Cape Peninsula University of Technology

IEC 61850 STANDARD-BASED RECLOSER CONTROL SCHEME FOR DISTRIBUTION SYSTEM

by

SIKHO NTSHIBA

Thesis submitted in fulfilment of the requirements for the degree

Master of Engineering: Electrical Engineering

in the Faculty of Engineering and Built in Environment

at the Cape Peninsula University of Technology

Supervisor: Dr Senthil Krishnamurthy

Bellville campus

7th December 2021

DECLARATION

I, Sikho Ntshiba, declare that the contents of this dissertation/thesis represent my own unaided work, and that the dissertation/thesis has not previously been submitted for academic examination towards any qualification. Furthermore, it represents my own opinions and not necessarily those of the Cape Peninsula University of Technology.

7th DEC 2021

Signed **Date**

ABSTRACT

The distribution system is a key component of the power system since it delivers power to clients and collects revenue. The distribution system is subject to unavoidable fault conditions. When these fault conditions occur, the distribution system's power lines are disrupted, and customers lose power for a few hours, depending on the sort of network malfunction. The distribution system serves hospitals, residential areas, factories, and schools. As a result of customer outages, power companies lose money and struggle to maintain reliability standards. When power is not delivered in accordance with the contract, power companies incur penalties from their customers. Previously, electric companies used a trouble call system to detect outages, in which a consumer experiencing a power outage would phone and report it. Field operators would be dispatched from control centers to restore power. Customers will be out of supply for an extended period of time as a result of this technique. As a result, using the IEC 61850 GOOSE message application, this study developed a recloser control technique to simulate the automatic reconfiguration of the distribution system under fault conditions.

The recloser control algorithm is designed for a radial distribution network. A 22kV distribution network is modeled and simulated using DIgSILENT software. Various faults are used at the feeder's upstream and downstream ends. The results of the DIgSILENT simulation are then used in a laboratory setting to implement the requested recloser control approach. A lab-scale test bench is built using three IEC 61850 compliant IEDs (two SEL-351A and one SEL-351), an Omicron CMC 356 injection device, an RSG 2288 Ethernet switch, and a PC. The recloser control system is tested using hardwired and IEC 61850 standard GOOSE signals. The DIgSILENT simulation results, a hardwired recloser control system, and an IEC 61850-based recloser control approach are compared and evaluated. The IEC61850-compliant GOOSE messaging program for a distribution system improves protection speed and reliability.

Through the construction of the distribution system recloser control technique, this research effort provides a standard benchmark for academic and industrial applications. The practical information gained through this research will instruct protection engineers on how to configure and deploy the recloser control scheme for

any industrial distribution network in order to increase network protection performance through autonomous reconfiguration under fault conditions.

Key Words: Distribution automation, Distribution system, Feeder automation, GOOSE message, IEC 61850 standard, Overcurrent protection, Recloser control scheme.

ACKNOWLEDGEMENTS

I wish to thank:

- God for the strength he given me.
- Dr Senthil Krishnamurthy for his support, advises, encouragement, patience, and availability throughout this project.
- All my colleagues at Centre for Substation Automation and Energy Management Systems (CSAEMS) for their support.

DEDICATION

The thesis is dedicated to my mother Pindiwe Patience Ntshiba.

Table of Contents

LIST OF FIGURES

LIST OF TABLES

GLOSSARY

AcSELerator Quickset - A software tool for configuring, commissioning, and managing power system devices for protection, metering, and monitoring.

AcSELerator Architect - A software tool that configures and documents IEC 61850 standard systems, which include GOOSE, sampled values, Manufacturing Message Specification for SCADA and process bus applications.

Alpha α **-** Slope constant for IEEE and IEC inverse overcurrent relay characteristic curves

Beta β **-** Slope constant for IEEE and IEC inverse overcurrent relay characteristic curves

Data attribute - describe the name format, range, and possible values associated with power system functions, which could be s status or measurement signals.

Distribution automation - Distribution automation (DA) is defined as the automatic control of the distribution system devices.

DIgSILENT - A software tool for modelling, simulation, and analyzing power system applications.

Distribution system - last section of the power system after generation and transmission that delivers electrical power to customers

Feeder - A conductor that connects a substation or local generation station to the load.

IEC 61850 - An international standard that defines the communication protocols for IEDs in substations.

Interoperability - Ability of IEDs to exchange and use the information for correct execution of specified functions, irrespective of the vendor.

Mesh network - A network where customers are supplied by more than one source of supply

Omicron CMC 356 - A relay test set and commissioning tool.

Overcurrent relay - A relay that operates when a current flow is greater than a pickup value

Physical device - contains one or more logical devices, each of which represents a set of functions, such as protection or control.

Radial network - A network that traditionally has one source of supply

Reliability indices - Performance measurements are used to measure the reliability of power utilities.

Recloser - A device that interrupts fault current and recloses under fault conditions

Relay coordination - The tripping of relays in an orderly manner in an electrical network

Relay operating time - The time that is taken by a relay to isolate a fault

SCADA - Supervisory Control and Data Acquisition is a computer-based system that remotely monitors and controls power system equipment in real-time.

Sectionalizer - A protection device that automatically isolates a faulty section of the line from the rest of the network

SEL-351A - Protection system relay

SEL-351 - Protection system relay

Test universe - A software tool for testing power system protection and measurement devices.

Time grading - The principle of operating relays in such a way that the relay closer to the fault operates first

Time delay - The amount of time given to a relay to wait before it operates

Transmission Control Protocol/Internet Protocol (TCP/IP) - A communication protocol used on the internet and similar computer networks

ABBREVIATION

ANSI - American National Standard Institute

CAIDI - Customer average interruption duration index

CB - Circuit breaker

CID - Configured IED Description

CT - Current transformer

CY - Cycle state

DER - Distributed energy resources

FDIR - Fault Detection Isolation and Restoration

GOOSE - Generic Object-Oriented Substation Event

ICD - IED Capability Description

IEC - International Electrotechnical Commission

IEEE - Institute of Electrical and Electronic Engineers

IED - Intelligent Electronic Devices

IDMT – Inverse definite minimum time

LN - Logical Node

LAN - Local Area Network

LD - Logical Device

LG fault - Single-phase-to-ground fault

LL fault - Double-phase-to-ground fault

LLL fault - Three-phase-to-ground fault

LO - Lockout state

MMS - IEC 61850 – Manufacturing Message Specification

NOP - Normal open point

OSI - Open Systems Interconnection

R1 - Relay 1

R2 - Relay 2

R3 - Relay 3

R4 - Relay 4

SVC - Static VAR Compensator

SCD - Substation Configuration Description

SCL - Substation Configuration description Language

SSD - System Specification Description

SLD - Single line diagram

SEL - Schweitzer Engineering Laboratories

SAIDI - System average interruption duration index

SAIFI - System average interruption frequency index

TMS - Time multiplier setting

VT - Voltage transformer

XML - Extensive markable language

XCBR - Logical node that represents a circuit breaker

51PP - Phase time overcurrent pickup

50P1P - Instantaneous overcurrent pickup

51G - Residual time overcurrent pickup

79LO - Lockout relay word bit

79CY - Reclose cycle relay word

79RS - Reset relay word bit

P51PTOC1 - logical node for 51PT

G51PTCO1 - logical node for 51GT

P67PTCOC1 - logical node for 67P1T

VB001 - virtual bit 1

VB002 - virtual bit 2

CHAPTER ONE

INTRODUCTION

1.1 Introduction

After the transmission system, the distribution system is responsible for distributing electricity to the various nodes in the network. Both transient (temporary) faults and permanent faults can occur in the distribution system network. These faults cause network disturbances, which have an impact on the resiliency of electricity supply to customers. The utilities and customer's trustworthiness in power delivery is a critical factor (Qin and Wu, 2014). Because of its significance and varying costs, distribution protection must be properly addressed. It's critical that the security of the system is both quick and dependable. Distribution system networks have been safeguarded with a variety of devices, such as overcurrent relays, Reclosers, sectionalizers, and fuses (Hosseinzadeh, 2008).

A 22kV distribution network is modeled and the simulation results are analyzed in this study. The simulation results are used to choose the pick-up settings for the lab-scale testing the auto-reclose scheme. The goal of this study is to implement a GOOSE auto-reclose control scheme for a distribution system based on the IEC 61850 standard. It also includes recloser protection, control, and condition monitoring features. The system detects faults and reconfigures the distribution network automatically to restore power to customers beyond the faulted section. The IEC 61850 GOOSE message is interoperable, which means that different vendors can use it.

This chapter describes an awareness of the problem in section 1.2, section 1.3 describes the problem statement, section 1.4 present the research aim and objectives, section 1.5 describes the hypothesis, Section 1.6 provide the delimitation of the research, the motivation of the research problem is provided in section 1.7, research assumptions are provided in section 1.8, Research methodology is presented in section 1.9, The breakdown of the thesis chapters is provided in section 1.10, and section 1.11 concludes the chapter.

1.2 Awareness of the problem

Through distribution automation, today's technology allows for better protection, monitoring, control, and quality of power in the distribution system. Communication technology capabilities are improving all the time. To find out about outages, power companies used a trouble call system in the past. A customer experiencing a power outage would call and report if there was a fault. Field operators were then dispatched to the field by the distribution control center. Following that, once the fault has been identified, the operators isolate and restore power. In South Africa, the traditional method is still used. In the event that a fault condition occurs in the network, advanced techniques should be applied to isolate the fault and automatically restore supply to customers without the need for human intervention.

As a result, a common technique for detecting, isolating, and restoring power is required to reduce outage duration and improve the quality and reliability of power in the distribution system. The research focuses on addressing the issues mentioned above.

As a result of the problem's awareness, IEC 61850 GOOSE message signals for the distribution system are being developed, as well as a recloser control scheme for automatic distribution system reconfiguration during event conditions.

1.3 Problem statement

The importance of distribution reliability, control monitoring, and protective functions to electric suppliers and end-users (customers) is undeniable but achieving them is a challenge. Various solutions have been implemented to address these issues, including the installation of additional protective equipment such as fuses, sectionalizers, switches, and reclosers, among others.

Electric suppliers developed automated strategies that can coordinate a large amount of responsibility using today's sophisticated technology. The current automation system is incompatible with other security devices from different manufacturers. As a result, a GOOSE message recloser control scheme based on the IEC61850 standard is required for automatic distribution system reconfiguration. To a large extent, all vendors will be able to use the proposed idea to implement automation and stabilize the distribution system.

Problem statement: ***The research work investigates the distribution system's reliability, control, monitoring, and protective functions. As a result, the research work implemented an IEC61850 standard-based recloser control scheme for automatic distribution system reconfiguration under fault conditions. The scheme is used to quickly isolate the faulted line section by detecting the fault operation and subsequent lockout of a recloser in the network. The scheme then closes the network's normally open point, re-energizing the healthy line section that had been de-energized when the fault had been cleared.***

1.3.1 Sub-problems

- Investigate the transition from a traditional hardwired protection system to a sophisticated wireless communication system using IEC61850 standard for transferring signals between protection and monitoring devices.
- Investigate the manual process of restoring power to customers, from fault location to automatic network reconfiguration without human intervention using IEC61850 standard.
- Engineering configuration of SEL-351 DIgSILENT Software version of the relay to perform and validate the auto-recloser function.
- Engineering configuration of SEL-351 IED to perform and validate the auto-recloser function at CSAEMS laboratory within DEECE at CPUT
- Engineering configuration of IEC61850 logical nodes P51PTOC1, G51PTCO1, P67PTCOC1, and OUT1GGIO3 to perform and validate the auto-recloser function at CSAEMS laboratory, at DEECE CPUT.
- Engineering configuration omicron test universe software to test the SEL-351 recloser protection function at CSAEMS laboratory, within DEECE at CPUT.
- Lab-scale implemenetation, test the recloser protection functions and analyse the simulation results.

1.4 Research aim and objectives

1.4.1 Aim

The goal of this study is to develop a recloser control scheme based on the IEC 61850 standard for automatic distribution system reconfiguration during fault conditions. The operation and subsequent lockout of the recloser in the network will be detected by this scheme, which quickly isolates the faulted line section and restores power to customers beyond the faulted location. Compare the hardwired simulation results to the recloser control scheme with IEC 61850 standard-based results.

1.4.2 Objectives

The literature review, development, implementation, and testing of the recloser protection functions are among the goals of this paper, which are detailed below.

1. The purpose of the literature work is to provide a review of the various approaches to recloser relay protection, control, and condition monitoring functions.
2. Perform engineering configuration of the DIgSILENT version of the SEL-351 auto-recloser relay.
3. Investigate the overcurrent and auto-reclose protection functions in the DIgSILENT environment.
4. Developed a recloser protection scheme for detecting faults, isolating them, and restoring power.
5. Perform engineering configuration of the SEL-351 auto-recloser IED.
6. To create GOOSE messages for an recloser control scheme based on the IEC 61850 standard.
7. Perform engineering configuration of the Test Universe configuration to validate the auto-recloser functions.
8. Test and analyse the recloser protection functions at lab-scale environment using SEL-351A relay and CMC devices.

9. Several case studies are simulated to verify the various power flow paths with parallel transformers and NOP Open/Close status in order to remove the faulted section of the network and restore power to rest of the distribution systems.
10. Compare DIgSILENT virtual relay simulation results with lab-scale simulation results.
11. Compare the simulation results of hardwired and IEC standard-based GOOSE message simulations for the auto-reclose scheme.

1.5 Hypothesis

The recloser control scheme based on the IEC 61850 standard allows automatic distribution system reconfiguration. The system is based on GOOSE messages for automatic distribution system reconfiguration during fault conditions. In comparison to traditional hardwired recloser schemes, IEC61850 communication improves the auto-reclose reconfiguration process, which is verified in this research work through lab-scale testing and simulation.

1.6 Delimitation of research

- This research work focuses on the application of IEC61850 in the distribution system auto-reclose scheme. A 22kV overhead distribution network is configured and modeled in the DIgSILENT Power Factory environment.
- Reclosers on a distribution network are considered in the project and reclosers on transmission and extra-high voltage networks are expected to be considered in future work.
- The recloser scheme was tested for the 22kV Distribution network because most faults in the SA distribution network require a solution based on modern technology, such as the implementation of the IEC61850 GOOSE message, to reduce outage times and improve protection speed, as well as the SAIFI and SAIDI indices.
- Due to the lumped load on the feeders, the distribution system is protected using reclosers.
- The fuse and sectionalizers are only considered on spur/branches with distributed loads on the network in comparison with the lump loads. Therefore the project is

limited to recloser protection on the main lines and protection on branches with fuses and sectionalizers are not considered.

- The investigations do not include recloser-sectionalizer and recloser-fuse coordination because the protection on the branches of the distribution network are not considered.

1.7 Motivation of the research project

The need to improve the distribution system's reliability, control, monitoring, and protection functions prompted the research project. The main goals of distribution system protection are to reduce the duration of a fault and the number of customers affected. Secondary goals include removing safety hazards as quickly as possible, limiting outages to the smallest section of the system, protecting customer equipment, protecting the network from avoidable disruptions, and removing faulty sections of the line (Hosseinzadeh, 2008).

The IEC 61850-based recloser control scheme is a cost-effective solution that allows for the isolation and restoration of electric power in a reasonable amount of time. By reconfiguring the network, it provides consumers such as industries, residential areas, and hospitals with the reliability of electric power during fault conditions. The IEC61850 standard-based recloser scheme isolates the faulty section of the network and restores power to a healthy section of the network without requiring human intervention.

As a result, the project work entails setting up a lab-scale and investigating the IEC 61850 GOOSE message application for distribution network automation using the SEL-351A auto-recloser IED and Omicron test injection device.

1.8 Assumptions

The following assumptions were used to guide the research:

- The distribution network is supplied by only one source of supply since it’s a radial system.
- The load is supplied by two parallel transformers, in order to provide an alternate power flow path during fault conditions.

- Even if the load can be supplied from different substations, reconfiguration can be done in the same way.
- There is one Normal Open Point (NOP) for the radial network without considering DGs.
- When the Normally Open Point (NOP) closes, power flow to the other side of the feeder is considered in the distribution system and its validated using DIgSILENT simulation.
- Implementation of the recloser control scheme improves distribution network reliability indices SAIFI and SAIDI.
- The omicron device's binary output is used to explore trip signals from the SEL-351A relay to emulate opening contacts of the circuit breaker.
- Hardwired protection signals are slower than IEC61850 GOOSE message communication.

1.9 Research Methodology

The goal of the study is to create a potential solution for automatic distribution system reconfiguration by establishing IEC 61850 standard GOOSE communication between adjacent reclosers in a distribution feeder. Without human intervention, the recloser should be able to detect faults, isolate them, and restore supply to customers beyond the faulted section. Information is gathered through online publications, related books, IEEE Std C37.104-2012, IEEE standard 141-1993, IEEE Std C37.110-1996, IEC 60255, IEEE C37.112, SEL-351 manual and test universe manual.

The methodology entails developing a recloser control algorithm for a 22kV distribution network, modeling, simulation, and lab-scale testing of the auto-recloser function at DEECE, CPUT's CSAEMS laboratory.

The implemented lab-scale test bench setup and positioning of the auto-reclosing relays in a distribution system network are shown in Figure 1.1. This auto-reclose scheme automatically restores power to line sections downstream that lost power due to faults upstream the distribution system line.

The auto-reclose SEL-351A relays configuration includes trip logic, close logic, and reclose logic. SEL-351A configuration settings of each relay include the definite time (50), inverse time overcurrent (51), tripping signals, and closing signals. The Omicron CMC 356 is used to inject currents and voltages signals to test the overcurrent and auto-reclose protection functions. The omicron test universe software provides an overcurrent test module and state sequencer module, which are used to test the overcurrent and auto-reclose protection functions of SEL-351A (R1) and SEL-351A (R2) relays. In this research, only the results for feeder A are documented, as the same results are applicable for feeder B.

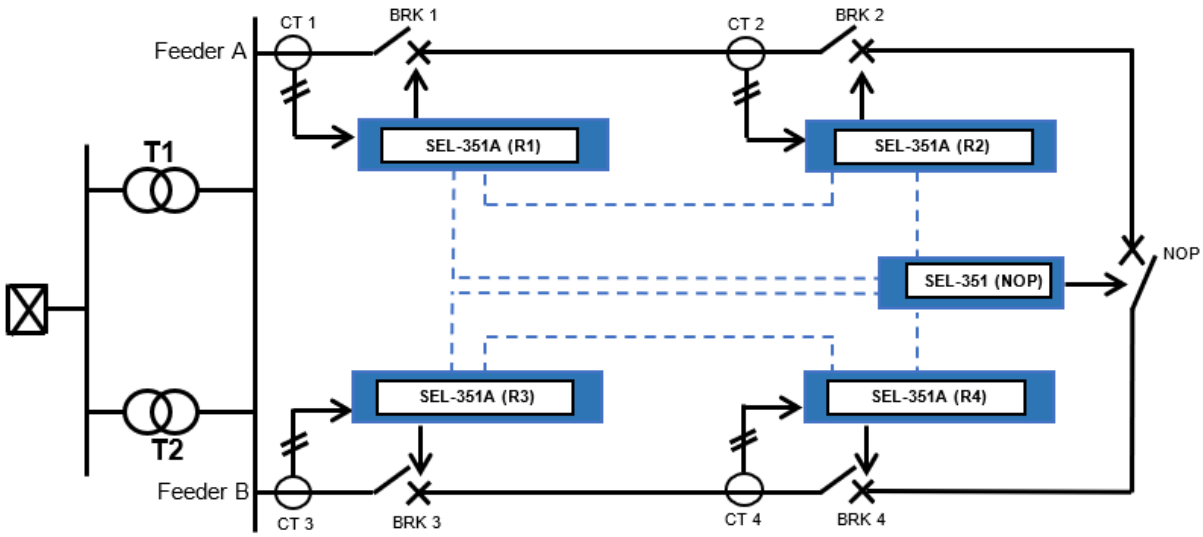

Figure 1.1: Recloser control scheme

1.9.1 Data collection

The data from the distribution network is gathered and analyzed. As shown in Figure 4.1 of Chapter 4 and Appendix A of this thesis, the data is used to model and simulate the distribution network.

1.9.2 Modeling and simulation

DIgSILENT software was used to conduct the simulations, to determine protection settings and system performance by performing power flow and short circuit analyses. Simulation of fault conditions in various sections of the distribution network is used to investigate the performance of the overcurrent relaying system. The distribution system recloser control scheme is investigated and evaluated.

1.9.3 Lab-scale test bench set up

The lab-scale setup is established at DEECE, CSAEMS laboratory at CPUT as shown in Chapter 6, Figures 6.1 to 6.4 respectively. The engineering configuration for the relay was done with the AcSELerator Quickset tool, the IEC 61850 GOOSE configuration was done with the AcSELerator Architect tool, and the Omicron device configuration was done with the test universe software.

1.10 Thesis chapter breakdown

There are seven chapters and one appendix in this thesis.

1.10.1 Chapter One

This chapter discusses the research problem, the problem statement, the research goal and objectives, the hypothesis, the research delimitation, the research motivation, the assumptions, and the research methodology.

1.10.2 Chapter Two

This chapter describes various methods formerly utilized in distribution networks for feeder automation. An overview of several types of distribution networks is examined (radial, ring, and mesh). The review of literature discusses the coordination of the recloser with other protective devices, reviews on reliability indices, and compares various approaches utilised on feeder automation, including procedures with and without the IEC 61850 standard.

1.10.3 Chapter Three

Distribution system faults overview, recloser application on a distribution system, recloser coordination, distribution system reliability measures, and distribution automation are all covered in this chapter.

1.10.4 Chapter Four

This chapter uses the DIgSILENT software to model the 22kV distribution network. DIgSILENT software-version of the recloser relay is configured and its protection

performance is investigated using fault study and recloser-recloser coordination simulations.

1.10.5 Chapter Five

This chapter describes the implementation and testing of the auto-reclose scheme test bench setup for the considered 22kV distribution system. The chapter provides the auto-reclose, overcurrent, and omicron test universe engineering configurations settings. Lab-scale testing of the recloser protection scheme and its simulation results are presented.

1.10.6 Chapter Six

The IEC 61850 standard-based GOOSE message for the recloser control scheme is described in this chapter. It also describes the logical node's configuration for the auto-reclose function and validates the IEC 61850 GOOSE messages simulation results.

1.10.7 Conclusion

This chapter summarizes the project deliverables, academic, research and industry application of the project, future work, and publications..

The next chapter provides a literature review investigation on recloser coordination with other protection devices, distribution automation, and reliability indices.

CHAPTER TWO

LITERATURE REVIEW

2.1 Introduction

Reclosers are critical components of a distribution network. They are strategically placed on a distribution system feeder. When there is a fault condition in a power line, reclosers detect, interrupt, and reclose power circuits. Reclosers are graded or coordinated with other field devices to reduce the number of power outages. Because the performance of the distribution system is measured using reliability measures known as "reliability indices," reducing the number of power outages improves system reliability. The reliability indices are calculated using sustained interruptions, load, and momentary interruptions.

Distribution automation enables a quick response to power outages as well as day-to-day distribution system operation (DA). DA employs modern communication computer-based technologies to remotely monitor, control, and coordinate field devices (Zhou *et al.*, 2016). DA includes automation at the substation, feeder, and customer's system. DA is essential for achieving system self-recovery and high power reliability.

Figure 2.1 depicts a graph of the number of publications reviewed from 1989 to 2021. These papers were chosen based on their relevance to distribution system feeder protection.The literature review collection includes 109 works on feeder protection from books, journals, standards, and user manuals. The graph illustrates that the number of feeder protection studies published increased from 2009, 2012, 2015 and 2018. The papers investigated for recloser coordination with other protection devices, (Recloser-Fuse (R-F), Recloser-Sectionerlizer (R-S), Recloser-Recloser (R-R)), distribution automation (FA), FDIR, and reliability indices are depicted in Figure 2.2.

Section 2.2 of this chapter discusses the overview of the distribution system. Section 2.3 examines distribution system concepts and recloser coordination with other protection devices. Section 2.4 gives a comparison of protection in various types of distribution networks. Section 2.5 contains an overview of related works on distribution system reliability indices. Section 2.6 provides an overview of distribution automation. Section 2.7 concludes the chapter.

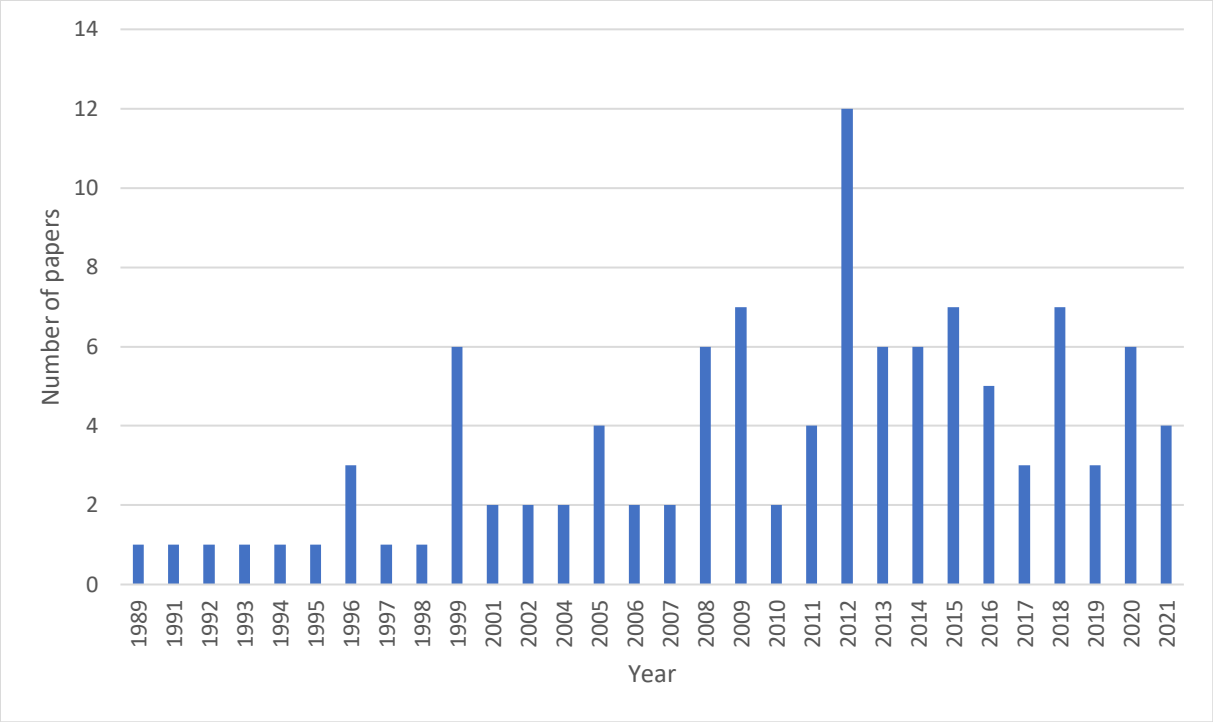

Figure 2.1: Number of papers vs publication

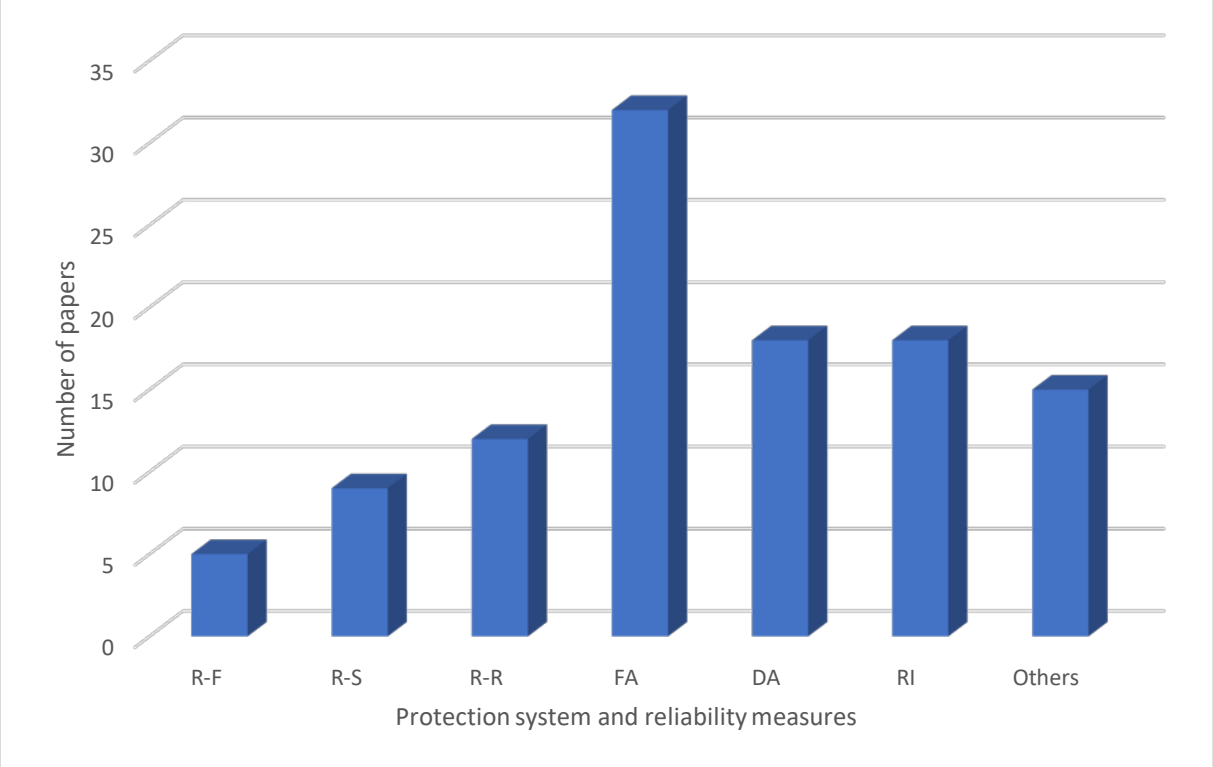

Figure 2.2: Type of protection and reliability measures vs number of papers

2.2 Distribution system overview

The final section of the electrical power system is the distribution system, which distributes electricity to end-users after generation and transmission. Power delivery reliability is a critical factor for both electrical utilities and customers, so this distribution section plays an important role. A distribution network is made up of a distribution substation, primary distribution feeders, secondary circuits, transformers, and field devices located along the distribution feeder (Prakash *et al.*, 2016) and(Mostafa, Elshahed and Elsobki, 2018). Reclosers, sectionalizers, fuses, voltage regulators, and other field devices are examples of this type of device. Floods, storms, and cyclones can all disrupt distribution networks.

Network faults are caused by natural disasters, trees falling on distribution lines, and other factors such as animals disturbing distribution lines. The reliability of the distribution system, as well as the security and quality of the electricity delivered, are all affected by faults (Salim *et al.*, 2009). Several types of protective devices are used to protect the distribution system from problems. Reclosers, overcurrent relays, and fuses are common distribution system protection devices (Fazanehrafat *et al.*, 2008). The system element or electrical equipment that needs to be protected, as well as the voltage level in the system, determine the type of protection used. There are broad guidelines on how these system elements or electrical equipment operate, even if there are no explicit standards for overall distribution system protection (Gers, 2004).

The most common distribution networks such as the radial network, ring network, and mesh network, are investigated. The benefits, limitations, operations, controls, management growth model of various types of distribution networks are discussed, as well as their advantages and disadvantages.

2.2.1 The fundamental principle of distribution networks

The following essential rules should be followed by distribution networks (Altuve, Zimmerman and Tziouvaras, 2015):

- The ability of the distribution network's protective devices to function effectively is referred to as reliability. The two main characteristics of reliability are dependability and security: when a fault occurs, the required operation should occur, and the erroneous operation should be avoided.

- To improve the protection speed, a network fault should be cleared to avoid equipment damage.
- Selectivity: Only disconnect the relevant portion of the distribution network in the event of a fault to ensure supply continuity.
- Cost: Make sure you're getting the best protection method in practise for the least amount of money.
- Customers should receive good electrical energy via distribution networks. This includes a constant voltage and supply frequency, a constant voltage magnitude, a harmonic-free voltage supply, and a power supply that is not interrupted.

2.2.2 Radial distribution network

At the distribution level, a substation has traditionally been the source of power. The substation supplies power to a typical radial distribution line that runs through several neighborhood areas (So and Li, 2002). A radial network topology is made up of a distribution transformer, circuit breakers, and protective devices (Fardo, 2009) and (Chan, 2009). A radial network is a flexible system that can be used to evaluate various topologies, fittings, controls, and security measures (Prakash *et al.*, 2016). Figure 2.3 depicts a simple radial distribution network that employs a single power source to feed several clients.

Radial networks make it easier to coordinate, develop, and determine component ratings. Reactive power compensation is used in voltage compensation techniques. The most cost-effective to set up and maintain is the radial distribution scheme (Prakash *et al.*, 2016). A radial distribution network is the least reliable in terms of continuous delivery because there is no alternate source of supply. When a problem occurs or protection devices open, many customers are disconnected. Power outages can occur for a variety of reasons, and supply restoration is dependent on how long it takes to fix the problem. Severe voltage swings may occur when consumers at the far end of the distribution line are heavily loaded (Cutler-Hammer, 1999).

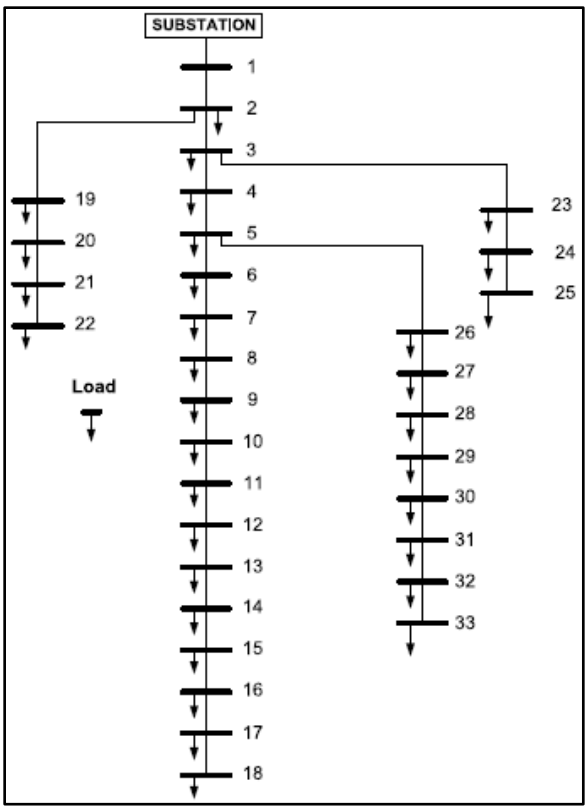

Figure 2.3: Typical radial distribution network (Prakash et al., 2016)

2.2.3 Ring or Loop distribution network

In densely populated areas, ring distribution networks are usually used. The network returns to its point of origin after looping through the service region. Switching devices are deliberately located in a ring network to ensure that clients are supplied from all directions. Switching devices open or close to preserve power source if a problem occurs or if power fails (Sadhu and Das, 2016)and (Cutler-Hammer, 1999). The ring structure provides improved voltage stability and reduced power loss. A common ring distribution network is seen in Figure 2.4.

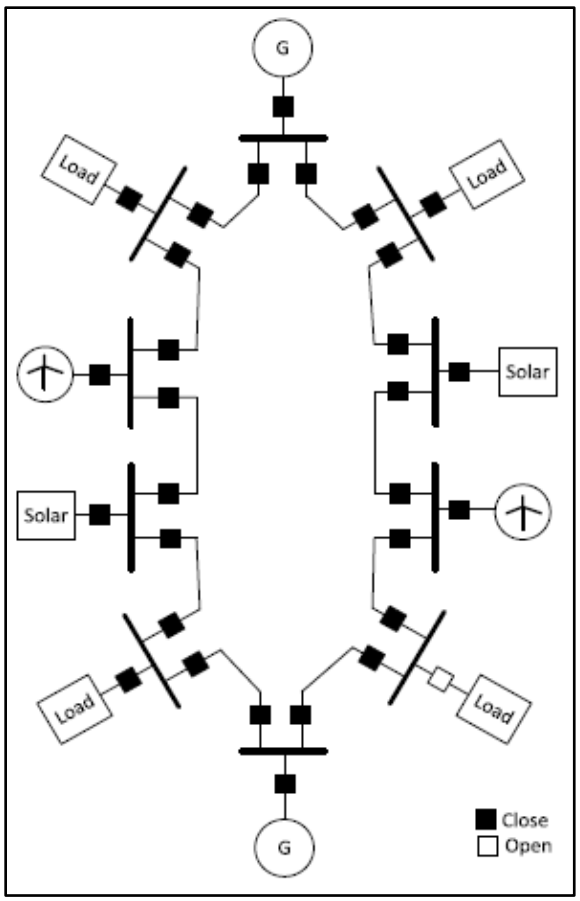

Figure 2.4: Typical Loop distribution network (Islam et al., 2017)

The ring network's main advantages include reduced real power loss, a balanced load system, improved bus voltage, increased system security, reliability, and improved power quality (Vasant, 2011). When compared to a simple radial distribution structure, the fundamental disadvantage of ring distribution structures is their high capacity cost. The ring structure design should meet all voltage drop and power requirements when fed from any side of the loop. When the distribution network is fed from either end, this distribution configuration necessitates additional capacity at both ends, and the conductor utilized should be large enough to carry the required power and voltage (Willis, 2004).

A distribution network with numerous connected rings is known as a multi-ring structure. A multi-ring construction features many power transfer pathways. Multi-path construction, on the other hand, makes the automatic operation of safety devices like reclosers or relays challenging since it can be difficult to identify, locate, and take necessary actions to minimize customer disruptions. (Islam *et al.*, 2017).

2.2.4 Mesh distribution network

In terms of supply continuity, a mesh distribution network is the most expensive and dependable type of distribution system. The mesh structure is made up of several linking circuits that operate at the same voltage (Cutler-Hammer, 1999). Consumers are served by more than one source of supply (Silos, Villafafila and Lloret, 2020). If one of the power supplies dies, customers are not disconnected. Other power sources are used to feed them. The network of a mesh structure is similar to that of a ring structure, but it includes redundant lines in addition to the mainline that provide an extra power supply route. This is done as a backup, to provide a backup power supply if the mainline fails. Figure 2.5 depicts the configuration of a mesh distribution network.

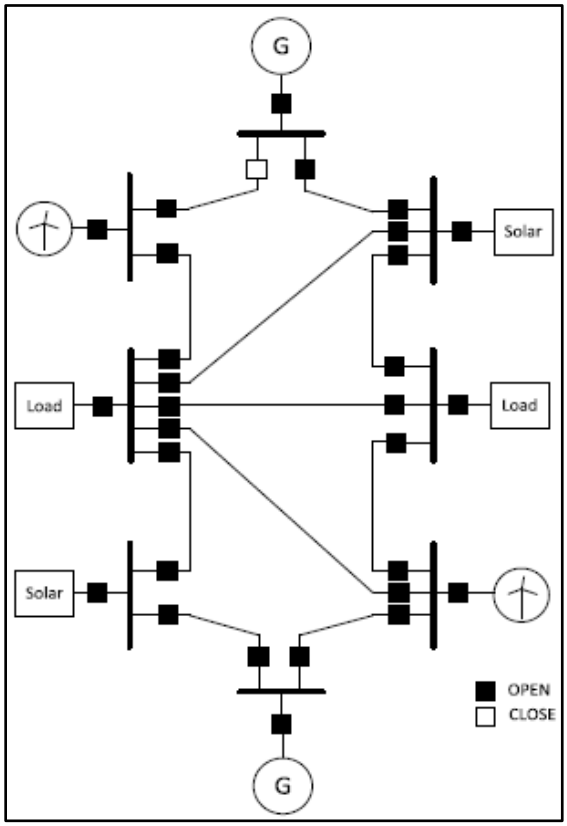

Figure 2.5: Typical Mesh distribution network (Islam et al., 2017)

2.2.5 Review summary on Radial, Ring and mesh distribution networks

In comparison to ring and mesh networks, radial distribution networks are simpler and less expensive to install. However, because there is only one source of power in a radial network, power delivery is the least reliable. When a fault condition occurs in a radial network, the length of time it takes to remove the fault condition from the network determines power restoration. In comparison to a radial network, a ring distribution network is more complex and expensive to create. Because of the alternate source of supply, power delivery in a ring network is superior than that in a radial network. Customers can be supplied with an alternate supply if a fault condition occurs in a ring network. When compared to radial and ring distribution networks, a mesh distribution network is more complex and expensive. Mesh networks are more expensive, but they provide the most reliable power delivery. When a fault occurs in a mesh network, customers are not left without power; instead, they are provided with an alternate source.

2.3 Distribution network protection devices and their coordination

The distribution system's protection devices are coordinated in such a way that the device closest to the fault operates first, followed by an upstream device locking out. This technique tries to limit fault-related service interruptions to a minimum in order to electrify as many consumers as possible. The automatic reclosing practice has an effect on the coordination of series-connected protection devices. When a recloser on the auto-reclose cycle reaches its dead time, the backup device begins to reset or, if a fuse, it cools down (IEEE Std C37.230, 2007).

The main distribution line is the focus of this thesis, which employs recloser-to-recloser coordination. The focus of this thesis was on lump load rather than distributed load. Fuse items are commonly used to protect line transformers on branches that are not connected to the main distribution line. Sectionalizers do not influence fault currents; rather, they count the number of operations performed by the upstream interrupting device and open when the device upstream has opened (IEEE Std C37.104-2012, 2012). For these reasons, recloser and fuse coordination, as well as recloser and sectionalizer coordination, are not used.

2.3.1 Recloser and fuse coordination

The position of these devices defines the critical criteria for selecting recloser and fuse coordination, which means that the fuse may be used as primary protection and the recloser as backup protection, or vice versa. If the fuse is closer to the source side and the recloser is downstream, the recloser operation should be faster than the fuse's minimum melting time. This is performed by multiplying the factors of the recloser's time/current characteristic curve to account for fuse link fatigue caused by the increased heat effect caused by prolonged operation of the recloser (Gers, 2004). Figure 2.6 depicts how the recloser and fuse interact, with the fuse serving as a backup and the recloser serving as primary protection. The recloser curve was modified with the appropriate factor, as seen in the diagram below (k).

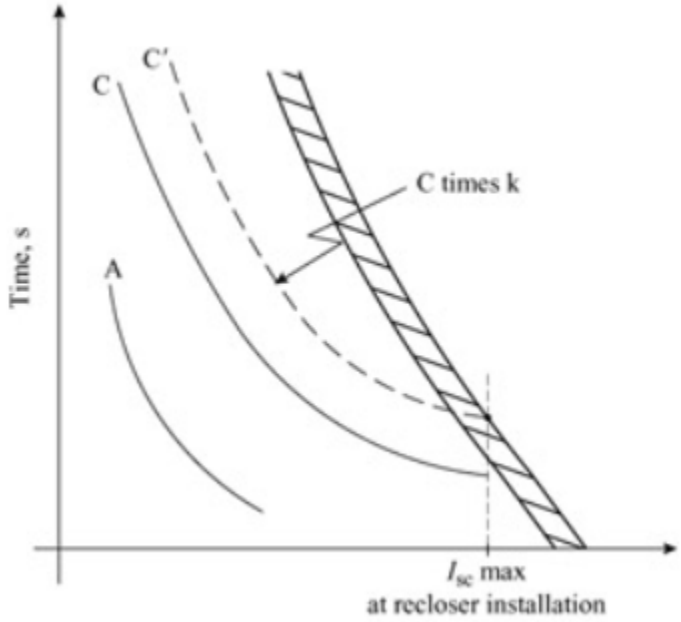

Figure 2.6: Typical representation of fuse (on the source side) and recloser coordination (Gers, 2004)

The shortest time for the fuse to melt while the recloser is closest to the source of supply as backup protection for the fuse downstream, which is the principal protection, must be higher than the recloser curve multiplied by the multiplication factor "k." The fuse clearing time should be shorter than the recloser curve without the multiplication

factor. An example recloser (on the source side) and fuse coordination diagram is shown in Figure 2.7.

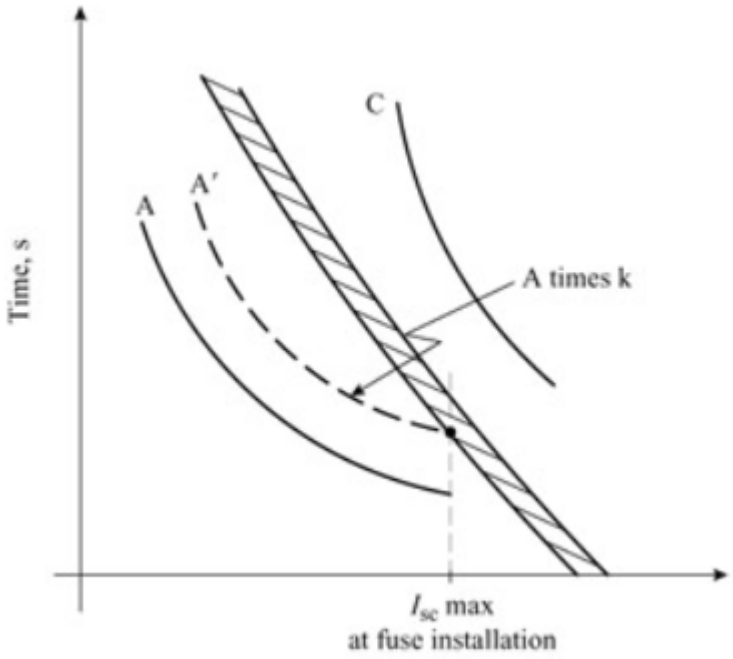

Figure 2.7: Typical representation of fuse (on the source side) and recloser coordination (Gers, 2004)

Because of the penetration of distributed energy resources, which affects the traditional radial distribution system, the authors (Brahma and Girgis, 2002) recommended new performance standards for recloser and fuse coordination. The distribution system loses its radial nature, causing coordination to be disrupted. The distribution system was modelled in PSCAD/EMTDC software, and adequate coordination between the recloser and the fuse was demonstrated. To address reliability concerns, the authors (Abidi and Yokoyama, 2005) built an appropriate distributed generation sizing as a backup to the distribution system. The coordination of the present recloser and fuse coordination was explored in the paper. The research is carried out in a simulation environment, and it confirms that the suggested method delivers adequate distributed generation sizing while maintaining protective coordination between the recloser and the fuse. Authors (Chaitusaney and Yokoyama, 2008) presented mitigation of degradation of dependability distribution system owing to recloser and fuse miscoordination caused by dispersed generation in 2008. The proposed updated protection system is useful in reducing distribution system reliability deterioration.

2.3.2 Recloser and sectionalizer coordination

Sectionalisers don't have a time/current property. The coordination is determined by the number of activities performed on the backup recloser. Sectionalizers are activated after sensing a predefined number of overcurrent surges. The following criteria influence the selection of a sectionalizer (Ruschel and Ashley, 1989) and (Rones and Vittal, 2013):

- Because sectionalizers only detect overcurrent surges on the load side, the downstream actuating current of the sectionalizer should be less than the upstream actuating current of the recloser.
- The number of downstream sectionalizer overcurrent counts should be less than the number of upstream recloser lockout settings.
- The memory term of the sectionalizer should be longer than the recloser's upstream accumulative tripping and reclosing period. This ensures that the sectionalizer counts all essential fault excursions.

(Arthi and Vittal, 2013) used PSCAD/EMTDC software to create a model of a recloser and sectionalizer coordination. The model was validated by deploying it in a distribution network sample and conducting several case studies. The purpose of this article is to offer information about the behavior of recloser and sectionalizer protection at the distribution system level. (Zeinalzadeh, Estebsari, and Bahmanyar, 2019) developed an algorithm for multi-objective placement of reclosers and sectionalizers in distribution system feeders in order to reduce customer outage expenses and enhancing system dependability. The algorithm's effectiveness is confirmed by simulation of the IEEE 85-node distribution feeder. When compared to scenarios where there are no overhead switches, the examined results show that the recloser and sectionalizer coordination provides statisfactory performance. The authors (Safari, Haghifam, and Zangiabadi, 2021) proposed a hybrid technique for recloser and sectionalizer positioning in the distribution system that takes into account device coordination, fault types, and equipment malfunctioning. This strategy tries to increase profitability for electricity companies while reducing service interruptions for

customers. To evaluate the suggested technique, a distribution network is simulated using Matlab software. The simulation results demonstrate the technique's effectiveness and robustness.

2.3.3 Recloser and recloser coordination

The downstream recloser should be set to operate faster than the upstream recloser, which is closer to the source of supply. The downstream recloser's fault clearance time and all reasonable time delays should be shorter than the upstream recloser's. The recloser is typically located closer to the source of supply in order to perform at least one quick reclosing operation, which clears transient faults between the source of supply and the load recloser. The time delay between time/current characteristics on electronic controlled and hydraulic controlled reclosers varies (Hao and Keckalo, 2021) and (Gers, 2004).

The authors (Razavi et al., 2008) used a genetic algorithm technique to optimize the coordination of overcurrent relays. The goal of this work is to overcome the problems of miscoordination and continuous or discrete-time multiplier or time dial setup. The suggested technique is validated on two distinct power system networks, and the findings show that the proposed method functions effectively, correctly, and flexibly. (Hussain, Rahim, and Musirin, 2013) gave a review of optimal overcurrent relay coordination for the protection system. The review discusses artificial intelligence, nature inspiration algorithms, and traditional overcurrent protection approaches. The authors (Chen, Lee, and Chang, 2012) presented a method for optimizing the overcurrent coordination of relays in a distribution network using a genetic algorithm, which included transformer protection. A typical single-ring distribution system is utilized to demonstrate the coordination and validate the suggested technique. Various types of curves, such as very inverse curves, typical inverse curves, and moderate inverse curves, as well as the transformer's damage curve, are considered and modelled. The simulation results show that the proposed strategy is both fast and accurate.

2.3.4 Review summary on types of distribution networks, protection devices, coordination and its relability analysis

This section provides comprehensive comparative study of radial, mesh, and ring distribution networks and their protective devices fuses, overcurrent protection, reclosers, sectionalizers, and their coordinations. The review summary examines the compensating devices utilized in the distribution network to improve the voltage profile and power factor by employing SVCs, FACTS, DGs, and transformer tap-changers (radial, ring and mesh). The review summary also emphasizes the distribution networks reviewed in this section's on power loss, power delivery reliability, and security status. Table 2.1 summarizes the types of protection devices used in radial, ring, and mesh network networks and emphasizes the necessity of compensating devices in maintaining the regulatory in distribution system and improving overall system performance (reliability, power supply, and security status).

Tables 2.1: A comparative analysis of protection in distribution networks

Paper / Authors	Aim	Network topology (Radial, Ring, Mesh)	Type of Protection device used (Fuse, OC, Recloser, Sectionalizer)	Voltage compensation device used (FACTS, Tap-changer, Voltage regulator, SVs, DGs)	Power Loss (Radial, Ring, Mesh)	Power delivery, security and reliability (Radial, Ring, Mesh)
(Ruschel and Ashley, 1989)	To investigate the coordination of relays, reclosers, and fuses for oil patch overhead distribution system lines.	Radial network	Coordination of relays, reclosers, and fuses.	No compesntaion device used.	High power loss due to radial structure.	Due to the radial structure and the lack of a backup supply, power delivery,security and reliability is extremely low.
(So and Li, 2002)	To create a method for coordinating overcurrent relays in order to protect ring-fed distribution networks that are integrated with DGs.	Ring network	Overcurrent relays	Voltage regulation is maintained by DG's	Because the network is ring-fed, integrated with DGs, and correctly coordinated, power loss is minimal.	Because of the ring topology and DG integration, there is a high level of security,power delivery and dependability.
(Fazanehrafat *et al.*, 2008)	To create a method for preserving recloser-to-fuse coordination in a DG integrated distribution system	Radial network	Recloser, and fuse	No compesntaion device used.	Because of the main supply and DER integration, power loss is minimum.	Because of the radial construction, security, power delivey and dependability are reduced.
(Motoki *et al.*, 2015)	To implement a computational system for analyzing power quality in a smart grid.	Radial work	Recloser	Transmission and distribution systems are both present in a simulated network. The transmission system used FACTS devices for compensation, distribution system simulated without compensation device	Because of the radial structure, there is a greater chance of power loss.	Because of the radial construction, security, power delivery and dependability are reduced.
(Islam *et al.*, 2017)	To improve existing distribution system structures, through a unique distribution system structure	Mesh network	Overcurrent	FACTS devices are used	Chances of power loss are minimized, customers have various routes to be back-fed in the mesh network.	Due to different routes to feed the load and multiple sources of supplies, there is very high-power security, power delivery and reliability.

(Mostafa, Elshahed and Elsobki, 2018)	To assess the influence of DERs on the dependability of the distribution system by incorporating SVCs.	Radial network	Recloser	SVC	The use of DERs and SVCs helps to reduce power loss.	Because there is only one source of supply, security,power delivery and dependability are compromised. If the source transformer fails, the DERs will be unable to meet the entire load.
(Silos, Villafafila and Lloret, 2020)	To design a fault location method for a mesh distribution network that includes DERs.	Mesh network	Overcurrent protection	No compesntaion device used.	Mesh topology and DER integration reduce power loss.	Because of the mesh topology and DER integration, the security, Power delivery and dependability are extremely good.

2.4 Review investigation on reliability indices

The papers in this section are a comparative examination of prior studies on reliability indices.

The performance of the distribution system and the statistics used to measure total customer service are affected by the system's exposure to hazardous conditions and its ability to survive the hazard conditions. As a result, the author (Gilligan, 1992) invented a method to examine network configuration and dangers. The information of the network configuration and dangers is then used to see how they affect the reliability indices. It is a matter of detecting the network's shortcomings and making state modifications based on the reliability indices results. The study approach includes looking at the length of the mainline, the network's vulnerability to dangerous circumstances, factors that could influence the conductor, and factors that could affect upstream protection devices (e.g., circuit breakers, reclosers).

Authors (Allan and Silva, 1995) provide models and methodologies for analyzing probability distributions for dependability indices in meshed networks in 1995. The research also offers a method for combining interruption costs with probability distributions of interruption lengths, as well as one for evaluating the cost of interruptions in meshed networks using CAIDI. Analytical techniques and the Monte Carlo method are used in the approach. Regardless of their future performance analysis, the analytical technique is based on the mean value of the dependability indices (Billinton and Wang, 1999). The Monte Carlo method is a popular solution for overcoming the analytical technique's limitations (Li, 2014). The results are studied and only illustrate that additional information may be obtained by employing reliability indices distributions.

Authors (Mo-yuen, Taylor and Mo-Suk, 1996) presented a method for evaluating and interpreting time of outage restoration (TOR) data in distribution systems in terms of time, effects, and environment. The correlation and analysis of statistical quantitative results and field engineering insight the method given in this study is easily adaptable to various electric utilities. This paper's technique and technical explanation are important for future research and development on TOR problems in distribution systems.

Authors (Goodin, Fahey and Hanson, 1999) published a comparative examination of distribution system reliability improvements that can be performed employing a variety

of outdoor distribution system devices during the beginning of 1999. The study begins with a discussion of the most common sorts of devices, such as reclosers, automatic sectionalizers, and manual switches. Then, calculate the total number of reliability improvements that can be obtained by using one or more of these distribution system devices. According to the paper, all of these distribution system devices improve system reliability. The switches improve the SAIDI (System Average Interruption Frequency Index). Midpoint switches are essential in tie-point applications where feeders can connect. The performance of sectionalizers and reclosers is comparable to that of other configurations, with the exception that reclosers provide higher improvement for MAIFI.

Authors (Makarov and Moharari, 1999) created a power system reliability and security integrated index in late 1999, which reflects both directly and indirectly. Direct characteristics are concerned with the risk of failing to fully supply the load at various load levels and contingencies. Indirect features are concerned with handling undesirable conditions such as circuit overload, voltage crises, poor stability margins, area interchange violations, insufficient generation reserves, and so on. Even if indirect characteristics may not always result in load losses, they do signal a diminished system security or reliability margin. The smaller margin may occasionally result in hardly foreseeable and quantified load losses (through corrective actions, islanding, and instability), unanticipated events (cascading outages), catastrophic system failures (voltage collapse), and other undesirable outcomes. Through the combining of varied contributing components utilizing a fuzzy logic-like methodology, this new integrated index provides a more thorough answer concerning the general degree of both reliability and security of the power system. The index is designed to be flexible enough to suit a variety of priorities and admissions of power utilities to specific index attributes.

The author (Roos, 2005) analyzed the application of reliability enhancement solutions on a test system from a socioeconomic standpoint. The average annual supply disruption cost to consumers supplied by the test system has been estimated for each of the solutions implemented on the test system. In addition, the maximum annual capital cost for implementing each test solution has been calculated. Following that, a reliability enhancement solution is considered socioeconomically justified if the financial expenditures connected with its deployment are less than the ensuing reduction in customer disruption cost.

Authors (Lei, Singh and Sprintson, 2014) demonstrate a novel reliability model and analysis method for current substation protection systems in early 2014. This method is used to study and assess an IEC 61850-based substation protection system that includes both physical and cyber components (Merging Units, IEDs, and process bus). The study's findings give thorough and crucial knowledge for reliability evaluation, paving the path for reliability analysis of complex and huge cyber and physical systems.

Authors (Nagaraj, Subramanyam and Richard, 2014) reported an effective Monte Carlo simulation method for assessing distribution system reliability in late 2014. The method analyzes real-world distribution system outage data to determine the failure and repair models that may be employed in the Monte Carlo simulation method. The paper also discusses the sensitivity of the reliability indices to model selection. The effect of safety devices on the statistical distribution of SAIFI for a real-world distribution system feeder is discussed. The sensitivity analyses revealed that the SAIFI results are essentially independent of the statistical model of the failure process, however the SAIDI is heavily dependent on the length of the repair duration model.

Authors (Huda and Rastko, 2016) create a new sequential multilevel Monte Carlo (MLMC) approach for estimating distribution system reliability in 2016. This method improves the computing efficiency of the Monte Carlo sequential method. The MLMC employs stochastic differential equations that are based on the approximation of reliability indices with multiple timesteps. The simulation results show that the MLMC approach gives appropriate reliability indices while taking less time to calculate than the sequential Monte Carlo method.

The authors (Bosisio *et al.*, 2019) offer a distribution system automation system logic that intends to increase reliability indices through the use of selective fault detection, quick network reconfiguration, and automatic back-feeding. Based on the IEC 61850 standard, electronic instruments, and an optical fiber communication network, a hierarchical smart substation strategy is given. Logic selectivity is used to coordinate the protection of the primary and secondary substations. This study shows and concludes that selective fault detection, quick network reconfiguration, and automatic back-feeding are possible.

The authors (Guner and Ozdemir, 2020) discuss the effects of electric vehicles. The impact that parking lots with grid-integrated battery storage have on the reliability of the

distribution system feeder. For feeder reliability indicators, the paper employs average interruption duration, average interruption frequency, and energy not served. For load point reliability, the reliability indices interruption frequency, interruption duration, and energy not served are utilized. The results show that the backup functioning of the parking lots increases the feeder reliability indices and the load point reliability indices.

The authors (Paci, Bualoti and Celo, 2021) offer a fuzzy logic that uses six input variables to evaluate the distribution system reliability indices of lines and transformers. Age, operation and maintenance, present loading exposure, and weather conditions are among the considerations (wind or temperature). The fuzzy logic is built on the IF-THEN rule learned through Matlab program. A thorough examination of the fuzzy system reveals that the variables under consideration are dynamically and precisely linked. This article finds that the fuzzy method ensures that engineering experience is taken into account, which is critical when tackling power system difficulties. Based on engineering expertise, the derived criteria correctly depict reliability indices.

Table 2.2 provides a brief summary of distribution network reliability indicies. The review summary describes the purpose of the publications studied on distribution network reliability indices, the methods used, and their accomplishments and limitations.

author and the year of the publication are compared, as well as the purpose of the research, the methods utilized, and the accomplishments or limits.

Tables 2.2: Review summary on distribution system reliability indices

Paper / Authors	Aim	Method used	Achievement/Limitations
(Gilligan, 1992)	To propose a mechanism for estimating the distribution system's reliability.	The suggested analysis method identifies network vulnerabilities and recommends improvements. The length of the line, exposure to hazards, and factors affecting upstream protective devices are all considered in the analysis.	The analysis's method improves the most exposed circuits at a minimal cost through the analysis method.
(Allan and Silva, 1995)	To create models and methodologies for assessing the reliability indices in a mesh distribution network. In addition, the study proposes a method for combining interruption costs with probability disruptions of interrupted duration and CAIDI to evaluate interruption costs in a mesh network.	The proposed method is based on a hybrid of analytical and Monte Carlo simulation.	The test findings show that more accurate estimates of interruption costs may be calculated. The method aids in determining whether or not targets are met.
(Mo-yuen, Taylor and Mo-Suk, 1996)	To conduct an analysis for the distribution system's time of outage restoration.	Statistical method used to evaluates and interprets time of outage restoration (TOR) data in a distribution system	This approach's design addresses the difficulties of modeling development for customer service and is effective for research and TOR improvement.
(Makarov and Moharari, 1999)	To establish a risk-based integrated index that directly and indirectly displays power system reliability and security. At varying load levels, direct characteristics are predicated on not fully supplying the load. Indirect features are based on dealing with undesirable events such as voltage crises, low stability, and circuit overload.	Fuzzy logic has been proposed. The logic make use of direct and indirect characteristics.	The developed security index meets the practical, flexible, and effective security and dependability needs of utilities
(Lei, Singh and Sprintson, 2014)	To develop a reliability model and analysis technique for a modern substation protection system based on IEC 61850.	The approach proposed is based on the IEC 61850 standard. It employs cyber components such as merging units, IEDs, and process buses, as well as physical electric components like as transformers, circuit breakers, and power lines.	The study's findings give thorough and crucial knowledge for reliability evaluation, paving the path for reliability analysis of complex and huge cyber and physical systems.
(Nagaraj, Subramanyam and Richard, 2014)	To build a model and analyze reliability indices SAIFI and SAIDI in the distribution system.	The Monte Carlo simulation approach is utilized.	The test results show that the sensitivity analyses show that the SAIFI results are essentially independent of the statistical model of the failure process, whereas the

			SAIDI is heavily dependent on the length of the repair duration model.
(Huda and Rastko, 2016)	To develop a sequential multilevel Monte Carlo (MLMC) approach for estimating distribution system reliability.	The proposed method employs a multilevel Monte Carlo (MLMC) algorithm..	The results of the tests show that the MLMC approach gives appropriate reliability indices while reducing calculation time when compared to the sequential Monte Carlo method.
(Bosisio *et al.*, 2019)	To design IEC 61850 automation system logic in order to increase distribution system reliability indices.	Based on the IEC 61850 standard, the suggested solution employs selective fault detection, quick network reconfiguration, and automatic back-feeding.	A logic selectivity is used to coordinate the protection of the primary and secondary substations. This study shows and concludes that selective fault detection, quick network reconfiguration, and automatic back-feeding are possible.This decreases the number of consumers without electricity service and increases the reliability indices.
(Guner and Ozdemir, 2020)	To create a method for improving distribution system dependability indices while taking into account electric vehicles Parking lots with grid-integrated battery storage.	For feeder reliability indices, the technique employs average interruption duration, average interruption frequency, and energy not served. For load point reliability, the reliability indices interruption frequency, interruption duration, and energy not served are utilized.	The simulation findings show that the backup functioning of the electric vehicles coupled with battery storage system increases the feeder and load point reliability indices, respectively.
(Paci, Bualoti and Celo, 2021)	To provide a fuzzy reasoning approach for assessing distribution system dependability indices.	The proposed solution employs fuzzy logic and is based on an IF-THEN rule created in Matlab software.	The developed fuzzy logic method ensures that engineering experience is taken into account while addressing distribution system dependability indices.. Based on engineering expertise, the derived criteria correctly depict reliability indices.

2.5 Distribution automation and its categories

Distribution automation (DA) was first proposed in the 1970s. The main inspiration was to employ emerging computer technology and communication protocols to improve the operating performance of the distribution system. Increasing efficiency was the primary driver of DA in its early stages. DA has now progressed to target reliability and distribution power quality improvements (Pahwa, 2005). Since then, DA has evolved into a distinct idea. DA encompasses all areas of distribution system planning, design, protection, dependability, load management, economic evaluation, and network control systems, often known as SCADA (Su and Teng, 2006). DA improves SCADA operations; formerly, field engineers had to manually activate devices for a specific system condition; now, field devices may react to system conditions automatically.

Some electric utilities have begun to incorporate Distribution Automation (DA) into their distribution circuit designs to achieve a quick reaction to outages as well as efficient daily distribution system functioning. The system operators can use DA to control many sectionalizing switches, circuit breakers, and reclosers remotely or locally. By remotely monitoring the analog values made available by DA-equipped equipment, DA also delivers real-time data to system field operators, such as voltage, current, power flow, and so on, for each circuit. The status points of these DA-equipped devices can also be monitored by the system operator. Because of DA's data-gathering capabilities, it is easy to pinpoint which parts of the distribution network are having problems. The system operator can remotely control or dispatch field engineers to isolate and repair sections of the distribution network using information from DA-equipped devices (IEEE Std C37.230, 2007).

One of the most important characteristics of an electric utility is how transmission and distribution resources are managed and maintained to ensure system dependability while improving operation and maintenance activities. Automation plays a significant role in data collection for control centers to monitor and operate the power system (Bakhtiari and Frarahani, 2012). As seen in Figure 2.8, this is done in a regulated framework with multiple layers.

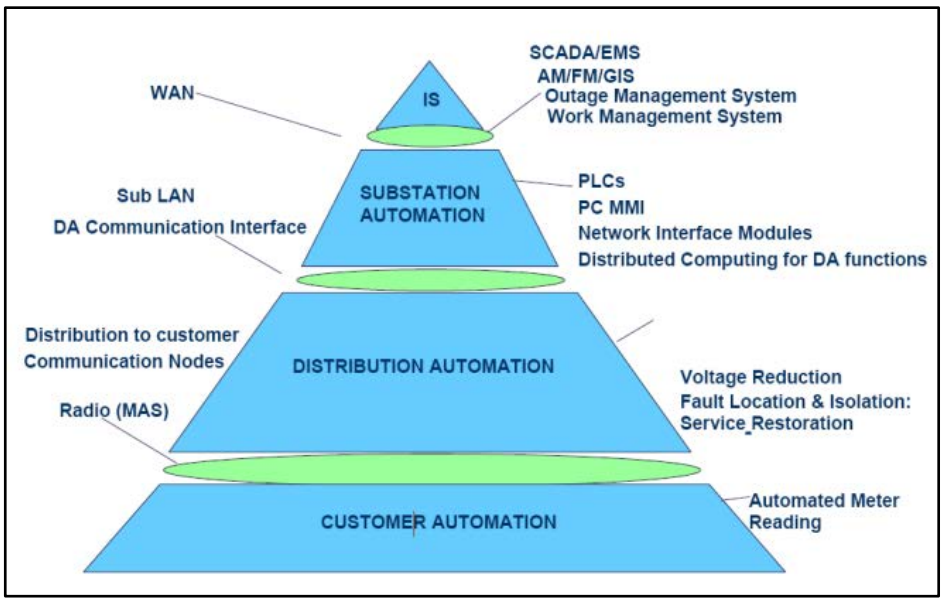

Figure 2.8: Automation functions pyramid (Bakhtiari and Frarahani, 2012)

- **Information system (IS):** The IS layer's primary functions include network planning and analysis, as well as information management. IS contains geographical information, component technical data, maintenance, statistics, and reporting.
- **Substation automation**: This layer addresses the control of circuit breakers in substations as well as IED communication.
- **Distribution automation**: This structure's function is to remotely operate and automate field equipment on the medium voltage system in real time.
- **Customer automation:** This layer's capabilities include automatic meter reading, load control, real-time pricing signalling, and automatic load connection and disconnection.

Distribution automation provides a number of capabilities and applications that can be deployed at various levels of the distribution system (Heidari, Fotuhi-firuzabad and Kazemi, 2015). As a result, automation has four primary functions: security, control, monitoring, and management. The protection function detects the problem, isolates it, and restores power to the network's healthy area. The control function, among other things, regulates transformer taps to provide a suitable voltage profile, load balancing,

and reactive power compensation. The monitoring function, among other things, keeps track of the condition of the distribution network switch position, protective actions, and analog data such as voltage, current, and power. To improve working efficiency and power quality, the management function employs sophisticated software to manage the equipment, user power supply, and outages (Zhou *et al.*, 2016). (Gruenemeyer, 1991) and (Markushevich, Herejk and Nielsen, 1994) classify Distribution automation categories into three types:

1. **Substation Automation:** DA at the substation includes:
    - Substation equipment such as bus voltage, circulating current, overload, load balancing, load tap changers (LTCs), and transformer protection such as fault isolation and transformer isolation are all controlled and monitored.
2. **Feeder Automation:** DA at the feeder include:
    - Automatic feeder switching and volt/Var control via voltage regulators and capacitor banks, and FDIR (Ruihua *et al.*, 2008). ***The aim of this thesis is on feeder automation, using FDIR method.***
3. **Customer Automation:** DA at the customer include:
    - Load control, real-time price signalling, reading meters remotely and billing, e.t.c

The thesis research work focused on feeder automation, but it is highlighted that substation automation and customer automation are interesting areas of investigation for future research. The following section of the review focuses into the feeder automation.

2.5.1 Review investigation on feeder automation

A comparative analysis of past research publications in the field of feeder automation was performed based on the research objective, network reconfiguration, load transfer, implementation, and system stability after load restoration. The comparison is shown in Table 2.3 below.

The most prevalent failure in overhead distribution networks is a line-to-ground fault with low or high impedance (Goryunov, Osipov and Dolgikh, 2016). The authors (Momoh,

Dias and Laird, 1997) proposed a fault diagnosis scheme for grounded or ungrounded distribution system designs. This approach detects, classifies, and locates fault states using an artificial neural network (ANN). For both grounded and ungrounded installations, the technique provides a tool for fault detection, feeder identification type, or phase classification. It lowers the number of false alarms and costs associated with physical fault location and feeder identification. (Teo and Gooi, 1998) developed a PC-based system that used artificial intelligence to diagnose faults and restore power to a linked distribution system. To restore power, the intelligence technique uses the condition of the post-fault network, tripped breakers, main protection alert, and conventional event. Authors (Souza *et al.*, 2001) described an ANN-based method for locating problems and categorizing alarms in a distribution system. The method has been evaluated in a seven-bus system and a Brazilian network, and it shows good discriminating capabilities as well as correct diagnosis of protection device failures, data loss, and alerts.

(Nagata *et al.*, 2005) suggested a multi-agent technique for restoring distribution system power. The approach employs a number of feeder and load agents. The feeder agents oversee the decision-making process, whereas the load agents represent the consumer loads. Using local data, the suggested technique can determine the target configuration and switching sequence. (Solanki, Sarika and Schulz, 2007) presented a multi-agent approach for exchanging information and determining an adequate power restoration strategy utilizing Java Agent Development as a framework. (Lin *et al.*, 2009) created an FDIR strategy for restoring electricity in a radial distribution network by utilizing a multi-agent-based distribution automation system. The authors (Bentarzi, Chafai, *et al.*, 2012) proposed a computer-based auto-recloser architecture that used a PC interfaced with an AD622 Acquisition card. The suggested framework obtains the real-time signal, processes it, and returns it to the system. It limits equipment damage, meets the principles and features of reclosers, and isolates damaged electrical network equipment as quickly as feasible.

(Zidan and El-Saadany, 2013) presented a service restoration genetic algorithm for the distribution system that prioritizes the most critical load, selects the lowest-cost restoration plan, maximizes restored loads, and reduces the projected number of switching operations. (Hussain, Choi and Lee, 2014) introduced a communication-based recloser method that uses recloser deadtime to reduce restoration time in smart

distribution systems. This approach begins the restoration procedure immediately after the recloser has completed two reclosing operations, presuming that a transient fault was cleared during the first two reclosing operations. (Saran and Fu, 2015) demonstrated an FDIR approach on a distribution system with and without distributed generators (DGs). To accomplish better fault isolation and restoration on the system, the technique used an overcurrent relay, fault locator, and sequential circuit breaker coordinator.

The theoretical aspects of FDIR in a distribution system are reviewed by the authors (Zidan *et al.*, 2017). The study discusses the technological, environmental, and economic challenges of distribution system self-healing. Authors (Konarski and Wegierek, 2018) reported an FDIR method that was implemented on an actual controlled short circuit test in a medium voltage overhead distribution system in mid-2018. Authors (Le *et al.*, 2018) developed a Fault, localization, isolation, and service restoration (FLISR) technique in late 2018 that uses signals from fault terminal units in conjunction with the status of the distribution network to swiftly discover and isolate the problematic area of the network.

To shorten service restoration time, the author (Parikh, Voloh and Mahony, 2013) suggested an FDIR method based on IEC 61850 GOOSE messages. The algorithm considers the capability constraints of the feeder, switches, and transformers. (Jamborsalamati *et al.*, 2015) implemented an IEC 61850 agent-based distributed FLSIR algorithm in a Real-Time Digital Simulator (RTDS) environment. The technique is tested in a generic radial distribution network with DGs and uses GOOSE messages to transmit status changes and pre-fault current measurements. The simulated results show the fault location, isolation of the faulty area, and power restoration of the network's healthy section via DGs. Furthermore, the results show that RTDS allows for the evaluation of the algorithm's time performance via an online dependability index computation. (Hoang, Tuan and Besanger, 2019) created a multiagent and IEC 61850 GOOSE-based fault location and isolation method for a PV-heavy distribution system. Local measurements are used in the designed technique, and fault direction data is transferred via IEC 61850 GOOSE messages. The design proves its ability to handle diverse fault scenarios while also reducing problem location and isolation time. (Habib, Fawzy and Brahma, 2020) proposed an IEC 61850 standard-based microgrid protection solution based on physical relays and hardware in the loop testing in an RTDS environment. The results show a

smooth data flow between physical relays and improved protection coordination. (Hong, Ishchenko and Kondabathini, 2021) suggested a fast FDIR (F-FDIR) technique for locating problematic sections of a microgrid system. In the loop test bench, the approach is tested and validated using genuine faults and errors scenarios utilizing real-time controller hardware. The test is performed with and without DGs, and it is shown to be resistant to potential communication and system failures.

Tables 2.3: Review comparative study on feeder automation.

Paper / Authors	Aim	Reconfiguration/ restoration using tie-switches, primary and secondary transformers or soft computing methods.	Load transfer capability using Manual/automatic with the aid of the SCADA and IEC61850 technology	Isolates/ restores power using either simulation/ lab-scale testing/ DSA	FDIR Stability analysis using either Parallel Transformers, tap-changers, Voltage-regulator, DGs
(Momoh, Dias and Laird, 1997)	To develop an artificial neural networks (ANN) integrated tool for fault diagnostics in both grounded and ungrounded distribution systems	The method utilized does not necessitate network reconfiguration.	There is no transfer of load. It's a hybrid ANN that's being employed. It collects data and uses it to validate results, reduce false alarms, and eliminate the need for manual defect detection and feeder identification.	This approach is compatible with Fortran and C programs simultaions, as well as the VMS operating system.	A transformer is stable and capable of carrying its load.
(Teo and Gooi, 1998)	Using artificial intelligence, develop a mechanism for problem diagnosis and power restoration for interconnected distribution networks.	Switching checks, restoration algorithms, and restoration procedures are utilized to recover the system..	The load is transmitted automatically. The intelligent approach makes advantage of the network post-fault state, tripped circuit breakers, protection alarms, and event log.	The lab-scale experiments were carried out using a PC-based distribution simulator.	The system's stability is maintained since the network is interconnected.
(Souza *et al.*, 2001)	To develop an ANN-based approach for detecting faults in an electrical power system.	The network has not been re-configured. It uses ANN classifiers to process alarms and fault locations.	There is no load transfer. The method is used generate real-time classifications and fault detection.	The ANN simulation method has been verified in a test system as well as a Brazilian system.	Because no reconfiguration is going place, the system does not show any stability issues.

(Nagata *et al.*, 2005)	To develop a multi technique using JAVA program for restoring electricity to distribution systems.	The system employs tie switches strategically placed to assist service restoration via feeder agents.	Sectionalizers are used to help in load transfer via feeder agents.	The developed methodis implemented using a computer and a JAVA software.	Transformers are employed to maintain stability following restoration.
(Solanki, Sarika and Schulz, 2007)	To implement an algorithm to provide fast restoration after a fault condition occurred in a distribution system	A multi-agent solution is used to restore power to loads via a switch agent.	Java program is used to facilitate load transfer among between agents.	Restore power using Java Agent development Framework (JADE) software	Generators are used to maintain stability after restoration. If overload occurs, the load is shed.
(Lin *et al.*, 2009)	Developed an FDIR for a distribution system following a contingency using a multi-agent-based technique.	-A section of a line that has become inoperable due to an upstream fault is restored by closing a tie switch between two supporting feeders; the main transformer must not be overloaded. -If the primary transformer becomes overloaded, the load is transferred to a secondary transformer. -If the main transformer becomes overloaded, the load is transferred to the supporting feeder if a large reserve is available. -The load is shed if the supporting feeder is overwhelmed.	Load transfer is carried out automatically by field agents via the SCADA system.	The FDIR model is validated using the JAVA Agent Development Framework (JADE) environment.	The load is transferred to supporting lines, supporting transformers, or load shedding to preserve stability.
(Zidan and El-Saadany, 2013)	To maintain stability, the load is moved to supporting lines,	The switching actions of sectionalizing tie	The load transfer approach is adaptable, with switches that can be	This load transfer procedure is emulated using	After load restoration, DGs are utilized to stabilize

	supporting transformers, or load shedding.	switches aid in service restoration.	operated. Influence of three differet types of switches was tested. Which are manually operated, partially automated, or fully automated.	computer software.	the system. When DG generation falls short of load demand, the load is shed.
(Saran and Fu, 2015)	To create an FDIR comparison tool for both active and passive distribution systems.	-There is no restoration in the passive distribution network. -The load is reconnected in the active distribution network by closing the circuit breaker to reconnect the healthy line and/or reconnecting DGs to the grid.	The designed algorithm automates load transfer.	On a Matlab-simulated distribution system, the FDIR technique is tested..	By integrating DGs to the grid, stability is maintained.
(Konarski and Wegierek, 2018)	Implementing a power restoration system to automate medium voltage distribution networks.	Sectional switches are used to restore load remotely.	Load transfer is carried out with the help of a SCADA technology that has been installed.	The proposed method is implemented using simulation software.	The transformer station ensures stability.
(Le *et al.*, 2018)	To design a Fault, Location, Isolation, and Service Restoration (FLISR) Scheme for the distribution system.	Restoration is accomplished by shutting the tie switch between adjacent feeders, assuming that the transformer is not overloaded following the restoration operation.	The proposed FLSIR technique restores power under fault conditions	The intended FLISR solution was carried out using E-Terra software, fault terminal units, reclosers, and overcurrent relays.	The usage of supporting transformers and supporting feeders ensures stability.
(Jamborsalamati *et al.*, 2015)	To develop an agent-based distributed FLSIR algorithm for a distribution system	Restoration is accomplished by closing the tie agents and utilizing the	To transmit load transfer status changes, the proposed approach uses the GOOSE protocol.	The proposed FLSIR algorithm is tested in an RTDS environment.	Transformers and DGs keep the system stable.

	in accordance with IEC 61850 standard.	GOOSE message from field agents.			
(Hoang, Tuan and Besanger, 2019)	To create a fault location and isolation approach for a photovoltaic distribution system that is multiagent and IEC 61850 GOOSE-based.	Load restoration is not available.	GOOSE Messages were utilized to facilitate load transferm fault location and isolation.	A Controller-Hardware-In-the-Loop facilitated the validation of the fault location and isolation technique (CHIL using RTDS).	No restoration taking place
(Habib, Fawzy and Brahma, 2020)	To design a microgrid protection strategy based on the IEC 61850 standard utilizing physical relays.	Load restoration is not available.	There is no load trasbfer What about	RTDS and physical relays are used to simulate a closed-loop test environment.	The distributed generation devices are employed to keep the system running in the event of a fault.
(Hong, Ishchenko and Kondabathini, 2021)	To design a self-healing microgrid utilizing IEC 61850 communication.	To restore power to healthy sections of the network once a problematic component has been disconnected, network controllers or field devices must first assess if the subsystem's total DER generation exceeds the total load; if so, the DER will support its load within the subsystem. If this is not possible, some of the load may be shifted to a possible subsystem, or local load shedding may be considered.	Load transfer is automated using IEC 61850 GOOSE messages and is controlled remotely using network controllers via the SCADA system.	The tests were run in real time with Hardware in the loop simulations.	The system's stability was maintained by the usage of DERs. Load is shed when DER generation is less than load demand.

2.5.2 Fault Detection Isolation and Restoration (FDIR)

To allow load transfer between feeders, traditional distribution networks use usually closed and normally open tie switches to interconnect feeders. If a problem is discovered, it should be located and isolated as soon as possible. The restoration operation then begins by switching impacted customers to the healthy feeder via tie switches, restoring power to them beyond the defective section. Without jeopardizing the switching operation or engineering limits, the restoration plan should be able to decrease the number of customers affected to the smallest amount practicable (Skoonpong and Sirisumrannukul, 2008). The critical function of fault detection, isolation, and restoration is to automatically restore power to clients who have been cut off. The majority of distribution networks are not fully automated at this time (Zidan and El-Saadany, 2012). Instead of automatically returning power to clients, field engineers must manually restore electricity. The following issues confront human operations (Chow, Taylor and Chow, 1996) and (Zidan *et al.*, 2017):

- Complexity and size of the restoration process
- The unreliable human operation, especially in bad weather conditions, at night and over weekends
- Manual power restoration takes more time than an automated system

Distribution automation reduces outage time and improves reliability indices. When a radial distribution network fails, the substation feeder often trips the entire feeder, forcing all customers on that feeder to lose power. These customers include residential districts, hospitals, industrial areas, and corporate places, among others. Figure 2.9 displays a distribution system restoration scenario without the usage of FDIR software. As illustrated in Figure 2.10, the fault management strategy typically takes three to four hours per outage.

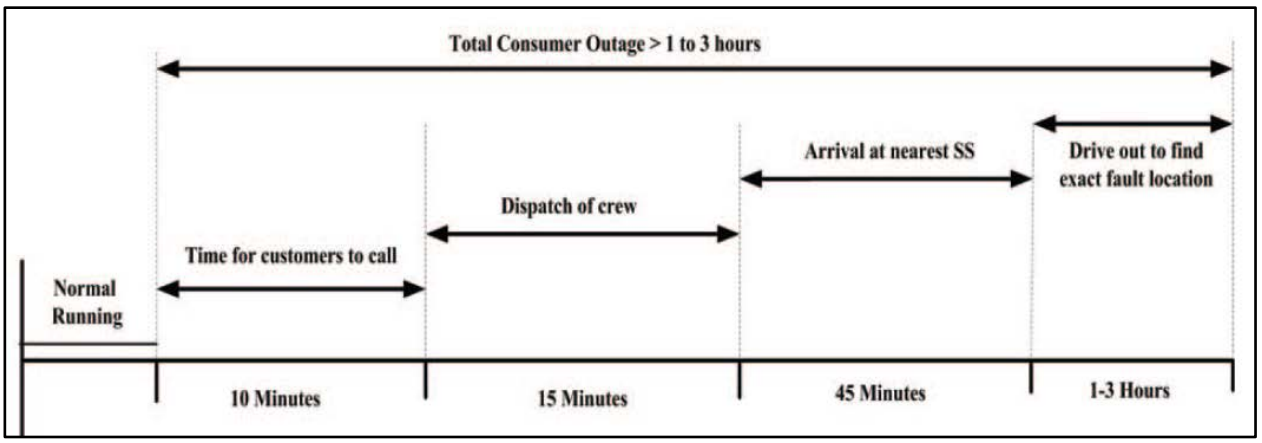

Figure 2.9: Fault management process without FDIR implementation (Parikh, Voloh and Mahony, 2013)

It should be emphasized that the time frame represented in Figure 2.10 is an estimate for analysis purposes only. When FDIR is not employed, the outage time increases, as illustrated in Figure 2.10. Many factors, such as the capacity of a backup feeder, the number of switching devices in the system, the number of manual switching devices, and so on, can affect outage time. Figure 2.11 depicts a scenario in which FDIR is used.

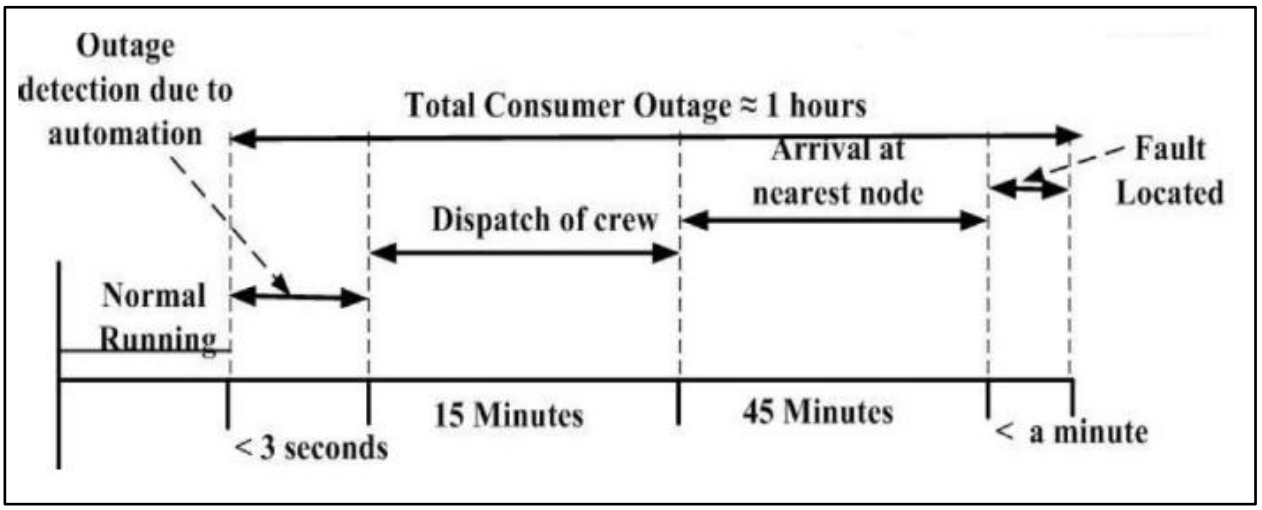

Figure 2.10: Fault management process with FDIR implementation (Parikh, Voloh and Mahony, 2013)

It should be noted that the time frame represented in Figure 2.11 is an estimate for analysis purposes only. In this case, it is determined that FDIR deployment can reduce outage time to approximately one hour per outage.

The author (Aguero, 2012) classified FDIR benefits into two categories: functional benefits and transitory benefits.

The following are some of the functional advantages:

- Indicators of reliability are being improved.
- Reduce the amount of energy that is not given.
- Provide the highest level of service possible.
- Reduce the time it takes to investigate the fault

The following are some of the immediate advantages:

- Increased income
- Reduce the cost of an outage to the client.
- Labor and vehicle cost savings
- Obtain regulatory benefits (when available)

FDIR can be divided into the following three architectures (Zidan and El-Saadany, 2012), (Shahin, 2013) and (Zidan *et al.*, 2017):

1. Centralized FDIR (C-FDIR)
2. De-Centralized FDIR (DC-FDIR)
3. Distributed FDIR (D-FDIR)

These architectures are illustrated in Figure 2.11 below (Valtari and Verho, 2011):

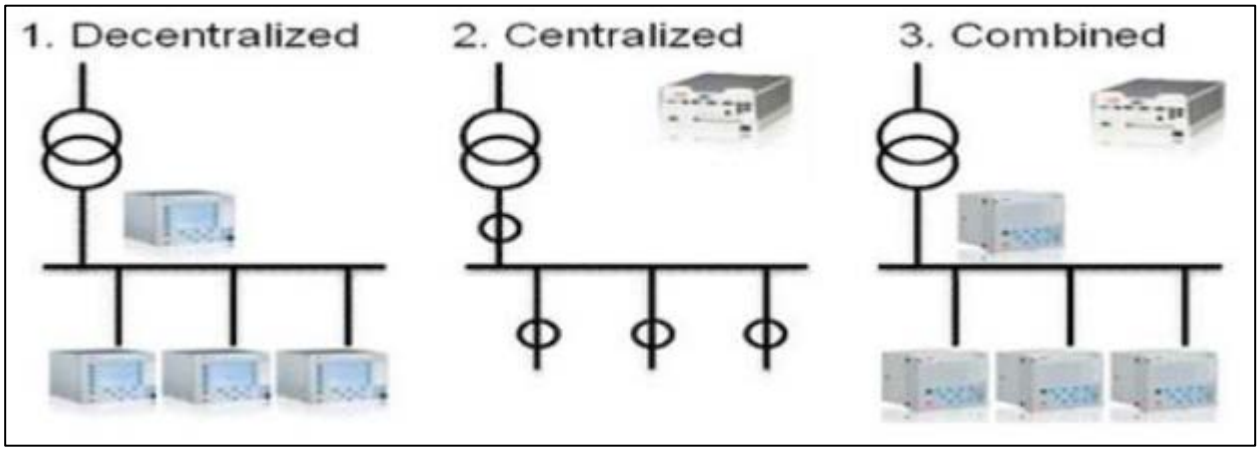

Figure 2.11: Possible architectures (Valtari and Verho, 2011)

In a centralized architecture, the control center receives all data from secondary substation devices and delivers the command to isolate the faulty portion (Zidan *et al.*,

2017). Using SCADA-enabled switches and sensors/IEDs strategically placed across the network, this architecture may be utilized to identify and locate the problematic area, isolate the fault, and restore power to the unaffected part of the distribution network. Every controlling device must communicate with the control center directly. A high-bandwidth communication network and exact load model information, on the other hand, maybe necessary. It may take longer to automate the entire process if you choose a centralized approach (Parikh, Voloh and Mahony, 2013). A centralized strategy could be subject to a single point of failure (Zidan *et al.*, 2017). If, for example, a central controller fails, the entire system fails.

At the substation level, a decentralized design is implemented. This design is built on monitoring devices communicating directly with one another. Local data is collected using intelligent sensors/IEDs, while remote data is collected through peer-to-peer connectivity with other controllers. IEDs handle data locally in the Decentralized method, therefore there is no need for a centralized station (Shahin, 2013). A communication network should be used to connect the remote input/output modules at each switch/recloser position to the distribution substation automation device. In comparison to a centralized system, a decentralized system is speedier and requires less bandwidth (Parikh, Voloh and Mahony, 2013). Each station exchanges its data with a neighboring substation to reorganize the network during power outages or faults.

Distributed architecture is widely used in large networks (Zidan *et al.*, 2017). A controlled device is present at every switch/recloser site in this architecture. These devices communicate with one another to detect the location of the fault and determine the best strategy to restore power. Because the IEDs (controllers) are dispersed throughout the network, IEC 61850-based GOOSE communication is the best solution for this architecture. This strategy necessitates the use of a controller rather than input/output units at each switching position (Parikh, Voloh and Mahony, 2013). This thesis focuses on a networked architecture that use GOOSE messages based on the IEC 61850 standard.

The recloser protection function simulated and tested in Chapter 6, section 6.10 employed ANSI code 51PT, and its equivalent IEC 61850 logical node (P51PTOC1) enabled distribution automation at the bay level. Other network subscribers may be able to subscribe to such data sets and execute distribution automation, which includes protection, automation, control, and monitoring.

2.6 Conclusion

This chapter examines into the literature review on distribution system protection in depth. The investigations include radial, ring, and mesh network topologies, as well as protection devices such as overcurrent relays, reclosers, fuses, sectionalizers, and coordination. The chapter gives detailed information on reliability measures based on the evaluated various indicators, as well as its economic implications for operation, maintenance, and providing continuity of supply to consumers. The distribution automation process, including feeder automation and FDIR, is thoroughly examined.

The following chapter explores into the mathematical components of fault types, reliability indices, and recloser control methods, as well as a broad overview of the IEC 61850 standard.

CHAPTER THREE

THEORY OF DISTRIBUTION SYSTEM FAULTS, RELOSER CONTROL, RELIABILITY INDEXES, AND THE IEC 61850 STANDARD

3.1 Introduction

Electrical failures can occur in the distribution system network in two ways: transient and permanent. These problems generate network disruptions, which have an impact on power distribution to customers. The protection system must be both rapid and dependable. The distribution system is protected with relays, reclosers, sectionalizers, and fuses, among other devices. These protection devices are linked together in such a way that the device closest to the fault is activated first, followed by an upstream device. This method ensures that as few customers as possible are affected by the service disruption.

The IEC 61850 standard for substation communication speeds up access to information on IEDs and improves device coordination. The IEC 61850 standard improves the protection and control of equipment in substations by allowing IEDs from various suppliers to communicate with one another. The IEC 61850 standard includes communication (Station Bus) between IEDs for monitoring, protection, and control, which replaces traditional hardwiring between IEDs and hardwiring from instrument transformers to IEDs (process bus).

The following is the content of this chapter: The overview of distribution system faults is covered in section 3.2, while the reclosing relay operating curves and coordination are described in sections 3.3 and 3.4, respectively. Recloser application in distribution system and principles settings are presented in section 3.5, and distribution system reliability measures are discussed in section 3.6. Section 3.7 discusses the IEC 61850 automation architecture, and section 3.8 concludes the chapter.

3.2 Distribution system feeder faults

In most cases, a distribution system is a three-phase balanced symmetrical network. When a network has defects, the symmetry is generally broken, resulting in an imbalanced current and voltage flow. Unsymmetrical faults are most commonly seen between phases or phase/(s)-to-ground, as listed below:

- Single line-to-ground fault (LG).
- Line-to-line fault (LL).
- Double Line-to-ground fault (LLG).

Single-phase representation is used to determine three-phase balanced faults. Because the magnitude and displacement between the phases are the same, symmetrical faults are considered unique. The following are examples of symmetrical faults:

- Three-phase short circuit fault (LLL).
- Three-phase-to-ground fault (LLLG).

The symmetrical component approach is used to investigate symmetrical and unsymmetrical faults by replacing the usual system sources with a supply source at the fault location (Grainger, 1999). In order to establish whether the fault must be cleared by discrimination or not, the boundary values of current at any relaying point must also be known. At the relaying point, the following information is required for each type of fault (Alstom Grid, 2011):

- Maximum fault current
- Minimum fault current
- Maximum throughout fault current

3.2.1 Three-phase symmetrical component

The most prevalent type of fault in low-voltage networks is a single-phase to earth fault, which can result in far higher fault current than three-phase faults. It is necessary to develop a system for analyzing faults that are imbalanced. Any common three-phase system can be described by three sets of balanced symmetrical vectors using the "principle of superposition" (Alstom Grid, 2011).

Two symmetrical vectors, known as positive and negative sequence vectors, are balanced but have opposite phase shifts, while a third symmetrical vector, known as zero sequence component, is balanced but has no phase shift between the phases. When a fault occurs in a balanced three-phase network, the negative and zero sequence vectors are uncoupled, leaving only a positive sequence fault current. In a balanced network, the

sequence vectors are interconnected at the fault position when the fault is unsymmetrical (Glover, Sarma and Overbye, 2012).

Superscripts 1, 2, and 0 are used to signify positive, negative, and zero sequence vectors, respectively. Dr. C.L. Fortescue introduced the symmetrical components approach in 1918. According to his theory, a three-phase system's unbalanced phasors can be resolved into three balanced phasor systems as follows (Saadat, 1999):

- A collection of balanced three-phase components with phase orders a, b, and c make up positive sequence components.
- A collection of balanced three-phase components with phase orders a, c, and b make up negative sequence components.
- Components in the zero-sequence are made up of three single-phase components with the same magnitude but zero phase angles.

For a three-phase system, phase voltages and symmetrical components in terms of the unbalanced voltages are represented in Equations 3.1 and 3.2, respectively.

$$\begin{aligned} V_a &= V_a^0 + V_a^1 + V_a^2 \\ V_b &= V_b^0 + V_b^1 + V_b^2 \\ V_c &= V_c^0 + \alpha\, V_c^1 + V_c^2 \end{aligned} \tag{3.1}$$

$$\begin{aligned} V_a^0 &= \frac{1}{3}(V_a + V_b + V_c) \\ V_a^1 &= \frac{1}{3}(V_a + \alpha V_b + \alpha^2 V_c) \\ V_a^2 &= \frac{1}{3}(V_a + \alpha^2 V_b + \alpha V_c) \end{aligned} \tag{3.2}$$

Where:

V_a is a phase a no-load voltage

V_b is phase b no-load voltage

V_c is phase c no-load voltage

α is phase angle at 120 degrees

α^2 is phase angle at 240 degrees

V_a^0, V_b^0, V_c^0 represents voltages for zero sequence components.

V_a^1, V_b^1 , V_c^1 represents voltages for positive sequence components.

V_a^2, V_b^2 , V_c^2 represents voltages for negative sequence components.

Similarly, the current in the power system network is given in equations 3.3 and 3.4 respectively

$$\begin{aligned} I_a &= I_a^0 + I_a^1 + I_a^2 \\ I_b &= I_a^0 + \alpha^2 I_a^1 + \alpha I_a^2 \\ I_c &= I_a^0 + \alpha I_a^1 + \alpha^2 I_a^2 \end{aligned} \tag{3.3}$$

$$\begin{aligned} I_a^0 &= \frac{1}{3}(I_a + I_b + I_c) \\ I_a^1 &= \frac{1}{3}(I_a + \alpha I_b + \alpha^2 I_c) \\ I_a^2 &= \frac{1}{3}(I_a + \alpha^2 I_b + \alpha I_c) \end{aligned} \tag{3.4}$$

Where:

I_a is phase A current

I_b is phase B current

I_c is Phase C current

I_a^1 , I_a^2, I_a^0 represents phase currents for positive, negative, and zero sequence components for phase A, respectively.

The three-phase apparent power in terms of symmetrical components may be expressed as follows:

$$S = 3(V_a^0 I_a^0 + V_a^1 I_a^1 + V_a^2 I_a^2) \tag{3.5}$$

Figures 3.1 to 3.4. provides the following unsymmetrical faults Single phase to ground fault

- Phase to phase fault
- Phase to phase to ground fault
- Three-phase to ground fault

The above formulas are used to calculate three-phase fault applied in the considered distribution system and its simulation results are presented in section 4.6 of Chapter 4.

3.2.1.1 Single-phase to ground fault

A single-phase to ground fault is shown in Figure 3.1. consider a single line to ground fault occurs in phase A as shown below. Assuming that the system is at no load, the boundary conditions for this fault type are represented as $\bar{V}a$ = 0, $\bar{I}b$ = 0 , $\bar{I}c$ = 0.

For symmetrical components, the currents can be deduced as shown in equation 3.6 below:

$$I_a^0 = I_a^1 = I_a^2 = \frac{\bar{V}a}{\bar{Z}1 + \bar{Z}2 + \bar{Z}0} \qquad (3.6)$$

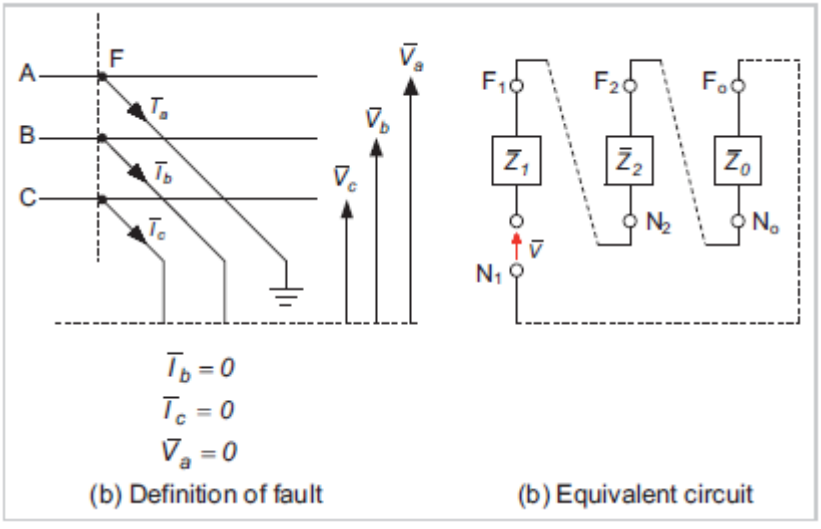

Figure 3.1: Single-phase to ground fault (Alstom Grid, 2011)

Where:

$\bar{V}a$ is the no-load voltage for phase A

$\bar{Z}1$ is the positive sequence impedance

$\bar{Z}2$ is the negative sequence impedance

$\bar{Z}0$ is the zero sequence impedance

The above formula is used to calculate the three-phase fault applied in the considered distribution system and its simulation results are presented in section 4.6 of Chapter 4.

3.2.1.2 Phase to phase fault.

When there is a short circuit between any two phases, the phase to phase fault occurs. A short circuit between phases B and C is shown in Figure 3.2 below as a fault state. The boundary conditions for this fault site are stated as, assuming the system is not loaded. $\bar{I}a = 0$, $\bar{I}b = -\bar{I}c$, $\bar{V}b = V_c$ and:

$$I_a^1 = \frac{\bar{V}a}{\bar{Z}1 + \bar{Z}2} = -I_a^2 \tag{3.7}$$

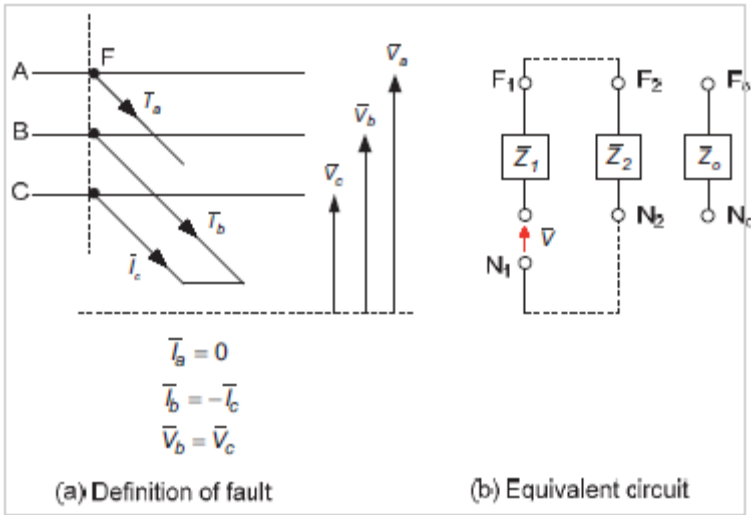

Figure 3.2: Phase to phase fault (Alstom Grid, 2011)

For a phase to phase fault as illustrated in Figure 3.2, Positive sequence and negative sequence components are involved. This means when a short circuit occurs between phases, and the ground is not involved, there will be no current flowing to the ground. Zero sequence components only get involved when there is a ground fault.

3.2.1.3 Phase to phase to ground fault

When there is a short circuit between two phases and ground, it is known as a phase to phase to ground fault. A short circuit on phase B and phase C through ground as shown in Figure 3.3 as a fault state. . Assuming that the system is at no load, the boundary conditions for this fault point are represented as $\bar{I}a$ = 0, $\bar{V}b = \bar{V}c$, = 0 and:

$$I_a^1 = \frac{\bar{V}a}{\bar{Z}1 + \frac{\bar{Z}0 \times \bar{Z}2}{\bar{Z}0 + \bar{Z}2}} \tag{3.8}$$

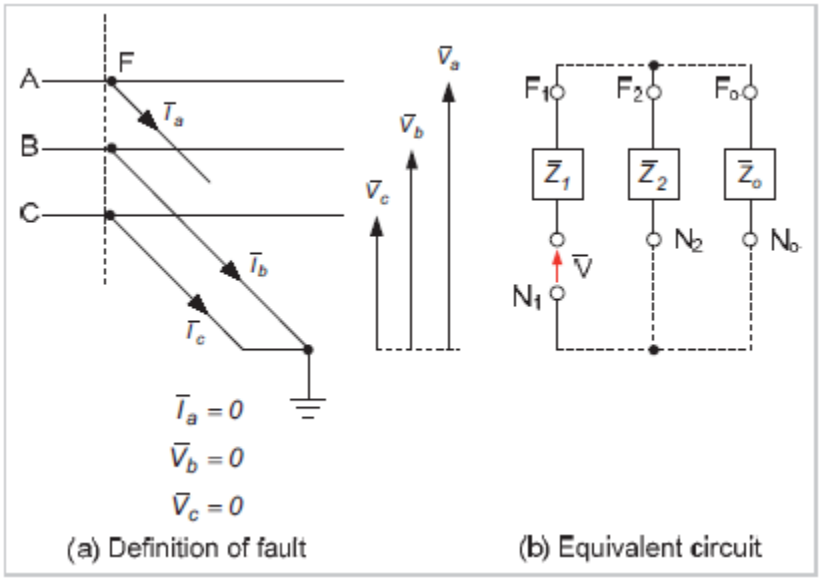

Figure 3.3: Phase to phase to ground fault (Alstom Grid, 2011)

3.2.1.4 Three-phase to ground fault

Three-phase to ground fault occurs when a short circuit between three-phase through ground, as illustrated in Figure 3.4. The boundary factors for this fault are represented as $\bar{I}a = \bar{I}b = \bar{I}c \neq 0$ and $\bar{V}a = \bar{V}b = \bar{V}c = 0$.

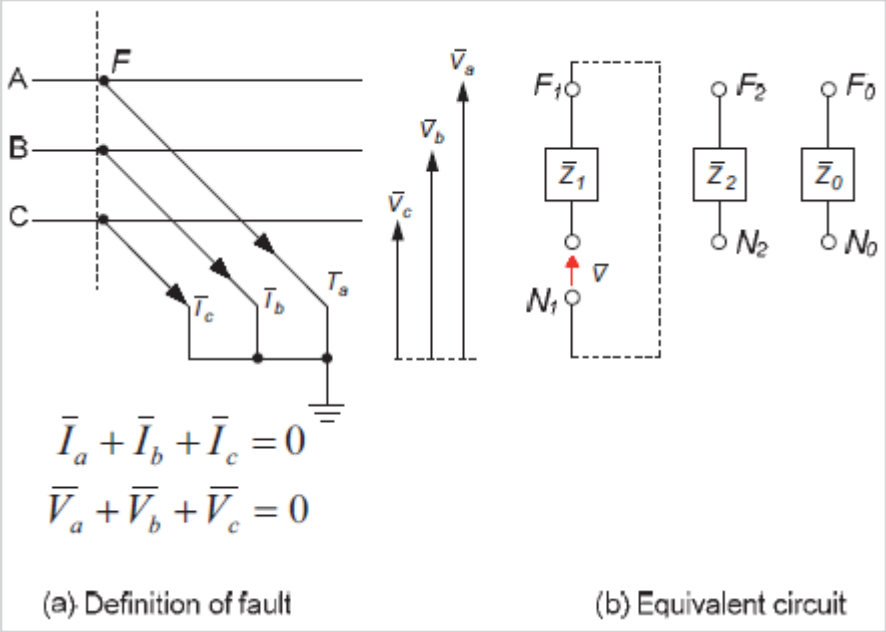

Figure 3.4: Three-phase to ground fault (Alstom Grid, 2011)

3.2.2 IEC 60909 short circuit calculations

Short circuits pose a substantial threat to electrical distribution system components and are a major problem when designing and implementing system protection. The current generated by a short circuit has the potential to harm or shorten the life of power system components. As a result, short circuit analysis is critical for planning the design and operation of a power system. The following are the main reasons for short circuit analysis (Weedy, 2012):

- To determine the magnitude of fault current and voltage on busbars during fault conditions
- To determine the circuit breaker's rated interrupting capacity
- To determine the relay settings
- Determination of unsymmetrical fault currents for single-phase faults, double phase to earth faults, phase to phase faults, and open circuit faults.
- Determination of minimum and maximum three-phase fault current.

The short circuit simulations are covered in chapter 4, section 4.4 of this thesis. The three-phase short circuit current $I_{k1}^{"}$, double phase short circuit current $I_{k2}^{"}$, single phase

to earth short circuit current $I_{kl}^{"}$ and the peak short circuit current I_p are simulated and taken into consideration. The minimum and maximum short circuit current are calculated using IEC 60909 standard. The equations for short circuit currents mentioned above and short circuit apparent power can be represented as shown from equations 3.9 to 3.14, respectively (IEC standard 60909, 2001).

$$I_{k1}^{"} = \frac{cV_n}{\sqrt{3}Z_k} \tag{3.9}$$

$$I_{k2}^{"} = \frac{\sqrt{3}}{2} I_{k1}^{"} \tag{3.10}$$

$$I_{kl}^{"} = \frac{\sqrt{3}cV_n}{\bar{Z}1 + \bar{Z}1 + \bar{Z}0} \tag{3.11}$$

$$k = 1.02 + 0.98e^{-3R/X} \tag{3.12}$$

$$I_p = k \times \sqrt{2} I_{k1}^{"} \tag{3.13}$$

$$S_k^{"} = \sqrt{3} I_{k1}^{"} V_n \tag{3.14}$$

Where:

$I_{k1}^{"}$ is the three-phase initial symmetrical short circuit current

$I_{k2}^{"}$ is the two-phase initial symmetrical short circuit current

$I_{kl}^{"}$ is the single-phase initial symmetrical short circuit current

c is the nominal voltage factor

V_n is the nominal voltage at the location of the fault

Z_k is the equivalent short circuit impedance

I_p is the peak short circuit current

DIgSILENT simulation calculated the fault current using the above equations (3.9) to (3.14), and the simulation results are presented in Chapter 4.6 for the various case studies considered.

3.3 Reclosing relay operating curves

Overcurrent protection is typically used to protect distribution system feeders. Overcurrent protection is made up of three primary components, each of which serves a

different purpose in the distribution system. Instrument transformers, also known as Current Transformers (CTs) and Voltage Transformers (VTs), are the first components. They step down high current and voltage magnitudes to detectable values. A relay is the second component, and a circuit breaker is the third (CB). When the current flowing through the relay exceeds the relay's setting, the relay sends a trip signal to the circuit breaker, which causes the circuit breaker's contacts to open, clearing the fault. The three overcurrent protection components are shown in Figure 3.5, which is an SLD of the distribution system feeder (CT, CB, and relay). on every feeder Overcurrent protection is mostly employed in the event of a short circuit.

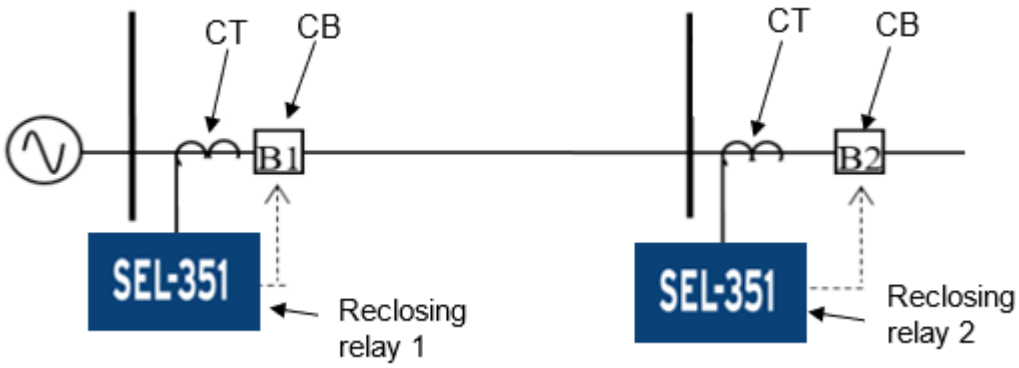

Figure 3.5: Distribution system feeder overcurrent protection

Overcurrent relays can be categorized into three groups namely, definite or instantaneous current characteristics, definite time characteristics, and inverse time characteristics. The relay characteristics curves and behavior are explained in the following subsections.

3.3.1 Definite current reclosing relays

When the measured current exceeds the preset current magnitude, the definite current relay activates instantly. The setting of the downstream relay controlling circuit breaker 2 (B2) in the radial distribution system depicted in Figure 3.5 is chosen so that it works first since it is further away from the source. This signifies that the downstream relay is only activated when the current magnitude is low. As the relay gets closer to the power source, the operational currents gradually increase. The fault is disconnected first by the relay with the lowest current setting. The definite time characteristic curve is depicted in Figure 3.6.

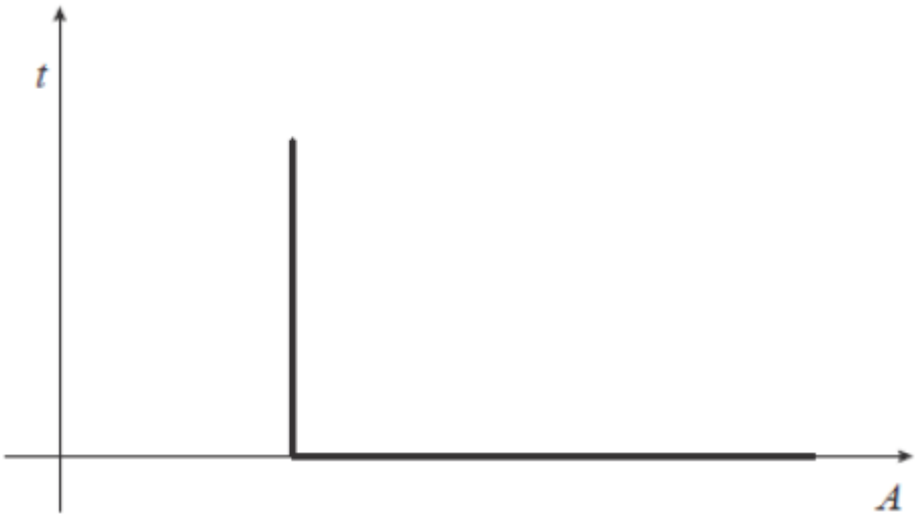

Figure 3.6: Definite current Overcurrent relay characteristic

3.3.2 Definite time reclosing relays

If the current flowing through the relay exceeds the preset value, definite time relays function after a defined amount of time. The settings for definite time relays can be designed so that the relay closest to the fault functions in a shorter time. The relay upstream of the source, on the other hand, takes longer to operate. If a defect occurs below the reclosing relay two in Figure 3.5, both relays will detect the problem. To isolate the fault, Relay 2 is activated first. In the event that Relay 2 fails to operate, Relay 1 operates after a certain time delay. The discrimination margin is the difference in operating time between the downstream and upstream relays. The definite time overcurrent relay characteristic is shown in Figure 3.7.

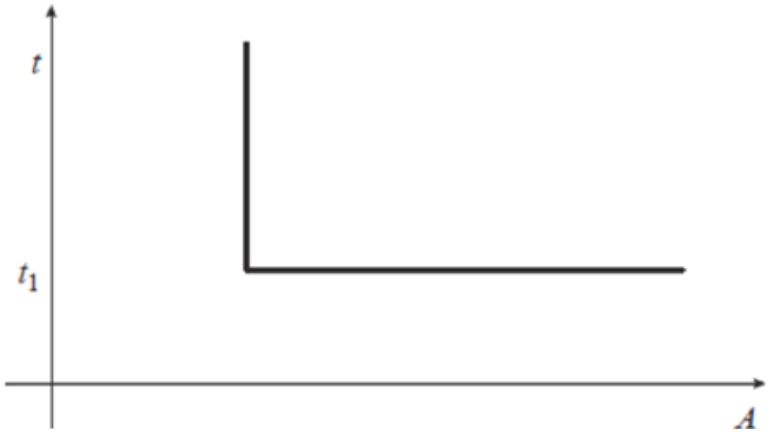

Figure 3.7: Definite time Overcurrent relay characteristic

3.3.3 Inverse time reclosing relays

As shown in Figure 3.8 characteristic curve, inverse time is inversely related to fault current amplitude. When a very high fault current is detected, this form of curve has the advantage of allowing for a faster tripping time without losing protection sensitivity. Inverse Definite Minimum Time is a combination of definite current and inverse time (IDMT). IDMT has the benefit of current discrimination and a decent time frame. An IDMT relay characteristic curve is shown in Figure 3.9.

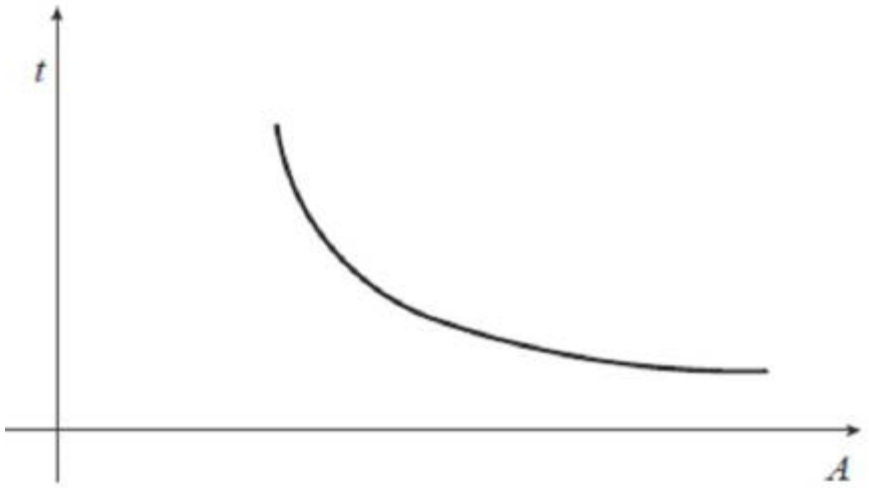

Figure 3.8: Inverse time overcurrent relay characteristic

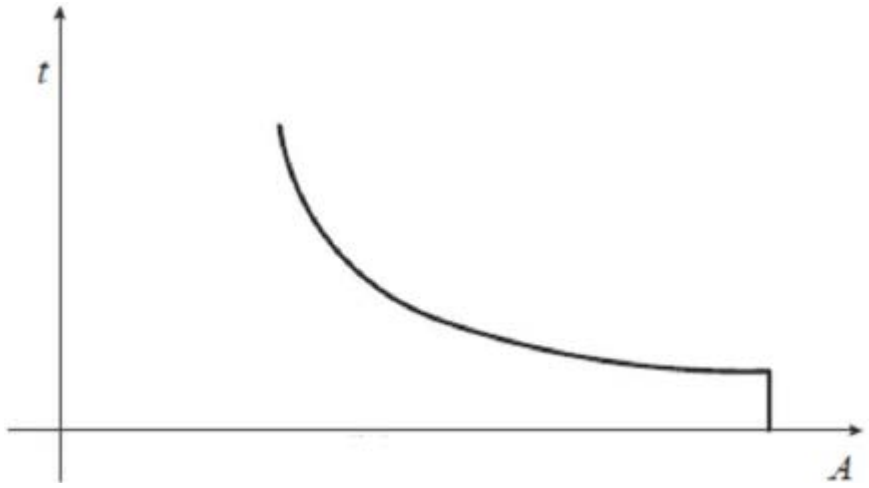

Figure 3.9: Inverse time with Instantaneous overcurrent relay characteristic

In chapter 4, the inverse time and IDMT characteristics curves are used. The IDMT curve was utilized for phase overcurrent elements at feeder A and feeder B, and the inverse time characteristic was employed for ground overcurrent elements. Both phase and

ground overcurrent components are designed with inverse time overcurrent in the downstream reclosing relays.

3.4 Reclosing relay grading principles

The protective principles utilized in the distribution system have an impact on the working speed, reliability, sensitivity, and selectivity. If the protective response is speedier, hazardous activities and damage to protected electrical equipment will be reduced. Furthermore, this assists in limiting the number of power outages to the lowest possible area of the network and provides a better understanding of the specific network segment that is troublesome (ABB, 2011). The following are examples of grading protection techniques: (Wright and Christopoulos, 1999).

- Current grading
- Time grading
- Time and current grading

3.4.1 Time grading

As demonstrated in section 4.6 of Chapter 4, this thesis used the time grading approach. The time-graded technique reclosers are coordinated so that the recloser nearest to the fault is the first to operate. The time grading principle is coordinated in such a way that the upstream recloser's tripping time is long enough that it does not send a tripping signal to its circuit breaker until the fault relay functions. An overcurrent reclosing relay with either definite time or inverse time characteristics is used to implement this theory. The time it takes for definite time relays to operate is unaffected by the size of the fault current. The larger the fault current magnitude, the shorter the operating duration in inverse time reclosing relays. Radial distribution networks are well served by inverse and definite time concepts. Overcurrent protection relays have four inverse time-current curves in general. The inverse time overcurrent relays curves are as follows, according to IEC 60255-151:

- Normal inverse
- Long-time inverse
- Very inverse

- Extremely inverse

In this chapter, the normal inverse curve is chosen for the simulation investigation. The grading margin is the maximum time allowed between the operation of two neighboring relays to provide correct discrimination. When overcurrent relays are not appropriately graded, multiple relays may function for the same fault, making pinpointing the specific site of the problem more difficult. This would result in unnecessarily lost supply to customers that aren't connected to the segment of the network that isn't affected (Alstom Grid, 2011). The following factors influence the grading margin:

- Circuit breaker interruption time
- Timing error of the relay
- Overshoot time of the relay
- CT error
- The final margin on completion of the operation

Typical timing errors for different relay technologies are tabulated in Table 3.1 below.

Table 3.1: Typical relay timing errors with standard IDMT (Alstom Grid, 2011).

	Overcurrent Relay/ Recloser controller			
	Electro-mechanical	Static	Digital	Numerical
Timing error (%)	7.5	5	5	5
Overshoot time (s)	0.05	0.03	0.02	0.02
Safety margin (s)	0.1	0.05	0.03	0.03
Overall grading margin – relay to relay(s)	0.4	0.35	0.3	0.3

The minimum grading time interval, " t' ", can be calculated using equation 3.15 below:

$$t' = \left(\frac{2E_R + E_{CT}}{100}\right)t + t_{CB} + t_o + t_s \quad (3.15)$$

Where:

E_R = relay or recloser timing error (IEC60255-4)

E_{CT} = CT ratio error (%)

t = operating time of relay or recloser closer to fault location (s)

t_{CB} = circuit breaker interrupting time (s)

t_o = relay or recloser overshoot time (s)

t_s = safety margin (s)

In instances where an overcurrent relay has an independent definite time-delay protection delay, the CT error is neglected. Therefore, the minimum grading time interval, t', can be calculated as follows:

$$t' = (\frac{2E_R}{100})t + t_{CB} + t_o + t_s \quad (3.16)$$

Since the virtual DIgSILENT version of digital relays is employed in Chapter 4, the grading margin used in this thesis is 0.3 seconds. This signifies that the upstream relay activates 0.3 seconds after the downstream relay.

3.4.2 Reclosing relay operating time

The relay operating time is defined by IEC 60255 and IEEE C37.112 and is given in Equation 3.17 below.

$$T_p = TMS \times \frac{\beta}{\left(\frac{I}{I_s}\right)^{\alpha} - 1} \quad (3.17)$$

Where:

T_p is the operating time of a relay

TMS is the multiplier setting

I is the current detected by the relay

I_s is current setting

α and β are slope constants

The slope constant defined by IEC 60255 and IEEE C37.112 is tabulated in Table 3.2. The pickup currents are determined using IEEE Guide for Protective Relay Applications to Distribution Lines.

Table 3. 2: Slope constants for IEEE and IEC inverse overcurrent relay characteristic curves (IEEE C37.112, 2018) and (IEC 60255, 2009)

IDMT curve description	Standard	α	β
Moderately inverse	IEEE	0.02	0.0515
Very inverse	IEEE	2	19.61
Extremely inverse	IEEE	2	28.2
Inverse	US-CO8	2	5.95
Short-time inverse	US-CO2	0.02	0.02394
Standard inverse	IEC	0.02	0.14
Very inverse	IEC	1	13.5
Extremely inverse	IEC	2	80.0
Long-time inverse	IEC	1	120

3.5 General overview of the auto-reclosers and its configuration settings

This section of the chapter gives an overview of auto-reclosers and their applications in distribution networks, while section 3.5.2 provides an overview of the number of reclosing attempts, deadtime, reclaim time, auto-reclosing reset time, and auto-reclosing-lockout.

3.5.1 Recloser application on the distribution system

A recloser is an electrical device designed primarily for overcurrent protection in secondary distribution systems that can detect, interrupt, and reclose under fault situations. An auto recloser is defined as a switching device, a controlling unit, and sensors for current and/or voltage signals (IEC 62271-111, 2012). When a fault condition

arises, the recloser disturbs the circuit by opening its circuit breaker for a predetermined open interval before automatically reclosing to reenergize the line. If the problem persists, the recloser will reclose for a predetermined number of shots before locking out. Reclosers are normally designed to have three open and close operations, followed by a lockout sequence on the final open and close operations. According to distribution system studies (IEC 62271-111, 2012), 70 to 80 percent of failures occur temporarily. Reclosers were created in the 1940s to address the lack of coordination in fuse operation, which results in a permanent suspension of supply even when no permanent fault exists (IEC 62271-111, 2012).

Reclosers come standard with three operating time/current characteristic curves. One of the curves is fast, while the other two are slower (Bentarzi, Chafai, *et al.*, 2012) and (Motoki *et al.*, 2015), and (Gers, 2004). Figure 3.10 is a standard illustration of the time/current characteristic curve for reclosers. The letter A represents a faster curve, while the letters B and C represent delayed curves.

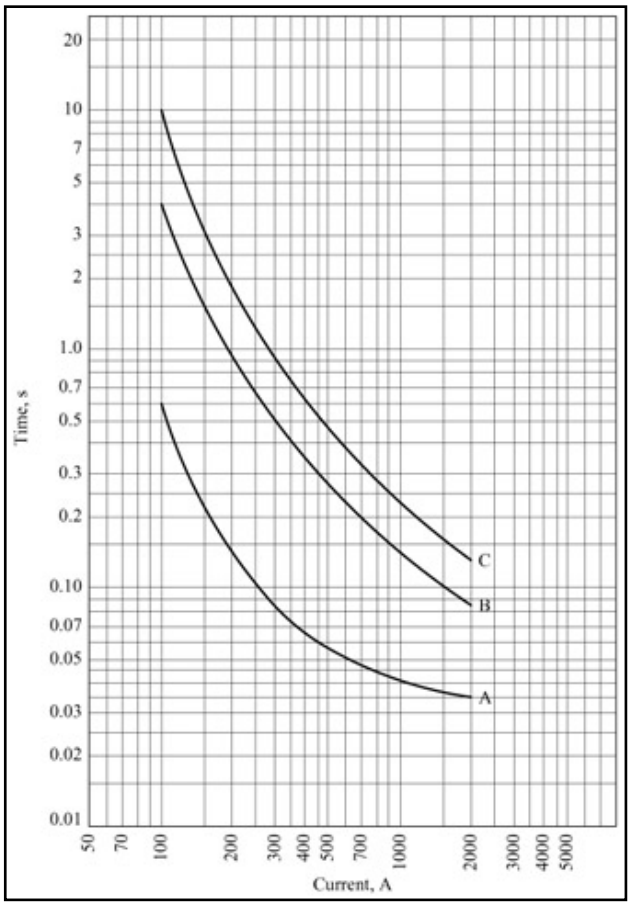

Figure 3.10: Recloser time/current curves (Hosseinzadeh, 2008)

A typical auto-reclose procedure is seen in Figure 3.11. This is a recurring fault sequence. To clear a momentary issue, the first shot on the far left was taken in instantaneous mode. The three shots that follow operate in a timed sequence using pre-programmed timing settings. When a permanent problem is discovered, the time delay function opens the protective devices closest to the fault, preventing the entire network from being disconnected.

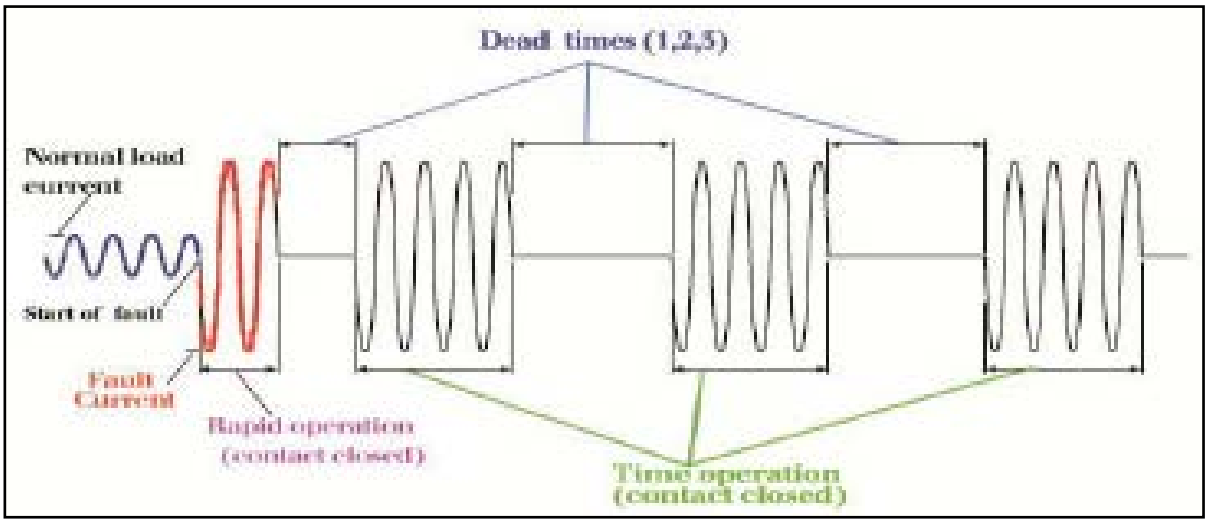

Figure 3.11: Typical recloser operation sequence (Bentarzi, Chafai, et al., 2012)

Reclosers use parameters such as deadtime, reclaim time, the number of reclosing tries, auto-reclosing reset time, and auto reclosing-lockout, as shown in Figure 3.11. These parameters are discussed in detail in the next section.

3.5.2 Principles of auto-reclosing settings

The main protection parameters and settings for auto-reclose schemes are defined by IEEE Std C37.104-2012 Guide for automatic reclosing of circuit breakers for AC Distribution and Transmission lines (IEEE Std C37.104-2012, 2012):

- Number of reclosing attempts
- Deadtime
- Reclaim time
- Auto-reclosing reset time and auto reclosing-lockout

3.5.2.1 The number of reclosing attempts

This is the predetermined number of attempts made by the recloser to clear a fault over a set period of time. There are no hard and fast rules for determining the number of reclosing procedures, but there are some considerations to consider.

(Bentarzi, Chafi, *et al.*, 2012). Circuit breaker restrictions and system circumstances are two of these considerations. Circuit breaker restrictions include the circuit breaker's ability to conduct several trips and close operations in a single session, as well as the impact of these multiple operations on the maintenance period. System circumstances are statistical data about a certain distribution system. The statistics show the types of problems that have happened on that particular power line in the past. Temporal faults, semi-permanent faults, and permanent faults are the three categories of faults. Three efforts at reclosing were made in this thesis.

3.5.2.2 Deadtime:

When reclosing, this is the time between the circuit interruption and the circuit re-establishment. Before attempting to auto-reclose a circuit breaker that has tripped due to a fault, several important things must be considered. System synchronism, load type, circuit breaker characteristics, protection reset time, and fault deionization are all issues to consider. Even though the goal is to restore supply to consumers as quickly as possible, auto-reclosing attempts that do not allow enough time for the dielectric to re-establish its strength result in a failed reclose attempt. If adequate time is not given for the gas to disperse, the ionized gas channels generated by the fault arc will begin conducting again after the auto-reclose. The length of time it takes to deionize a circuit is determined by the voltage, the distance between conductors, the amount of the fault current, and the weather. Equation 3.18 can be used to compute the time delay for deionization of air at the fault point:

$$t = 10.5 + \frac{V_{L-L}}{34.5} \tag{3.18}$$

where:

t is time in cycles

V_{L-L} is rated line to line voltage in Kilo volts

Table 3.3 shows typical recloser dead time intervals at a distribution system level as defined by IEEE Std. C37.104-2012.

Table 3.3: Recloser dead time intervals for distribution system

Deadtime interval	Typical time setting range in seconds
The initial trip to first reclose	0-5
Second trip to second reclose	10-20
Third trip to third reclose	10-30

This thesis used 3 seconds, 10 seconds and 10 seconds for the first initial reclose, the second trip to reclose, and the third trip to reclose, respectively.

3.5.2.3 Reclaim time:

As described in IEEE Std. C37.104-2012, reclaim time is affected by the type of protection utilized and the circuit breaker's spring winding time. The time it takes for the counting mechanism to return to its starting position after one or more counting operations is known as reclaim time. The reset time in an auto-reclosing device is the amount of time that must pass after a completed closing operation, measured from the contact that the closing contacts make before the reclosing device commences a new reclosing sequence if the fault remains.

3.5.2.4 Auto-reclosing reset time and auto reclosing-lockout:

The time it takes for a reclosing relay to reset after a successful auto-reclosure is known as the reset time. After the reset time delay ends, the reclosing relay returns to its reset state if auto reclosing was successful. The nature of the issue and the predicted clearing time may influence how long the reset time delay is chosen. For intermittent problems, a longer reset delay decreases the risk of excessive tripping and auto-reclosing. The reclosing will reset if the time between intermitted faults is lower than the period between intermitted faults, preventing lockout. Increased reset time on the reclosing relay reduces excessive operations, however, it may result in unwanted lockout actions.

When auto-reclosing attempts fail, the reclosing relay enters a lockout condition, preventing the circuit breaker from closing automatically. After a predetermined number of unsuccessful tries to re-energize the line, auto-reclose is disabled. Lockout conditions prevent persistent faults from causing harm to the device and the entire distribution system.

Reclosing relays are classified based on whether they are single-phase or three-phase, the type of regulating unit (hydraulic or electronic), and the arc extinguishing medium they employ (oil, air, SF6, or vacuum). Reclosing relays are designed to meet the electrical, mechanical, and rating standards of IEC 62271-111 and IEEE C37.60TM, with this study applying a three-phase reclosing concept.

3.5.3 Types of reclosers

This section of the chapters discusses many types of reclosing choices, such as single-phase, three-phase, high-speed auto-reclosing, and delayed auto-reclosing.

3.5.3.1 Single-phase reclosing

The most common fault in overhead lines is a single phase-to-earth fault. Single-phase reclosing is most commonly used to protect single-phase lines in a three-phase feeder, such as branches or taps (IEC 62271-111, 2012). Auto-reclosing is performed in a single-phase arrangement by integrating a tripping or close mechanism in each circuit breaker pole. When a single phase-to-earth fault occurs, a single-phase reclosing scheme trips and auto-recloses only the associated circuit breaker pole (Alstom Grid, 2011). This means that each phase of a relay's auto-reclose function consists of three distinct steps. When there is a single phase-to-earth permanent fault, one phase can lock out while the other two phases continue to work normally.

3.5.3.2 Three-phase reclosing

Three-phase reclosing is used to avoid single-phasing of three-phase loads on three-phase motors when lockout of all three phases is forecast for a permanent fault (IEC 62271-111, 2012).

3.5.3.3 High-speed auto-reclosing

In high voltages, high-speed auto-reclosing is commonly used. Aside from the time required to extinguish the arc, high-speed auto-reclosing closes the circuit breaker without delay. Auto-reclose attempts for transient faults have a high success rate, according to IEEE C37.104TM-2012, hence high-speed auto-reclose should be considered. Some of the benefits of high-speed reclosing (IEEE Std C37.104-2012, 2012) are as follows:

They are

- Quick restoration of power to customers
- Maintain system stability
- Restores the system's capability and integrity.

Power system studies are required before high-speed reclosing may be implemented. Knowing how long the system can withstand a disturbance before losing stability, understanding protection and circuit breaker characteristics, and the time required for fault arc de-ionization, as well as selecting deadtime, reclaim time, and the number of reclosing tries, are all part of this (Alstom Grid, 2011).

3.5.3.4 Delayed auto-reclosing

Based on the study and analysis of the system architecture, delayed auto-reclosing may be acceptable. A failing initial high-speed auto-reclose attempt and successive reclosing attempts may cause reclosure to be delayed (Alstom Grid, 2011).

3.6 Distribution system reliability measures

The distribution system's job is to meet customers' energy needs as cheaply as feasible while maintaining supply consistency and quality at a suitable level (Kumar, Sekhar and Ramamoorty, 2017). As a result, the distribution system necessitates great levels of dependability. The point of load indication and performance indicators, which include failure frequency, the average duration of failure, and average time per year, all contribute to high-reliability expectations in a distribution network (Fahmi *et al.*, 2014). The reliability of a distribution system can be assessed using reliability indices that have

been analyzed. Indexes based on prolonged interruptions, load-based indices, and indices based on transient interruptions are the three types of indices available. However, not all utilities have the data needed to generate the indices (IEEE Std 1366, 2012). In the following sections, different types of indices based on IEEE Std 1366TM - 2012 are discussed.

The reliability indices discussed in this chapter help to better understand the financial aspects of distribution system management and maintenance. Certain indices were not calculated in the Thesis because the DIgSILENT distribution system considered in Figure 4.1 assumed lumped load rather than distributed load.

3.6.1 Reliability indices based on sustained interruptions

The sustained outage is a long-term outage caused by a permanent malfunction. When failures cause a continuous outage, field experts are called in to repair and restore the electric network (Paci, Celo and Bualoti, 2018). To be called a prolonged interruption, an interruption must last longer than five minutes (IEEE Std 1366, 2012). Long-term interruption indices are as follows:

System average interruption frequency index (SAIFI*).* SAIFI is used to calculate the average number of disruptions a customer experiences due to persistent defects over a given time period. SAIFI is calculated using equation (3.19)

$$\text{SAIFI} = \frac{\Sigma \text{ Total number of customers interrrpted}}{\text{Total number of customers served}} = \frac{\Sigma N_j}{N_t} \quad (3.19)$$

Where N_j = sum of customers disrupted each time a permanent fault occurs during a duration of time given to report

N_t = Sum of customers served for that particular area

System average interruption duration index (SAIDI). SAIDI denotes the average time between interruptions for every client who receives electricity. SAIDI is calculated using equation (3.20)

$$\text{SAIDI} = \frac{\Sigma \text{ Customer Minutes of Interruption}}{\text{Total number of customers served}} = \frac{\Sigma r_i N_j}{N_t} \quad (3.20)$$

Where r_i = time taken to restore power for each disruption

Customer average interruption duration index (CAIDI). CAIDI is the average time it takes to restore electricity when a permanent fault occurs. CAIDI is calculated using equation (3.21)

$$\text{CAIDI} = \frac{\Sigma \text{ Customer Minutes of Interruption}}{\text{Total number of customers interrupeted}} = \frac{\Sigma r_i N_j}{\Sigma N_j} = \frac{\text{SAIDI}}{\text{SAIFI}} \quad (3.21)$$

Customer Total Average Interruption Duration Index (CTAIDI). CTAIDI is the average amount of time consumers were without power. CTAIDI is a hybrid of CAIDI that is calculated in the same way as CAIDI, except that consumers that experience disruptions are only counted once. CTAIDI is computed using the equation (3.22). CTAIDI is the average amount of time consumers were without power. CTAIDI is a hybrid of CAIDI that is calculated in the same way as CAIDI, except that consumers that experience disruptions are only counted once. CTAIDI is computed using the equation (3.22)

$$\text{CTAIDI} = \frac{\Sigma \text{ Customer Minutes of Duration}}{\text{Total number of Distinct Customers Interrupted}} = \frac{\Sigma r_i N_j}{\text{CN}} \quad (3.22)$$

Where CN = sum of customers that experiencing a permanent fault during a time given to report

Customer Average Interruption Frequency Index (CAIFI). CAIFI is designed to identify the average number of times clients with long-term disruptions have long-term interruptions s. CAIFI is calculated using equation (3.23) below.

$$\text{CAIFI} = \frac{\Sigma \text{ Customer Minutes of Duration}}{\text{Total number of Distinct Customers Interrupted}} = \frac{\Sigma N_j}{\text{CN}} \quad (3.23)$$

Average Service Availability Index (ASAI). ASAI is the percentage of time that a client has power during a year or a specified reporting period. ASAI can be expressed mathematically as seen in equation (3.24).

$$\text{ASAI} = \frac{\Sigma \text{ Customer hours service available}}{\text{Customers hours service demand}} = \frac{N_t \times \left(\text{Number of} \frac{\text{hours}}{\text{year}}\right) - \Sigma r_i N_j}{N_t \times \left(\text{Number of} \frac{\text{hours}}{\text{year}}\right)} \quad (3.24)$$

Customers Experiencing Multiple Interruptions (CEMIn). CEMIn represents the percentage of individual customers that experience n or more continuous interruptions to the total number of customers served. CEMIn can be expressed mathematically as seen in equation (3.25).

$$\text{CEMIn} = \frac{\text{Total number of customers that are expected } n \text{ or more sustained interruptions}}{\text{Total number of customers served}} \quad (3.25)$$

To calculate CEMIn, equation (3.26) below can be used.

$$\text{CEMIn} = \frac{CN_{(k \geq n)}}{N_T} \quad (3.26)$$

Where CN = Total number of distinct customers who have experienced a sustained Interruption during the reporting period

$CN_{(k \geq n)}$ = number of customers who have experienced *n* or more sustained interruptions during the reporting period

k = the number of disconnections experienced by an individual customer in a reporting period

Customers Experiencing Prolonged Interruptions (CELID). CELID is the percentage of customers that encounter service interruptions that last longer or shorter than a predetermined amount of time. The duration of a single interruption (s) or the amount of time (t) that a customer was affected during a reporting period is the amount of time (t) that a customer was disrupted. The equation for a single interruption time period is provided in equation (3.27), whereas the equation for total interruption duration is shown in equation (3.28). (3.28)

Single interruption duration is calculated as follows:

$$\text{CELID-t} = \frac{\text{Total number of customers that experienced S or more hours}}{\text{Total number of customers served}} \quad (3.27)$$

To calculate this index equation (3.32) below can be used.

$$\text{CELID-s} = \frac{CN_{(k \geq S)}}{N_T} \quad (3.28)$$

Total interruption duration is calculated as follows:

$$\text{CELID-t} = \frac{\text{Total number of customers that experienced T or more hours}}{\text{Total number of customers served}} \quad (3.29)$$

To calculate this index equation (3.30) below can be used.

$$\text{CELID-t} = \frac{CN_{(k \geq T)}}{N_T} \tag{3.30}$$

3.6.2 Reliability Indices based load

Index of average system disruption frequency (ASIFI) ASIFI was designed to calculate reliability based on load rather than the number of consumers. This rating is crucial in locations where the bulk of clients are industrial or commercial. ASIFI is also used by utilities that do not have precise tracking systems. As depicted in equation 3.31, ASIFI can be stated analytically (3.31).

$$\text{ASIFI} = \frac{\text{Total Connected KVA interrupted}}{\text{Total connected KVA served}} \tag{3.31}$$

To calculate ASIFI, equation (3.32) below can be used.

$$\text{ASIFI} = \frac{\Sigma L_i}{L_T} \tag{3.32}$$

Where L_i = supplied kVA load disconnected for each interruption event

L_T = Total load served in kVA

Average system interruption duration index (ASIDI). This index is used to keep track of how many times a customer has been interrupted for more than n minutes. Its purpose is to assist in the discovery of consumer issues that are not visible through averages. ASIDI can be stated mathematically, as seen in the equation (3.33).

$$\text{ASIDI} = \frac{\Sigma \text{ Total Connected KVA interrupted}}{\text{Total connected KVA served}} \tag{3.33}$$

To calculate ASIDI, equation (3.34) below can be used.

$$\text{ASIDI} = \frac{\Sigma r_i L_i}{L_T} \tag{3.34}$$

3.6.3 Momentary Indices

Momentary Average Interruption Event Frequency Index (MAIFI). MAIFI indicates the average rate of short disturbances. MAIFI may be stated analytically as seen in equation (3.35).

$$\text{MAIFI} = \frac{\Sigma \text{ Total number of customer momentary interrption events}}{\text{Total number of customers served}} \quad (3.35)$$

To calculate MAIFI, equation (3.36) below can be used.

$$\text{MAIFI} = \frac{\Sigma \text{IM} N_{mi}}{N_T} \quad (3.36)$$

Momentary Average Interruption Event Frequency Index (MAIFI_E). The average rate of temporary interruptions events is indicated by MAIFIE. MAIFIE can be expressed mathematically as seen in equation (3.37).

$$\text{MAIFI}_E = \frac{\Sigma \text{ Total number of customer momentary interrption events}}{\text{Total number of customers served}} \quad (3.37)$$

To calculate MAIFI_E, equation (3.38) below can be used.

$$\text{MAIFI}_E = \frac{\Sigma IM_E N_{mi}}{N_T} \quad (3.38)$$

Customers Experiencing Multiple Sustained Interruption and Momentary Interruption Events (CEMSMI_n). CEMSMIn is the proportion of specific customers who have had n or more sustained and temporal interruption events to the total number of customers served. This indication is quite valuable for clients who are unable to be tracked by averages. As shown in the equation, CEMSMIn can be stated numerically (3.39).

$$\text{CEMSMI}_n = \frac{\Sigma \text{ Total number of customers Experiencing or more interruptions}}{\text{Total number of customers served}} \quad (3.39)$$

To calculate CEMSMI_n, equation (3.40) below can be used.

$$\text{CEMSMI}_n = \frac{CNT_{(k \geq n)}}{N_T} \quad (3.40)$$

This thesis's reliability investigation is not calculated because it only considers lumped load models working on the specified distribution system. However, the author intends to use distribution network reliability analysis in his future work with distributed load rather than lump load modeling.

3.7 IEC 61850-based communication architecture for substation automation

The IEC 61850 is an Ethernet communication standard for substations. It is a standard that validates the interoperability of substation gear used for protection, monitoring,

metering, control, and automation (Janaka *et al.*, 2012). The IEC 61850 standard's goal is to create a communication standard that keeps up with technological advances, performance, and nominal costs (Adamiak, Baigent and Mackiewicz, 2009). The IEC 61850 standard divides substation communication into three levels:

- Station level
- Bay level
- Process level

The three IEC 61850 communication levels are depicted in Figure 3.12. The station level, as shown in Figure 3.12, includes a substation computer, an operator's desk, and interface with equipment outside the substation. IED protection, metering, and control are all part of the bay level. I/O devices, sensors, and switches are all part of the process level.

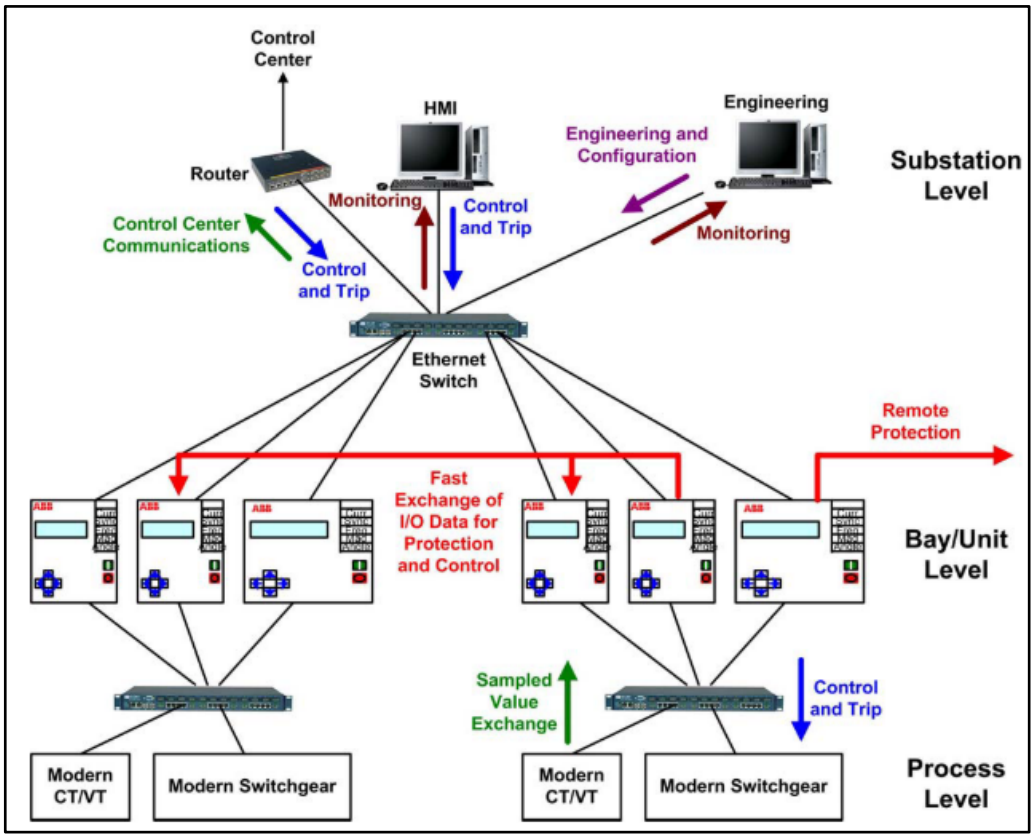

Figure 3.12: Substation communication architecture base on IEC 61850 (Mohagheghi, Stoupis and Wang, 2009)

Part 8 of the IEC 61850 standard defines communication between stations and bay levels, while Part 9 of the IEC 61850 standard defines communication between bay levels and process levels.

3.7.1 Substation Configuration Language Files (SCL)

SCL interchange of database configurations from various vendors (SEL-351A Instruction manual, 2020). SCL has four types of files, as stated in IEC 61850-6 of the standard (Mohagheghi, Stoupis and Wang, 2009), namely: files are Extensive Markable Language (XML)-based configuration files used to facilitate the

1. IED Capability Description file (.ICD): The ICD file defines the IED's capabilities, data type templates, logical node types, optional communication section, and substation section.

2. System Specification Description (.SSD) file: The SSD file defines the substation single line diagram and logical nodes needed for that specific application.

3. Substation Configuration Description file (.SCD): The SCD file contains a complete description of the power system, a description of each IED, a section for communication configuration, and a description of the substation.

4. The Configured IED Description file (.CID) is used to exchange data and settings between the IED and the configuration tool. CID files also have a communication component, which includes the address of the IED utilized in the project.

The flow of information starts with the extraction of system data and ICD data from the SSD and ICD files. The system configurator then creates an SCD file that contains functions and information on each IED. The IED configurator collects the SCD file and creates the CID file that enables the format suitable for each IED via GOOSE and MMS.

The process of configuring an IEC 61850 system is illustrated in Figure 3.13 below.

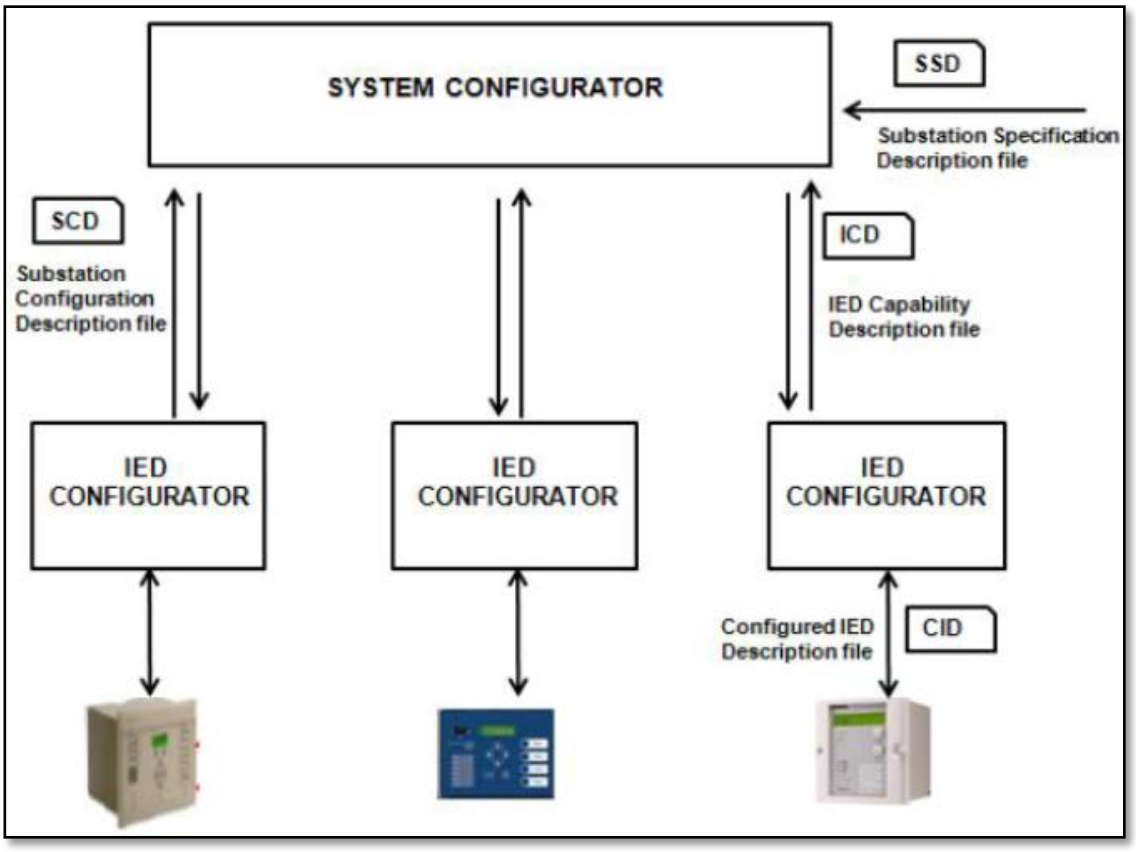

Figure 3.13: Configuration process for IEC 61850 configurator (Baningobera, 2018)

3.7.2 Manufacturing Message Specification (MMS)

MMS is an international standardized massaging system that is used to mimic real devices and operations, as well as to share real-time data and supervisory control information between networked devices and/or computer programs in an independent manner (SISCO, 1995). MMS was created in the 1980s and standardized as ISO 9506 as a network independent data exchange protocol for industrial networks (SEL-351 Instruction manual, 2019). In theory, IEC 61850 can be mapped to any protocol, but mapping objects and services to a protocol that merely offers access to simple data points via registers or index numbers can be quite difficult. MMS supports sophisticated named objects as well as flexible services that enable for simple mapping of IEC 61850. This is why IEC kept MMS in the IEC 61850 standard (SEL-351A instruction manual, 2018). The MMS object model is shown in Figure 3.14 conveying real-time data and supervisory control information between network devices and/or computer applications.

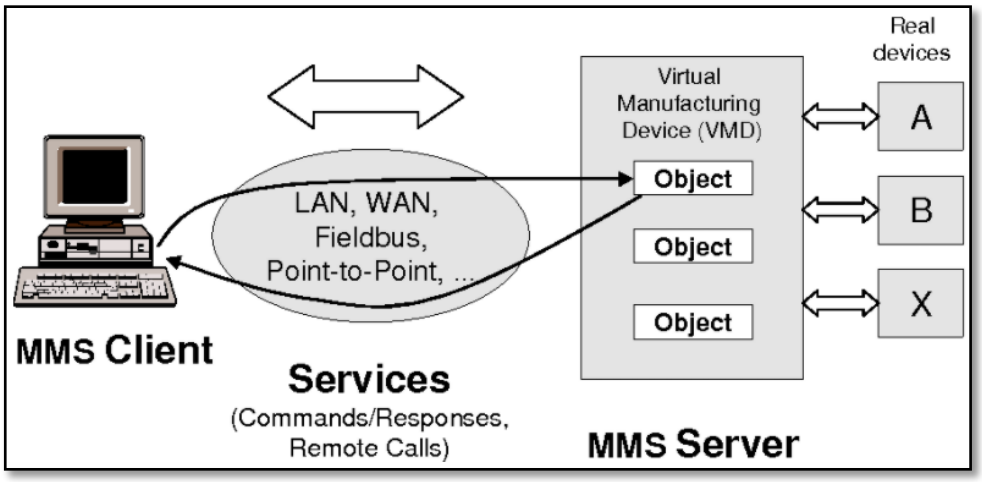

Figure 3.14: MMS client/server object model (Schwarz, 2020)

3.7.3 IEC 61850 Generic Object Oriented Substation Event (GOOSE) message

The IEC 61850 GOOSE message is used for high-speed control messaging. GOOSE broadcasts messages across the network that contain status, controls, and measured quantities that can be used by other devices (SEL-351A Instruction manual, 2020). The GOOSE message protocol is an event-based protocol. The GOOSE principle is that the publisher sends messages continually when an event occurs (e.g trip or close). Because the GOOSE protocol is a publisher or subscriber-based protocol, there is no assurance that the published message was properly received by the subscriber, which means that continual posting reduces the risks of losing the published GOOSE message. Every GOOSE message is published under a certain topic. The subscriber gets all GOOSE messages published by the publisher system, then filters them down to only those with the subscribed topic. Because the GOOSE protocol is a publisher or subscriber protocol, communication is limited to the Local Area Network (LAN) and Wide Area Network (WAN) (Hou and Dolezilek, 2010). Figure 3.15 depicts the GOOSE message being retransmitted indefinitely. When an event happens, the continuous GOOSE transmission interval reduces and eventually increases to a stable constant after the event, as shown in Figure 3.15

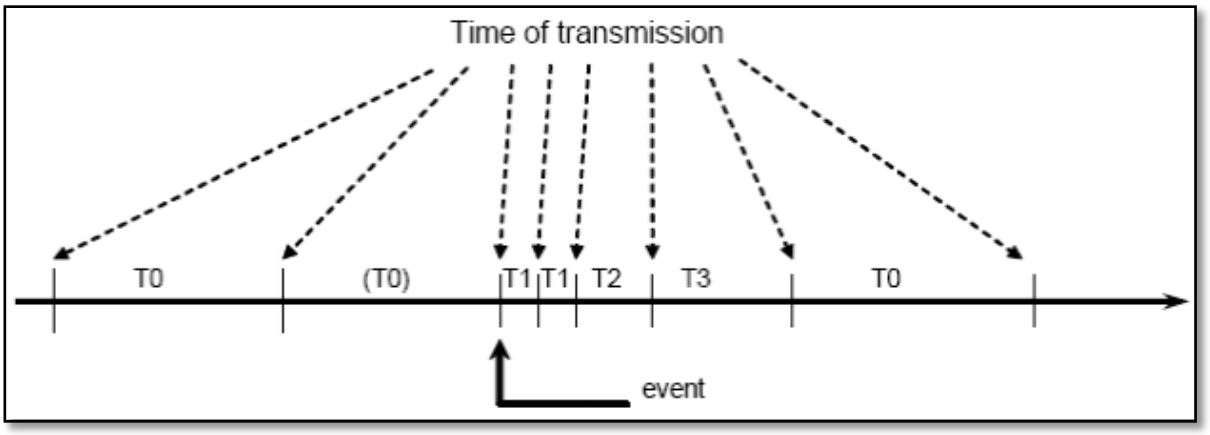

Figure 3.15: GOOSE message publication (Hou and Dolezilek, 2010)

3.7.4 IEC 61850 data modelling and logical nodes

The substation automation system is made up of numerous IEDs that communicate via a network. Modeling is required to identify the data items and objects of each IED participating in automated functions. As shown in Figure 3.16, the IEC 61850 standard modeling begins with the Physical Device (PD), which is the IED that connects to the system.

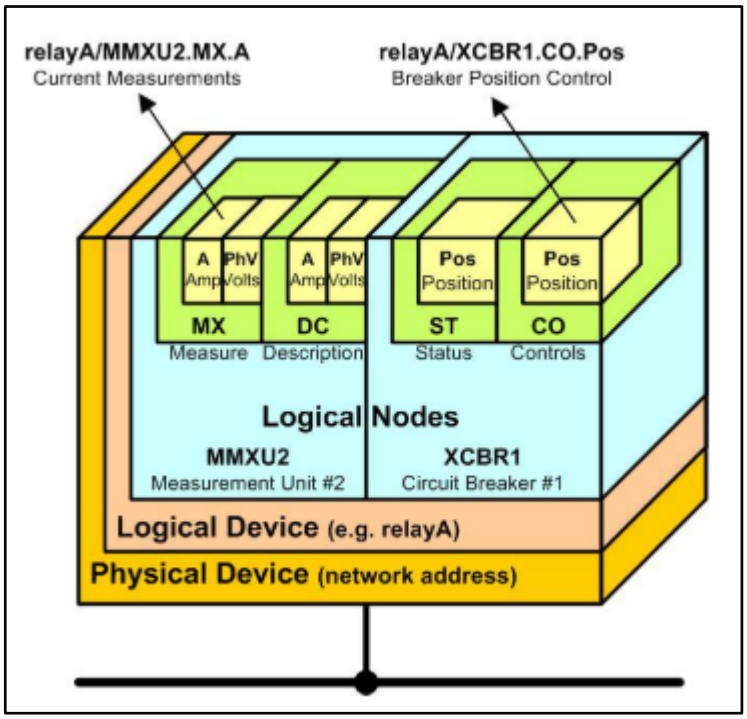

Figure 3.16: Object model of IED in IEC 61850 standard (Mohagheghi, 2010)

A physical device contains one or more Logical Devices (LD), each of which represents a set of functions, such as protection or control. The LD is made up of one or more Logical Nodes (LN) or objects. Each LN has Data Attributes (DA), which describe the name format, range, and possible values associated with power system functions, which could be status or measurement signals.

Figure 3.17 depicts a logical node hierarchical structure of a Circuit Breaker (XCBR). The circuit breaker is represented by the XCBR section of the LN. The LN contains numerous data objects, each of which belongs to a specific data class. As shown in Figure 6.6, each data item can have several data properties.

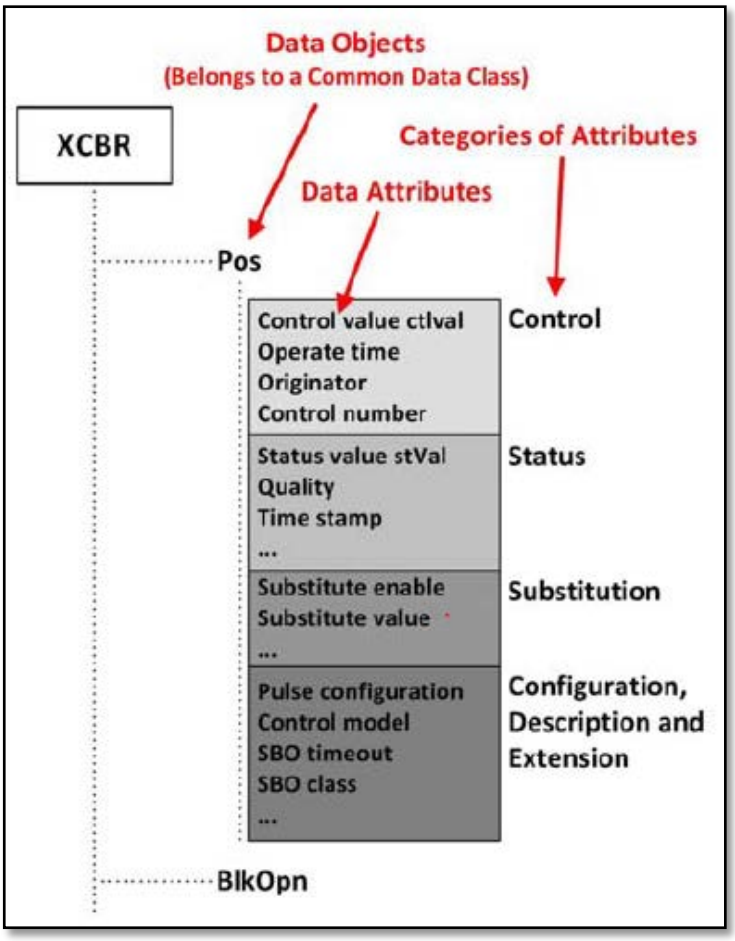

Figure 3.17: Logical node hierarchical structure (Mohagheghi, 2010)

IEC 61850 device modeling is a virtualized model that begins with the device abstract and ends with the object defined in IEC 61850-7. In IEC 61850-8-1, the abstract model is mapped to a specific protocol stack based on MMS, TCP/IP, and Ethernet. The model

simplifies referring to a specific object. Figure 3.18 depicts an example of an object name structure in accordance with IEC 61850. Relay 1 is the name of the logical device that controls a single circuit breaker logical node XCBR1. Pos denotes the circuit breaker position, and stVal denotes the status.

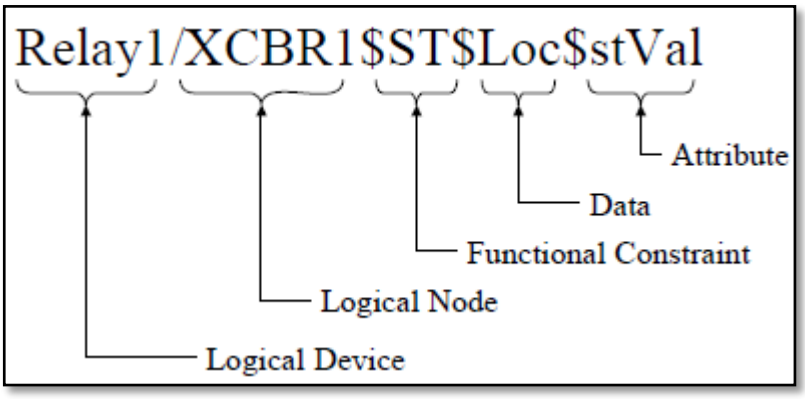

Figure 3.18: Object name structure based on IEC 61850 (Mackiewicz, 2006)

Logical node groupings and group indicators from IEC 61850-7-4 are given in Table 3.4.

Table 3.4: IEC 61850 Logical node groups and group indicators

Logical node groups	Group indicator
Automatic control	A
Supervisory control	C
Generic function references	G
Interfacing and archiving	I
System logical nodes	L
Metering and measurement	M
Protection functions	P
Protection related functions	R
Sensors and monitoring	S
Instrument transformers	T
Switchgear	X
Power transformer and related functions	Y
Further (power system) equipment	Z

Table 6.1 in Section 6.4 of chapter 6 shows the logical nodes and datasets that were utilized to design the recloser control system in chapter 6.

3.8 Conclusion

An overview of the mathematical components used to determine short circuit currents, recloser relay operating characteristics curves, grading principles for reclosing and automatic recloser settings are among the topics covered in this chapter. Distribution network reliability indicators and the IEC 61850 standard are also covered.

This chapter laid the theoretical groundwork for the DigSilent simulation of recloser protection functions and its simulation results are presented in section 4.6. As a result of this, the lab-scale implementation and testing of the recloser protection functions using both hardwired and IEC61850 GOOSE message applications are included in the simulation results and investigations, as discussed in sections 5.4, and 6.5 respectively.

The following chapter discusses DIgSILENT simulation studies of the distribution network in order to build its recloser protective mechanism and examine its performance.

CHAPTER FOUR

DIgSILENT IMPLEMENTATION OF THE AUTO-RECLOSE PROTECTION SCHEME FOR DISTRIBUTION SYSTEM

4.1 Introduction

The distribution system is an important part of the power system since it delivers power to users and collects revenue. The distribution system is vulnerable to unavoidable fault conditions. When these fault conditions occur, the power lines of the distribution system are disrupted, and clients are left without power. Customers include hospitals, residential areas, factories, and schools, among others. Power utilities lose income and struggle to maintain reliability standards when consumers are out of service. Power utilities also obtain penalties from customers who have contracts with them when power is not supplied in accordance with the terms of the contract (Wang et al., 2018).

This chapter's simulation study models a 22kV distribution network with two radial feeder lines protected by four overcurrent relays and analyzes the simulation findings. The simulation examines the performance and coordination of overcurrent protective reclosing relays. As illustrated in Figure 4.1, each feeder in the considered distribution network includes two reclosing relays, one SEL-351 relay at the feeder's outgoing end and a second SEL-351 relay downstream of the distribution line.

The overcurrent relaying system's performance is investigated by simulating fault conditions in various areas of the distribution network. The auto-reclose function is being researched and analyzed. The simulation findings show that auto reclosers are required to restore power downstream of the distribution lines due to network faults upstream.

Sections 4.2 and 4.3 present the DIgSILENT model and load flow simulation results for the distribution network. Section 4.4 examines the short-circuit simulation, current transformer selection, and simulation results. Section 4.5 describes the overcurrent protection configuration settings. Section 4.6 shows the simulation findings for the four case studies under consideration, and Section 4.7 provides the conclusion.

4.2 Modelling of the distribution system network

This section's goal is to build and model the distribution network in DIgSILENT software. Figure 4.1 depicts the distribution network under consideration. This grid-connected distribution network has two feeders A and B, busbars, transformers, overhead cables, three loads in each feeder, and a Normal Open Point (NOP).

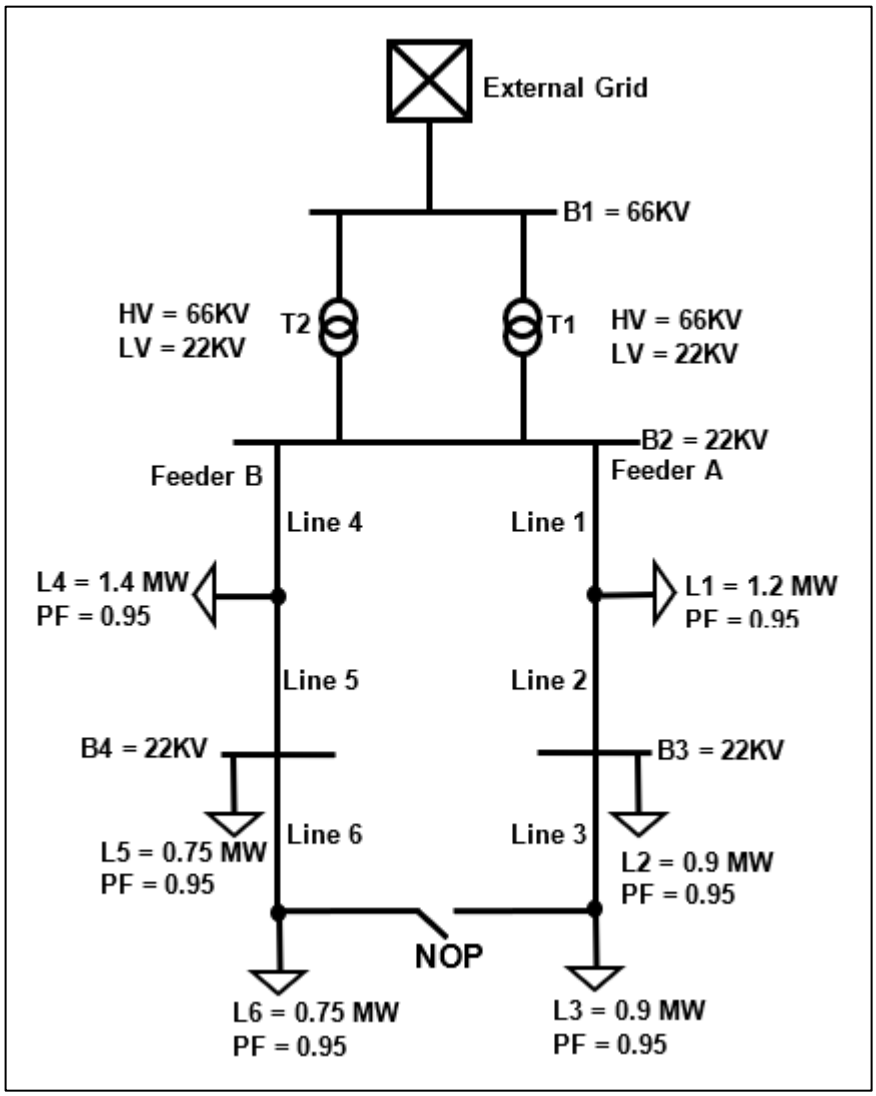

Figure 4.1: Single line diagram of the distribution system

The DIgSILENT workflow of the studied distribution network, with investigations carried out in the order shown in Figure 4.2.

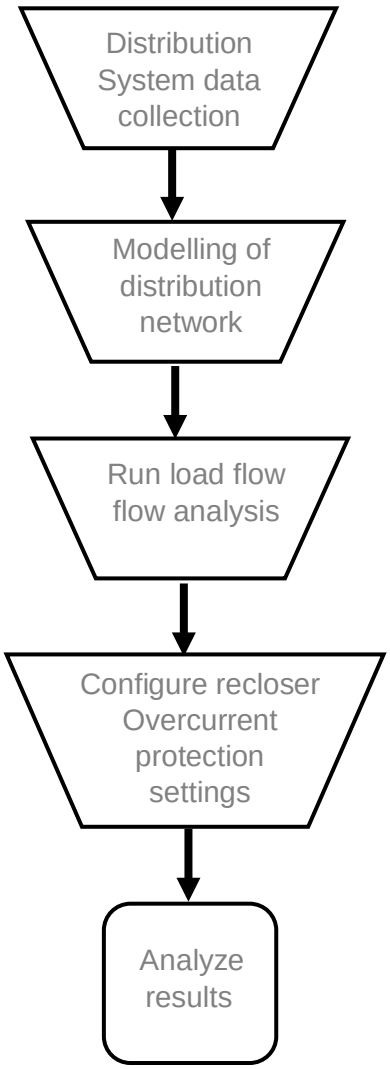

Figure 4.2: Workflow diagram of DIgSILENT simulation

The written description that follows provides an overview of the sequence diagram seen in Figure 4.2.

- Data collection entails obtaining the parameters of each piece of equipment, which includes the grid, transformers, overhead lines, loads, and reclosing relays.
- Building the Power System Single line diagram Figure 4.1 and configuring the network data are part of the modeling of the researched distribution network.
- The load flow analysis is performed to study the power system network's steady-state studies.

- The SEL-351 overcurrent reclosing relay elements are configured after a satisfactory load flow analysis.
- Short circuit analysis, overcurrent reclosing relay operation, overcurrent recloser grading, and auto-reclosing are all part of the simulation results analysis.
- The comprehensive modeling of the external grid, busbars, transformer, overhead line, and load is included in Appendix A.

4.3 Load flow analysis

This section examines the load flow simulation findings. To be considered successful under three-phase steady-state conditions, a power system network's generation must supply load and losses, the voltage on busbars must remain close to the actual rated values, generator operation must remain within stipulated real and reactive power limits, and overhead transmission lines, distribution lines, and transformers must not be overloaded (Glover, Sarma and Overbye, 2012).

It should be noted that the load flows are carried out with both transformers operational and the tap changer set to position two. The reason for setting the tap changer position to tap two is that it can provide the entire load from both feeders A and B with the NOP open, and either feeder A or B when the NOP is closed, without affecting the voltage profile. The load flows are run for the three configurations listed below, with reference to the network diagram with load flow shown in Figure 4.3.

1. When the NOP is open and both feeder circuit breakers (A and B) are closed, Feeder A is supplying it own load, and feeder B is supplying its own load.
2. When the NOP is closed, the circuit breaker at feeder B is open, and the entire distribution system network is supplied by feeder A.
3. When the NOP is closed, the circuit breaker at feeder A opens, and feeder B supplies the full distribution system network.

Under normal conditions, the studied distribution system operates with the two parallel transformers in service and NOP open as shown in Figure 4.3. Two transformers are present to prevent outages if the transformer fails or needs to be serviced. . When the NOP is closed due to a maintenance or fault condition in one feeder, the feeder that is not under maintenance or fault condition will back feed the network via the NOP.

With the NOP open, the load flow for the first configuration is conducted to guarantee that each feeder can supply its load. The load flow for the second configuration is done to guarantee that feeder A can supply the whole distribution system via NOP. The load flow for the third configuration is done to verify that feeder B can supply the whole distribution system via NOP. The load flows of the three configurations are run in common to validate that the voltage profiles of each configuration are within the limitations established in IEEE standard 141-1993 criteria (IEEE Std 141, 1993). To ensure that none of these arrangements overload transformers and overhead wires, and that power system standards and regulations are not breached. The load flow analysis calculates the rate of flow of current, real and reactive power in the distribution system under consideration.

This part, which is explained further below, offers the load flow results for each setup. The Newton-Raphson method is used to compute the load flow. In two iterations, the load flow results for configuration one are successfully executed and converged. Figure 4.3 illustrates the distribution system load flow results in a single line diagram. As illustrated by the animated power flow with arrows in Figure 4.3, power flows from feeders (A and B) to the NOP, with no power flowing across the NOP. This signifies that feeder A is supplying its load and feeder B is supplying its load. CB (A and B) in Figure 4.3 are Feeder circuit breakers (A and B).

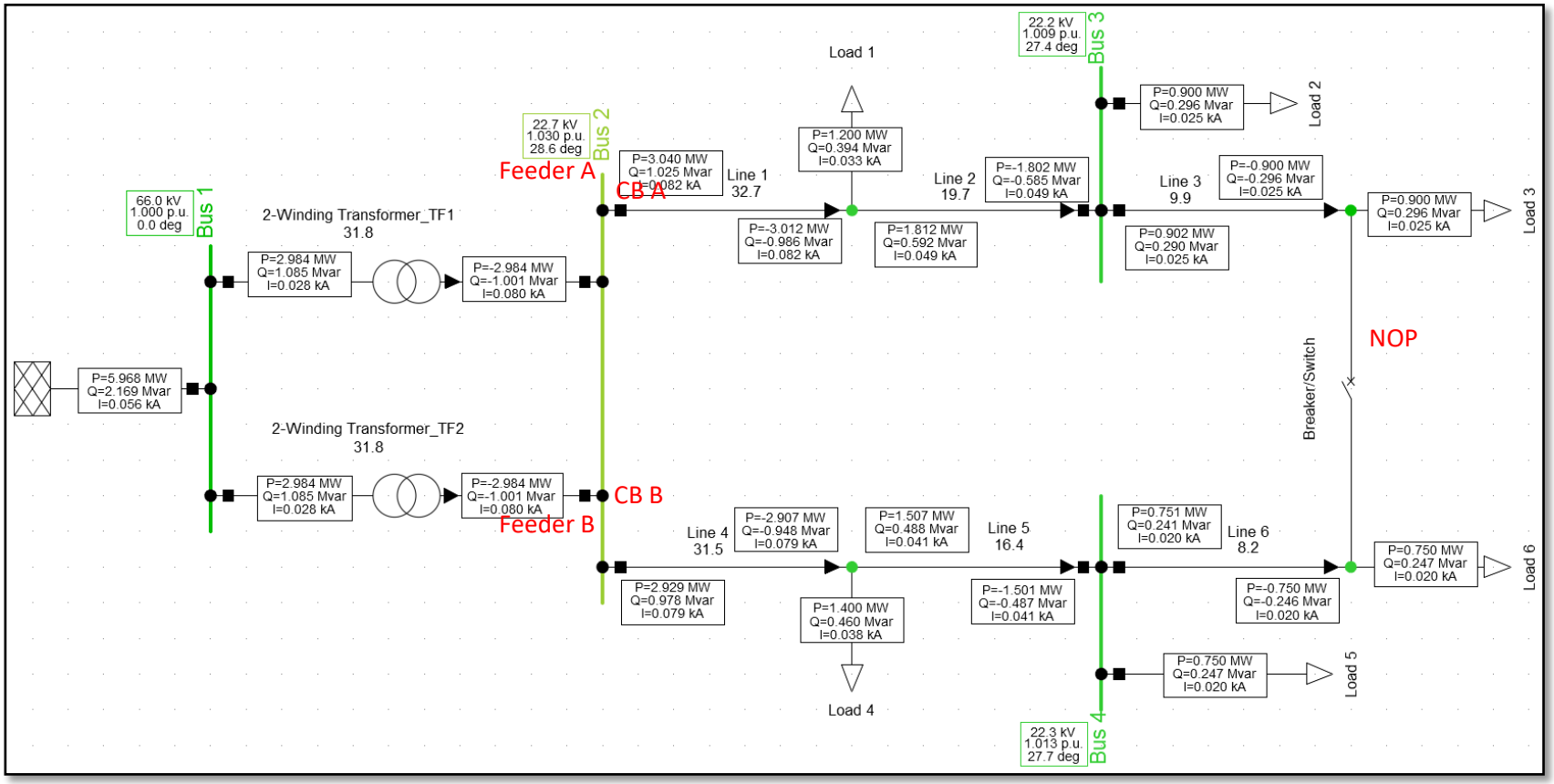

Figure 4.3: Diagram showing the network's load flow when NOP is open and CBs A and B are closed

Figures 4.4 and 4.5 show the simulation results for three-phase voltages and currents, respectively. Figure 4.4 shows the simulation results for feeder A with the NOP open, while Figure 4.5 shows the simulation results for feeder B with the NOP open.

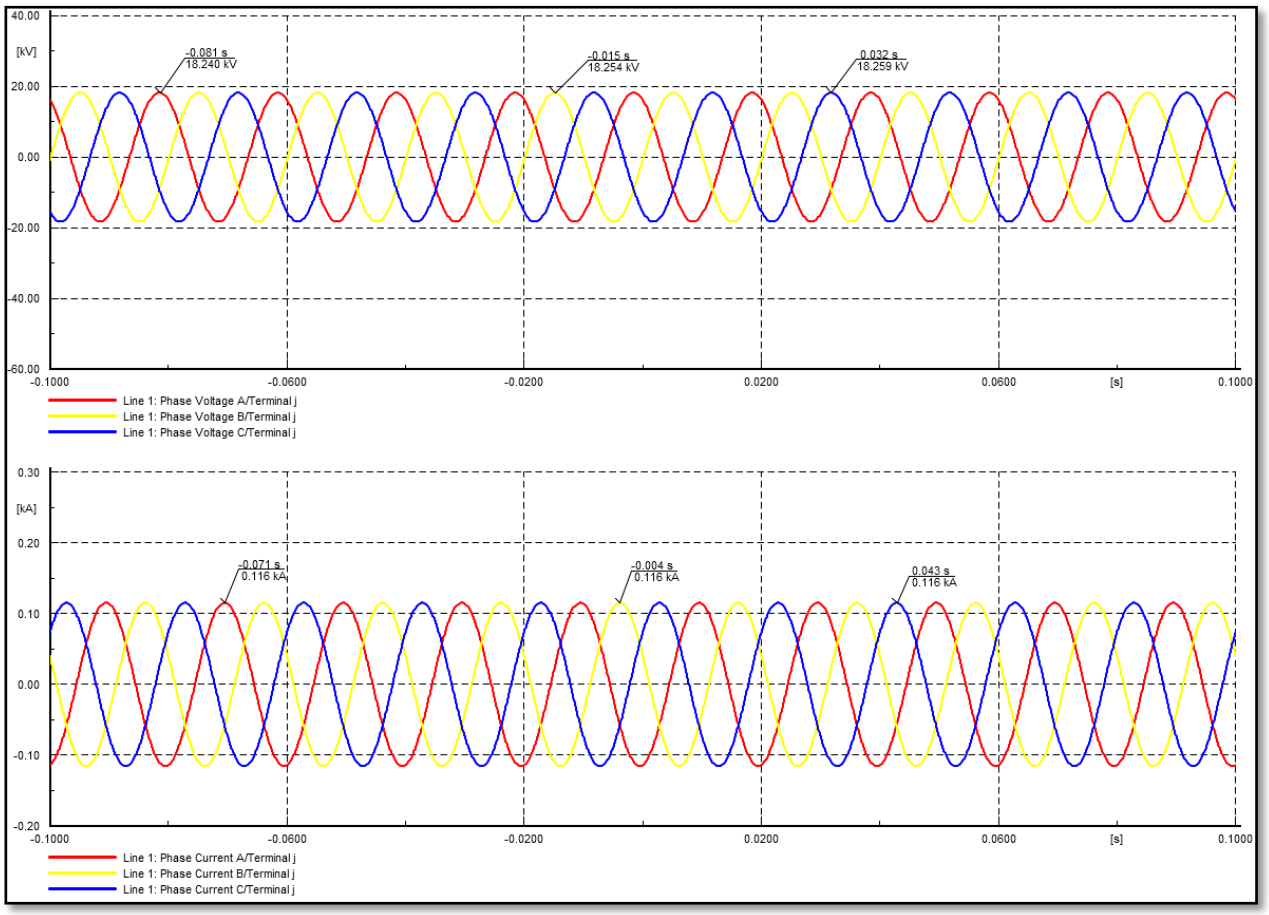

Figure 4.4: Signals measuring three-phase voltage currents at the feeder A network upstream

The values shown in Figure 4.4 are the RMS magnitude of phase voltages and currents at line 1 which corresponds to $V_L = 18.24kV \times \frac{\sqrt{3}}{\sqrt{2}} = 22.34kV$ and $I_L = \frac{0.116kA}{\sqrt{2}} = 82.02A$ respectively.

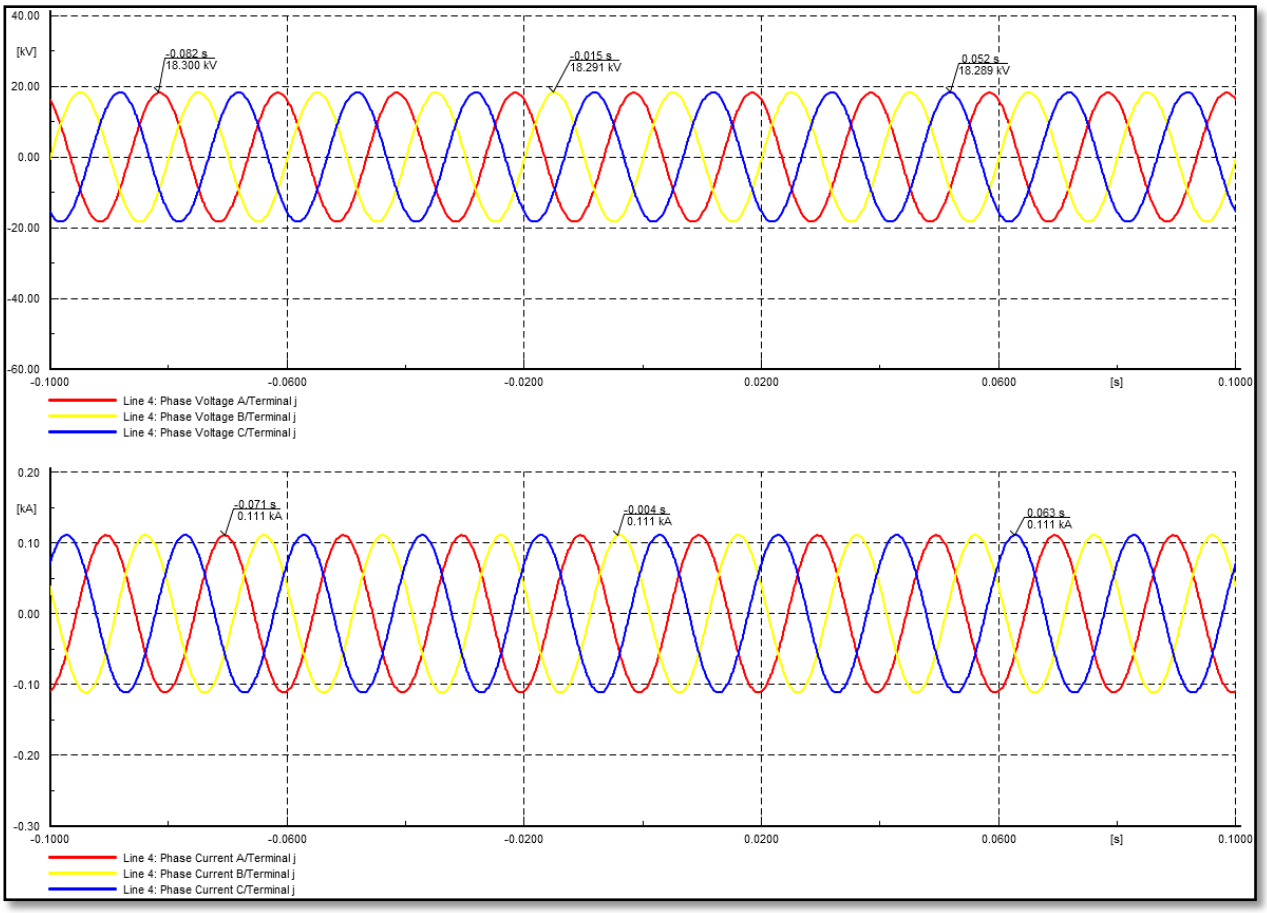

Figure 4.5: Three-phase voltage and currents signals measured at feeder B upstream of the network

The values of the phase voltage and current RMS magnitudes in Figure 4.5 corresponds to $V_L = 18.33kV \times \frac{\sqrt{3}}{\sqrt{2}} = 22.45kV$ and $I_L = \frac{0.111kA}{\sqrt{2}} = 78.49A$

Table 4.1 shows the voltage profile of the simulated distribution system. According to the simulation results, the distribution system maintains a lower voltage limit of 1 per unit and a higher voltage limit of 1.03 per unit, both of which are within IEEE 141-1993 standard criteria.

Table 4.1: The voltage profile of the distribution network for configuration one (NOP open and CBs A and B closed)

Load Flow Calculation					Complete System Report: Substations, Voltage Profiles, Grid Interchange
AC Load Flow, balanced, positive sequence			Automatic Model Adaptation for Convergence		No
Automatic tap adjustment of transformers		No	Max. Acceptable Load Flow Error		
Consider reactive power limits		No	Bus Equations(HV)		1.00 kVA
			Model Equations		0.10 %

Grid: Grid	System Stage: Grid		Study Case: Study Case		Annex: / 3

	rtd.V [kV]	Bus - voltage [p.u.]	[kV]	[deg]	Voltage - Deviation [%] −10	−5	0	+5	+10
Bus 1									
	66.00	1.000	66.00	0.00					
Bus 2									
	22.00	1.030	22.66	28.57					
Bus 3									
	22.00	1.009	22.19	27.45					
Bus 4									
	22.00	1.013	22.29	27.69					

The complete load flow results are shown in Table 4.2. The findings show the total real power, reactive power, and apparent power supplied by the transformers to both feeders of the distribution network. According to the load flow data, external grid generation supply 5.97 MW and reactive power support of 2.17Mvar with grid losses of 0.7MW. In this situation, the external grid generation supplies the overall power demand without taking into account the spinning reserve.

Table 4.2: Power flow results for configuration one (NOP open and CBs A and B closed)

Load Flow Calculation					Grid Summary
AC Load Flow, balanced, positive sequence			Automatic Model Adaptation for Convergence		No
Automatic tap adjustment of transformers		No	Max. Acceptable Load Flow Error		
Consider reactive power limits		No	Bus Equations(HV)		1.00 kVA
			Model Equations		0.10 %

Grid: Grid	System Stage: Grid	Study Case: Study Case	Annex: / 1

Grid: Grid	Summary						
No. of Substations	0	No. of Busbars	4	No. of Terminals	4	No. of Lines	6
No. of 2-w Trfs.	2	No. of 3-w Trfs.	0	No. of syn. Machines	0	No. of asyn.Machines	0
No. of Loads	6	No. of Shunts/Filters	0	No. of SVS	0		

Generation	=	0.00 MW	0.00 Mvar	0.00 MVA	
External Infeed	=	5.97 MW	2.17 Mvar	6.35 MVA	
Inter Grid Flow	=	0.00 MW	0.00 Mvar		
Load P(U)	=	5.90 MW	1.94 Mvar	6.21 MVA	
Load P(Un)	=	5.90 MW	1.94 Mvar	6.21 MVA	
Load P(Un-U)	=	0.00 MW	0.00 Mvar		
Motor Load	=	0.00 MW	0.00 Mvar	0.00 MVA	
Grid Losses	=	0.07 MW	0.23 Mvar		
Line Charging	=		-0.06 Mvar		
Compensation ind.	=		0.00 Mvar		
Compensation cap.	=		0.00 Mvar		
Installed Capacity	=	0.00 MW			
Spinning Reserve	=	0.00 MW			
Total Power Factor:					
Generation	=	0.00 [-]			
Load/Motor	=	0.95 / 0.00 [-]			

The system report, shown in Table 4.3 below, comprises active power, reactive power, transformer loads, and overhead lines. According to the simulation findings, both transformers are loaded to 32 percent, and the lines (lines 1–6) are loaded between 8 and 32 percent.

Table 4.3: Summary of the distribution system network for configuration one (NOP open and CBs A and B closed)

Grid: Grid			System Stage: Grid			Study Case: Study Case				Annex:				/ 1
	rated Voltage [kV]	Bus-voltage [p.u.]	[kV]	[deg]	Active Power [MW]	Reactive Power [Mvar]	Power Factor [-]	Current [kA]	Loading [%]	Additional Data				
Bus 1														
	66.00	1.00	66.00	0.00										
Cub_3	/Xnet	External Grid			5.97	2.17	0.94	0.06		Sk":	778.49 MVA			
Cub_1	/Tr2	2-Winding Transfor			2.98	1.08	0.94	0.03	31.75	Tap:	2.00	Min:	1	Max: 17
Cub_4	/Tr2	2-Winding Transfor			2.98	1.08	0.94	0.03	31.75	Tap:	2.00	Min:	1	Max: 17
Bus 2														
	22.00	1.03	22.66	28.57										
Cub_1	/Tr2	2-Winding Transfor			-2.98	-1.00	-0.95	0.08	31.75	Tap:	2.00	Min:	1	Max: 17
Cub_3	/Lne	Line 1			3.04	1.02	0.95	0.08	32.73	Pv:	27.39 kW	cLod:	0.01 Mvar	L: 7.00 km
Cub_4	/Lne	Line 4			2.93	0.98	0.95	0.08	31.50	Pv:	21.75 kW	cLod:	0.01 Mvar	L: 6.00 km
Cub_5	/Tr2	2-Winding Transfor			-2.98	-1.00	-0.95	0.08	31.75	Tap:	2.00	Min:	1	Max: 17
Bus 3														
	22.00	1.01	22.19	27.45										
Cub_3	/Lod	Load 2			0.90	0.30	0.95	0.02		Pl0:	0.90 MW	Q10:	0.30 Mvar	
Cub_1	/Lne	Line 2			-1.80	-0.59	-0.95	0.05	19.72	Pv:	9.94 kW	cLod:	0.01 Mvar	L: 7.00 km
Cub_2	/Lne	Line 3			0.90	0.29	0.95	0.02	9.90	Pv:	2.32 kW	cLod:	0.01 Mvar	L: 6.50 km

Grid: Grid			System Stage: Grid			Study Case: Study Case				Annex:				/ 2
	rated Voltage [kV]	Bus-voltage [p.u.]	[kV]	[deg]	Active Power [MW]	Reactive Power [Mvar]	Power Factor [-]	Current [kA]	Loading [%]	Additional Data				
Bus 4														
	22.00	1.01	22.29	27.69										
Cub_3	/Lod	Load 5			0.75	0.25	0.95	0.02		Pl0:	0.75 MW	Q10:	0.25 Mvar	
Cub_1	/Lne	Line 5			-1.50	-0.49	-0.95	0.04	16.35	Pv:	5.85 kW	cLod:	0.01 Mvar	L: 6.00 km
Cub_2	/Lne	Line 6			0.75	0.24	0.95	0.02	8.20	Pv:	1.22 kW	cLod:	0.01 Mvar	L: 5.00 km

The load flow simulation results for configuration two with Feeder A feeding the distribution network via NOP are presented in the following section. The circuit breaker on feeder A is closed, the NOP is closed, and the circuit breaker on feeder B is open, as shown in Figure 4.6. This indicates that feeder A is feeding the entire power demand of the distribution system, and the animation provides the direction of the power flow with arrows, as shown in Figure 4.6.

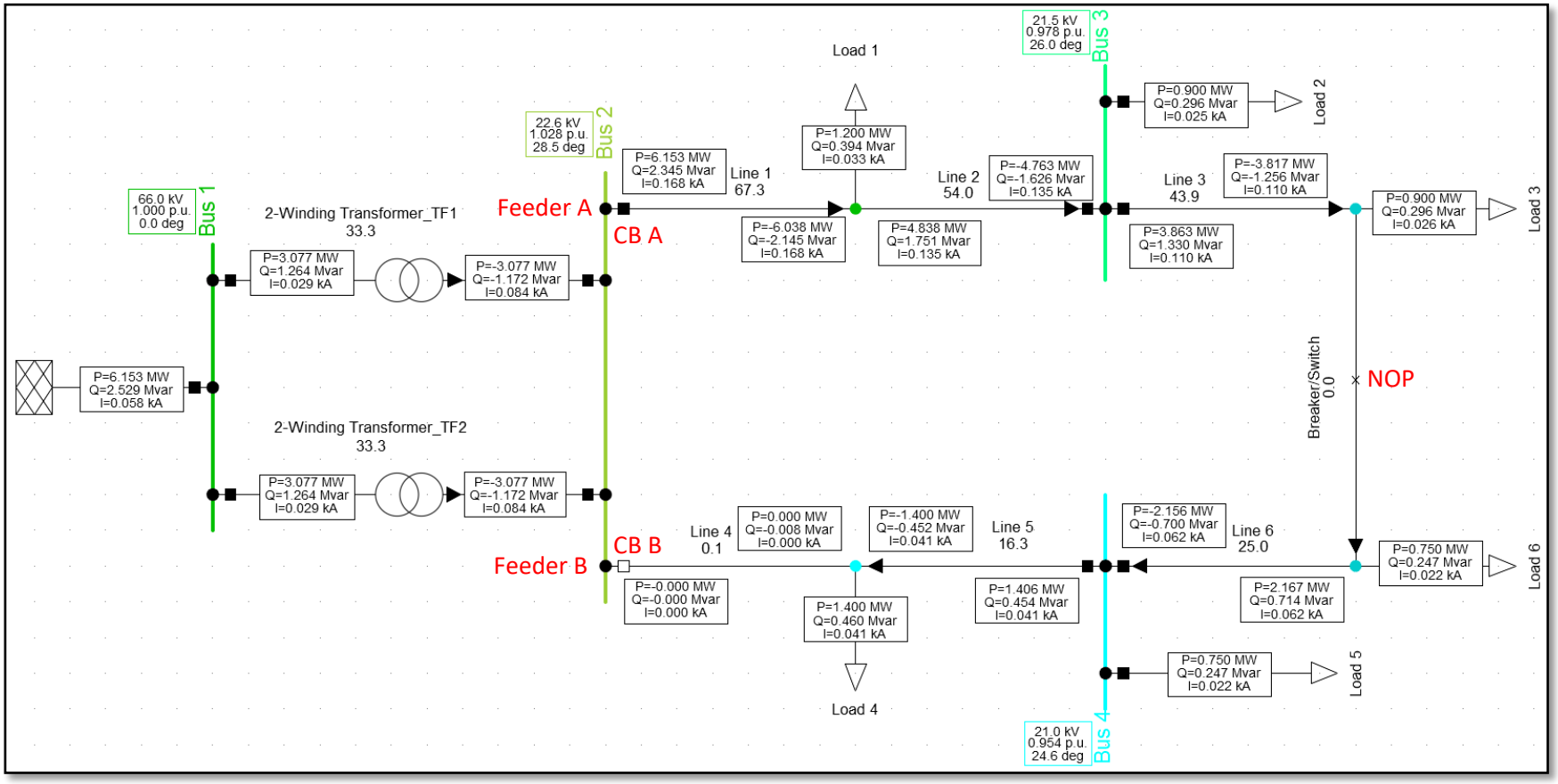

Figure 4.6: With the NOP closed, a single line diagram of the distribution network load flow results feeding on feeder AThe simulation

results for three-phase voltage and currents for configuration 2 with feeder A feeding the network with NOP closed are shown in Figure 4.7 below.

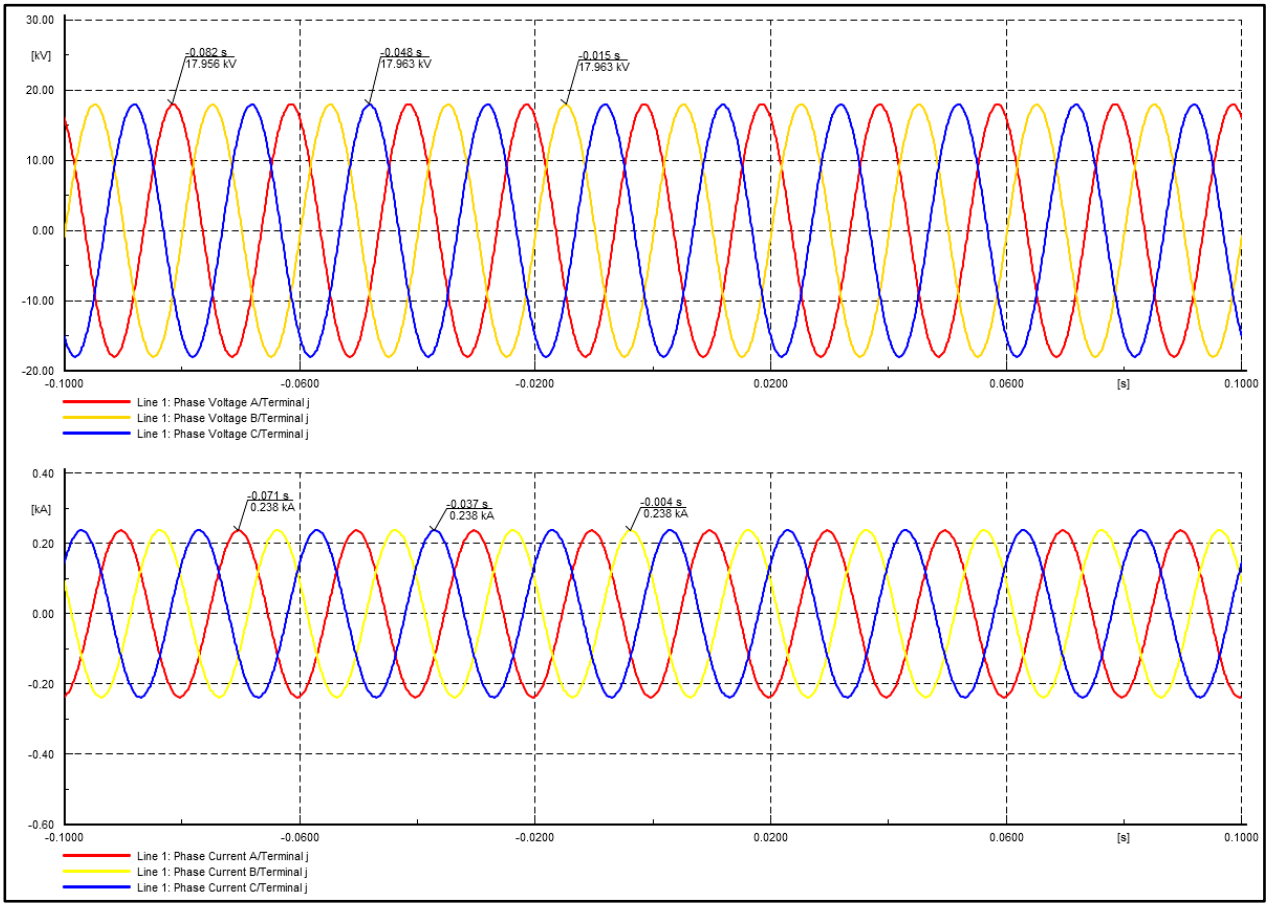

Figure 4.7: Signals measuring three-phase voltages and currents at feeder A upstream of the network while CB A is closed and CB B is open

Line 1 RMS magnitude of phase voltages and currents corresponds to VL = 17.956kV × $\frac{\sqrt{3}}{\sqrt{2}}$ = 21.99kV and $I_L = \frac{0.238kA}{\sqrt{2}}$ = 168.29A respectively.

Table 4.4 shows the voltage profile for configuration two (Feeder A feeds the network with NOP closed).

According to the simulation results, the distribution system maintains a minimum voltage limit of 0.954 per unit and a maximum voltage limit of 1.028 per unit. The simulated distribution network's voltage profile meets IEEE 141-1993 standard criteria.

Table 4.4: Voltage profile of the distribution system for configuration two (Feeder A feeds the network with NOP closed)

Load Flow Calculation			Complete System Report: Substations, Voltage Profiles, Grid Interchange
AC Load Flow, balanced, positive sequence		Automatic Model Adaptation for Convergence	No
Automatic tap adjustment of transformers	No	Max. Acceptable Load Flow Error	
Consider reactive power limits	No	Bus Equations (HV)	1.00 kVA
		Model Equations	0.10 %

Grid: Grid	System Stage: Grid	Study Case: Study Case	Annex: / 3

	rtd.V [kV]	Bus - voltage [p.u.]	[kV]	[deg]	Voltage - Deviation [%] −10 −5 0 +5 +10
Bus 1					
	66.00	1.000	66.00	0.00	
Bus 2					
	22.00	1.028	22.62	28.52	
Bus 3					
	22.00	0.978	21.51	25.96	
Bus 4					
	22.00	0.954	20.98	24.65	

The complete load flow findings for configuration two are shown in Table 4.5 below (Feeder A feeds the network with NOP closed). When feeder A provides the network with the NOP closed, the results show the whole distribution system network's real power, reactive power, and apparent power supplied by both transformers. According to the load flow data, external grid generation provides 6.15 MW and reactive power support of 2.53 Mvar with grid losses of 0.25MW. In this situation, the external grid generation supplies the overall power demand without taking into account the spinning reserve.

Table 4.5: Summary of power flow results for configuration two (Feeder A supplying the network with NOP closed)

Grid: Grid	System Stage: Grid	Study Case: Study Case	Annex: / 1

Grid: Grid — Summary

No. of Substations	0	No. of Busbars	4	No. of Terminals	4	No. of Lines	6	
No. of 2-w Trfs.	2	No. of 3-w Trfs.	0	No. of syn. Machines	0	No. of asyn.Machines	0	
No. of Loads	6	No. of Shunts/Filters	0	No. of SVS	0			

Generation	=	0.00	MW	0.00	Mvar	0.00 MVA
External Infeed	=	6.15	MW	2.53	Mvar	6.65 MVA
Inter Grid Flow	=	0.00	MW	0.00	Mvar	
Load P(U)	=	5.90	MW	1.94	Mvar	6.21 MVA
Load P(Un)	=	5.90	MW	1.94	Mvar	6.21 MVA
Load P(Un-U)	=	0.00	MW	-0.00	Mvar	
Motor Load	=	0.00	MW	0.00	Mvar	0.00 MVA
Grid Losses	=	0.25	MW	0.59	Mvar	
Line Charging	=			-0.06	Mvar	
Compensation ind.	=			0.00	Mvar	
Compensation cap.	=			0.00	Mvar	
Installed Capacity	=	0.00	MW			
Spinning Reserve	=	0.00	MW			

Total Power Factor:		
Generation	=	0.00 [-]
Load/Motor	=	0.95 / 0.00 [-]

The system report in Table 4.6 shows active power, reactive power, and transformer and overhead line loads. According to the simulation results, both transformers are loaded to 33.26 percent, and the lines (lines 1 to 3, 5 to 6) are loaded between 16 and 67 percent. It is crucial to note that by opening CB B on the Feeder B circuit, line 4 is taken out of operation, therefore any planned maintenance or issue on that segment of the line will be readily resolved.

Table 4.6: Summary of distribution network simulation results for configuration two (Feeder A supply the network with NOP closed)

Grid: Grid	System Stage: Grid	Study Case: Study Case	Annex: / 1

		rated Voltage [kV]	Bus-voltage [p.u.]	Bus-voltage [kV]	Bus-voltage [deg]	Active Power [MW]	Reactive Power [Mvar]	Power Factor [-]	Current [kA]	Loading [%]	Additional Data
Bus 1											
		66.00	1.00	66.00	0.00						
Cub_3	/Xnet	External Grid				6.15	2.53	0.92	0.06		Sk": 778.49 MVA
Cub_1	/Tr2	2-Winding Transfor				3.08	1.26	0.92	0.03	33.26	Tap: 2.00 Min: 1 Max: 17
Cub_4	/Tr2	2-Winding Transfor				3.08	1.26	0.92	0.03	33.26	Tap: 2.00 Min: 1 Max: 17
Bus 2											
		22.00	1.03	22.62	28.52						
Cub_1	/Tr2	2-Winding Transfor				-3.08	-1.17	-0.93	0.08	33.26	Tap: 2.00 Min: 1 Max: 17
Cub_3	/Lne	Line 1				6.15	2.34	0.93	0.17	67.26	Pv: 115.70 kW cLod: 0.01 Mvar L: 7.00 km
Cub_4	/Lne	Line 4				-0.00	-0.00	-1.00	0.00	0.09	Pv: 0.00 kW cLod: 0.01 Mvar L: 6.00 km
Cub_5	/Tr2	2-Winding Transfor				-3.08	-1.17	-0.93	0.08	33.26	Tap: 2.00 Min: 1 Max: 17
Bus 3											
		22.00	0.98	21.51	25.96						
Cub_3	/Lod	Load 2				0.90	0.30	0.95	0.03		P10: 0.90 MW Q10: 0.30 Mvar
Cub_1	/Lne	Line 2				-4.76	-1.63	-0.95	0.14	54.04	Pv: 74.69 kW cLod: 0.01 Mvar L: 7.00 km
Cub_2	/Lne	Line 3				3.86	1.33	0.95	0.11	43.90	Pv: 45.77 kW cLod: 0.01 Mvar L: 6.50 km

Grid: Grid	System Stage: Grid	Study Case: Study Case	Annex: / 2

		rated Voltage [kV]	Bus-voltage [p.u.]	Bus-voltage [kV]	Bus-voltage [deg]	Active Power [MW]	Reactive Power [Mvar]	Power Factor [-]	Current [kA]	Loading [%]	Additional Data
Bus 4											
		22.00	0.95	20.98	24.65						
Cub_3	/Lod	Load 5				0.75	0.25	0.95	0.02		P10: 0.75 MW Q10: 0.25 Mvar
Cub_1	/Lne	Line 5				1.41	0.45	0.95	0.04	16.29	Pv: 5.81 kW cLod: 0.01 Mvar L: 6.00 km
Cub_2	/Lne	Line 6				-2.16	-0.70	-0.95	0.06	24.95	Pv: 11.37 kW cLod: 0.01 Mvar L: 5.00 km

The load flow for the third configuration (Feeder B feeding the network with NOP closed) was successfully completed and converged after three iterations. The entire distribution system is supplied by feeder B, as shown in power flow Figure 4.8.

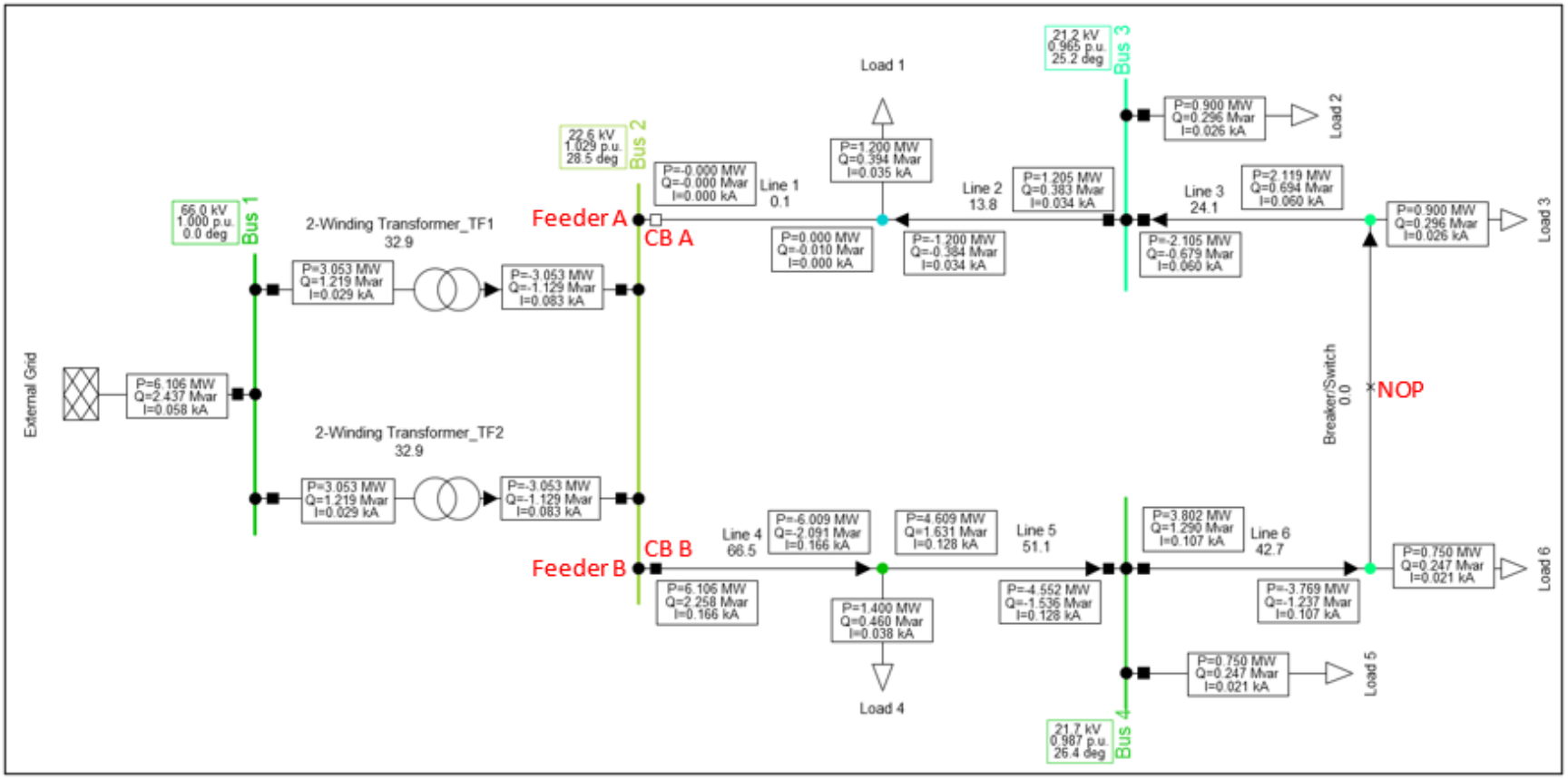

Figure 4.8: Load flow diagram using Feeder B as the source when the NOP is closed and Feeder A is open.

The simulation results for three-phase voltage and currents for configuration 3 with feeder B feeding the network with NOP closed are shown in Figure 4.9 below.

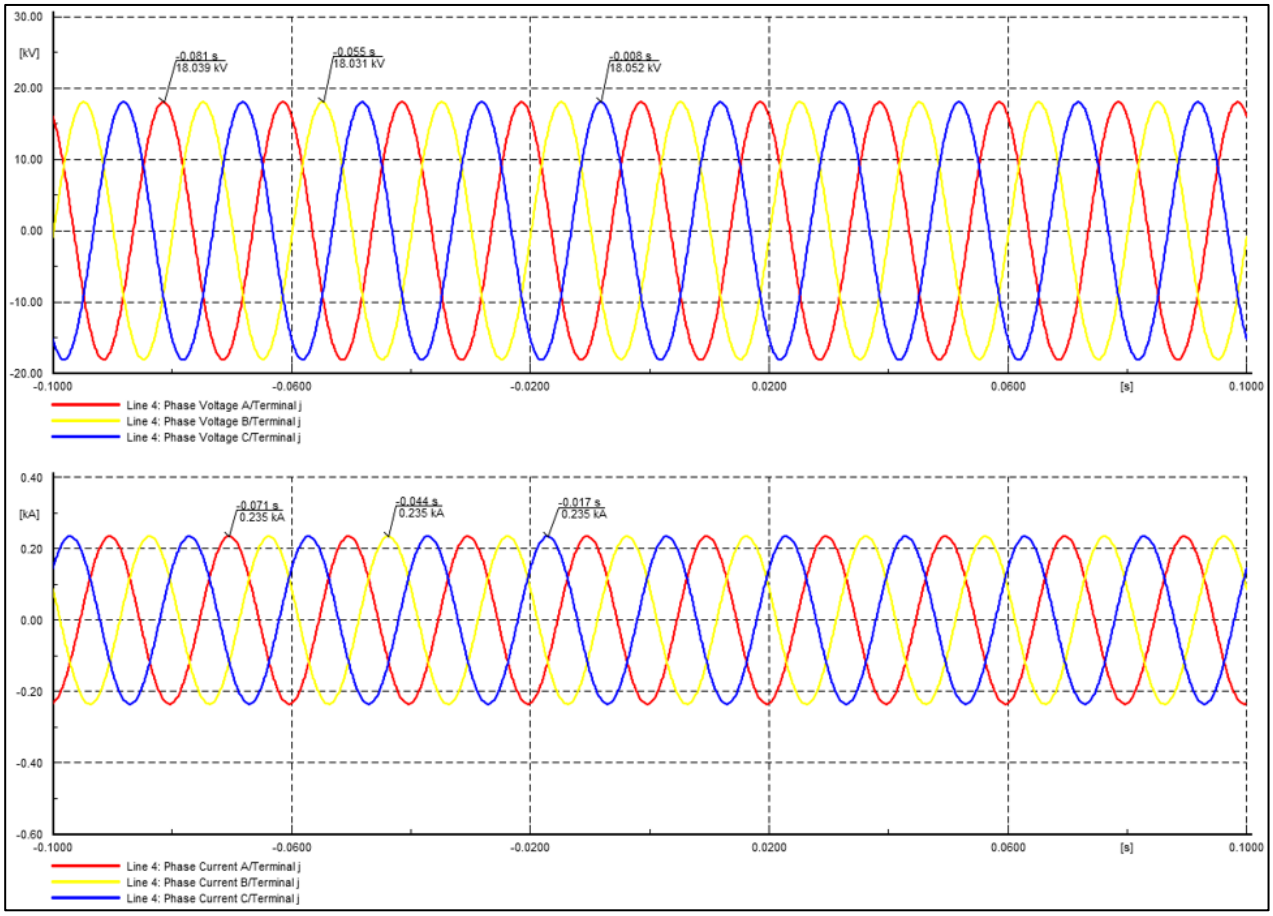

Figure 4.9: Feeder A's three-phase voltages and currents

The RMS magnitude of phase voltages and currents for line 4 corresponds to V_L = 18.039kV × $\frac{\sqrt{3}}{\sqrt{2}}$ = 22.09kV and $I_L = \frac{0.235kA}{\sqrt{2}}$ = 166.17A respectively.

Table 4.7 shows the network's voltage profile, which has a low voltage of 0.965 per unit and a high voltage of 1.029 per unit, indicating that the voltage profile of the simulated distribution network satisfies IEEE 141-1993 standard standards.

Table 4.7: Voltage profile of the distribution system network for configuration three

Grid: Grid	System Stage: Grid	Study Case: Study Case	Annex: / 3

	rtd.V [kV]	Bus - voltage [p.u.]	[kV]	[deg]	Voltage - Deviation [%] −10	−5	0	+5	+10
Bus 1									
	66.00	1.000	66.00	0.00					
Bus 2									
	22.00	1.029	22.63	28.53					
Bus 3									
	22.00	0.965	21.24	25.22					
Bus 4									
	22.00	0.987	21.71	26.40					

Table 4.8 shows the total load flow results for configuration three. The findings show the total real power, reactive power, and apparent power of the distribution system network. According to the load flow statistics, external grid generation supply 6.11 MW and reactive power support of 2.44 Mvar, with grid losses of 0.21MW.

Table 4.8: Summary of power flow results for configuration three

Load Flow Calculation				Grid Summary
AC Load Flow, balanced, positive sequence		Automatic Model Adaptation for Convergence		No
Automatic tap adjustment of transformers	No	Max. Acceptable Load Flow Error		
Consider reactive power limits	No	Bus Equations (HV)		1.00 kVA
		Model Equations		0.10 %

Grid: Grid	System Stage: Grid	Study Case: Study Case	Annex: / 1

Grid: Grid — Summary

No. of Substations	0	No. of Busbars	4	No. of Terminals	4	No. of Lines	6
No. of 2-w Trfs.	2	No. of 3-w Trfs.	0	No. of syn. Machines	0	No. of asyn.Machines	0
No. of Loads	6	No. of Shunts/Filters	0	No. of SVS	0		

Generation	=	0.00 MW	0.00 Mvar	0.00 MVA	
External Infeed	=	6.11 MW	2.44 Mvar	6.57 MVA	
Inter Grid Flow	=	0.00 MW	0.00 Mvar		
Load P(U)	=	5.90 MW	1.94 Mvar	6.21 MVA	
Load P(Un)	=	5.90 MW	1.94 Mvar	6.21 MVA	
Load P(Un-U)	=	0.00 MW	-0.00 Mvar		
Motor Load	=	0.00 MW	0.00 Mvar	0.00 MVA	
Grid Losses	=	0.21 MW	0.50 Mvar		
Line Charging	=		-0.06 Mvar		
Compensation ind.	=		0.00 Mvar		
Compensation cap.	=		0.00 Mvar		
Installed Capacity	=	0.00 MW			
Spinning Reserve	=	0.00 MW			
Total Power Factor:					
Generation	=	0.00 [-]			
Load/Motor	=	0.95 / 0.00 [-]			

Table 4.9 shows the power system data for configuration three. The system report includes active power, reactive power, transformer loading, and overhead line loading.

Table 4.9: Summary of the distribution system network for configuration three

Grid: Grid	System Stage: Grid	Study Case: Study Case	Annex: / 1

	rated Voltage [kV]	Bus-voltage [p.u.]	Bus-voltage [kV]	Bus-voltage [deg]	Active Power [MW]	Reactive Power [Mvar]	Power Factor [-]	Current [kA]	Loading [%]	Additional Data
Bus 1										
	66.00	1.00	66.00	0.00						
Cub_3 /Xnet	External Grid				6.11	2.44	0.93	0.06		Sk": 778.49 MVA
Cub_1 /Tr2	2-Winding Transfor				3.05	1.22	0.93	0.03	32.87	Tap: 2.00 Min: 1 Max: 17
Cub_4 /Tr2	2-Winding Transfor				3.05	1.22	0.93	0.03	32.87	Tap: 2.00 Min: 1 Max: 17
Bus 2										
	22.00	1.03	22.63	28.53						
Cub_1 /Tr2	2-Winding Transfor				-3.05	-1.13	-0.94	0.08	32.87	Tap: 2.00 Min: 1 Max: 17
Cub_3 /Lne	Line 1				-0.00	-0.00	-1.00	0.00	0.11	Pv: 0.00 kW cLod: 0.01 Mvar L: 7.00 km
Cub_4 /Lne	Line 4				6.11	2.26	0.94	0.17	66.46	Pv: 96.85 kW cLod: 0.01 Mvar L: 6.00 km
Cub_5 /Tr2	2-Winding Transfor				-3.05	-1.13	-0.94	0.08	32.87	Tap: 2.00 Min: 1 Max: 17
Bus 3										
	22.00	0.97	21.24	25.22						
Cub_3 /Lod	Load 2				0.90	0.30	0.95	0.03		P10: 0.90 MW Q10: 0.30 Mvar
Cub_1 /Lne	Line 2				1.20	0.38	0.95	0.03	13.78	Pv: 4.85 kW cLod: 0.01 Mvar L: 7.00 km
Cub_2 /Lne	Line 3				-2.10	-0.68	-0.95	0.06	24.05	Pv: 13.73 kW cLod: 0.01 Mvar L: 6.50 km

Grid: Grid	System Stage: Grid	Study Case: Study Case	Annex: / 2

	rated Voltage [kV]	Bus-voltage [p.u.]	Bus-voltage [kV]	Bus-voltage [deg]	Active Power [MW]	Reactive Power [Mvar]	Power Factor [-]	Current [kA]	Loading [%]	Additional Data
Bus 4										
	22.00	0.99	21.71	26.40						
Cub_3 /Lod	Load 5				0.75	0.25	0.95	0.02		P10: 0.75 MW Q10: 0.25 Mvar
Cub_1 /Lne	Line 5				-4.55	-1.54	-0.95	0.13	51.10	Pv: 57.26 kW cLod: 0.01 Mvar L: 6.00 km
Cub_2 /Lne	Line 6				3.80	1.29	0.95	0.11	42.73	Pv: 33.36 kW cLod: 0.01 Mvar L: 5.00 km

The distribution system under consideration is generally operated with two transformers in service. When one transformer fails or requires maintenance, the second transformer should be able to supply the entire distribution system's load. Appendix A depicts the load flow findings when just one transformer is in operation. The findings also show that the probability of consumers going out of service due to transformer failure or maintenance is reduced.

The load flow investigations in Table 4.10 below are based on three scenarios: 1) NOP open with CBs A and B closed, 2) Feeder A feeds the network with NOP closed, and 3) Feeder B feeds the network with NOP closed.

Table 4.10: Summary of the three simulation results

Load flow solutions	Scenario 1	Scenario 2	Scenario 3
	Voltage in p.u		
Bus 1 (Slack Bus)	1	1	1
Bus 2 (PV Bus)	1.03	1.028	1.029
Bus 3 (PQ Bus)	1.009	0.978	0.965

Bus 4 (PQ Bus)	1.013	0.954	0.987
	Transformer summary		
Transformer 1	2.98MW 1.08Mvar 0.94 PF 0.03kA 31.75% loading	3.08MW 1.26Mvar 0.92 PF 0.03kA 33.26% loading	3.05MW 1.22Mvar 0.93 PF 0.03kA 32.87% loading
Transformer 2			
	Line summary		
Line 1	3.04MW 1.02Mvar 0.95 PF 0.08kA 32.73% loading	6.15MW 2.34Mvar 0.93 PF 0.17kA 67.26% loading	0MW 0Mvar 1 PF 0kA 0.11% loading
Line 2	1.8MW 0.59Mvar 0.95 PF 0.05kA 19.72% loading	4.76MW 1.63Mvar 0.95 PF 0.14kA 54.04% loading	1.2MW 0.38Mvar 0.95 PF 0.03kA 13.78% loading
Line 3	0.9MW 0.29Mvar 0.95 PF 0.02kA 9.9% loading	3.86MW 1.33Mvar 0.95 PF 0.11kA 43.9% loading	2.1MW 0.68Mvar 0.95 PF 0.06kA 24.05% loading
Line 4	2.93MW 0.98Mvar 0.95PF 0.08kA 31.5% loading	0MW 0Mvar 1 PF 0kA 0.09% loading	6.11MW 2.26Mvar 0.94 PF 0.17kA 66.46% loading
Line 5	1.5MW 0.49Mvar 0.95 PF 0.04kA 16.35% loading	1.41MW 0.45Mvar 0.95 PF 0.04kA 16.35% loading	4.55MW 1.54Mvar 0.95 PF 0.13kA 51.1% loading
Line 6	0.75MW 0.24Mvar 0.95 PF 0.02kA 8.2% loading	2.16MW 0.7Mvar 0.95 PF 0.06kA 24.95% loading	3.8MW 1.29Mvar 0.95 PF 0.11kA 42.73% loading
	Load summary		
Load 1	1.2MW 0.394Mvar 0.95 PF 0.033kA	1.2MW 0.394Mvar 0.95 PF 0.033kA	1.2MW 0.394Mvar 0.95 PF 0.035kA
Load 2	0.9MW 0.3Mvar	0.9MW 0.3Mvar	0.9MW 0.3Mvar
Load 3	0.95 PF 0.025kA	0.95 PF 0.03kA	0.95 PF 0.03kA
Load 4	1.4MW 0.46Mvar 0.95 PF 0.038kA	1.4MW 0.46Mvar 0.95 PF 0.041kA	1.4MW 0.46Mvar 0.95PF 0.038kA

Load 5	0.75MW 0.25Mvar 0.95 PF 0.02kA	0.75MW 0.25Mvar 0.95 PF 0.02kA	0.75MW 0.25Mvar 0.95 PF 0.02kA
Load 6			
	External infeed and Grid losses summary		
External infeed	5.97MW 2.17Mvar 0.94 PF 0.06kA	6.15MW 2.53Mvar 0.92 PF 0.06kA	6.11MW 2.44Mvar 0.93 PF 0.06kA
Grid losses	0.07MW 0.23Mvar	0.25MW 0.59Mvar	0.21MW 0.5Mvar

4.4 Short circuit simulation

The DIgSILENT software tool was used in this chapter to perform short circuit analysis on the distribution system feeder. Various case studies on the used distribution network are carried out using the DIgSILENT software program. The three-phase short circuit current $I_{k1}^{"}$, double phase short circuit current $I_{k2}^{"}$, single phase to earth short circuit current $I_{kl}^{"}$ and the peak short circuit current I_p are all simulated and analyzed. Formulas to calculate these short circuits are presented in section 3.2.2 of chapter 3.

Short circuits are used in both feeders of the distribution system network, at the following locations: lines 1 and 3 on feeder A, and lines 4 and 6 on feeder B. The outcomes of all short circuits used will be discussed in the following sections.

4.4.1 Simulation of a three-phase short circuit on feeder A (line 1)

Table 4.11 shows the single-phase to ground short circuit simulated in line 1. The type of short circuit used is indicated in blue. The fault is indicated in green, and it is located between the red phase and ground. The single-phase to ground fault is applied at 1% of line 1, and the measured fault current is 5.81kA.

The findings of the three-phase short circuit in line 1 are shown in Table 4.12. The blue color indicates the type of fault, while the green color indicates that the fault affects all phases. A three-phase fault was also applied at 1% of the line, resulting in a fault current of 4.89kA.

Table 4.11: Single-phase to ground short circuit results for feeder A (line 1)

Short-Circuit Calculation IEC 60909					Single Phase to Ground			/ Max. Short-Circuit Currents		
Asynchronous Motors Always Considered		Grid Identification Automatic			Short-Circuit Duration Break Time				0.10 s	
					Fault Clearing Time (Ith)				1.00 s	
		Conductor Temperature User Defined		No	Voltage factor c Voltage factor c				Standard	
Fault Distance from Line:	Terminal i: \sntsh\Dx network\Network Model\Network Data\Grid\Line 1	... ork Model\Network Data\Grid\Bus 2			Absolute Relative				0.07 km 1.00 %	
Grid: Grid					System Stage: Grid					

		rtd.V. [kV]	Voltage [kV]	Voltage [deg]	c- Factor	Sk" [MVA]	Ik" [kA]	Ik" [deg]	ip [kA]	Ib [kA]	Sb [MVA]	EFF [-]
Fault Location:												
Line 1	A	0.00	0.00	1.10	73.80	5.81	-87.99	15.77	5.81	73.80	0.00	
	B	12.76	-109.92		0.00	0.00	0.00	0.00	0.00	0.00	0.91	
	C	12.96	109.59		0.00	0.00	0.00	0.00	0.00	0.00	0.93	

Table 4.12: Three-phase short circuit results for feeder A (line 1)

Short-Circuit Calculation IEC 60909					3-Phase Short-Circuit			/ Max. Short-Circuit Currents		
Asynchronous Motors Always Considered		Grid Identification Automatic			Short-Circuit Duration Break Time				0.10 s	
					Fault Clearing Time (Ith)				1.00 s	
Decaying Aperiodic Component (idc) Using Method	B	Conductor Temperature User Defined		No	Voltage factor c Voltage factor c				Standard	
Fault Distance from Line:	Terminal i: \sntsh\Dx network\Network Model\Network Data\Grid\Line 1	... ork Model\Network Data\Grid\Bus 2			Absolute Relative				0.07 km 1.00 %	
Grid: Grid					System Stage: Grid					

	rtd.V. [kV]	Voltage [kV]	Voltage [deg]	c- Factor	Sk" [MVA]	Ik" [kA]	Ik" [deg]	ip [kA]	Ib [kA]	Sb [MVA]	Ik [kA]	Ith [kA]
Fault Location:												
Line 1	0.00	0.00	1.10	186.21	4.89	-88.36	13.27	4.89	186.21	4.89	5.17	

4.4.2 Feeder A has a single-phase to ground short circuit and a three-phase short circuit at line 3

Table 4.13 shows the results of the single-phase to ground short circuit simulation at line 3. The type of short circuit used is indicated in blue. The fault is indicated in green, and it is located between the red phase and ground. The fault is located at 1% of line 3, and the generated fault current is 1kA.

The findings of the three-phase short circuit in line 3 are shown in Table 4.14. The blue color indicates the type of fault, while the green color indicates that the fault affects all phases. The three-phase fault was also used at 1% of the line and generated 1.68kA.

Table 4.13: Single-phase to ground short circuit results for feeder A (line 3)

Short-Circuit Calculation IEC 60909					Single Phase to Ground			/ Max. Short-Circuit Currents			
Asynchronous Motors Always Considered		Grid Identification Automatic			Short-Circuit Duration Break Time				0.10 s		
					Fault Clearing Time (Ith)				1.00 s		
		Conductor Temperature User Defined		No	Voltage factor c Voltage factor c				Standard		
Fault Distance from Line:	Terminal i: ... ork Model\Network Data\Grid\Bus 3 \sntsh\Dx network\Network Model\Network Data\Grid\Line 3				Absolute Relative				0.06 km 1.00 %		
Grid: Grid					System Stage: Grid						
	rtd.V. [kV]	Voltage [kV]	[deg]	c- Factor	Sk" [MVA]	Ik" [kA]	[deg]	ip [kA]	Ib [kA]	Sb [MVA]	EFF [-]
Fault Location:											
Line 3	A	0.00	0.00	1.10	12.73	1.00	-75.46	1.92	1.00	12.73	0.00
	B	18.04	-134.55		0.00	0.00	0.00	0.00	0.00	0.00	1.29
	C	17.00	138.14		0.00	0.00	0.00	0.00	0.00	0.00	1.22

Table 4.14: Three-phase short circuit results for feeder A (line 3)

Short-Circuit Calculation IEC 60909					3-Phase Short-Circuit				/ Max. Short-Circuit Currents				
Asynchronous Motors Always Considered		Grid Identification Automatic			Short-Circuit Duration Break Time					0.10 s			
					Fault Clearing Time (Ith)					1.00 s			
Decaying Aperiodic Component (idc) Using Method	B	Conductor Temperature User Defined		No	Voltage factor c Voltage factor c					Standard			
Fault Distance from Line:	Terminal i: ... ork Model\Network Data\Grid\Bus 3 \sntsh\Dx network\Network Model\Network Data\Grid\Line 3				Absolute Relative					0.06 km 1.00 %			
Grid: Grid					System Stage: Grid								
	rtd.V. [kV]	Voltage [kV]	[deg]	c- Factor	Sk" [MVA]	Ik" [kA]	[deg]	ip [kA]	Ib [kA]	Sb [MVA]	Ik [kA]	Ith [kA]	
Fault Location:													
Line 3	0.00	0.00	1.10	64.02	1.68	-70.24	3.22	1.68	64.02	1.68	1.69		

4.4.3 Feeder B has a single-phase to ground short circuit and a three-phase short circuit at line 4

Table 4.15 shows the results of a single-phase to ground short circuit simulation at line 4. The type of short circuit used is indicated in blue. The fault is indicated in green, and it is located between the red phase and ground. The fault is applied at 1% of line 4, and the fault current generated is 5.83kA.

The findings of the three-phase short circuit on line 4 are shown in Table 4.16. The blue color indicates the type of fault, while the green color indicates that the fault affects all phases. The three-phase fault was applied to 1% of the line, resulting in a fault current of 4.89kA.

Table 4.15: A Single-phase to ground short circuit occurs on feeder B at line 4

Short-Circuit Calculation IEC 60909					Single Phase to Ground			/ Max. Short-Circuit Currents	
Asynchronous Motors		Grid Identification			Short-Circuit Duration				
Always Considered		Automatic			Break Time			0.10 s	
					Fault Clearing Time (Ith)			1.00 s	
		Conductor Temperature			Voltage factor c				
		User Defined		No	Voltage factor c			Standard	
Fault Distance from	Terminal i:	... ork Model\Network Data\Grid\Bus 2			Absolute			0.06 km	
Line:	\sntsh\Dx network\Network Model\Network Data\Grid\Line 4				Relative			1.00 %	
Grid: Grid					System Stage: Grid				

		rtd.V. [kV]	Voltage [kV]	Voltage [deg]	c- Factor	Sk" [MVA]	Ik" [kA]	Ik" [deg]	ip [kA]	Ib [kA]	Sb [MVA]	EFF [-]
Fault Location:												
Line 4	A	0.00	0.00	1.10		74.05	5.83	-88.04	15.84	5.83	74.05	0.00
	B	12.75	-109.77			0.00	0.00	0.00	0.00	0.00	0.00	0.91
	C	12.94	109.45			0.00	0.00	0.00	0.00	0.00	0.00	0.93

Table 4.16: Feeder B endured from a three-phase short circuit at line 4

Short-Circuit Calculation IEC 60909					3-Phase Short-Circuit			/ Max. Short-Circuit Currents	
Asynchronous Motors		Grid Identification			Short-Circuit Duration				
Always Considered		Automatic			Break Time			0.10 s	
					Fault Clearing Time (Ith)			1.00 s	
Decaying Aperiodic Component (idc)		Conductor Temperature			Voltage factor c				
Using Method	B	User Defined		No	Voltage factor c			Standard	
Fault Distance from	Terminal i:	... ork Model\Network Data\Grid\Bus 2			Absolute			0.06 km	
Line:	\sntsh\Dx network\Network Model\Network Data\Grid\Line 4				Relative			1.00 %	
Grid: Grid					System Stage: Grid				

	rtd.V. [kV]	Voltage [kV]	Voltage [deg]	c- Factor	Sk" [MVA]	Ik" [kA]	Ik" [deg]	ip [kA]	Ib [kA]	Sb [MVA]	Ik [kA]	Ith [kA]
Fault Location:												
Line 4	0.00	0.00	1.10		186.45	4.89	-88.40	13.29	4.89	186.45	4.89	5.18

4.4.4 Feeder B has a single phase to ground short circuit and a three-phase short circuit at line 6

Table 4.17 displays the simulation results for the short circuit simulated on line 6. The type of short circuit used is indicated in blue. The fault is indicated in green, and it is located between the red phase and ground. The fault is applied at 1% of line 6, with a fault current of 1.1kA.

The findings of the three-phase short circuit on line 6 are shown in Table 4.18. The blue color indicates the type of fault, while the green color indicates that the fault affects all phases. A three-phase fault was also applied at 1% of line 6, resulting in a fault current of 1.86kA.

Table 4.17: Single-phase to ground short circuit results for feeder B (line 6)

Short-Circuit Calculation IEC 60909	Single Phase to Ground	/ Max. Short-Circuit Currents
Asynchronous Motors Always Considered	Grid Identification: Automatic	Short-Circuit Duration: Break Time 0.10 s; Fault Clearing Time (Ith) 1.00 s
	Conductor Temperature: User Defined No	Voltage factor c: Voltage factor c Standard
Fault Distance from Line:	Terminal i: ... ork Model\Network Data\Grid\Bus 4 \sntsh\Dx network\Network Model\Network Data\Grid\Line 6	Absolute 0.05 km; Relative 1.00 %

Grid: Grid | System Stage: Grid

		rtd.V. [kV]	Voltage [kV]	Voltage [deg]	c-Factor	Sk" [MVA]	Ik" [kA]	Ik" [deg]	ip [kA]	Ib [kA]	Sb [MVA]	EFF [-]
Fault Location: Line 6	A		0.00	0.00	1.10	14.46	1.14	-75.81	2.21	1.14	14.46	0.00
	B		17.83	-134.20		0.00	0.00	0.00	0.00	0.00	0.00	1.28
	C		16.88	137.44		0.00	0.00	0.00	0.00	0.00	0.00	1.21

Table 4.18: Feeder B suffer from a three-phase short circuit at line 6

Short-Circuit Calculation IEC 60909	3-Phase Short-Circuit	/ Max. Short-Circuit Currents
Asynchronous Motors Always Considered	Grid Identification: Automatic	Short-Circuit Duration: Break Time 0.10 s; Fault Clearing Time (Ith) 1.00 s
Decaying Aperiodic Component (idc) Using Method B	Conductor Temperature: User Defined No	Voltage factor c: Voltage factor c Standard
Fault Distance from Line:	Terminal i: ... ork Model\Network Data\Grid\Bus 4 \sntsh\Dx network\Network Model\Network Data\Grid\Line 6	Absolute 0.05 km; Relative 1.00 %

Grid: Grid | System Stage: Grid

	rtd.V. [kV]	Voltage [kV]	Voltage [deg]	c-Factor	Sk" [MVA]	Ik" [kA]	Ik" [deg]	ip [kA]	Ib [kA]	Sb [MVA]	Ik [kA]	Ith [kA]
Fault Location: Line 6		0.00	0.00	1.10	70.89	1.86	-71.22	3.61	1.86	70.89	1.86	1.87

Table 4.19 summarizes the short circuit simulation findings for all of the faults simulated for the distribution system network described above. The results of the short circuit simulation show the amount of fault current where the protection devices will be fitted. Table 4.19 shows a summary of three-phase and single-phase faults in the distribution network, along with their locations.

Table 4.19: Results of short circuit simulation for distribution system feeders A and B upstream and downstream

Fault type	Fault location	$S_k^{"}$ (MVA)	$I_{k1}^{"}$ (kA)
Single-phase to ground fault	Feeder A (Line 1 at 1%)	73.8	5.81
Three-phase fault	Feeder A (Line 1 at 1%)	186.21	4.89
Single-phase to ground fault	Feeder A (Line 3 at 1%)	12.73	1.0
Three-phase fault	Feeder A (Line 3 at 1%)	64.02	1.68
Single-phase to ground fault	Feeder B (Line 4 at 1%)	74.05	5.83
Three-phase fault	Feeder B (Line 4 at 1%)	186.45	4.89
Single-phase to ground fault	Feeder B (Line 6 at 1%)	14.46	1.14
Three-phase fault	Feeder B (Line 6 at 1%)	70.89	1.86

The fault current results show the short circuit currents with respective fault locations, where the protection relays are situated.

4.4.5 Current transformer (CT) selection

According to IEEE Std C37.110-1996, the maximum design load current of a power system network should not exceed the rated CT primary current when using current transformers for protection relaying reasons. To reduce wiring weight and provide the best capability and performance, the highest CT ratio permissible should typically be chosen. Under maximum symmetrical primary fault current, the CT ratio should be large enough that the CT secondary current should not exceed 20 times the rated current (IEEE Std C37.110, 1996).

The CT ratio chosen is 300:1. When Feeder A supplies the whole distribution system, as shown in Figure 4.6 with 168A, the highest feasible load current of the investigated distribution system network is reached. Because it is less than CT primary current, this current conforms with the IEEE guidelines. As shown in Table 4.19, the maximum symmetrical three-phase fault current of the analyzed distribution system network is 4.89kA. If the maximum symmetrical fault current is divided by the CT ratio (4.89kA/300 = 16.3A), the rated current is less than 20 times the maximum symmetrical primary fault current.

When a single phase to ground fault is simulated, the maximum fault current is the highest. This value is 5.83kA, as given in Table 4.19 above. When the maximum fault current is divided by the CT ratio (5.83kA/300 = 19.43A), the result is less than 20 times the rated CT secondary current. All four reclosing relays utilized in this Chapter have a CT ratio of 300:1.

4.5 Overcurrent protection configuration settings

This section contains overcurrent protection configuration settings, relay location, stage, type of characteristic curve utilized, pick up current, time dial, and direction. The overcurrent protection settings for relays 1, 2, 3, and 4 are shown in tables 4.20 to 4.23 below. For protective relay applications to distribution lines, the pickup currents were established in accordance with IEEE Std C37.110-1996. Phase overcurrent protection elements in accordance with ANSI codes 50, 51, or 67 detect single-phase, double-phase, and three-phase overcurrent. The earth fault protection element and its ANSI code 50N, 51N, 50G, or 51G detect earth faults. When the fault current exceeds the relay threshold, the Protection function executes the procedure. Because the virtual DIgSILENT version of digital relays is employed, the grading margin between the upstream and downstream relay is 0.3 seconds. Section 3.4 of Chapter 3 goes over how to choose a grading margin.

Table 4.20: Configuration of the Relay 1 phase and residual overcurrent elements

Prote-ction device name	Branch	Stage (Phase /Residual)	Characte-ristic curve	I Pick up primary	I Pick up Secondary With CT ratio 300:1	Time dial	Direction
Relay 1	Line 1	51P	IEC Normal inverse	168×1.5 = 252A	0.84A	0.13	Non-Directional
		67P1	IEC Definite time	3900A	13A	0	
		51G	IEC Normal inverse	252×0.25 = 63A	0.21A	0.17	

Table 4.21: Configuration of the Relay 2 phase and residual overcurrent elements

Prote-ction device name	Branch	Stage (Phase)	Characte-ristic curve	I Pick up primary	I Pick up Secondary With CT ratio 300:1	Time dial	Direction
Relay 2	Line	51P	IEC Normal inverse	135×1.5 = 202.5A	0.68A	0.05	Non-Directional
		51G		202.5×0.25 =50.63A	0.17A		

Table 4.22: Configuration of the Relay 3 phase and residual overcurrent elements

Prote-ction device name	Branch	Stage (Phase)	Characte-ristic curve	I Pick up primary	I Pick up Secondary with CT ratio 300:1	Time dial	Direction
Relay 3	Line 4	51P	IEC Normal inverse	166×1.5 = 249A	0.83A	0.13	Non-Directional
		67P1	IEC Definite time	3900A	13A	0	
		51G	IEC Normal inverse	249×0.25 =62.25A	0.21A	0.16	

Table 4.23: Configuration of the Relay 4 phase and residual overcurrent elements

Protection device name	Branch	Stage (Phase)	Characteristic curve	I Pick up primary	I Pick up Secondary With CT ratio 300:1	Time dial	Direction
Relay 4	Line 5	51P	IEC Normal inverse	128×1.5 = 192A	0.64A	0.05	Non-Directional
		51G		192×0.25 =192A	0.16A		

In Figure 4.10, the relay locations of the 22kV distribution system are shown. Feeder A is protected by Relay 1 in the event of a fault between lines 1 and 2. Feeder A is protected by Relay 2 in the event of a fault between line 3 and NOP. Relay 3 protects feeder B in the event of a fault between lines 4 and 5. Relay 4 protects feeder B in the event of a fault between line 6 and the NOP.

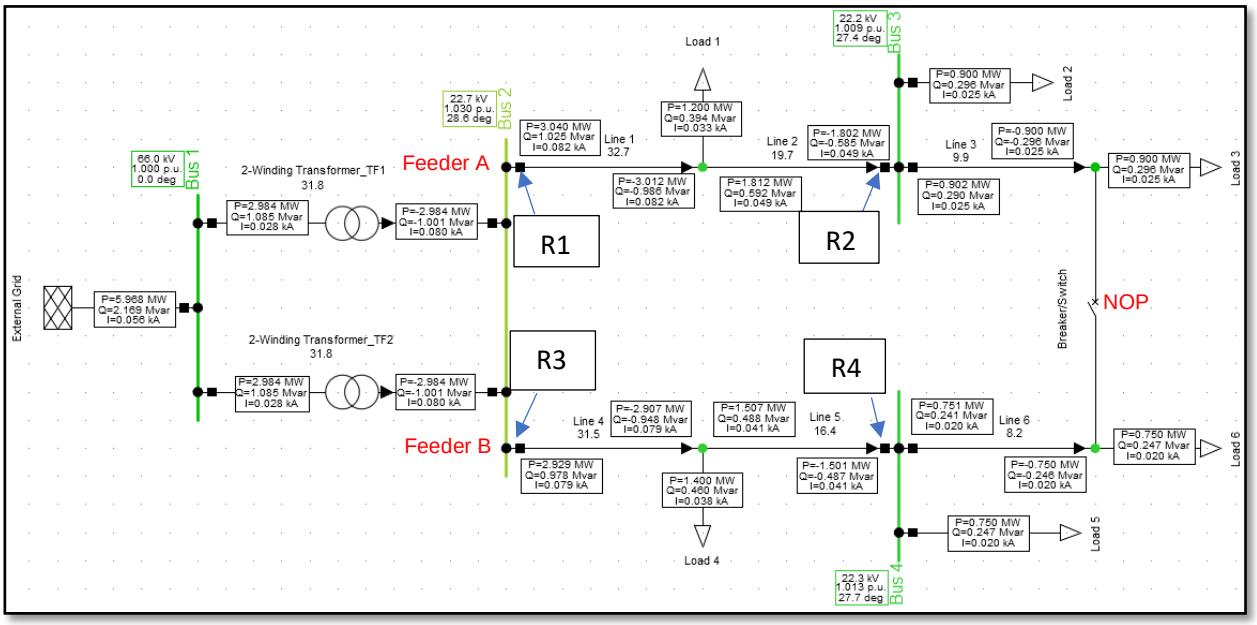

Figure 4.10: Protection devices for a 22kV distribution system with 1 to 4 relays

Distribution system automation, as defined by the Institute of Electrical and Electronic Engineers (IEEE), is a system that allows an electric power utility to monitor, coordinate, and operate distribution components in real-time from a remote location. The scope of the distribution system automation is determined by the geographical and demographic characteristics of the service region in question, as well as the characteristics of the existing distribution system network (Koozehkanani, Salemi and Sadr, 2015). To assist analysis, distribution system automation can be grouped into three categories:

Substation automation, Feeder automation, and Customer automation, according to the various classifications.

The protection of feeders is the focus of this chapter. The automation of feeders is a component of distribution automation. Data acquisition and supervisory control of line equipment, FDIR via reclosers, Volt/VAR via voltage regulators and capacitor bank, sectionalizers, and switches are all part of the distribution system automation at the feeder (Sardina, 2015).

This chapter focuses on the overcurrent and auto-reclose functions, which are used in Chapter 5, Section 5.4, to achieve FDIR using SEL-351 IEDs. The following steps can be used to achieve FDIR:

1. Fault detection: The first stage is to identify a fault, which is caused by protection devices (Intelligent Electronic Devices, IED or recloser). After the faulty feeder has been tripped, the faulty section of the tripped feeder must be removed. The part of the feeder line between reclosers or IEDs is referred to as a faulty section.
2. Fault Isolation: Once the problematic piece of the feeder has been identified, both sides of the fault must be isolated using reclosers or IEDs.
3. Estimation is required after isolating the faulty section of the feeder and before power is restored to the faultless section to evaluate if power can be restored to a healthy feeder.

4.6 Case studies

Four case studies were simulated on DIgSILENT software to assess the performance of the overcurrent auto-reclose scheme for the distribution system. The performance of each overcurrent relay in the considered distribution network shown in Figure 4.1 was investigated in the following scenarios.

1. Case one: A three-phase fault and a single-phase to ground fault on Feeder A between relays R1 and relay R2
2. Case two: A three-phase fault and a single-phase to ground fault on Feeder A between relays R2 and NOP

3. Case three: A three-phase fault and a single-phase to ground on Feeder B between relays R3 and relay R4
4. Case three: A three-phase fault and a single-phase to ground on Feeder B between relays R4 and NOP

Three reclosing attempts were used in this thesis. For the first initial reclose, the second trip to reclose, and the third trip to reclose, the dead time intervals are 3 seconds, 10 seconds, and 10 seconds, respectively. Section 3.5.2 of Chapter 3 discusses the selection of reclosing attempts and open intervals.

4.6.1 Case one: Three-phase fault and single-phase to ground fault on Feeder A between relays 1 and relay 2

4.6.1.1 Three-phase fault on Feeder A between relays 1 and relay 2

Using the EMT simulation study mentioned below, this case study aims to analyze the SEL-351 overcurrent relay characteristics and auto-reclose feature using DIgSILENT software. A three-phase short circuit is created by simulating a three-phase short circuit between busbars 2 and 3 (Line 1-Line 2) of feeder A. It is intended that if a transient fault develops at this section of the line, power will be restored when the SEL-351 relay is reset (relay R1). When a three-phase permanent fault occurs at this section of the line, relay R1 is expected to auto-reclose three times, and if the fault persists, relay R1 is expected to lockout, send an open signal to SEL-351 (relay R2) downstream at busbar 3, and send a close signal to the NOP to back feed the section of the line between busbar 3 (Line 3) and NOP.

An EMT simulation was run for 25.5 seconds in DIgSILENT to emulate the aforementioned auto-reclose function. At 0.1 seconds, a three-phase fault was introduced in the section of the line and cleared after 0.385 seconds. Because the initial reclose occurred after 3 seconds, the entire Feeder A line was dead for 3 seconds. Feeder A has another 10 seconds of dead-time. The fault was still simulated, and after 0.385 seconds, a second reclose happened, and the fault was cleared. Feeder A has another 10 seconds of dead-time. After 0.385 seconds, the fault was still simulated and cleared. It is evidence that the fault is permanent after three reclosure attempt, and the relay will trip and lockout. Table 4.24 contains an overview of the auto-reclose sequence depicted in Figure 4.11. Figure 4.11 depicts the usual load current prior to the fault being

introduced between 0 and 0.1 seconds, as well as the three reclosures attempts until the lockout stage.

Table 4.24: Auto-reclose operation for a three-phase fault on Feeder A between relays R1 and R2 (between Line 1-Line 2)

Recloser operation modes	Dead Time	Fault current	Fault initiated	Fault cleared	Fault duration
Recloser first attempt	-	2536.76 A	0.1s	0.485s	0.385s
Recloser second attempt	3s	2536.76 A	3.485s	3.87s	0.385s
Recloser third attempt	10s	2536.76 A	13.87s	14.255s	0.385s
Recloser fourth attempt	10s	2536.76 A	24.255s	24.255	0.385s

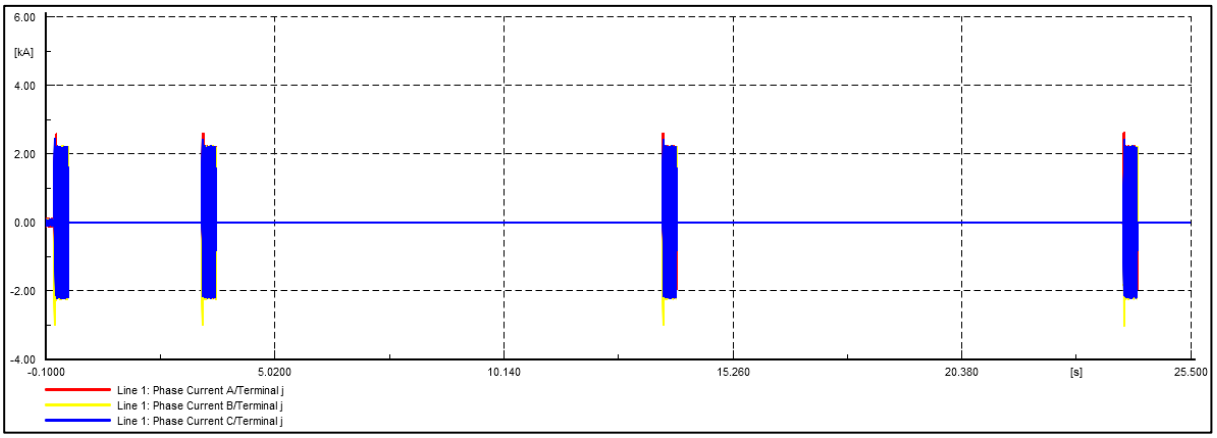

Figure 4.11: Auto-reclose simulation results for a three-phase fault between relays R1 and relay R2

Figure 4.12 depicts the power flow results on the distribution network after a fault was introduced in feeder A at 50% of the line between relays (R1) and (R2). It is seen that when R1 is triggered and the circuit breaker is opened, feeder A is out of supply from the outgoing of the feeder till the normal open point (NOP). It is also seen that the fault impacts the segment of the line between R2 and NOP, despite the fact that that segment of the line is fault-free. Customers lying between line sections R2 and NOP are thus unduly affected. As a result, there is a requirement to automatically configure the distribution network and supply consumers located between R2 and NOP via feeder B. Only feeder B receives power from the outgoing feeder until the NOP, as shown by the

power flow arrows in Figure 4.12. It should be noted that the network reconfiguration in this chapter was accomplished through the use of EMT simulations.

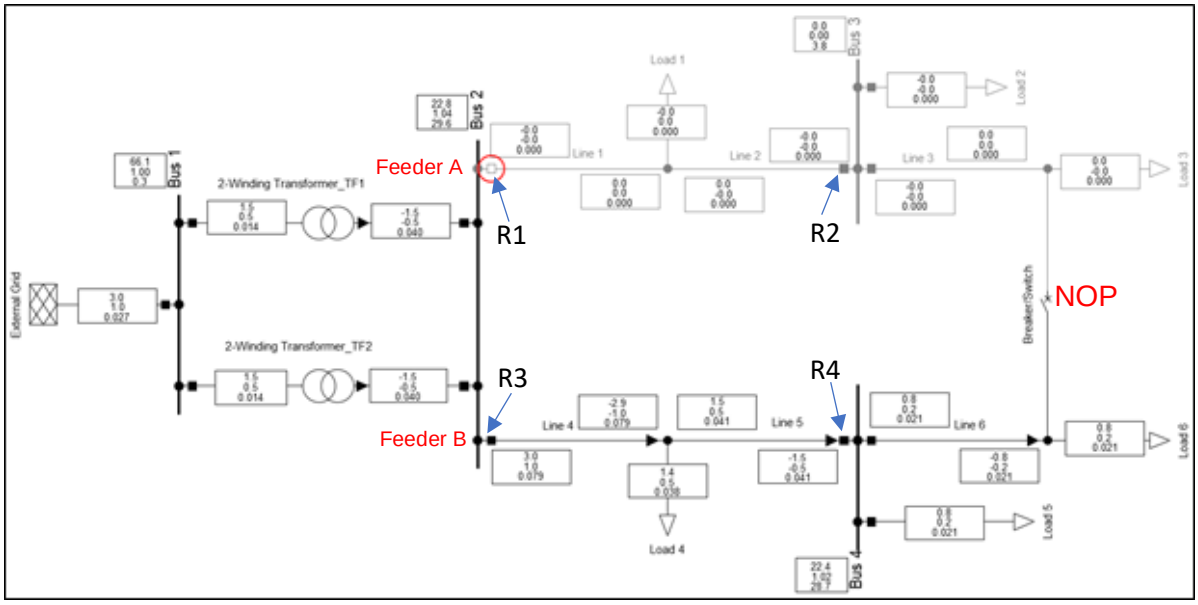

Figure 4.12: Power flow simulation results as a result of a fault occurs between relays 1 and 2

Figure 4.13 depicts a three-phase current for line 3 (the segment between R2 and NOP) after a permanent fault between busbars 2 and 3 occurred. Figure 4.9 shows that a normal load current of 0.035kA was flowing between 0 and 0.1 seconds. When the fault was introduced at 0.1 seconds, the auto-reclose cycle happened, R1 locked out and R2 opened, the NOP closed, and feeder B back fed line 3 via the NOP. Figure 4.9 further shows that once the auto-reclose cycle was finished and the faulty section was separated, normal load current was flowing on line 3 to supply loads 2 and 3.

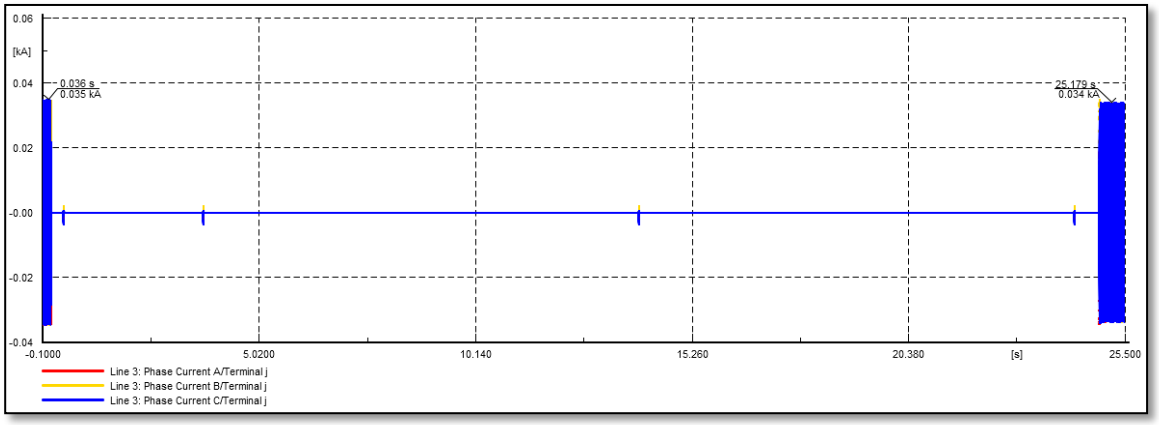

Figure 4.13: Power flow simulation results as a back feed for the line section between busbar 3 and NOP (line 3)

Figure 4.14 depicts the power flow after the faulty section of the line between busbars 2 and 3 was disconnected. The power flow arrows show that electricity flows from feeder B to line 3 via the NOP, supplying loads 2 and 3.

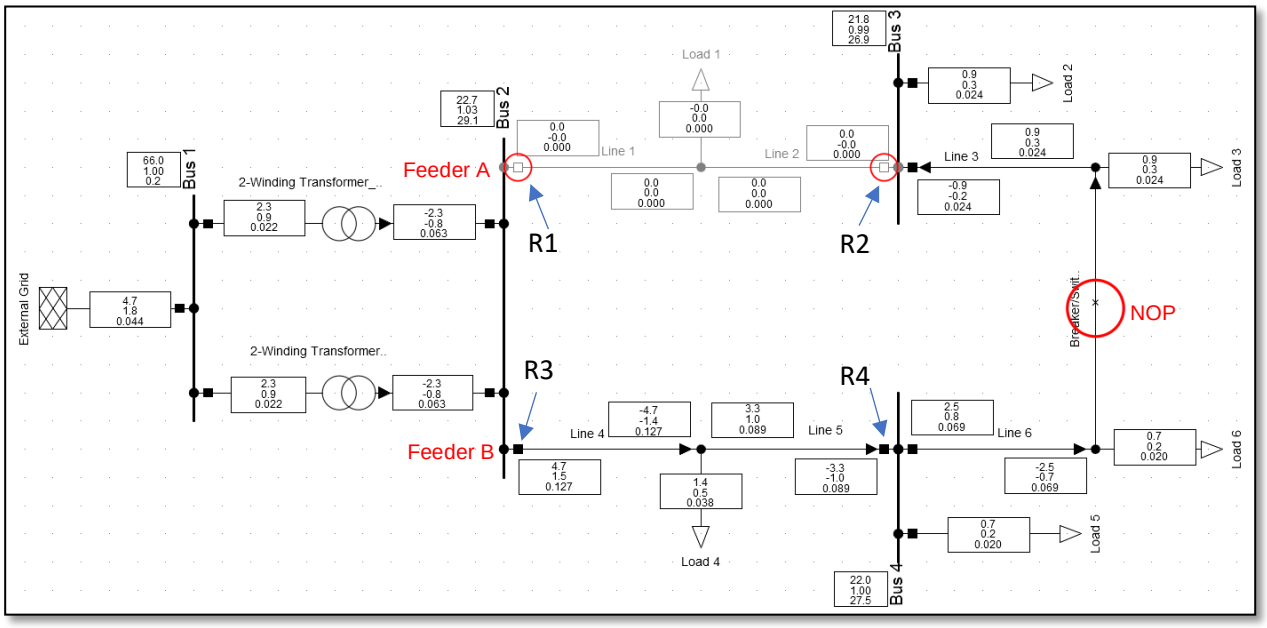

Figure 4.14: Power flow simulation results after isolating the line busbars 2 and 3

Table 4.25: Response of Relay R1 to a three-phase short circuit between Relays R1 and R2.

Grid: Grid	System Stage: Grid	Study Case: Study Case	Annex: / 1

Relay 1(IED1)	Relay Type : SEL 351-1A-300V					
Ct : Current Transformer	Location : Busbar	: Bus 2	/	Ratio	: 300A/1A	
	Branch	: Line 1		Connection	: Y	
CoreCt: Current Transformer	Location : Busbar	: Bus 2	/	Ratio	: 300A/1A	
	Branch	: Line 1		Connection	: Y	
51P : 51P	(IEC: I>t ANSI: 51)		Current [sec.A]	[pri.A]		Tripping Time
Current Setting :	0.840 sec.A 252.00 pri.A 0.840 p.u.		A : 8.456	2536.76		0.385 s
Time Dial :	0.130 Time Shift : 1.000		B : 8.456	2536.76		
Characteristic :	C1 - IEC Class A (Standard Inverse)		C : 8.456	2536.76		
67P1 : 67P1	(IEC: I>> ANSI: 50)		Tripping Current	[pri.A]		Tripping Time
Pickup Current :	13.000 sec.A 3900.00 pri.A 13.000 p.u.		A : 8.456	2536.76		9999.999 s
Time Setting :	0.000 s		B : 8.456	2536.76		
Total Time :	0.020 s		C : 8.456	2536.76		
51G : 51G	(IEC: IE>t ANSI: 51N)		Tripping Current	[pri.A]		Tripping Time
Current Setting :	0.210 sec.A 63.00 pri.A 0.210 p.u.		0.000	0.00		9999.999 s
Time Dial :	0.160 Time Shift : 1.000					
Characteristic :	C1 - IEC Class A (Standard Inverse)					
Logic : Logic						
Breaker	Cubicle	Branch	Busbar	/ Substation	Fault Clearing Time	

Overcurrent protection settings are provided in section 4.5. Tables 4.20 to 4.23 show the setup options for the overcurrent relays (R1 to R4). The operation of the relays is thoroughly examined in this section. The tripping time for R1 for a three-phase secondary fault current of 8.456 A is shown in Table 4.25. At 0.385 seconds, the inverse time

overcurrent phase element (51P) was operational. The definite time phase overcurrent element (67P1) and the inverse time residual element (51G) both did not issue trip signals. Because the fault current is less than the 67P1 pick up current, 67P1 did not operate (13A secondary). 51G elements only operate for ground faults; in this situation, 51G did not operate because it was a phase fault. The time stamp 9999.999s indicates that the relay did not operate in accordance with the DIgSILENT relay programming (DIgSILENT, 2020).

The overcurrent curve used to examine the performance of relay R1 is shown in Figure 4.15 below. The inverse time overcurrent element (51P1) operated at 0.385 seconds, as shown in the curve. The operational time of the definite time element (67P1) is 9999.999s because it did not operate.

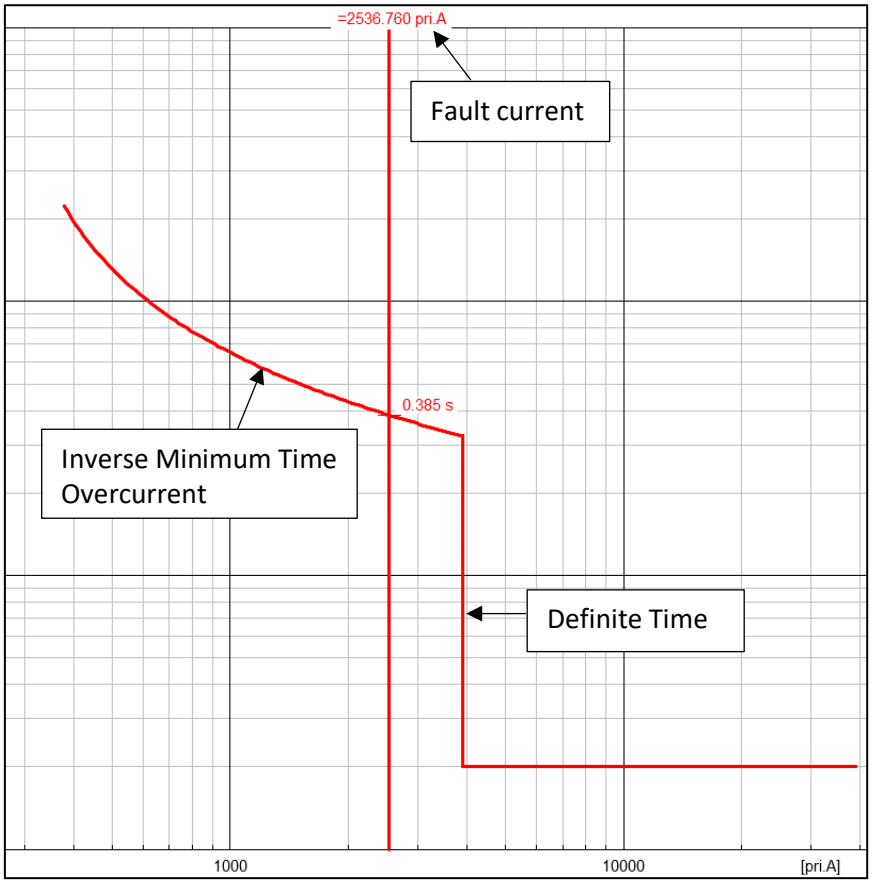

Figure 4.15: Relay R1 responds to a three-phase fault on the line section between relays R1 and R2

4.6.1.2 Single-phase to ground fault between relays R1 and relay R2

The overcurrent relay operation to a single phase to ground fault on the line between relays R1 and R2 on feeder A is investigated in this case study. The auto-reclose function is not programmed for ground faults in this protection study due to safety aspects of humans and animals. When there is a ground fault, the relay is set to trip and isolate the faulty section of the line.

The tripping duration for the single-phase to ground fault simulated between the red phase and ground is shown in Table 4.26. At 0.348 seconds, the residual inverse time overcurrent element (51G) was operational. The primary fault current is 1727.7A, whereas the secondary fault current is 5.757A.

Table 4.26: Relay R1 response to a single-phase ground fault between busbars 2 and 3

```
| Relay 1(IED1)                  Relay Type : SEL 351-1A-300V                                                          |
|   Ct    : Current Transformer  Location   : Busbar       : Bus 2              /                 Ratio       : 300A/1A  |
|                                             Branch       : Line 1                               Connection  : Y        |
|                                                          :                                                          |
|   CoreCt: Current Transformer  Location   : Busbar       : Bus 2              /                 Ratio       : 300A/1A  |
|                                             Branch       : Line 1                               Connection  : Y        |
|                                                          :                                                          |
|   51G     : 51G                ( IEC: IE>t  ANSI: 51N  )         Tripping Current       [pri.A]           Tripping Time |
|     Current Setting :   0.210 sec.A     63.00 pri.A   0.210 p.u.              5.757       1727.10              0.348 s  |
|     Time Dial       :   0.170     Time Shift  :   1.000                                                              |
|     Characteristic  :   C1 - IEC Class A (Standard Inverse)                                                          |
|   Logic     : Logic                                                                                 :                |
|     Breaker           Cubicle      Branch                  Busbar               / Substation       Fault Clearing Time |
|      Switch            Cub_3        Line 1                  Bus 2               /                            0.348 s  |
|   load enc i threshold threshold ( IEC: I>>   ANSI: 50   )         Tripping Current       [pri.A]           Tripping Time |
|     Pickup Current  :   0.100 sec.A     30.00 pri.A   0.100 p.u.              1.918        575.50              0.001 s  |
|     Time Setting    :   0.000 s                                                                                      |
|     Total Time      :   0.001 s                                                                                      |
```

The residual overcurrent curve used to examine the performance of relay R1 is shown in Figure 4.16 below. The residual inverse time overcurrent element (51G) operated at 0.348 seconds, as shown on the curve.

The resulting power flow diagram for a single-phase to ground fault between busbars 2 and 3 is identical to the one shown in Figure 4.14. Because the auto-reclose mechanism is not configured for ground faults, R1 trips on the first attempt of a temporary or permanent ground fault in the network.

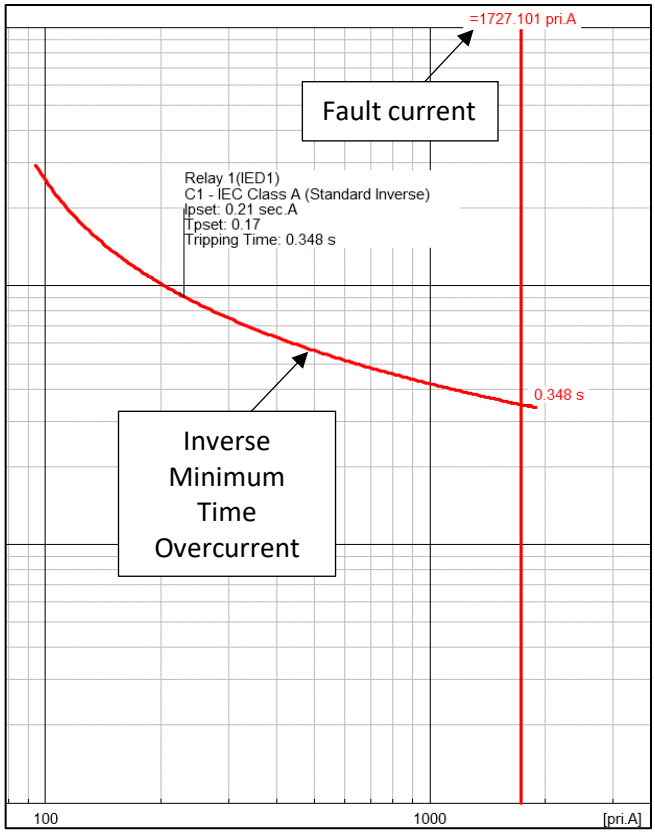

Figure 4.16: Relay R1 operation to a single phase to ground between busbars 2 and 3.

4.6.2 Case two: Three-phase fault and single-phase to ground fault on Feeder A between relays 2 and NOP

4.6.2.1 Three-phase fault on Feeder A between relays 2 and NOP

The purpose of this case study is to look into the SEL-351 overcurrent relay for a three-phase fault between busbar 3 and NOP (Line 3). An EMT simulation lasts 25.5 seconds. A three-phase fault was introduced on line 3 at 0.1 seconds and cleared after 0.175 seconds. line 3 until the NOP was dead for 3 seconds and the first reclose occurred after 3 seconds The fault was still present, and it was cleared after 0.175 seconds. Line 3 has another ten-second delay. The fault was still there, thus a second reclose happened, and the fault was cleared after 0.175 seconds. Line 3 will be dead for another ten seconds. The fault remained and was cleared after 0.175 seconds. After three reclosure efforts, the fault is deemed to be permanent, and the relay trip and lockout occur. Table 4.27 summarizes the auto-reclose sequence. Figure 4.17 depicts the usual load current

before the fault was introduced between 0 and 0.1 seconds, as well as the three reclosers until lockout.

Table 4.27: Auto-reclose operation for a three-phase fault on Feeder A between R2 and NOP (Line 3)

Recloser operation modes	Dead Time	Fault current	Fault initiated	Fault cleared	Fault duration
Recloser first attempt	-	1456.65A	0.1s	0.275s	0.175s
Recloser second attempt	3s	1456.65A	3.275s	3.45s	0.175s
Recloser third attempt	10s	1456.65A	13.45s	13.625s	0.175s
Recloser fourth attempt	10s	1456.65A	23.625s	23.8	0.175s

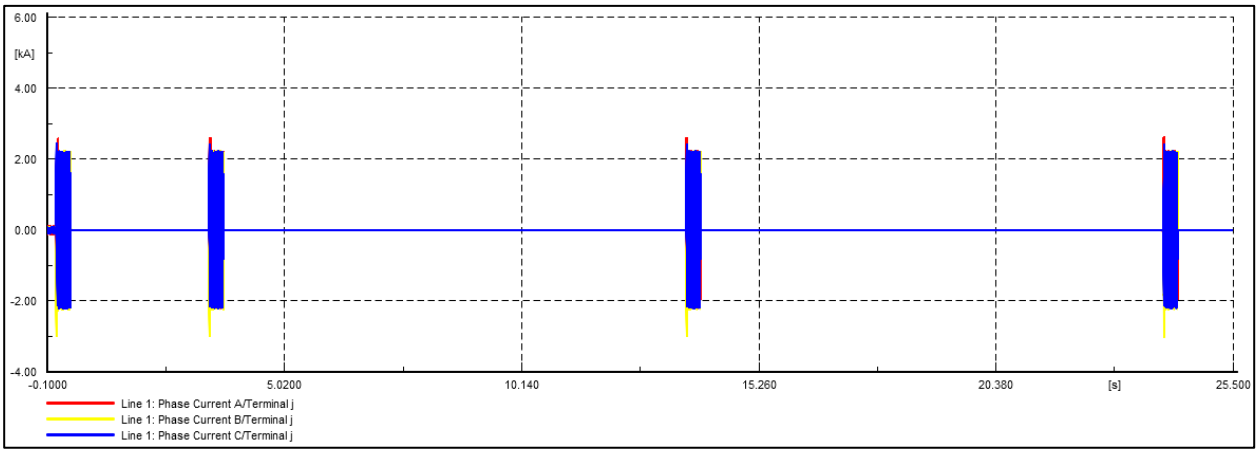

Figure 4.17: Auto-reclose simulation results for a three-phase fault between relays R2 and NOP

Table 4.28 shows the tripping times for three-phase faults. Because the fault is seen by both relays, the table shows both operating times for Relays R2 and R1. 1456.65A is the simulated short circuit current. R2 phase inverse time overcurrent element (51P) was the first to operate at 0.175 seconds, followed by relay R1 phase inverse time overcurrent element (51P) at 0.51 seconds. The two relays are graded with a 0.3-second grading margin. The goal is for relay R2 to operate at 0.175 seconds in order to clear the fault. If relay R2 fails to clear the fault, relay R1 should clear the fault in 0.51 seconds. The phase definite time time overcurrent element (67P1) did not operate because the fault current threshold was lesser than its pickup setting, and the residual inverse time overcurrent element (51G) did not operate because there was no ground fault involved.

Both 67P1 and 51G have an operational time of 9999.999 s, indicating that no operation took place.

Table 4.28: Relays R1 and R2 operation to a three-phase fault between busbars 3 and NOP (line 3)

```
| Relay 1(IED1)                    Relay Type : SEL 351-1A-300V
|   Ct    : Current Transformer    Location   : Busbar       : Bus 2             /                 Ratio       : 300A/1A
|                                               Branch       : Line 1                              Connection  : Y
|                                               :
|   CoreCt: Current Transformer    Location   : Busbar       : Bus 2             /                 Ratio       : 300A/1A
|                                               Branch       : Line 1                              Connection  : Y
|                                               :
|   51P     : 51P                  ( IEC: I>t   ANSI: 51   )          Current  [sec.A]       [pri.A]           Tripping Time
|     Current Setting :   0.840 sec.A    252.00 pri.A   0.840 p.u.      A :     4.856       1456.65               0.510 s
|     Time Dial       :   0.130     Time Shift :   1.000                B :     4.856       1456.65
|     Characteristic  :   C1 - IEC Class A (Standard Inverse)           C :     4.856       1456.65
|   67P1    : 67P1                 ( IEC: I>>   ANSI: 50   )          Tripping Current       [pri.A]           Tripping Time
|     Pickup Current  :  13.000 sec.A   3900.00 pri.A  13.000 p.u.      A :     4.856       1456.65            9999.999 s
|     Time Setting    :   0.000 s                                       B :     4.856       1456.65
|     Total Time      :   0.020 s                                       C :     4.856       1456.65
|   51G     : 51G                  ( IEC: IE>t  ANSI: 51N  )          Tripping Current       [pri.A]           Tripping Time
|     Current Setting :   0.210 sec.A     63.00 pri.A   0.210 p.u.            0.000         0.00            9999.999 s
|     Time Dial       :   0.170     Time Shift  :   1.000
|     Characteristic  :   C1 - IEC Class A (Standard Inverse)
|   Logic     : Logic                                                                                :
|     Breaker           Cubicle      Branch                  Busbar               / Substation        Fault Clearing Time
```

```
| Relay 2 (IED2)                   Relay Type : SEL 351-1A-300V
|   Ct    : Current Transformer    Location   : Busbar       : Bus 3             /                 Ratio       : 300A/1A
|                                               Branch       : Line 2                              Connection  : Y
|                                               :
```

```
| Grid: Grid                System Stage: Grid           | Study Case: Study Case               | Annex:                / 3  |
```

```
|   CoreCt: Current Transformer    Location   : Busbar       : Bus 3             /                 Ratio       : 300A/1A
|                                               Branch       : Line 2                              Connection  : Y
|                                               :
|   51P     : 51P                  ( IEC: I>t   ANSI: 51   )          Current  [sec.A]       [pri.A]           Tripping Time
|     Current Setting :   0.680 sec.A    204.00 pri.A   0.680 p.u.      A :     4.856       1456.65               0.175 s
|     Time Dial       :   0.050     Time Shift :   1.000                B :     4.856       1456.65
|     Characteristic  :   C1 - IEC Class A (Standard Inverse)           C :     4.856       1456.65
|   51G     : 51G                  ( IEC: IE>t  ANSI: 51N  )          Tripping Current       [pri.A]           Tripping Time
|     Current Setting :   0.170 sec.A     51.00 pri.A   0.170 p.u.            0.000         0.00            9999.999 s
|     Time Dial       :   0.050     Time Shift  :   1.000
|     Characteristic  :   C1 - IEC Class A (Standard Inverse)
|   Logic     : Logic                                                                                :
|     Breaker           Cubicle      Branch                  Busbar               / Substation        Fault Clearing Time
|      Switch            Cub_1        Line 2                  Bus 3               /                         0.175 s
|   load enc i threshold threshold ( IEC: I>>   ANSI: 50   )          Tripping Current       [pri.A]           Tripping Time
|     Pickup Current  :   0.100 sec.A     30.00 pri.A   0.100 p.u.            4.856       1456.65               0.001 s
|     Time Setting    :   0.000 s
|     Total Time      :   0.001 s
```

Figure 4.18 depicts the overcurrent curve used to evaluate the performance of R1 and R2. Only the inverse time overcurrent element (51P) of relay R2 operated at 0.175 seconds, as shown on the curve, and if R2 fails to operate, relay R1 will operate at 0.51 seconds. The obtained grading margin is 0.335 seconds. The phase definite time element (67P1) did not operate, and its operational time is 9999.999 seconds.

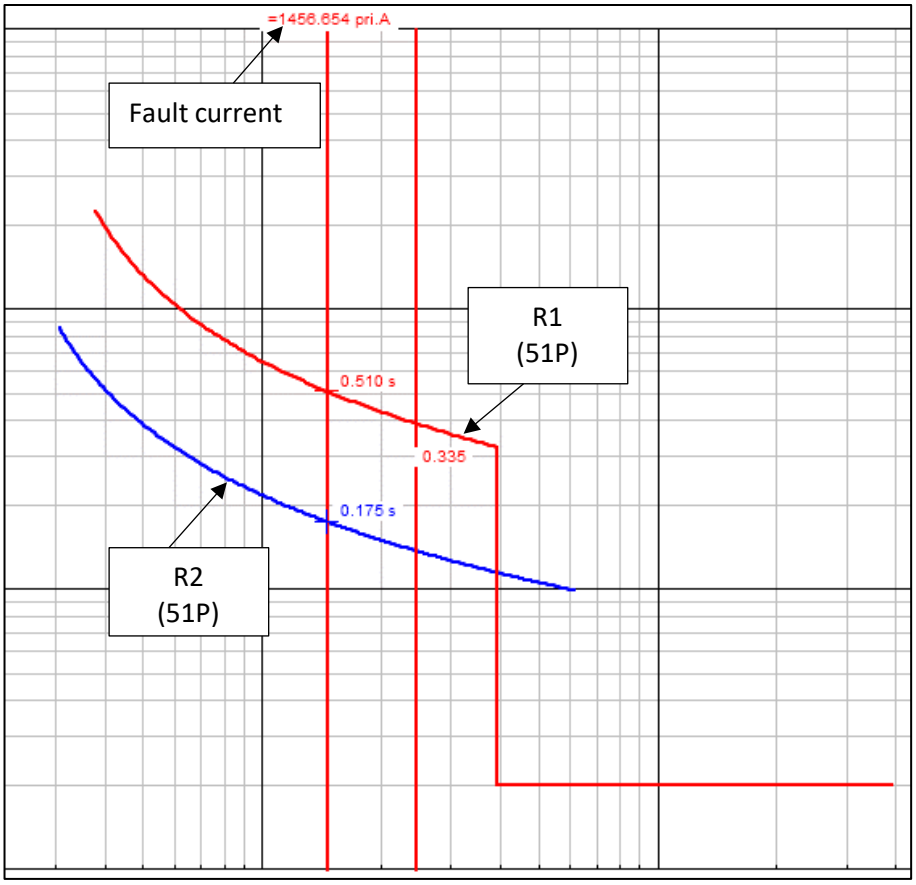

Figure 4.18: Relays R1 and R2 operation for a three-phase fault between busbar 3 and NOP (line 3)

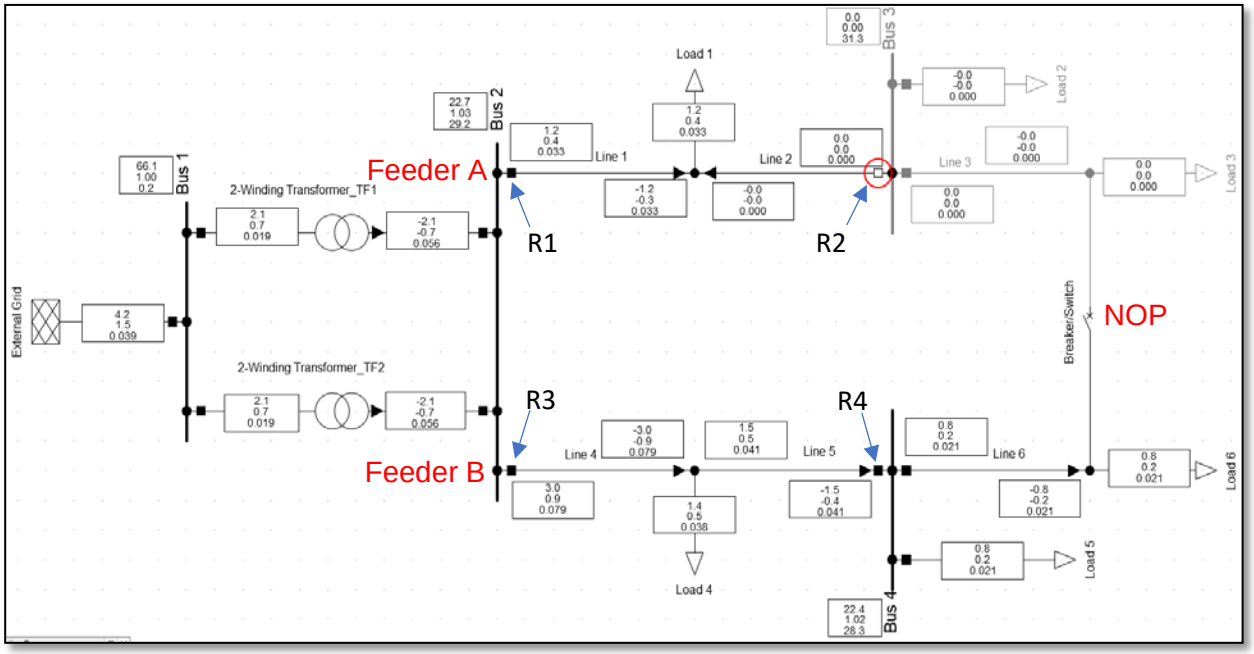

Figure 4.19: Power flow simulation results due to a fault between relays 2 and NOP

Figure 4.19 depicts the distribution network's power flow, when line 3 is disconnected. Power flows from feeder A's outgoing to relay R2, but there is no power from relay R2 to NOP, due to the fault that is isolated on that section of the network.

4.6.2.2 Single-phase to ground fault between Relay 2 and NOP

The purpose of this case study is to look at the overcurrent response of the SEL-351 relay to a single phase to ground fault on the line between busbar 3 and the NOP of feeder A. Ground faults are not programmed for auto-reclose function in this investigation for the safety of humans and animals. When there is a ground fault, the relay is set to trip and isolate the faulty segment of the line.

The tripping times for the single-phase to ground fault simulated between red phase and ground are shown in Table 4.29. Because both relays detected the fault, the data indicate the operation of the relays R1 and R2. Primary fault current is 843.12A, and secondary fault current is 2.81A. The residual inverse overcurrent time element (51G) operated at 0.121 seconds, while R2's 51G operated at 0.447 seconds. R2 was the first to operate because the fault was in its line segment (line 3). If R2 fails to operate, R1 will operate effectively at 0.326 seconds. This indicates that the two relays are properly discriminated.

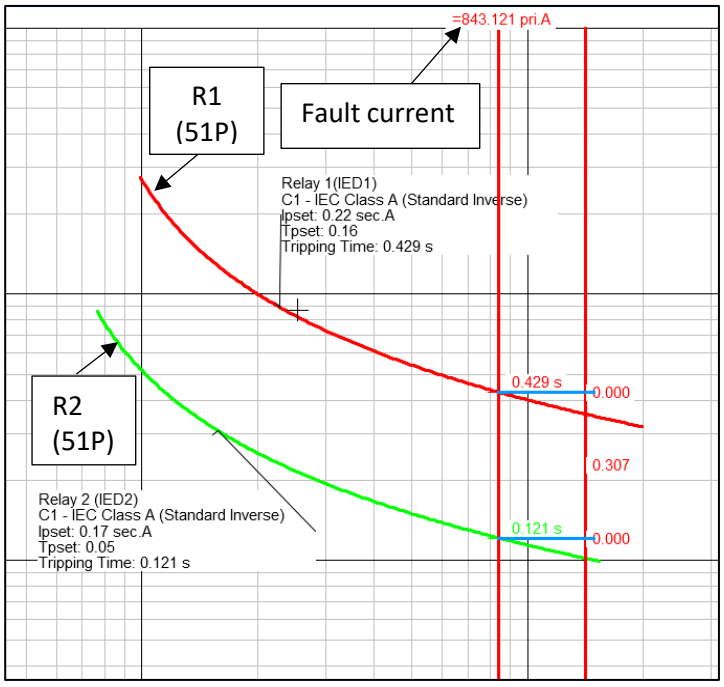

Figure 4.20: Relays R1 and R2 operation for a single-phase to ground fault between busbar 3 and NOP (line 3)

Figure 4.20 depicts the overcurrent relay curve used to analyze relays R1 and R2 performance for a single-phase to ground fault. Only the residual inverse time overcurrent element (51G) of relay R2 operated at 0.121 seconds, as shown on the curve, and if relay R2 fails to operate, relay R1 will operate at 0.429 seconds. The obtained grading margin is 0.307 seconds.

Table 4.29: Relays R1 and R2 operation for a single-phase to ground short circuit between busbars 3 and NOP

Relay 1(IED1)		Relay Type : SEL 351-1A-300V							
Ct : Current Transformer		Location : Busbar	: Bus 2	/		Ratio	: 300A/1A		
		Branch	: Line 1			Connection	: Y		
			:						
CoreCt: Current Transformer		Location : Busbar	: Bus 2	/		Ratio	: 300A/1A		
		Branch	: Line 1			Connection	: Y		
			:						
51G : 51G		(IEC: IE>t ANSI: 51N)		Tripping Current	[pri.A]	Tripping Time			
Current Setting :	0.210 sec.A	63.00 pri.A	0.210 p.u.	2.810	843.12	0.447 s			
Time Dial :	0.170	Time Shift :	1.000						
Characteristic :	C1 - IEC Class A (Standard Inverse)								
Logic : Logic						:			
Breaker Switch	Cubicle Cub_3	Branch Line 1	Busbar Bus 2	/ Substation /		Fault Clearing Time 0.447 s			
load enc i threshold threshold (IEC: I>>		ANSI: 50)		Tripping Current	[pri.A]	Tripping Time			
Pickup Current :	0.100 sec.A	30.00 pri.A	0.100 p.u.	0.936	280.88	0.001 s			
Time Setting :	0.000 s								
Total Time :	0.001 s								

Relay 2 (IED2)		Relay Type : SEL 351-1A-300V							
Ct : Current Transformer		Location : Busbar	: Bus 3	/		Ratio	: 300A/1A		
		Branch	: Line 2			Connection	: Y		
			:						
CoreCt: Current Transformer		Location : Busbar	: Bus 3	/		Ratio	: 300A/1A		
		Branch	: Line 2			Connection	: Y		
			:						
Grid: Grid		System Stage: Grid		Study Case: Study Case		Annex:	/ 3		
51G : 51G		(IEC: IE>t ANSI: 51N)		Tripping Current	[pri.A]	Tripping Time			
Current Setting :	0.170 sec.A	51.00 pri.A	0.170 p.u.	2.810	842.88	0.121 s			
Time Dial :	0.050	Time Shift :	1.000						
Characteristic :	C1 - IEC Class A (Standard Inverse)								
Logic : Logic						:			
Breaker Switch	Cubicle Cub_1	Branch Line 2	Busbar Bus 3	/ Substation /		Fault Clearing Time 0.121 s			
load enc i threshold threshold (IEC: I>>		ANSI: 50)		Tripping Current	[pri.A]	Tripping Time			
Pickup Current :	0.100 sec.A	30.00 pri.A	0.100 p.u.	0.936	280.88	0.001 s			
Time Setting :	0.000 s								
Total Time :	0.001 s								

4.6.3 Case three: Three-phase fault and single-phase to ground on Feeder B between relays 3 and relay 4

4.6.3.1 Three-phase fault on Feeder B between relays R3 and relay R4

The purpose of this case study is to look into the SEL-351 overcurrent relay characteristics and auto-reclose function for a three-phase short circuit between busbar 2 and busbar 4 (line 4-line 5) of feeder B. According to this case study, if a temporal fault

develops at this segment of the line, power will be restored when the SEL-351 relay R3 is reclosed. It is also expected that if a three-phase permanent fault occurs at this section of the line between busbar 2 and busbar 3, relay R1 should auto-reclose three times, and if the fault remains, relay R3 should lockout, send an open signal to SEL-351 (relay R4) downstream at busbar 4, and send a close signal to the NOP to back feed the section of the line between busbar 4 and NOP (line 6). This will supply loads 5 and 6.

For 25.5 seconds, an EMT simulation is performed. A three-phase fault was introduced in the segment of the line at 0.1 seconds and cleared 0.371 seconds later. The entire Feeder B line was dead for 3 seconds, until the first reclose happened after 3 seconds. The fault was still present, and it was cleared after 0.371 seconds. Feeder B is subjected to another 10 second period of dead time. The fault was still there, thus a second reclose happened, and the fault was cleared after 0.371 seconds. Feeder B is subjected to another 10 second period of dead time. The fault remained and was cleared after 0.371 seconds. After three reclosure attempt, the fault is deemed to be permanent, and the relay trip and lockout occur. The auto-reclose cycle is summarized in Table 4.30 below. Figure 4.21 depicts the usual load current before the fault was introduced between 0 and 0.1 seconds, as well as the three reclosures till lockout.

Table 4.30: Auto-reclose operation for a three-phase fault on Feeder B between relays R3 and R4 (Line 4-Line 5)

Recloser operation modes	Dead Time	Fault current	Fault initiated	Fault cleared	Fault duration
Recloser first attempt	-	2731.47A	0.1s	0.471s	0.371s
Recloser second attempt	3s	2731.47A	3.471s	3.842s	0.371s
Recloser third attempt	10s	2731.47A	13.842s	14.213s	0.371s
Recloser fourth attempt	10s	2731.47A	24.213s	24.584	0.371s

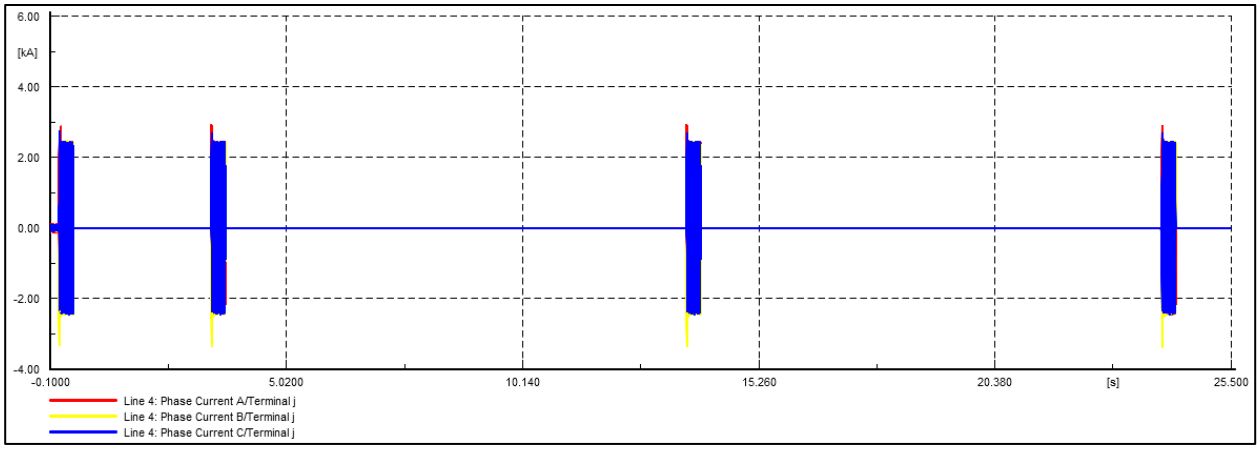

Figure 4.21: Auto-recloser simulation results for a three-phase fault between relays R3 and R4

Figure 4.22 depicts the distribution network's power flow results after a fault occurred in feeder B at (50 percent) of the line between relays R3 and R4. When relay R3 operates and opens its circuit breaker, feeder B is closed from the incoming feeder till the NOP. The line segment between relay R4 and NOP (Line 6) is also affected by the fault, despite the fact that that segment of the line is fault-free. Customers on the section of the line between relay R4 and NOP are affected unnecessarily, since the fault is not in that section of the line. There is a requirement for the network to automatically reconfigure and provide the line section between relay R4 and NOP via the NOP from feeder A. As seen by the power flow arrows, only feeder B receives power from the incoming feeder till the NOP.

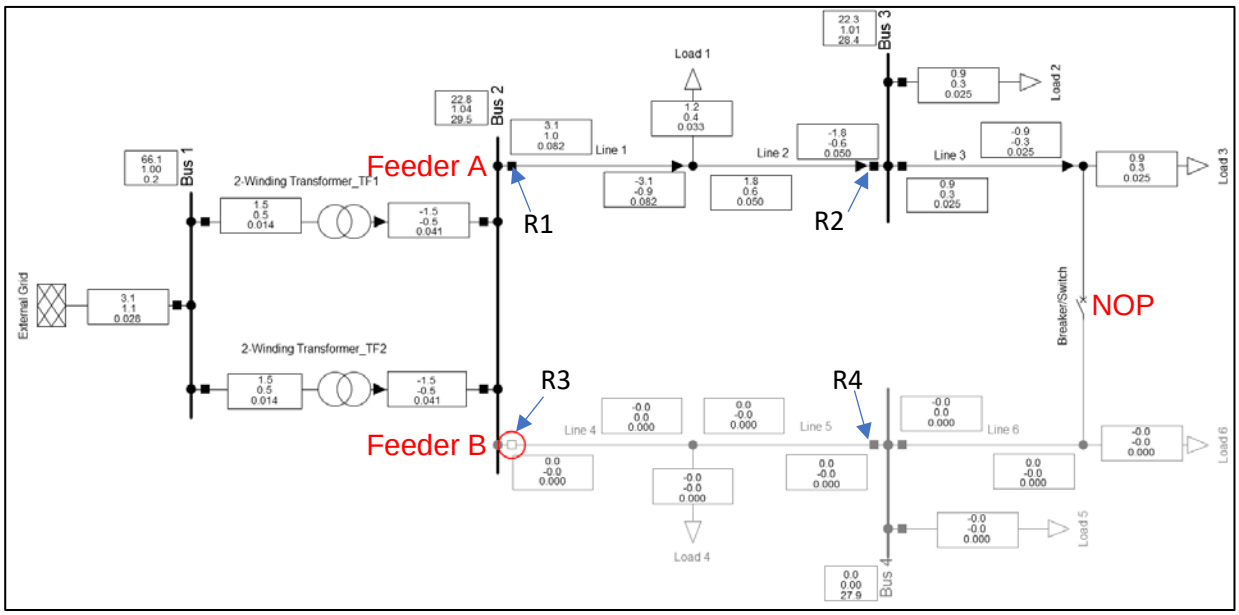

Figure 4.22: Power flow simulation results after isolating the line relays R3 and R4

Figure 4.23 depicts a three-phase current for line 6 during the permanent fault between busbars 2 and 4. A normal load current of 0.029kA was recorded to flow between 0 and 0.1 seconds. When the fault was introduced at 0.1 seconds, the auto-reclose cycle happened, Relays R3 locked out and R4 opened, the NOP closed, and feeder A back fed line 6 via the NOP. It has been noticed that when the auto-reclose cycle has been finished and the faulty section has been isolated, the usual load current flows on line 6 to supply loads 5 and 6 respectively.

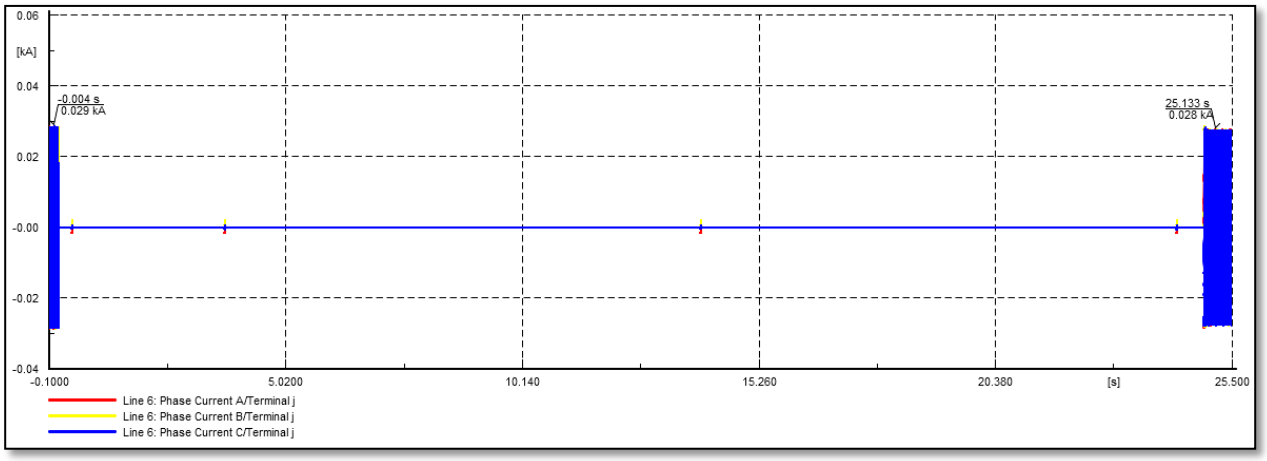

Figure 4.23: Back feed simulation results for the line section between busbar 4 and NOP (line 6)

Figure 4.24 depicts the power flow after the faulty section of the line between busbars 2 and 4 was disconnected. The Power flow simulation results in Figure 4.24 show that power flows from feeder A to line 6, via the NOP, to supply loads 5 and 6.

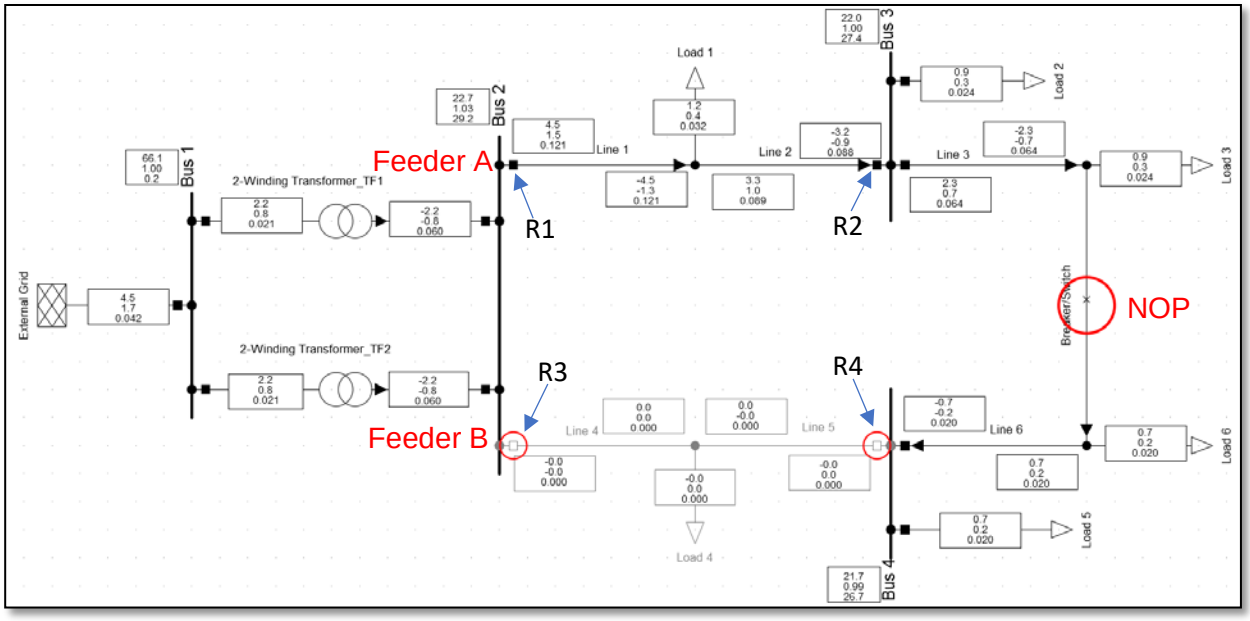

Figure 4.24: Power flow simulation results after isolating the line busbars 2 and 4

Table 4.31: Relay 3 operation for a three-phase short circuit occurs between relays R3 and R4

```
| Relay 3 (IED3)                  Relay Type : SEL 351-1A-300V
|   Ct    : Current Transformer   Location   : Busbar       : Bus 2              /                Ratio       : 300A/1A
|                                              Branch       : Line 4                              Connection  : Y
|                                                           :
|   CoreCt: Current Transformer   Location   : Busbar       : Bus 2              /                Ratio       : 300A/1A
|                                              Branch       : Line 4                              Connection  : Y
|                                                           :
|   51P     : 51P                 ( IEC: I>t   ANSI: 51   )         Current  [sec.A]       [pri.A]          Tripping Time
|     Current Setting :   0.830 sec.A    249.00 pri.A   0.830 p.u.      A :     9.105       2731.47             0.371 s
|     Time Dial       :   0.130     Time Shift :   1.000               B :     9.105       2731.47
|     Characteristic  :   C1 - IEC Class A (Standard Inverse)          C :     9.105       2731.47
|   67P1    : 67P1                ( IEC: I>>   ANSI: 50   )         Tripping Current       [pri.A]          Tripping Time
|     Pickup Current  :  13.000 sec.A   3900.00 pri.A  13.000 p.u.      A :     9.105       2731.47          9999.999 s
|     Time Setting    :   0.000 s                                       B :     9.105       2731.47
|     Total Time      :   0.020 s                                       C :     9.105       2731.47
|   51G     : 51G                 ( IEC: IE>t  ANSI: 51N  )         Tripping Current       [pri.A]          Tripping Time
|     Current Setting :   0.210 sec.A     63.00 pri.A   0.210 p.u.            0.000         0.00          9999.999 s
|     Time Dial       :   0.170     Time Shift  :   1.000
|     Characteristic  :   C1 - IEC Class A (Standard Inverse)
|   Logic     : Logic                                                                                :
|     Breaker          Cubicle      Branch                  Busbar              / Substation        Fault Clearing Time
|      Switch           Cub_4        Line 4                  Bus 2              /                          0.371 s
|   load enc i threshold threshold ( IEC: I>>   ANSI: 50   )         Tripping Current       [pri.A]          Tripping Time
|     Pickup Current  :   0.100 sec.A     30.00 pri.A   0.100 p.u.            9.105       2731.47             0.001 s
|     Time Setting    :   0.000 s
|     Total Time      :   0.001 s
```

Table 4.31 shows the tripping time for relay 3 in the event of a three-phase fault. At 0.371 seconds, the inverse time overcurrent phase element (51P) was operational. The definite time phase overcurrent element (67P1) and the inverse time residual element (51G) were both non-opertional. Because the fault current is less than the 67P1 threshold pickup current setting, therefore 67P1 element not operate. Because of

the ground fault is not introduced in the network, the inverse time residual overcurrent element (51G) did not operate.

The overcurrent characteristic curve used to examine the performance of relay R3 as depicted in Figure 4.25. The inverse time overcurrent element (51P) was the only one that operated at 0.371 seconds. The operational time of the definite time element (67P1) is 9999.999s, indicating that no operation occurred.

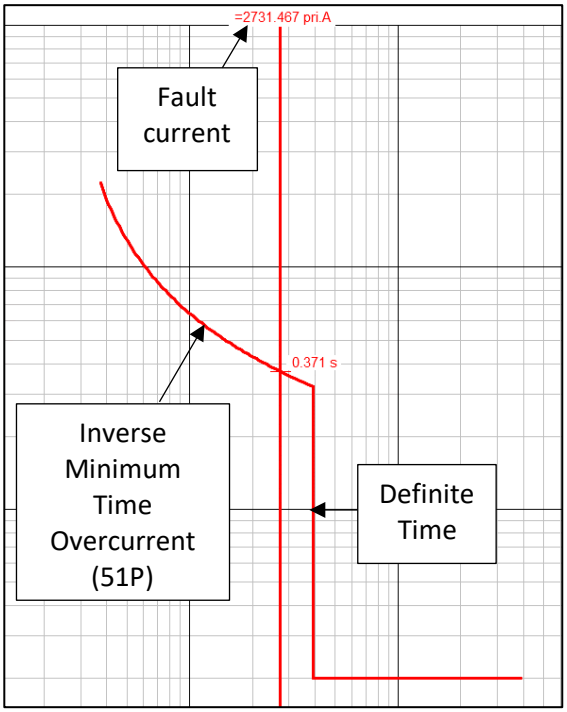

Figure 4.25: Relay R3 operation for a three-phase fault between busbars 2 and 4 (Line 4-Line 5)

4.6.3.2 Single-phase to ground fault between busbars 2 and 4

The purpose of this case study is to look into the overcurrent relay operation for a single-phase to a ground fault on the feeder B line between busbars 2 and 4 (Line 4-Line 5). Ground faults are not configured to perform auto-reclose in this case study for the safety of humans and animals. When a ground fault develops, the relay is set to trip and isolate the faulty segment of the line.

The tripping duration for the single-phase to ground fault simulated between red phase and ground is shown in Table 4.32. At 0.338 seconds, the residual inverse overcurrent

time element (51G) was operational. Primary fault current is 1923.46A, and secondary fault current is 6.412A.

Table 4.32: Relay R3 response for a single-phase to ground short circuit between busbars 2 and 4 (Line 4-Line 5)

Relay 3 (IED3)		Relay Type : SEL 351-1A-300V					
Ct : Current Transformer		Location : Busbar	: Bus 2	/		Ratio	: 300A/1A
			Branch : Line 4			Connection	: Y
			:				
CoreCt: Current Transformer		Location : Busbar	: Bus 2	/		Ratio	: 300A/1A
			Branch : Line 4			Connection	: Y
			:				
51G : 51G		(IEC: IE>t ANSI: 51N)		Tripping Current	[pri.A]		Tripping Time
Current Setting :	0.210 sec.A	63.00 pri.A	0.210 p.u.	6.412	1923.46		0.338 s
Time Dial :	0.170	Time Shift :	1.000				
Characteristic :	C1 - IEC Class A (Standard Inverse)						
Logic : Logic						:	
Breaker	Cubicle	Branch	Busbar	/ Substation		Fault Clearing Time	
Switch	Cub_4	Line 4	Bus 2	/			0.338 s
load enc i threshold threshold (IEC: I>> ANSI: 50)				Tripping Current	[pri.A]		Tripping Time
Pickup Current :	0.100 sec.A	30.00 pri.A	0.100 p.u.	2.137	640.99		0.001 s
Time Setting :	0.000 s						
Total Time :	0.001 s						

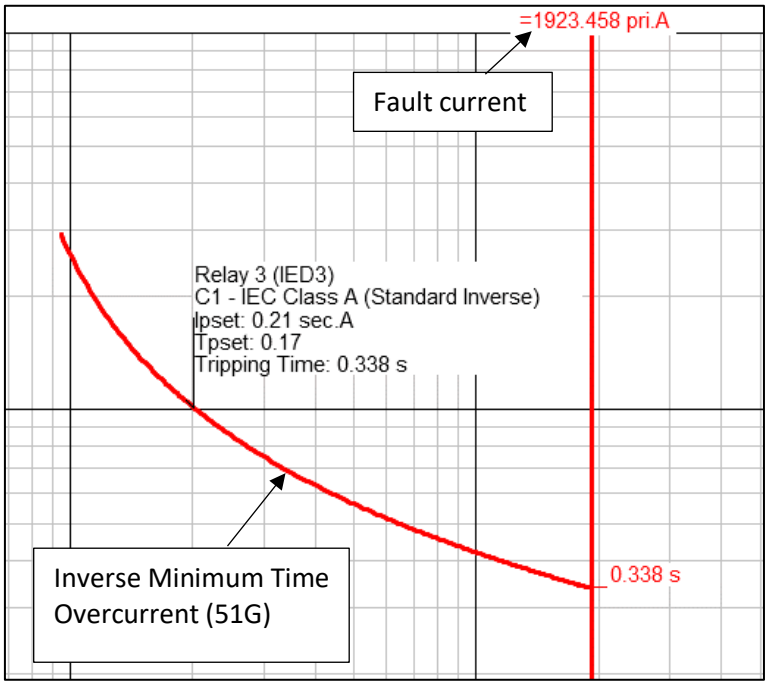

Figure 4.26: Overcurrent Relay R3 operation for a single-phase to ground between busbars 2 and4 (Line 4-Line 5)

Figure 4.26 depicts the residual overcurrent curve used to assess relay R3's performance. Only the residual inverse time overcurrent element (51G) operated at 0.338 seconds, as seen on the curve below.

4.6.4 Case four : Three-phase fault and single-phase to ground on Feeder B between relays 4 and NOP

4.6.4.1 Three-phase fault between relays 4 and NOP

The purpose of this case study is to look into the SEL-351 overcurrent relay in the event of a three-phase fault between busbar 4 and NOP (Line 6). For 25.5 seconds, an EMT simulation is performed. A three-phase fault was introduced in line 6 at 0.1 seconds and cleared 0.159 seconds later. line 3 till the NOP was dead for 3 seconds and the first reclose happened after 3 seconds The fault remained, and it was cleared after 0.159 seconds. Line 3 experiences another ten-second dead time. The fault remained, and after 10 seconds, a second reclose happened, and the fault was cleared. Line 6 will be non-operational for another 10 seconds. The fault remained, and it was cleared after 0.159 seconds. It is presumed that the fault is permanent after three reclosure attempts, and the relay trip and lockout occur. Table 4.33 contains a summary of the discussed auto-reclose operation. Figure 4.27 depicts the usual load current prior to the fault being introduced between 0 and 0.1 seconds, as well as the three reclosures till lockout.

Table 4.33: Auto-reclose operation for a three-phase fault on Feeder B between relays R4 and NOP (Line 6)

Recloser operation modes	Dead Time	Fault current	Fault initiated	Fault cleared	Fault duration
Recloser first attempt	-	1645.76A	0.1s	0.259s	0.159s
Recloser second attempt	3s	1645.76A	3.259s	3.418s	0.159s
Recloser third attempt	10s	1645.76A	13.418s	13.577s	0.159s
Recloser fourth attempt	10s	1645.76A	23.577s	23.736s	0.159s

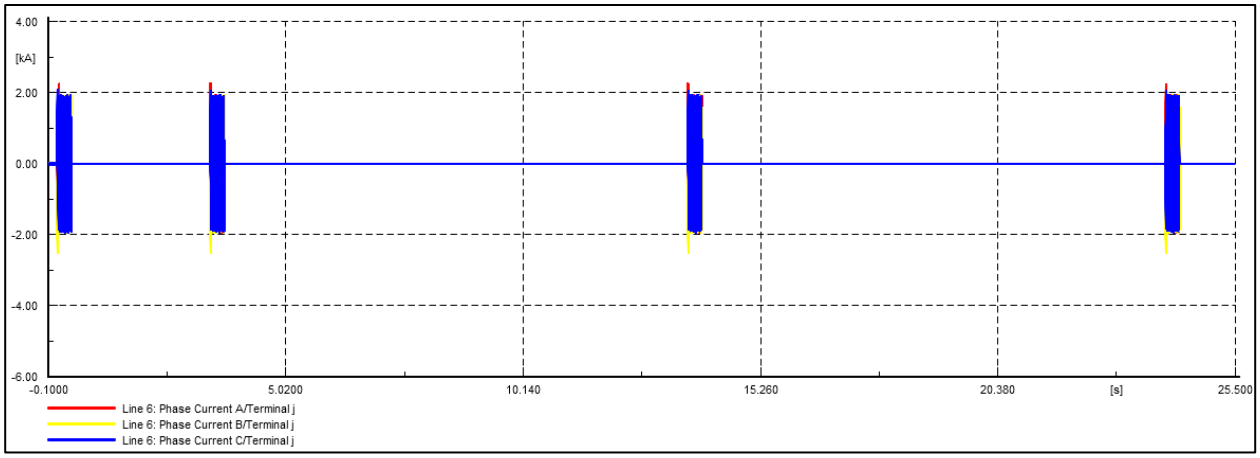

Figure 4.27: Auto-reclose simulation results for a three-phase fault between relays 4 and NOP (line 6)

Table 4.33 shows the tripping times for three-phase faults. Because the fault is detected by both relays, the table shows both operating times for R3 and R4. The short circuit current was 1645.76A. Relay R4 phase inverse time overcurrent element (51P) was the first to operate at 0.159 seconds, followed by relay R3 phase inverse time overcurrent element (51P) operated at 0.473 seconds. The grading margin between the two relays is 0.314 seconds. Relay 4 operates first, followed by relay R3 operated at 0.51 seconds later to clear the fault if relay R4 fails to operate. The phase definite time time overcurrent element (67P1) did not operate because the fault current threshold setting was lesser in comparsion with its pickup setting, and the residual inverse time overcurrent element (51G) did not operate because there was no ground fault involved. Both 67P1 and 51G have an operational time of 9999.999 s, indicating that no operation took place.

Figure 4.28 depicts the overcurrent curve that was utilized to evaluate the performance of relay R3 and R4. Only the inverse time overcurrent element (51P) for R4 operated at 0.159 seconds, as shown on the curve, and if relay R3 fails to work, relay R1 will operate at 0.473 seconds. The obtained grading margin is 0.313 seconds. The phase definite time overcurrent element (67P1) non-operational indicated as 9999.999 s.

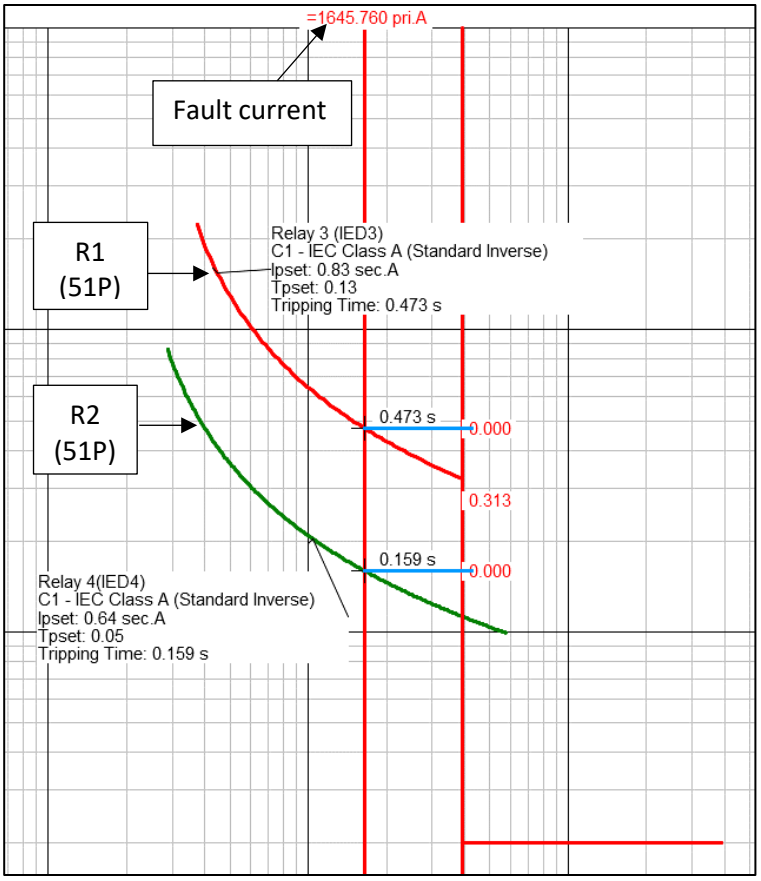

Figure 4.28: Relays R3 and R4 operation for a three-phase short circuit between busbar 4 and NOP (Line 6)

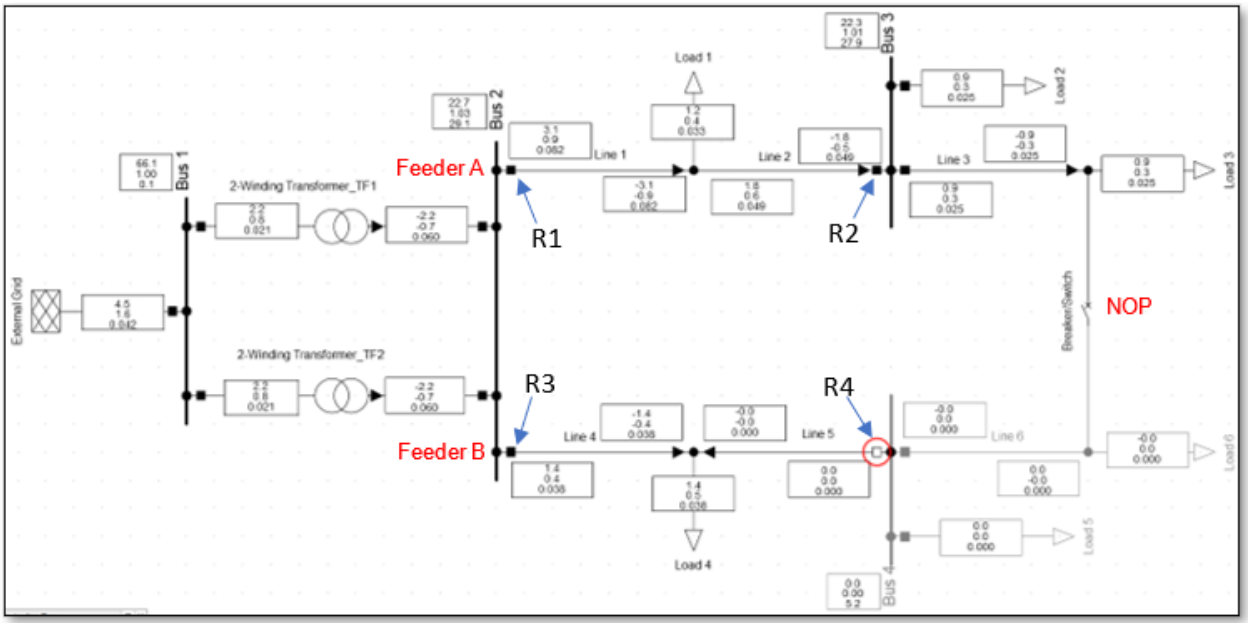

Figure 4.29: Power flow simulation results with section of the line between busbar 4 and NOP is isolated due to a fault

Figure 4.29 depicts the resultant power flow of the studied distribution network when the section of the line between busbar 4 and NOP is disconnected due to a fault.

4.6.4.2 Single-phase to ground fault between busbar 4 and NOP

The purpose of this case study is to look at the overcurrent response to a single phase to ground fault on the feeder B line between busbar 4 and NOP (Line 6). Ground faults are not configured to perform auto-reclose function in this investigation for the safety of humans and animals. When a ground fault develops, the relay is set to trip and isolate the faulty segment of the line.

The tripping duration for the single-phase to ground fault simulated between red phase and ground is shown in Table 4.34. The primary fault current is 977.37 amps, and the secondary fault current is 3.258 amps. Relay R4 residual inverse overcurrent time element (51G) operated at 0.113 seconds. Relay R3 will operate at 0.422 seconds if relay R4 fails to operate.

Table 4.34: Relays R3 and R4 operation for a single-phase to ground fault between busbars 4 and NOP

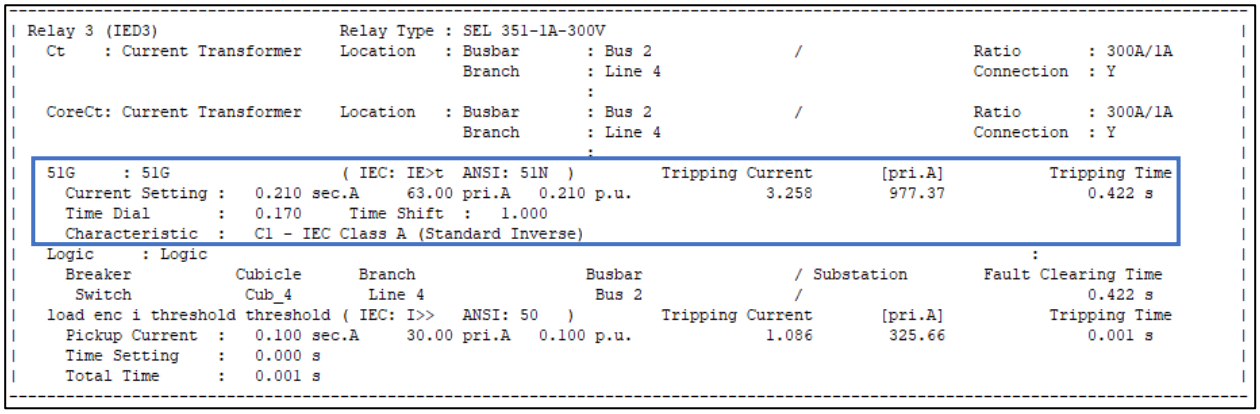

```
| Relay 3 (IED3)                  Relay Type : SEL 351-1A-300V                                                                |
|   Ct    : Current Transformer   Location   : Busbar      : Bus 2            /                Ratio       : 300A/1A       |
|                                              Branch      : Line 4                            Connection  : Y             |
|                                             :                                                                           |
|   CoreCt: Current Transformer   Location   : Busbar      : Bus 2            /                Ratio       : 300A/1A       |
|                                              Branch      : Line 4                            Connection  : Y             |
|                                             :                                                                           |
|   51G     : 51G                 ( IEC: IE>t  ANSI: 51N  )        Tripping Current       [pri.A]          Tripping Time |
|     Current Setting :   0.210 sec.A     63.00 pri.A   0.210 p.u.            3.258       977.37             0.422 s      |
|     Time Dial       :   0.170     Time Shift  :   1.000                                                                 |
|     Characteristic  :   C1 - IEC Class A (Standard Inverse)                                                             |
|   Logic     : Logic                                                                                    :                |
|     Breaker           Cubicle      Branch                 Busbar              / Substation       Fault Clearing Time    |
|      Switch            Cub_4        Line 4                 Bus 2              /                          0.422 s        |
|   load enc i threshold threshold ( IEC: I>>   ANSI: 50   )        Tripping Current       [pri.A]          Tripping Time |
|     Pickup Current  :   0.100 sec.A     30.00 pri.A   0.100 p.u.            1.086       325.66             0.001 s      |
|     Time Setting    :   0.000 s                                                                                         |
|     Total Time      :   0.001 s                                                                                         |
```

```
| Relay 4(IED4)                   Relay Type : SEL 351-1A-300V                                                                |
|   Ct    : Current Transformer   Location   : Busbar      : Bus 4            /                Ratio       : 300A/1A       |
|                                              Branch      : Line 5                            Connection  : Y             |
|                                             :                                                                           |
|   CoreCt: Current Transformer   Location   : Busbar      : Bus 4            /                Ratio       : 300A/1A       |
|                                              Branch      : Line 5                            Connection  : Y             |
|                                             :                                                                           |
|   51G     : 51G                 ( IEC: IE>t  ANSI: 51N  )        Tripping Current       [pri.A]          Tripping Time |
|     Current Setting :   0.160 sec.A     48.00 pri.A   0.160 p.u.            3.257       977.16             0.113 s      |
|     Time Dial       :   0.050     Time Shift  :   1.000                                                                 |
|     Characteristic  :   C1 - IEC Class A (Standard Inverse)                                                             |
|   Logic     : Logic                                                                                    :                |
|     Breaker           Cubicle      Branch                 Busbar              / Substation       Fault Clearing Time    |
|      Switch            Cub_1        Line 5                 Bus 4              /                          0.113 s        |
|   load enc i threshold threshold ( IEC: I>>   ANSI: 50   )        Tripping Current       [pri.A]          Tripping Time |
|     Pickup Current  :   0.100 sec.A     30.00 pri.A   0.100 p.u.            1.086       325.66             0.001 s      |
|     Time Setting    :   0.000 s                                                                                         |
|     Total Time      :   0.001 s                                                                                         |
```

Figure 4.30 depicts the overcurrent curve used to analyze relays R3 and R4 performance for a single-phase to ground fault. Only the residual inverse time overcurrent element (51G) for relay R4 operated at 0.113 seconds, as shown on the curve, and if relay R4 fails to work, relay R3 will operate at 0.422 seconds. The obtained grading margin is 0.307 seconds.

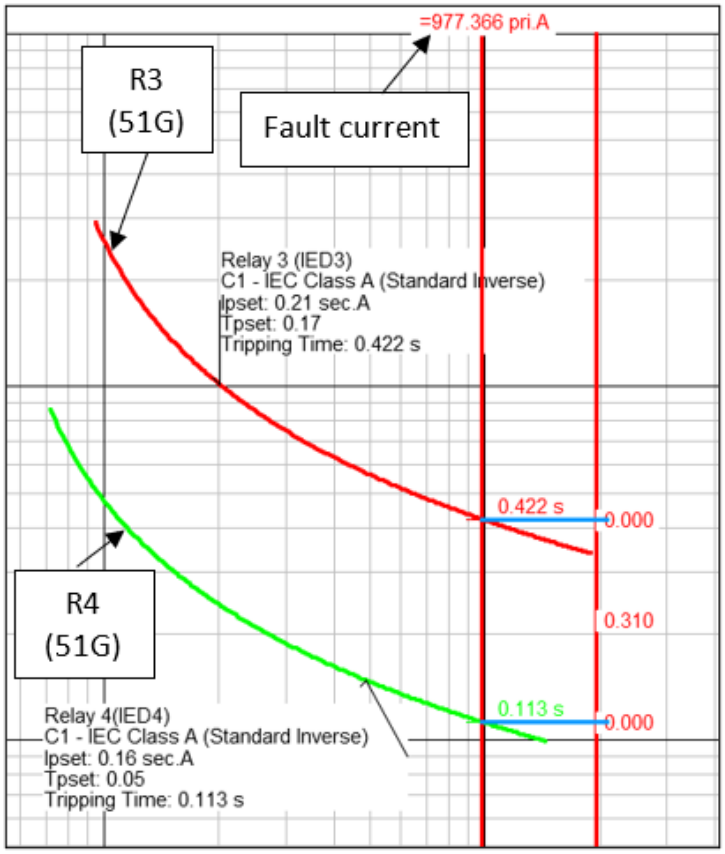

Figure 4.30: Relay R3 and R4 operation for a single phase to ground fault between busbars 4 and NOP

The resultant SLD of the distribution system network when line 6 is isolated due to a single phase to ground fault will be the same as the one shown in Figure 4.29.

4.6.5 Summary on the Three-phase and single-phase to ground fault scenario applied on Feeder A and Feeder B

In summary, the simulation findings reported in this section (Figures 4.11–4.30 and Tables 4.24–4.44) show that overcurrent relay performance for recloser functions is

studied for both temporary and permanent phase faults in the network. The ground fault scenario is studied for a permanent fault in the network while keeping human and animal safety in mind. The relay performance was satisfactory in both situations, three-phase and ground fault scenarios, and met the protection requirements speed, selectivity and relability. The simulation knowledge gained in this chapter will instruct protection engineers on how to implement the recloser scheme for any industrial distribution network in order to increase distribution network protection performance.

4.7 Conclusion

The auto-reclose overcurrent protection scheme for industrial distribution systems was presented in this chapter. The DIgSILENT software simulation tool is used to model and simulate the distribution network. Load flow simulation is performed under various network operating conditions, and the simulation results are thoroughly examined. Short circuits study are investigated for faults in various locations along the distribution network.

The SEL-351 overcurrent relays utilized in the recloser protection study were equipped with the DIgSILENT software. For upstream and downstream coordination of the recloser overcurrent relays, both current and time discriminations are used. According to the simulation results, when the outgoing feeder fails, the downstream segment of the network can be automatically back-fed by the healthy feeder.

The simulation findings reported in this section demonstrate that overcurrent relay performance for the recloser functions is studied in the network for both temporary and permanent phase faults. The ground fault scenario is studied for a permanent fault in the network while keeping human and animal safety in mind. The relay performance was satisfactory and met the protection requirements.

CHAPTER FIVE
IMPLEMENTATION OF THE LAB-SCALE TEST BENCH AND TESTING THE AUTO-RECLOSE PROTECTION SCHEME FOR THE DISTRIBUTION SYSTEM

5.1 Introduction

This chapter explains the hardwired lab-scale implementation of the distribution system's recloser control scheme. The auto-reclose technique is implemented using the SEL-351A (R1), SEL-351A (R2), and SEL-351 overcurrent reclosing relays. The SEL-351A relay (R1) is positioned at the outgoing feeder, the SEL-351A relay (R2) is positioned downstream of the SEL-351A relay (R1), and the SEL-351 relay is positioned at the NOP, as shown in Figure 5.1. Figure 5.1 depicts the lab-scale test bench setup and placement of the auto-reclosing relays in a distribution system network. This recloser control scheme restores power to line sections downstream that have lost power owing to faults in the distribution system line.

Trip logic, close logic, and reclose logic are all included in the auto-reclose SEL-351A relays configuration. Each relay's SEL-351A configuration options include definite time (50), inverse time overcurrent (51), tripping signals, and close signals. The Omicron CMC 356 is used to analyze the overcurrent and auto-reclose protection functions by simulating current and voltage signals. Overcurrent and auto-reclose protection functionalities of SEL-351A (R1) and SEL-351A (R2) relays are tested using the omicron test universe software's overcurrent test module and state sequencer module.

Two case studies are considered:

Three-phase fault and a single-phase to ground fault on the SEL-351A relay (R1)

Three-phase fault and a single-phase to ground fault on the SEL-351A relay (R2)

The recloser control scheme's lab-scale test bench simulation results are studied and compared to DIgSILENT simulation findings.

The following is a summary of the chapter's content: Section 5.2 describes the relay configuration settings for auto-reclose and overcurrent protection relays, whereas Section 5.3 describes the omicron test universe configuration parameters for auto-reclose and overcurrent protection. Section 5.4 presents recloser control scheme lab-

scale testing and simulation results, as well as a comparison of recloser control scheme lab-scale test bench simulation results to DIgSILENT.

5.2 Configuring reclosing relays for auto-reclose and overcurrent protection

This section describes the hardwired lab-scale test bench setup for the recloser control scheme. Figure 5.1 depicts an auto-reclose scheme in a distribution system network, and the portion encircled red on feeder A is the developed recloser control scheme demonstrating how the SEL-351A (R1), SEL-351A (R2), and SEL-351 (NOP) relays are positioned to protect and automatically reconfigure the distribution network under fault conditions. The setup and functioning of the auto-reclose system on feeder A is the same as for feeder B. In order to avoid recurrence.

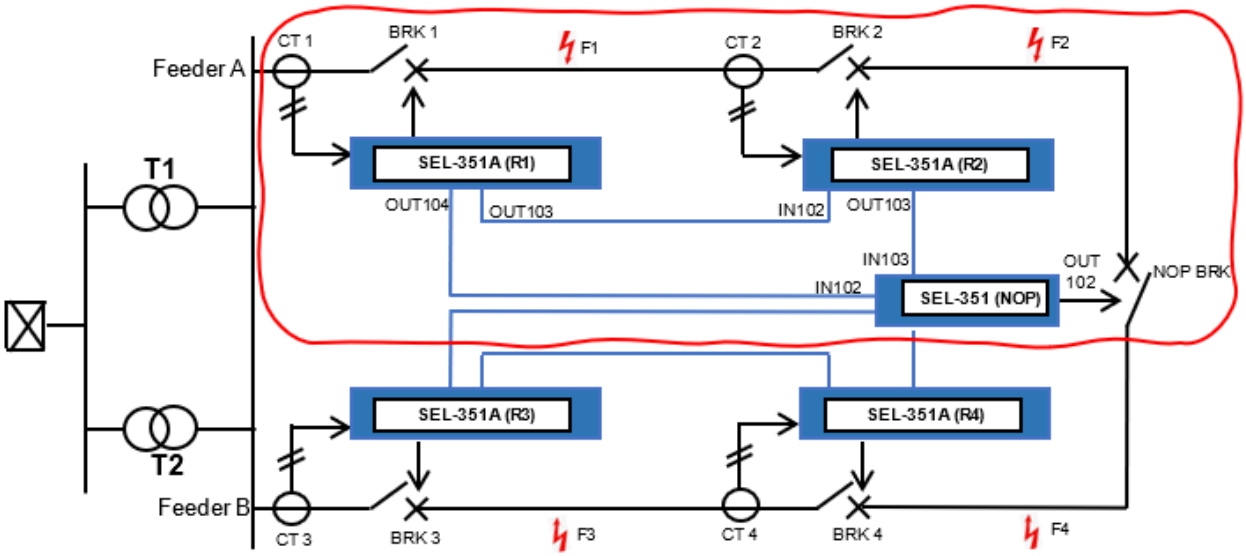

Figure 5.1: Auto-reclose scheme in a distribution system network

The recloser control scheme uses the SEL-351A (R1), SEL-351A (R2), and SEL-351 (NOP) relays. F1 to F4 represent faults 1 to 4.

AcSELerator Quickset software is used to setup the three auto-reclose relays and overcurrent configuration parameters. The Omicron CMC 356 injection device is used to test the auto-reclose and overcurrent protection functions by simulating currents and voltages. omicron test universe software is used to configure the omicron CMC 356 configuration settings. A personal computer is used to configure both the AcSELerator

Quickset and the test universe software. All of these devices communicate with one another via the Ruggedcom RSG2288 Ethernet switch, as shown in Figures 5.2 and 5.3.

Figure 5.2 below shows the hardwired auto-reclose scheme lab-scale test bench configuration for a fault (F1) occurring on the distribution line between SEL-351A relays (R1) and (R2) in Figure 5.1. Figure 5.3 shows the auto-reclose scheme lab-scale test bench configuration for a fault (F2) occurring on the line between SEL-351A relay (R2) and SEL-351 relay (NOP).

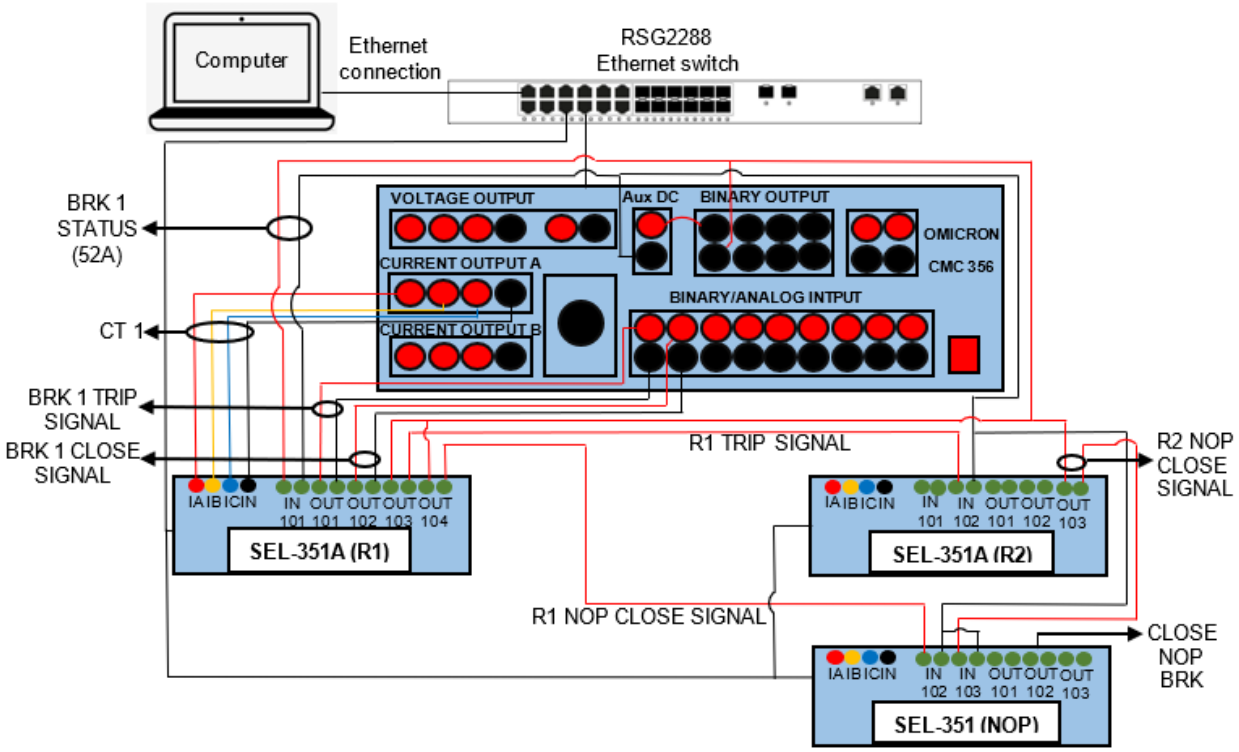

Figure 5.2: Hardwired auto-reclose scheme for a fault (F1) between SEL-351A (R1) and SEL-351A (R2)

CT1 current signals are injected into SEL-351A (R1) using an omicron CMC 356 to simulate faults on the distribution line between SEL-351A (R1) and SEL-351A. (R2). CT2 current signals are injected into SEL-351A (R2) using an omicron CMC 356 to simulate faults on the distribution line between SEL-351A (R2) and SEL-351 (NOP). The trip and close signals of circuit breakers BRK1 and BRK2 are represented by binary signals attached to SEL-351A (R1) and SEL-351A (R2) output ports OUT101 and OUT102, respectively. OUT101 and OUT102 are then mapped to the Omicron CMC 356 device's binary inputs 1 and 2, as shown in Figures 5.2 and 5.3.

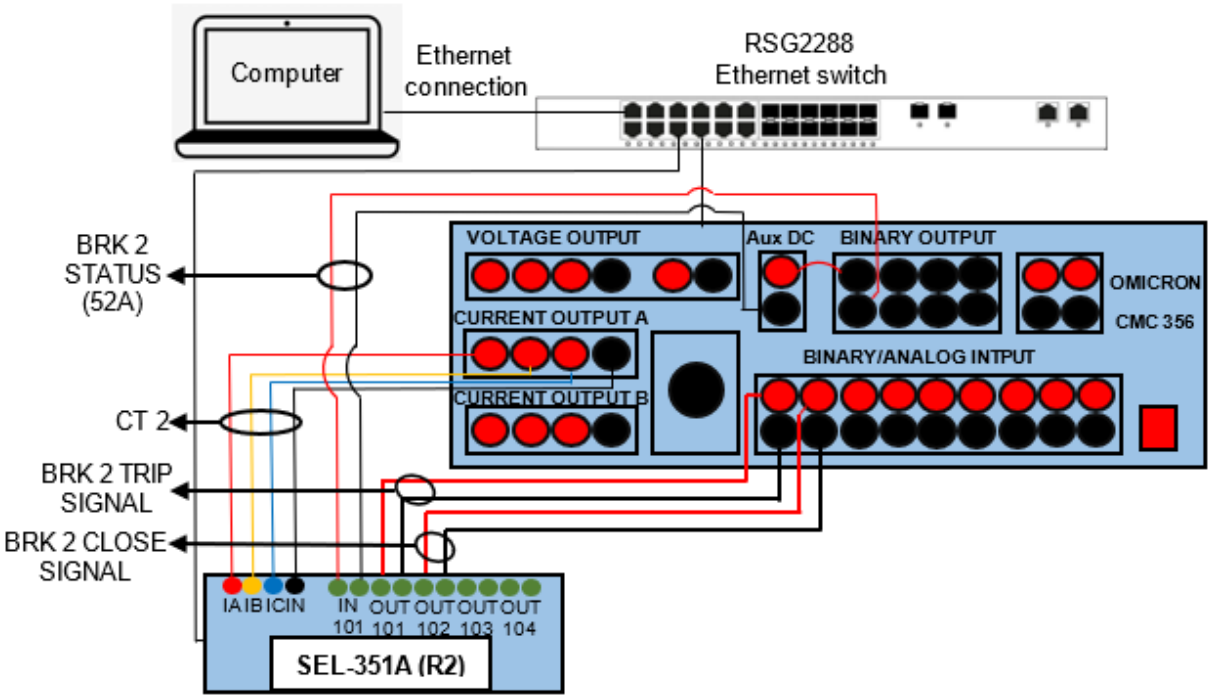

Figure 5.3: Hardwired auto-reclose scheme for a fault (F2) between SEL-351A (R2) and SEL-351A (NOP)

The input port IN101 is connected to the circuit breaker status (52A) of SEL-351A (R1) and SEL-351A (R2). When the circuit breaker is closed, 110V DC is provided to IN101 via the CMC 356's AUX DC connection. IN101 is de-energized when the circuit breaker is tripped. The output ports OUT103 and OUT104 of the SEL-351A (R1) are linked to the input ports IN102 of the SEL-351A (R2) and SEL-351A (R3) (NOP). The SEL-351A (R2) output port OUT103 is linked to the SEL-351A input port IN103 (NOP). When both trip signals from SEL-351A (R1) and SEL-351A (R2) are received, output port OUT102 of SEL-351A (NOP) sends a close command to the NOP circuit breaker.

5.2.1 Communication configuration settings for reclosing relays SEL-351A (R1), SEL-351A (R2), and SEL-351 (NOP)

AcSELerator quickset software is used to configure the SEL-351 engineering configuration parameters. This is a Schweitzer Engineering Laboratories (SEL) tool that allows engineers to configure, commission, and manage IEDs for power system protection, control, metering, and monitoring. The communication parameters of the

SEL-351A (R1), SEL-351A (R2), and SEL-351 (NOP) relays are shown in Figure 5.4 below.

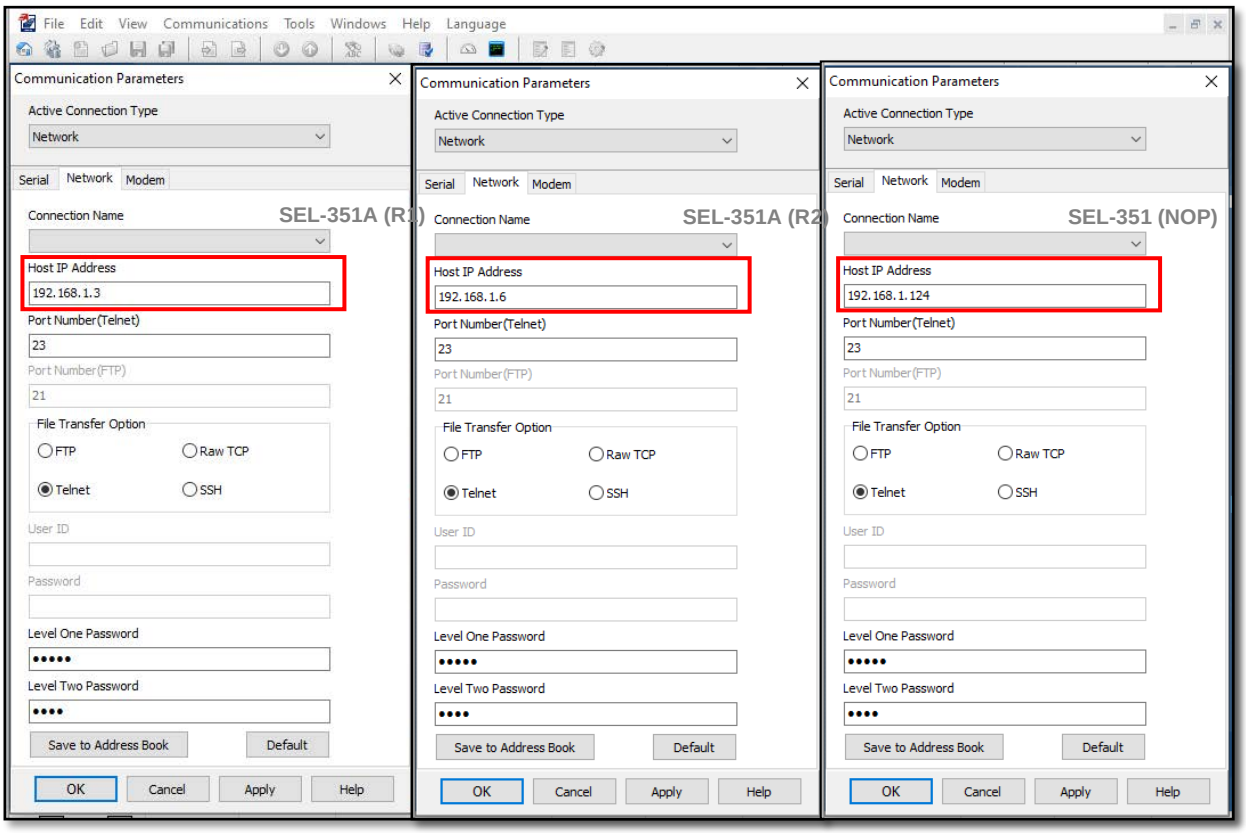

Figure 5.4: AcSELerator Quickset communication configuration settings for reclosing relays SEL-351A (R1), SEL-351A (R2), and SEL-351 (NOP)

The SEL-351A (R1), SEL-351A (R2), and SEL-351 (NOP) relays communication setup parameters depicts in Figure 5.4. The connection type should be network, the IP addresses of the SEL-351A (R1), SEL-351A (R2), and SEL-351 (NOP) relays are 192.168.1.3, 192.168.1.6, and 192.168.1.124, respectively, the transfer file choice is telnet, and the passwords are set to default as OTTER and TAIL for level 1 access.

The Internet Protocol (TCP/IP) settings are specified in the sections illustrated in Figure 5.5 below to enable communication between the computer and the three relays. The IP address of the computer should be in the same domain as the IP address of the host relay, and the Subnet mask is 255.255.255.0. The operator can read, update, and send settings from and to three relays utilized in the project to create the auto-reclose scheme. once the communication configuration parameters are correct and the connection is established.

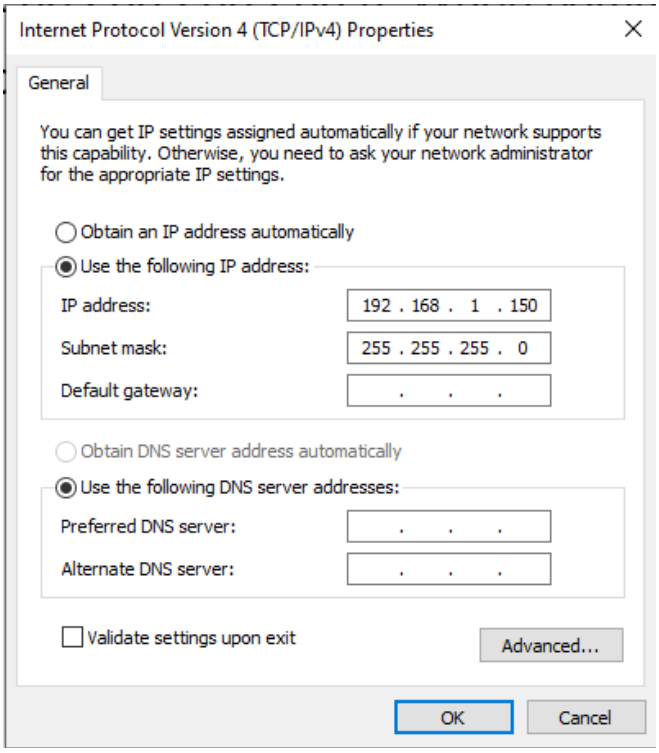

Figure 5.5: Properties of the Internet protocol (TCP/IP)

5.2.2 Configuration of the engineering settings for the relay SEL-351A (R1)

This section describes how to use the AcSELerator Quickset software program to configure the SEL-351A relay (R1) protection configuration parameters to configure the auto-reclose scheme. Once contact between the Personal Computer and the SEL relay is established, AcSELerator Quickset displays the SEL-351A (R1) engineering setup window, as shown in Figure 5.6 below. The SEL-351A relay includes six configurable groups that allow users to configure it for a variety of applications. Only group 1 is configured in this project. Figure 5.6 shows the usual setup settings for Groups 1–6, Global, Report, DNP Map, and ports.

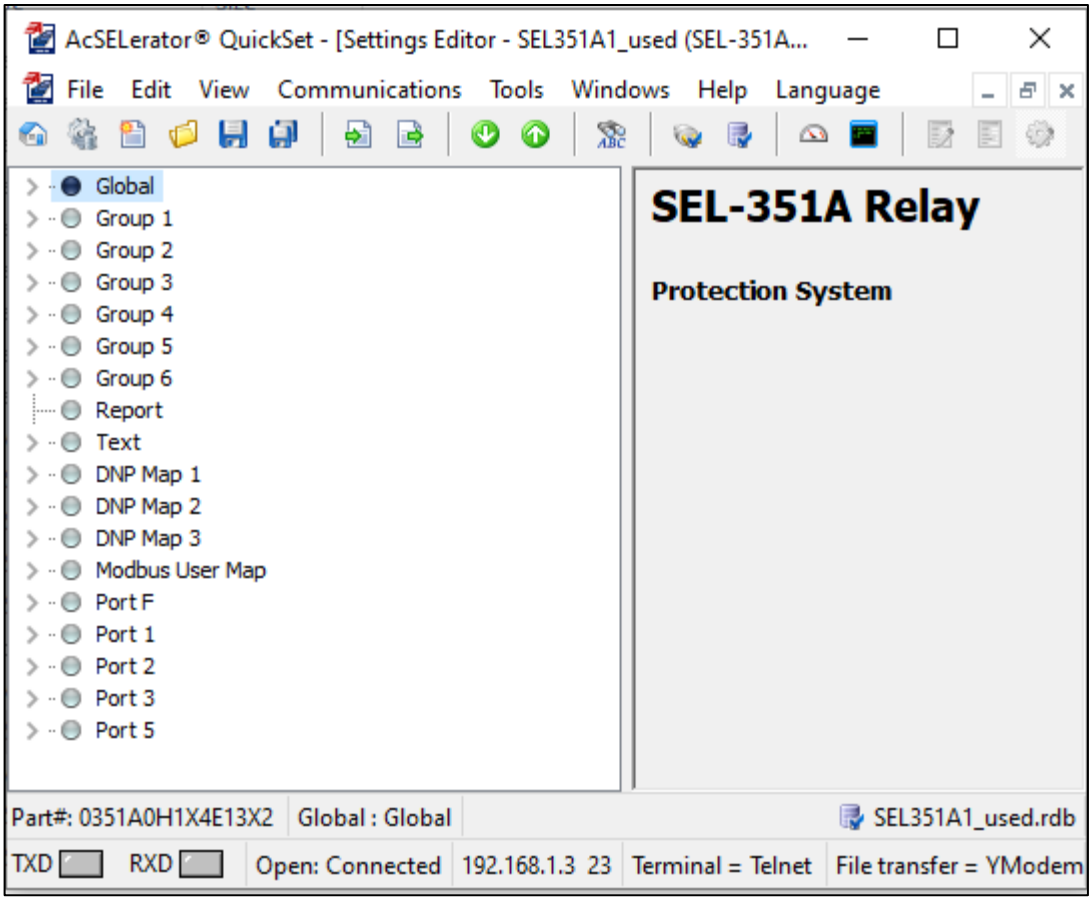

Figure 5.6: Setting the home page for the SEL351A (R1) relay configuration

The first item under Global function is General configuration settings, and the power system parameters are configured as follows. As illustrated in Figure 5.7, the nominal frequency is set to 50Hz, and the phase rotation is set to ABC.

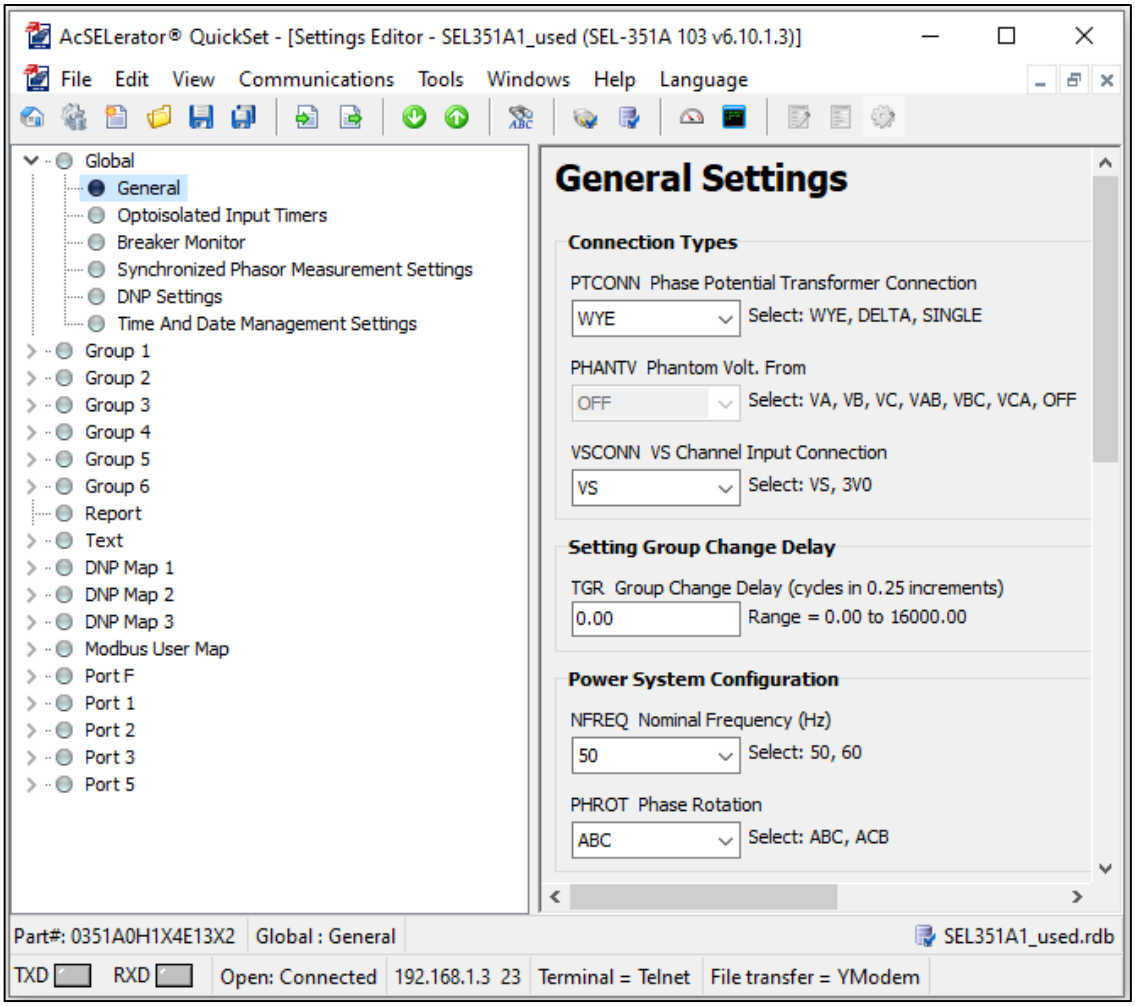

Figure 5.7: SEL-351A (R1) relay global general settings

Set 1 under group 1 is selected in Figure 5.8 below. Set 1 contains 20 items that must be configured for the relay SEL-351A. (R1). General settings, Phase Overcurrent Elements (50), Phase Time-Overcurrent Elements (67), Residual Ground Time-Overcurrent Elements (51), Directional element (32), and Reclosing relay (79) are configured for the lab-scale test bench set up in this section to test the auto-reclose and overcurrent protection functions of the SEL-351A relay (R1). The other configuration options are left at their default values.

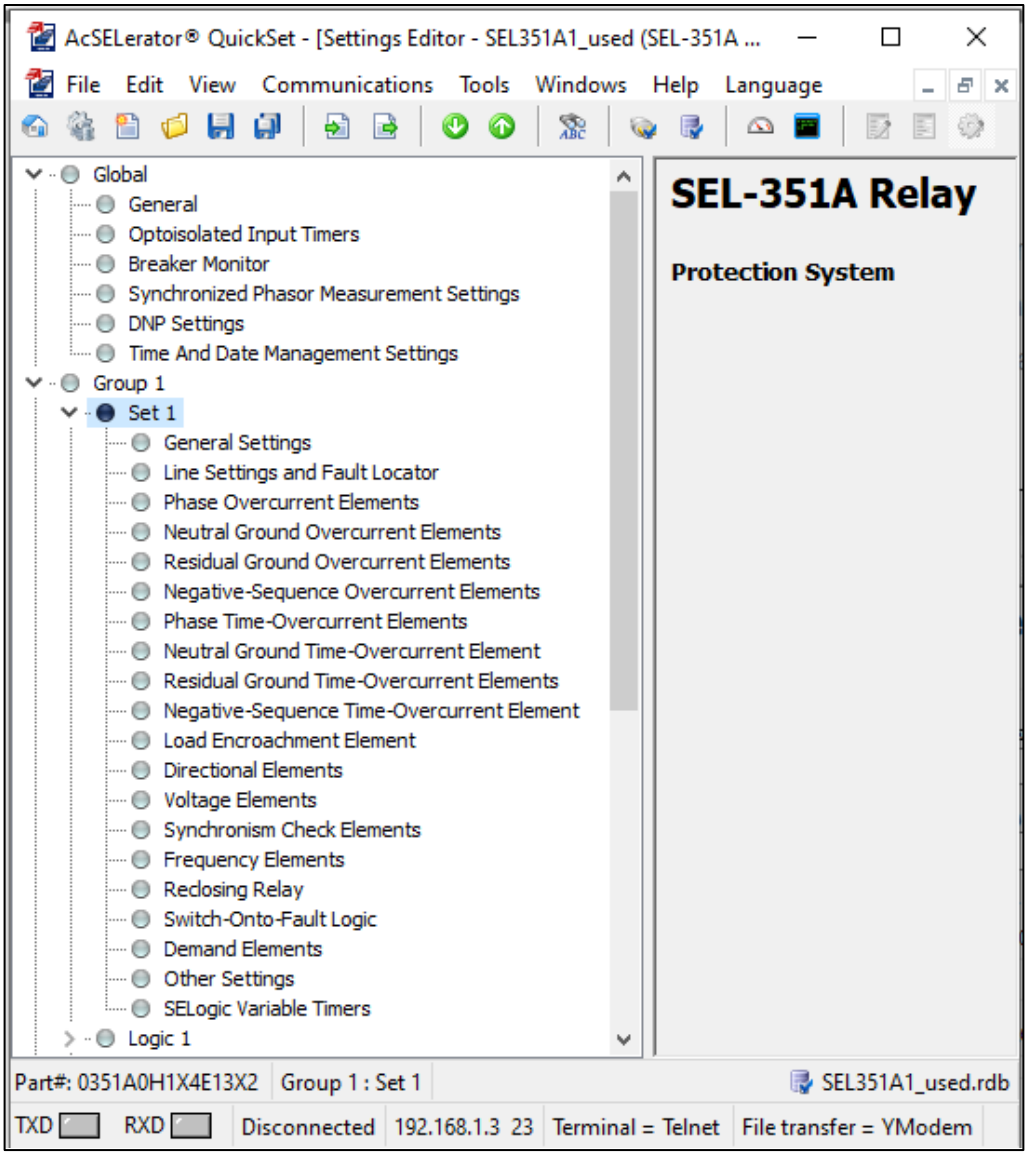

Figure 5.8: Set 1 configuration settings for the SEL-351A (R1) relay

In Figure 5.8, Set 1 under Group 1 is selected, and in Figure 5.9, Set 1 under Group 1's General settings are selected. The CT ratio for this project is configured in this section. As illustrated in Figure 5.9, the CT ratio for both phase and neutral elements is set to 300:1 amperes. Section 4.4.5 of Chapter 4 describes the CT selection procedure.

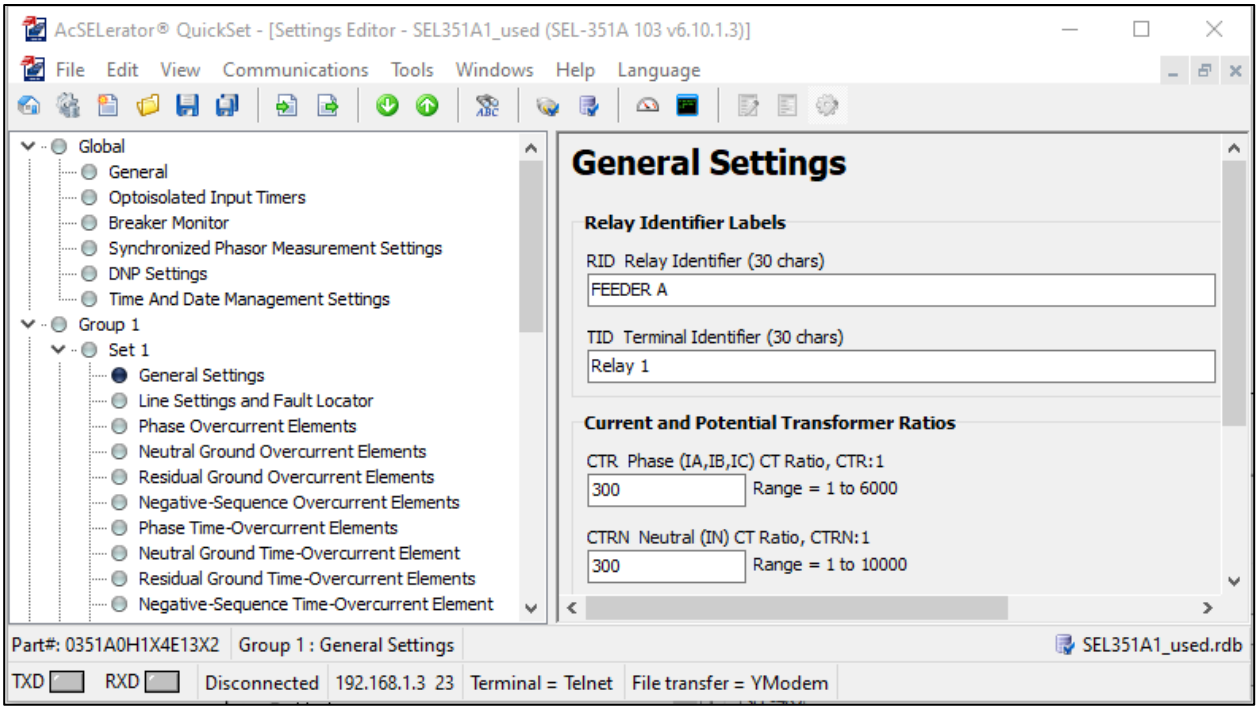

Figure 5.9: SEL-351A (R1) relay current transformer settings

The connection utilized to build the lab-scale test bench arrangement is depicted in Figure 5.10. A full wiring diagram is shown in Appendix B. Current input terminals Z01 through Z07 are provided on the SEL-351A relay (R1), where three-phase current signals are supplied into the relay via the test injection device. The output ports OUT 101 and 102 are connected to the TRIP and CLOSE signals, respectively, while the input port IN101 is mapped to the circuit breaker status.

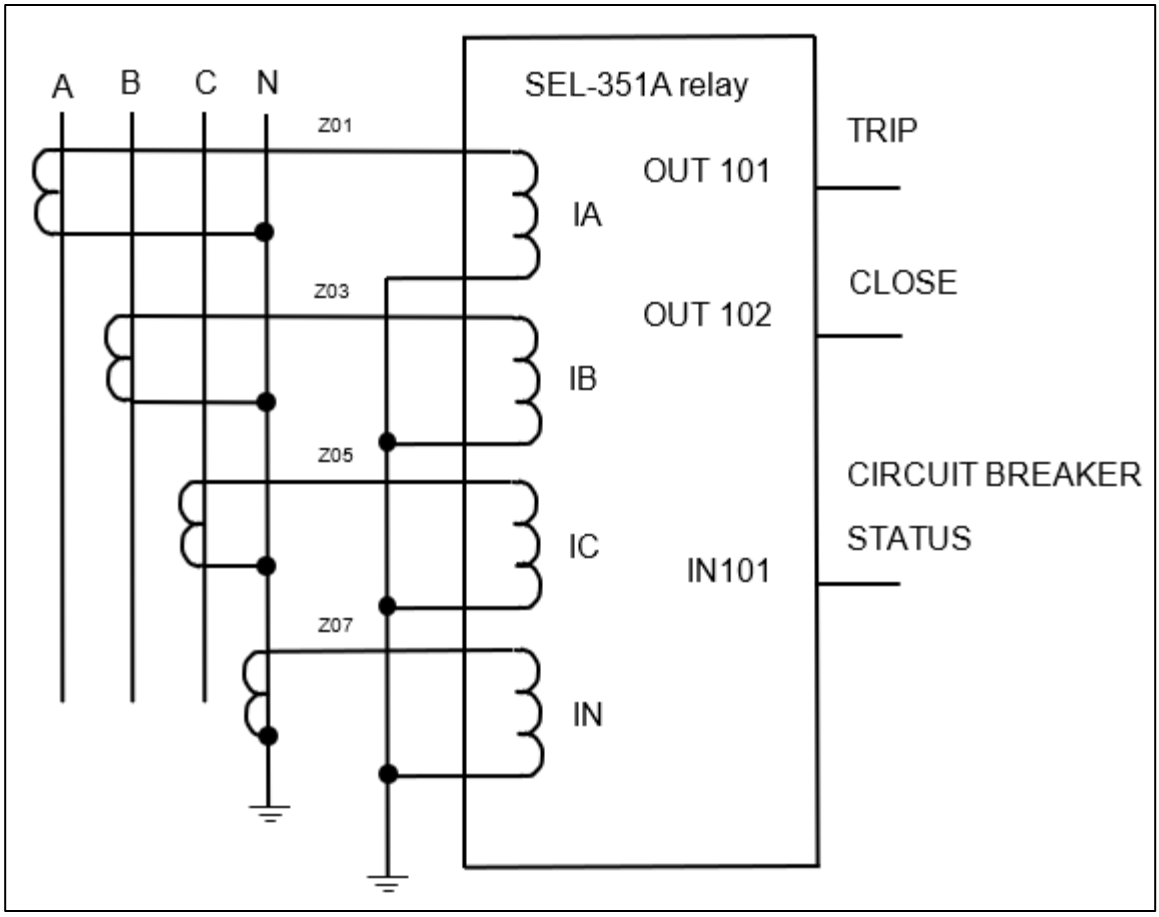

Figure 5.10: SEL-351A (R1) relay three-phase current connections

The overcurrent protection elements are the next set of parameters to be set up. On the SEL-351A relay, you can specify up to six levels of overcurrent protection for phase instantaneous/definite-time elements (R1). To make use of these features you'll need to Enable the E50P option, as shown in Figure 5.13. Only the element at level 1 is being utilized in this project. Figure 5.10 shows the input current signals (IA, IB, IC, and IN) flowing into the comparator. All the input current signals are tested against the 50P1P preset. The comparator's output is proportional to the current it receives. 50A1, 50B1, and 50C1 are all set to high if current signals IA, IB, or IC in Figure 5.10 are greater than Figure 5.11's pre-selected 50P1P (logical 1) setting. It is set to low if the current in IA, IB or IC is less than the pre-set 50P1P value (logical 0). At least one of the present signals 50A1, 50B1, 50C1 must be high for 50P1 to be a logical 1.

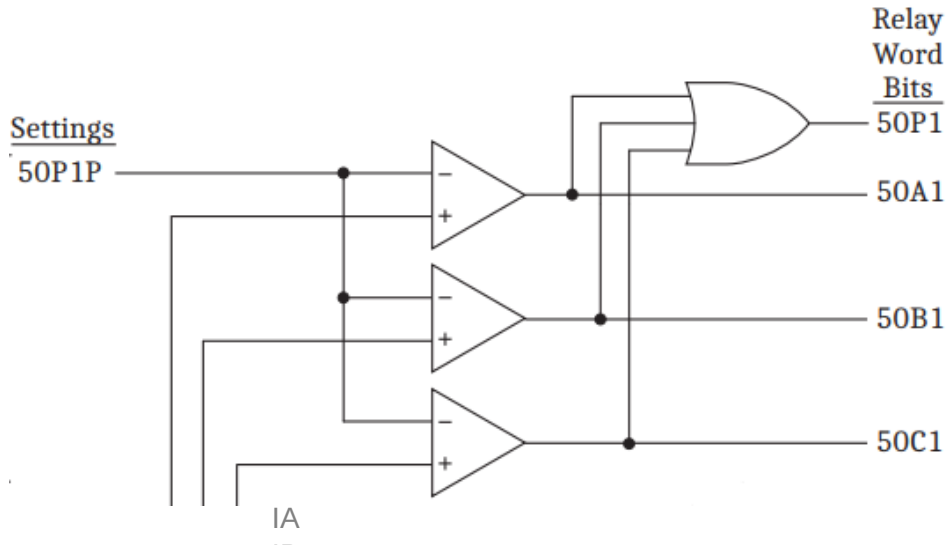

Figure 5.11: Level 1 phase Instantaneous overcurrent element of the SEL-351A (R1) relay

As shown in Figure 5.11, a relay word bit 50P1 is used as the input to Figure 5.12. In this project, the directional control element (E32) in Figure 5.12 has been set to "N". Since there is no direction control, E32 will be constantly asserted (logical 1).

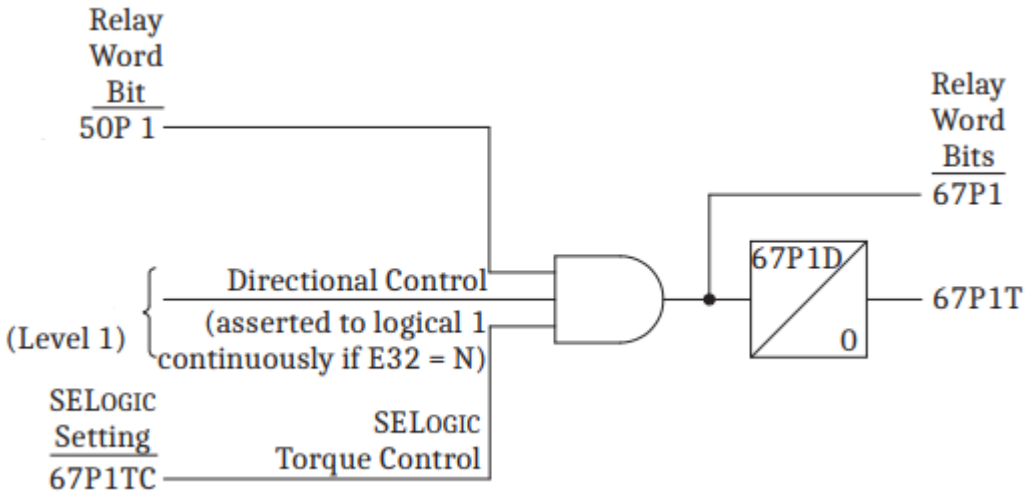

Figure 5.12: Level 1 phase Instantaneous overcurrent element with directional control (SEL-351A Instruction manual, 2020)

Directly in the SEL-351A relay, the torque control (67P1TC) has been set to logical 1. As demonstrated in Figure 5.12, the instantaneous overcurrent elements (67P1T) would be non-operational if the torque control was set to logical 0. The AND gate's output 67P1 is asserted when all three of its inputs 50P1, E32, and 67P1TC are high, as shown in Figure 5.12. After the pre-set time delay, the AND gate 67P1D transmits a trip signal to the 67P1T element, which is the phase definite time overcurrent element with time delay (in seconds). This trip signal is provided to the circuit breaker for the load to be shed through output 101 in Figure 5.10.

In the SEL-351A (R1) relay, the aforesaid logic is set up in group 1 settings, under phase overcurrent elements, as shown in Figure 5.13 below. It is set to 1, then 50P1P pick up element is set to 13A, time delay elements 67P1d is set to zero cycles, and all other elements are disabled.

The phase time-overcurrent setting is the next setting to configure. There are four time-overcurrent elements in the SEL-351A (R1). E51P, the enable setting, turns these features on. There are four phase time-overcurrent elements, each having an enabling setting and operating currents, listed in Table 5.1 below.

Table 5.1: All phases of the SEL-351A (R1) time-overcurrent elements

Time-Overcurrent Element	Enable setting (E51P= N,1 or 2)	Operating current
51PT	1 or 2	Maximum phase current (IP)
51AT	2	A-Phase (IA)
51BT	2	B-Phase (IB)
51CT	2	C-Phase (IC)

For example, if E51P is equal to N, it indicates phase time overcurrents are disabled; if E51P is equal to 1, it means the maximum phase overcurrent element (IA, IB, and IC) is enabled; and if E51P is equal to 2, it means the phase overcurrent elements (IA, IB, and IC) are enabled.

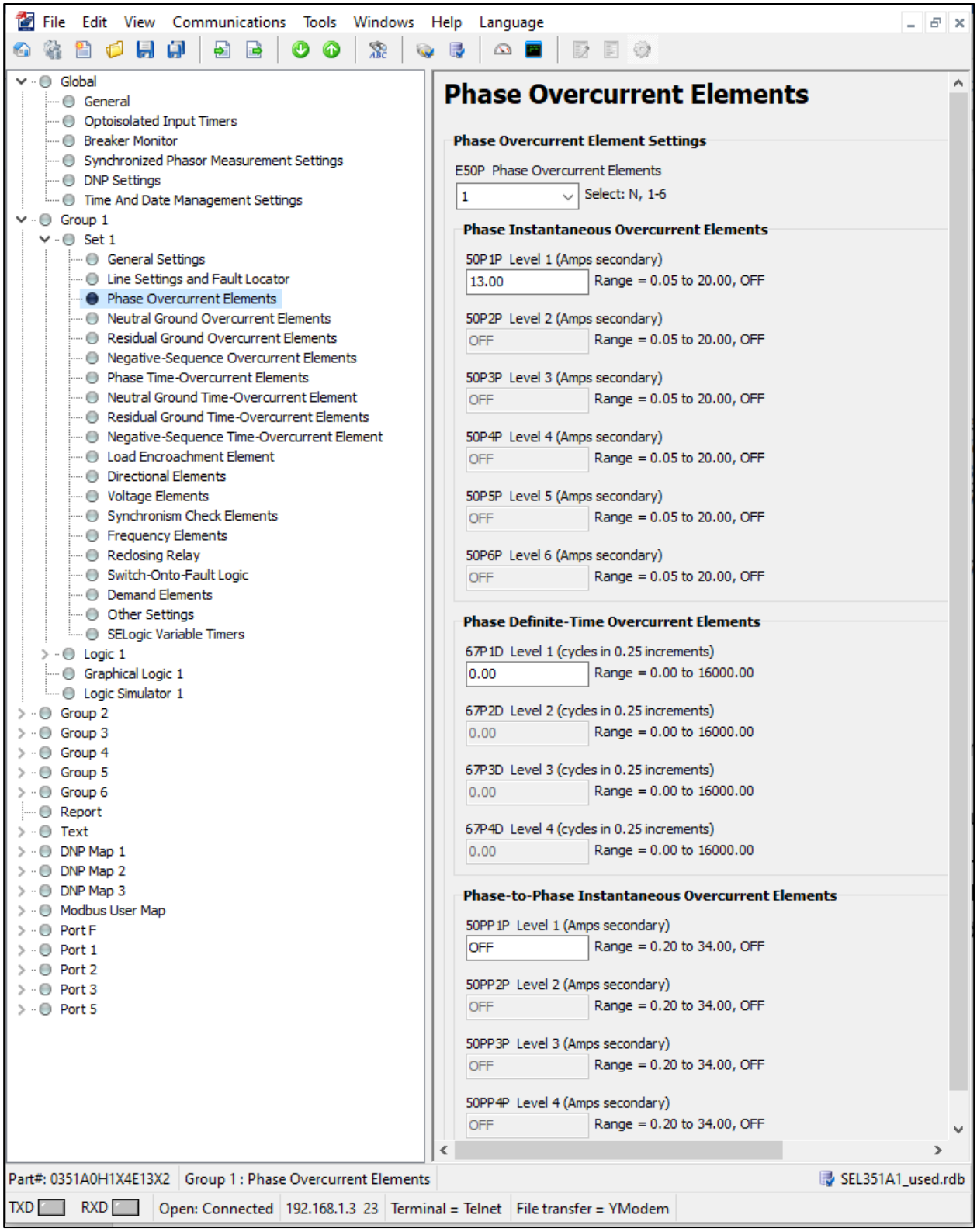

Figure 5.13: Phase overcurrent configuration settings of the SEL-351A (R1) relay

Maximum phase overcurrent logic is explained in this part because it was employed in this project. Three more phase time overcurrent elements (IA, IB and IC) operate in exactly the same way as the maximum phase time-overcurrent element mentioned above. The maximum phase time-overcurrent configuration parameter used in this project is shown in Table 5.2 below.

Table 5.2: Maximum phase time-overcurrent configuration settings of the SEL-351A (R1) relay

Relay word bits	Definition	Threshold value
51PP	Pickup	0.84A
51PC	Type of curve	C1
51PTD	Time dial	0.13 seconds
51PRS	Electromacanical reset timing	N
51PTC	SELOGIC for torque control setting	1

Fig. 5.14 shows the directional control element (E32) with its value set to "N". This is why E32 and the directional control are always asserted (logical 1). The SEL-351A (R1) relay has the torque control (51P1TC) set to logical 1. The torque control switch closes when the AND gate's two input signals are both logical 1. A comparison is made between these three-phase currents (I_P) and the comparator's 51PP pickup setting (see Figure 5.14). As soon as the phase time overcurrent has timed out on its curve due to an Ip exceeding the 51PP pickup setting, the comparator pickup's output will have the 51P element. As illustrated in Figure 5.11, when these conditions are met, the relay contact output port OUT101 receives a trip signal, making 51PT logical 1. If Ip is less than pickup 51PP, the comparator's output is a logical 0, and as a result, assertions 51P and 51PT are de-asserted.

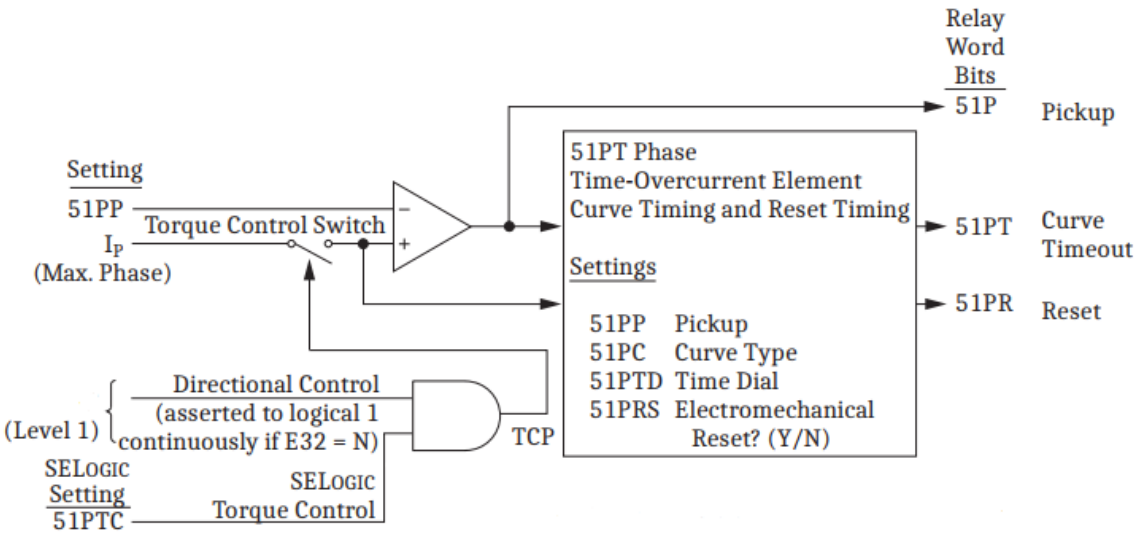

Figure 5.14: Phase time-overcurrent logic for level 1 element (SEL-351A Instruction manual, 2020)

Figure 5.15 shows the SEL-351A relay (R1) with the logic mentioned previously. Phase time-overcurrent elements can be found in Group 1 settings.

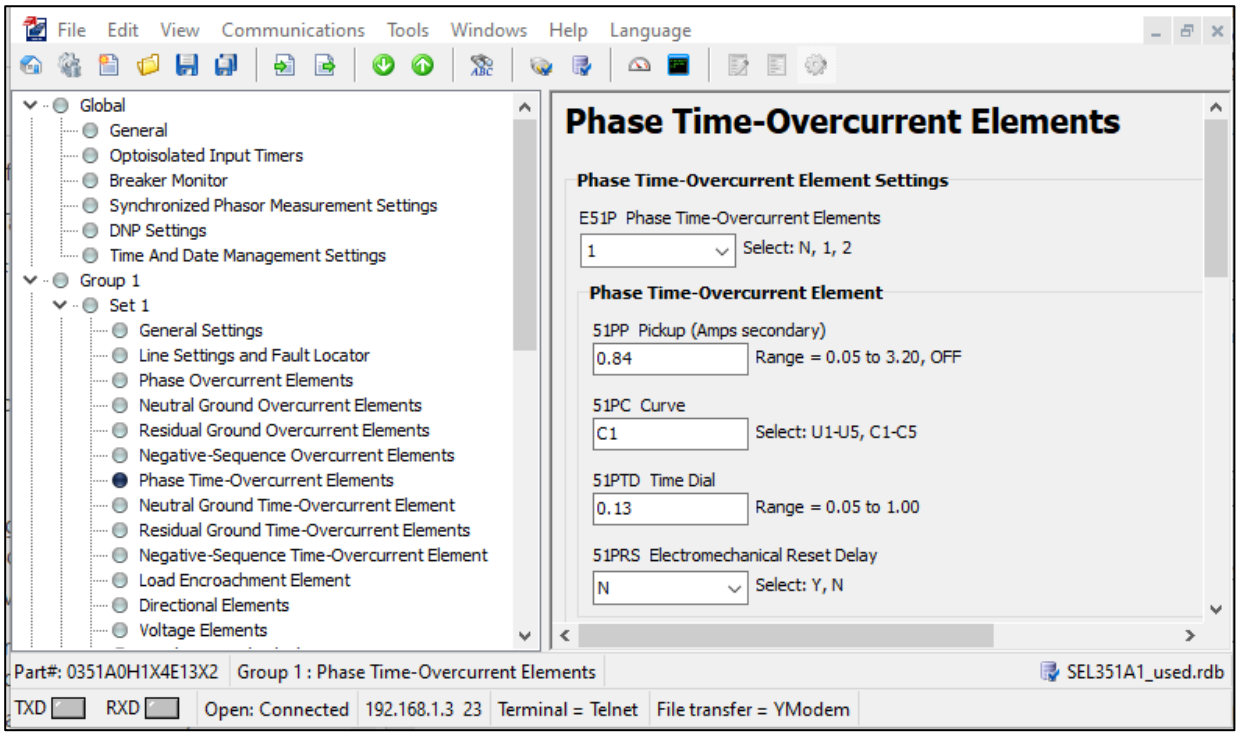

Figure 5.15: Phase time-overcurrent element configuration settings of the SEL-351A (R1) relay

On the SEL-351A relay, two residual ground time-overcurrent components are provided using the AcSELerator Quickset software (R1). Only the level1 element is utilized in this project. Table 5.3 and Figure 5.16 show the settings for residual ground time-

overcurrent. Residual ground time overcurrent logic is shown in Figure 16. Using Figure 5.14's explanation of phase time overcurrent logic, the maximum phase current "I_P" can be replaced with residual ground current "I_G," and other settings and relay word bits can be replaced as well.

Table 5.3: Residual ground time-overcurrent element configuration settings

Setting	Difinition	Settings on SEL-351 IED
51GP	Pickup	0.21A
51GC	Type of curve	C1
51GTD	Time dial	0.17 seconds
51GRS	Electromacanical reset timing	N
51GTC	SELOGIC for torque control setting	1

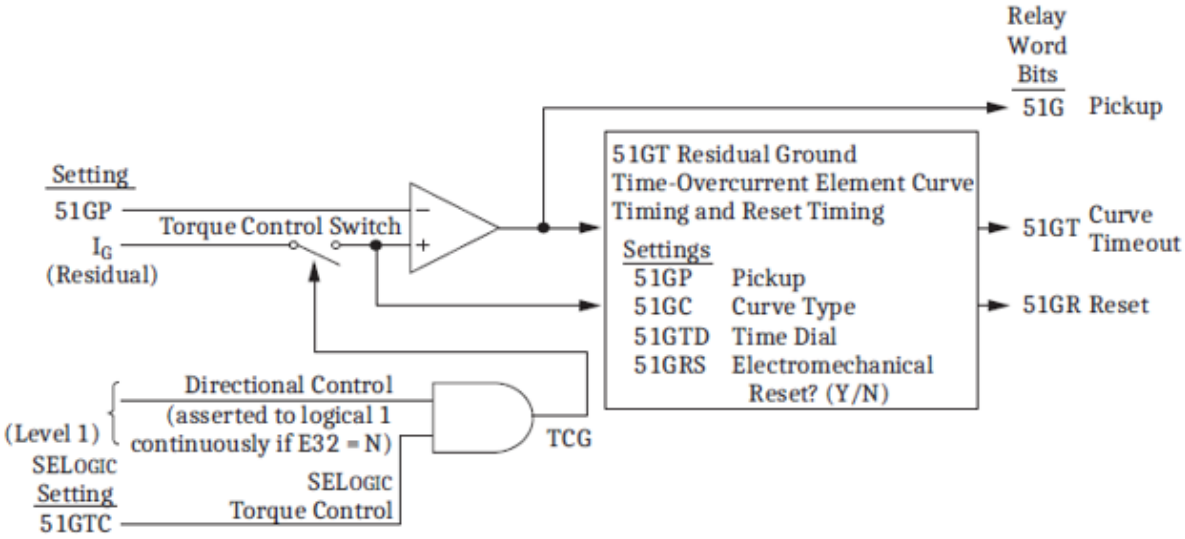

Figure 5.16: Residual ground time-overcurrent for level 1 element (SEL-351A Instruction manual, 2020)

Figure 5.17 shows the AcSELerator Quickset software's Residual ground time-overcurrent elements configuration parameters.

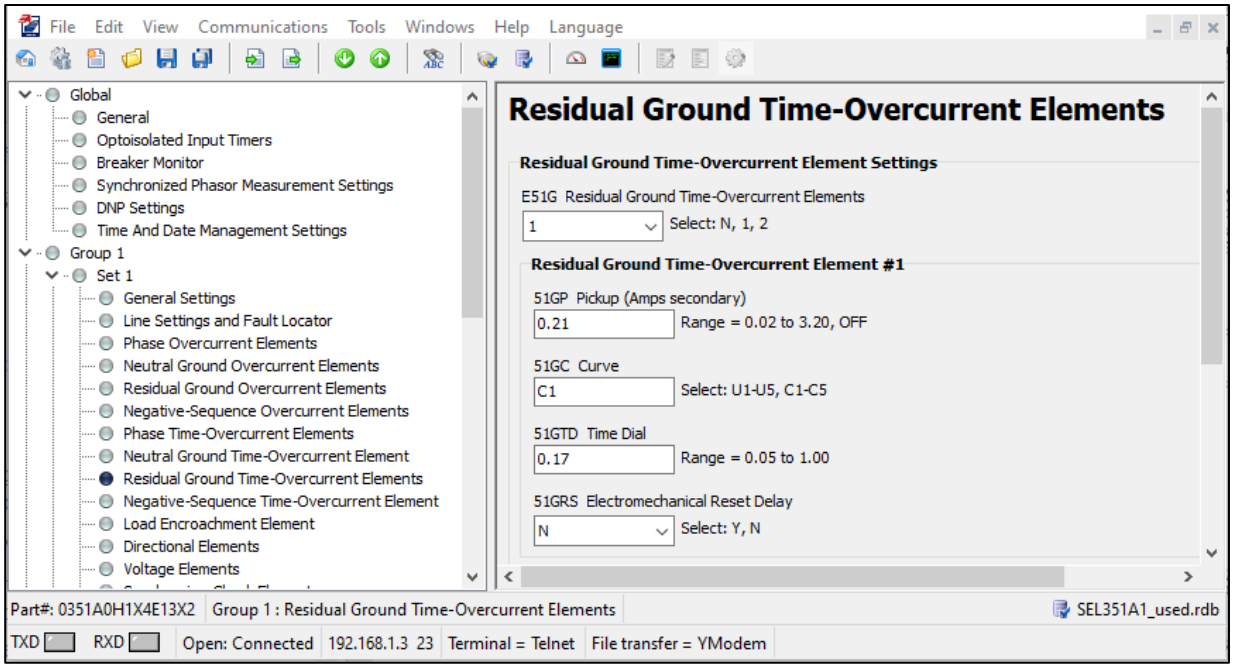

Figure 5.17: Residual time-overcurrent elements configuration settings

The last group 1 settings are those for the reclosing relay. The E79 reclose setting can be used to activate the reclose settings for the reclosed relays. E79 regulates the number of open interval time settings. Three open intervals are employed in this project. IEEE Std. C37.104-2012 dictates the selection of open intervals and reset time for the data. Following this Table 5.4 has the ANSI code 79 elements setup for the SEL-351A reclosing relay (R1). The overcurrent and auto-reclose settings obtained from the SEL-351A relay terminal window are shown in Appendix C.

Table 5.4: Reclosing relay open interval settings

Recloser relay word bits	Recloser time delays in cycles	Description of the relay word bits
Reclosing relay open interval 1 (79OI1)	150 cycles	The required time of CB time to stay open from the first shot
Reclosing relay open interval 2 (79OI2)	500 cycles	The required time of CB time to stay open from the second shot
Reclosing relay open interval 3 (79OI3)	500 cycles	The required time of CB time to stay open from the third shot
Reset time from reclosing cycle (79RSD)	750 cycles	Qualifies automatic closure, when the relay is in reclose cycle state

Reset time from lockout (79RSLD)	750 cycles	Qualifies closure when the relay is in the lockout position
Reclose supervision time limit (79CLSD)	0 cycles	Inoperative

The reclosing relay settings are configured in the AcSELerator Quickset software as shown in Figure 5.18 below.

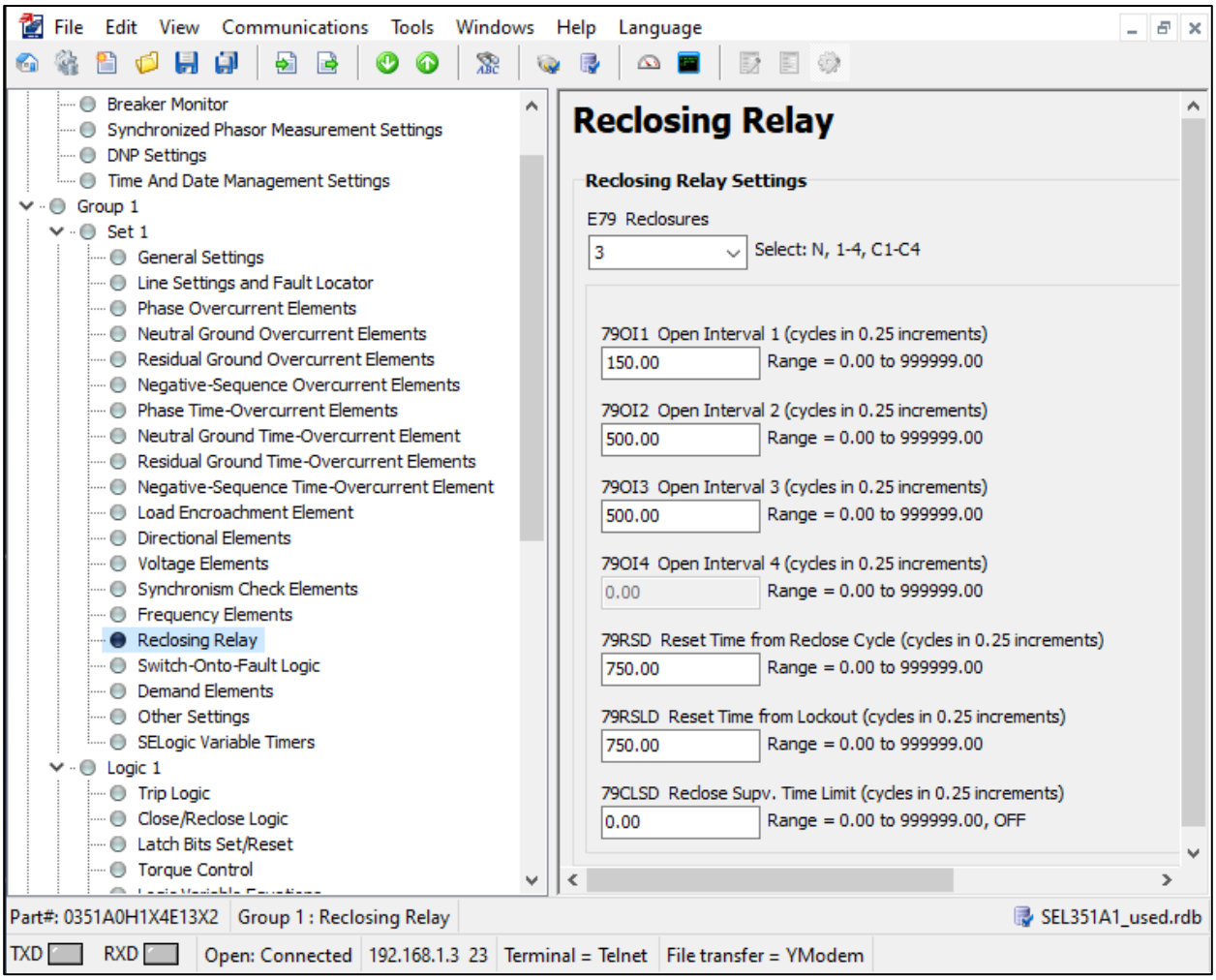

Figure 5.18: Reclosing relay configuration settings

This table lists the SEL-351A (R1) relay reclosing states, together with its relay word bit and LED status, as seen in Table 5.5 and Figure 5.19.

Table 5.5: SEL-351A (R1) reclosing state along with its relay word bits and front panel LED status

SEL-351A reclosing states	Relay word bit	Front panel LED
Reset	79RS	RS
Reclose cycle	79CY	CY
Lockout	79LO	LO

According to IEEE Std. C37.104-2012 and SEL-351A instruction manual, the following Figure 5.19 shows the relay reclosing states and auto-reclose general function.

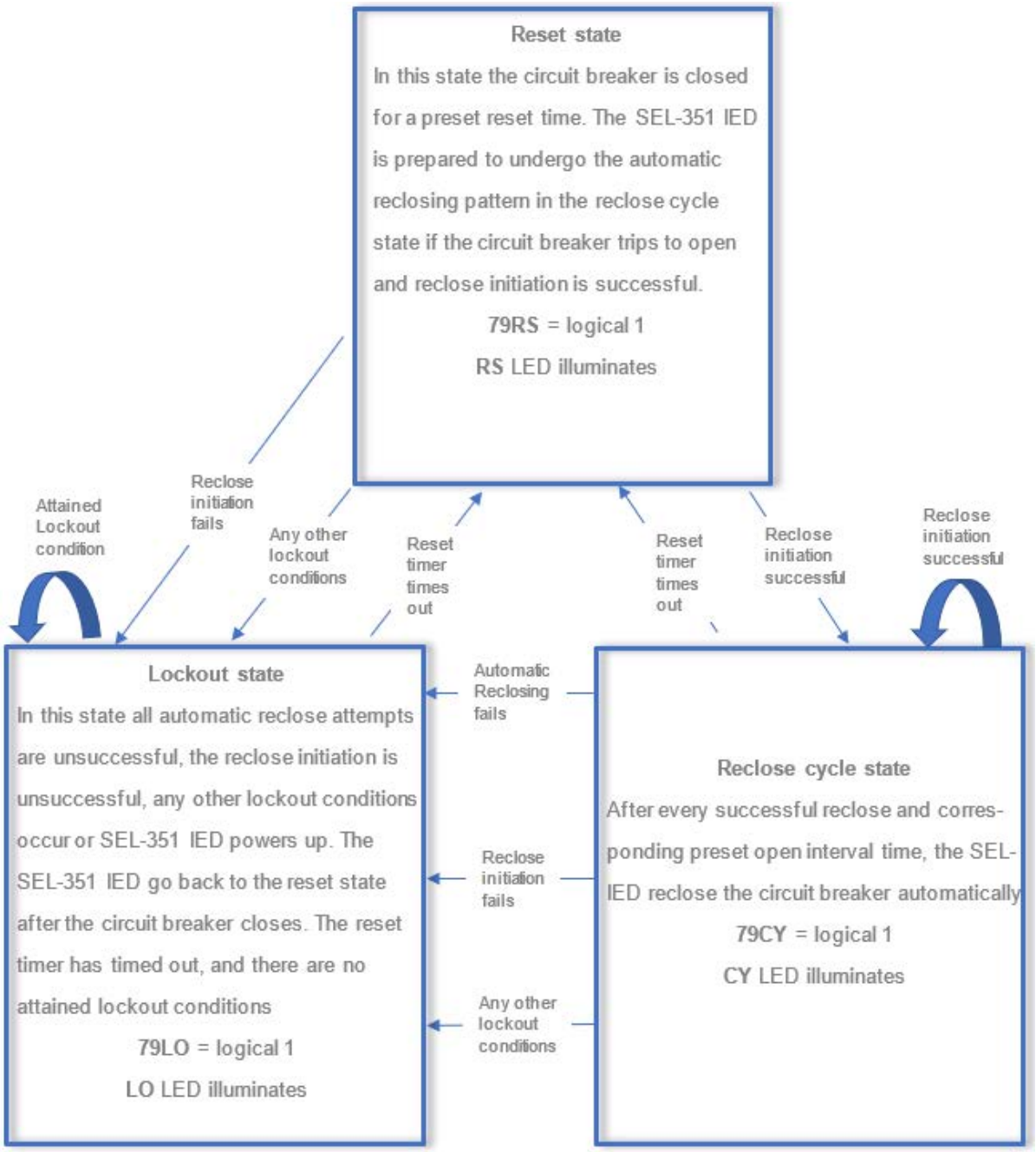

Figure 5.19: The relay auto-reclose states

The parameters for Logic 1 can be seen in the following Figure, 5.20. Logic 1 includes a total of 14 configurable options. Output contacts and other trip/communication-assisted trip elements are only configured in this chapter. Below are the instantaneous and time overcurrent trip elements that correspond to the set phase overcurrent elements, residual ground time overcurrent elements, and phase time-overcurrent elements. In this section, all of the other settings are pre-configured.

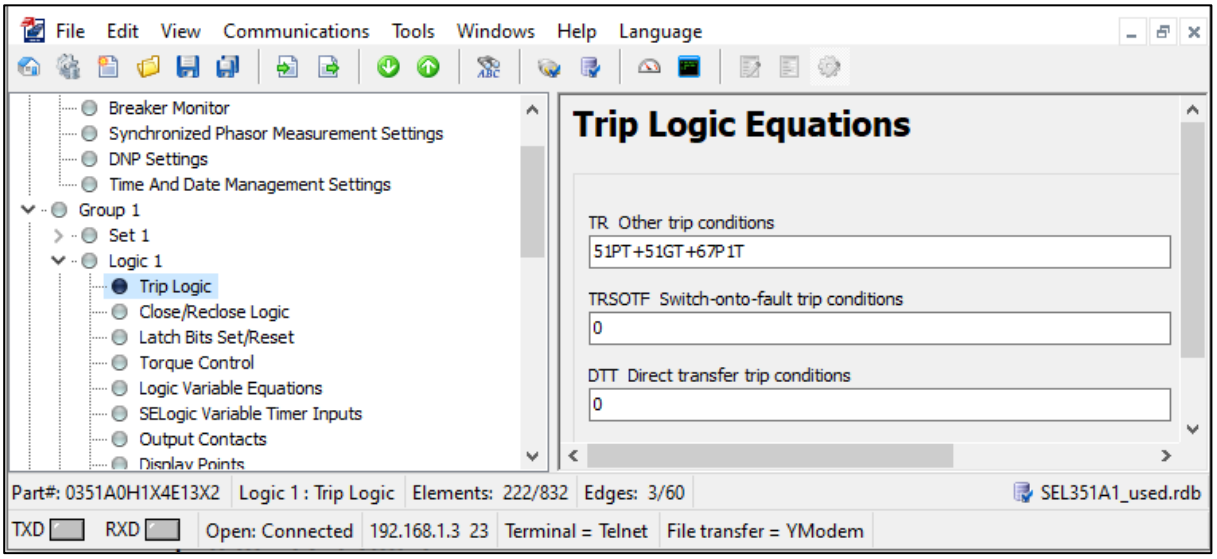

Figure 5.20: SEL-351A (R1) relay trip/communication-assisted logic

Figures 5.21 and 5.22 illustrate the SEL-351A (R1) relay's close logic and close/Reclose configuration. SEL-351A relay status (52A) reveals that the initial setting circuit breaker status (IN101) is mapped to the input contact port (IN101) of the SEL-351A relay (R1). Other from automated re-closing, the close criteria are set as default.. The unlatch close condition is set at 52A. The initial setting reclose initiate (79RI) is set to be 51PT element, which means that only 51PT must begin the auto-reclose procedure. In the setting reclose initiate supervision, 79RI is a rising edge detection element (79RIS). In order for open interval timing to start, 51PT must be set to logical 0 and 79RIS must be logical 1.

51PT's logical 0 to logical 1 transition enables the next open interval while 52A or 79CY is in the "enabled" state, and this is the reason 52A is there. Circuit breakers are closed (logical 1) at the time of the first trip in an auto-reclose cycle, which is when the SEL-351A relay (R1) is able to start the timer for the first open interval.

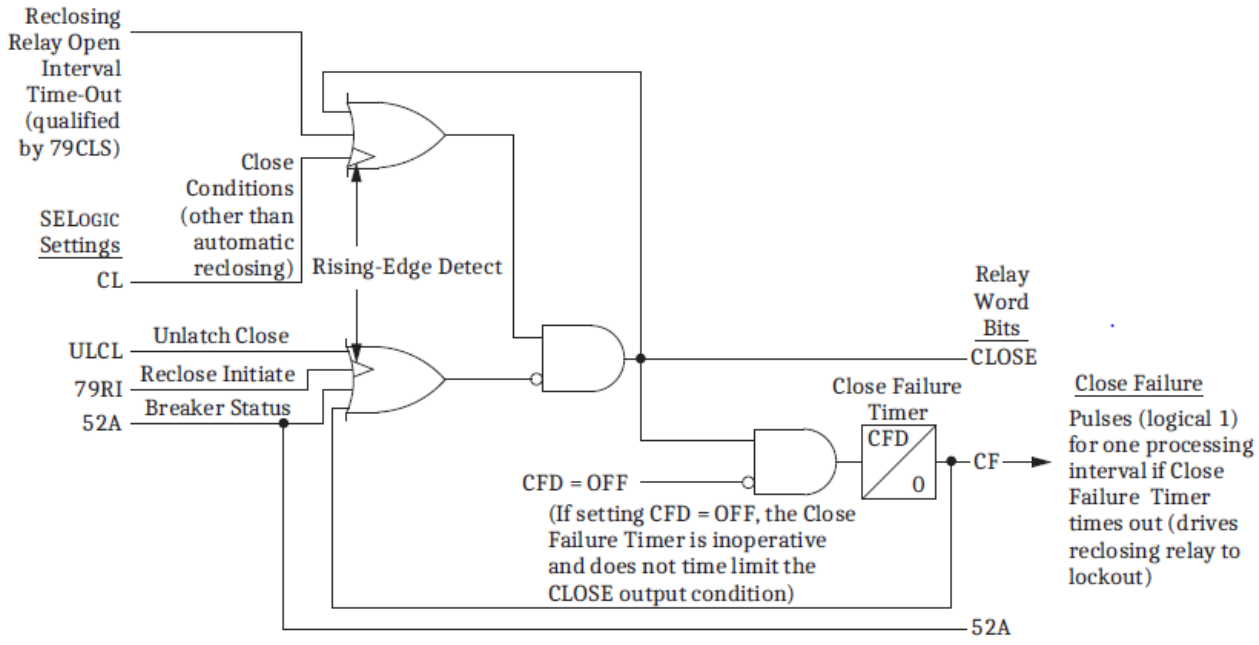

Figure 5.21: SEL-351A (R1) relay close logic (SEL-351A Instruction manual, 2020)

The reclose cycle state is still deactivated at the time of the first trip. In this case, 79CY is part of the re-initiate supervision settings for subsequent trips after the first trip. To put it another way, the R1 SEL-351A relay (79CY) has entered the reclose cycle state, while 52A has entered the open state.

A lockout has been placed on the 79DLS drive to last shot setting (79LO). When the shot counter is equal or greater than the last shot and the circuit breaker is open, the SEL-351A (R1) relay is driven to the last shot. There is no reclose supervision logic (79CLS) and all other options are set to 0.

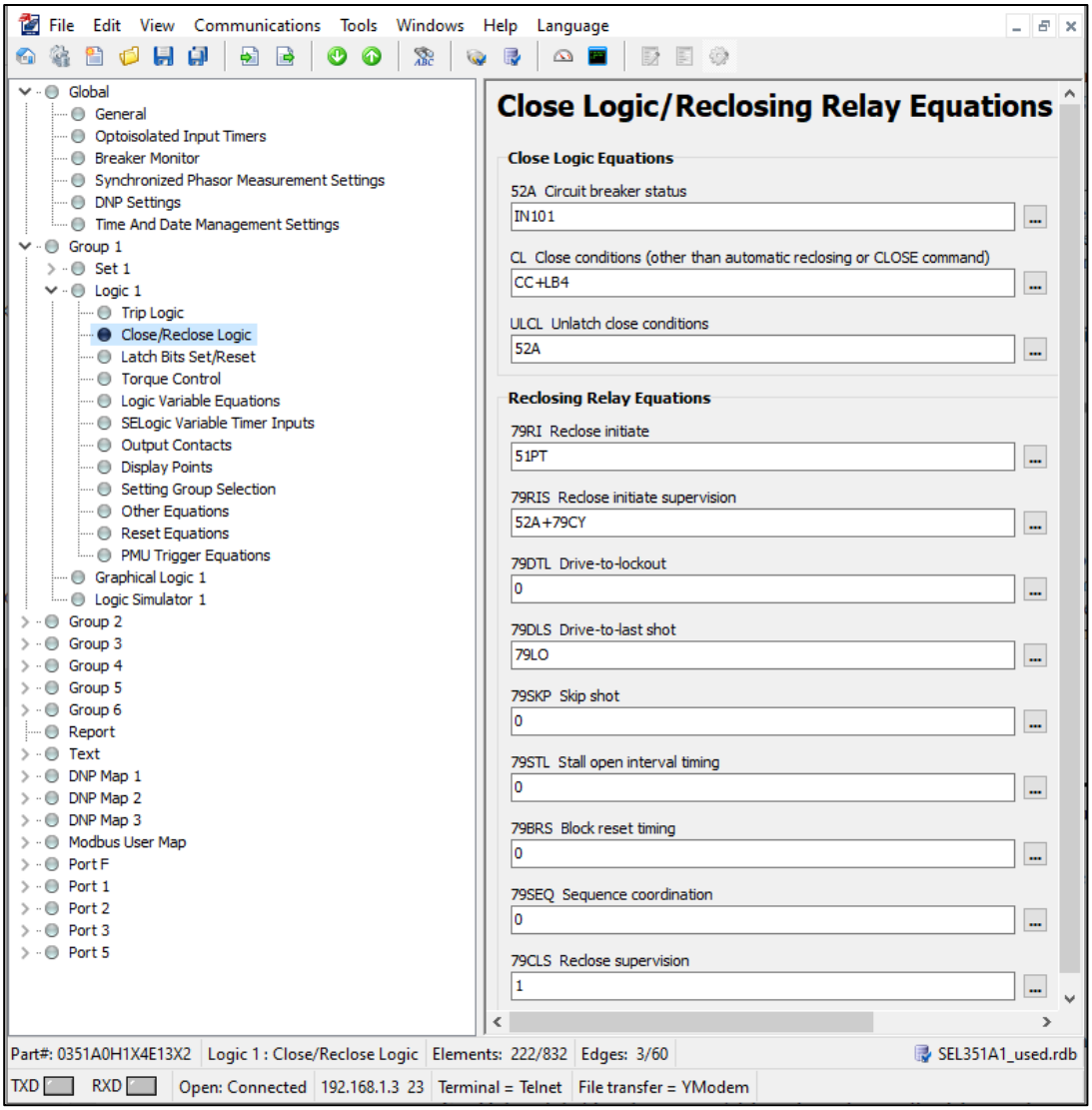

Figure 5.22: SEL-351A (R1) Reclosing relay close logic configuration

Graphical logic and output contact equations for relay SEL-351A are shown in the following Figures 5.23 and 5.24. There is a CLOSE command signal setting on relay output port OUT102 as well as the phases instantaneous, time-phase and residual time-overcurrent trip components all assigned to relay output contact port OUT101. There are two output ports that are used to send signals to SEL-351A (R2) and SEL-351 (NOP) in order to confirm that SEL-351A (R1) has been locked out owing to 51GT, 67P1T or 67P1T commencement. SEL-351A (R2) and SEL-351 (NOP) are controlled by these signals. Default values are used for the remaining setup options.

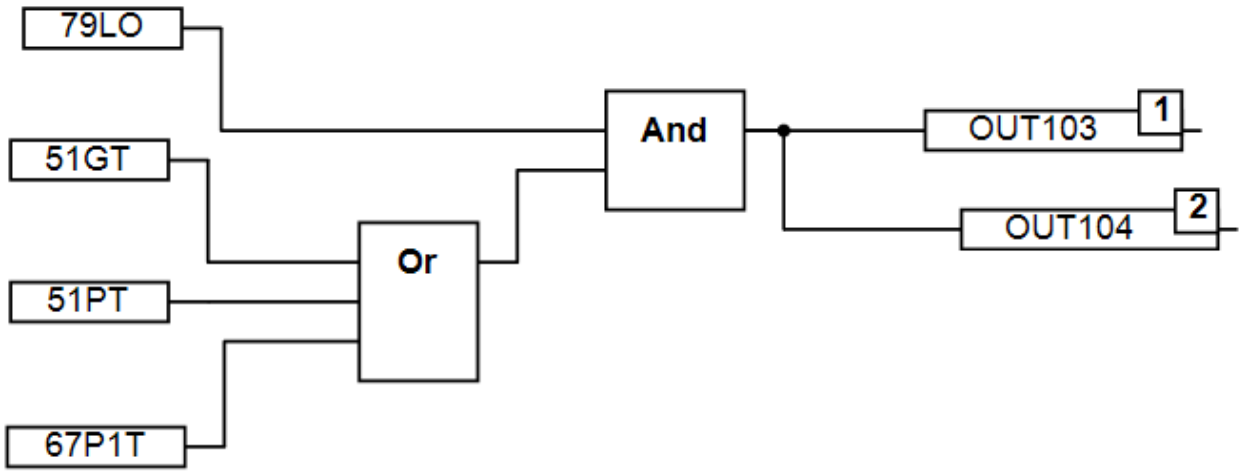

Figure 5.23: SEL-351A (R1) **relay** output ports logic congfiguration

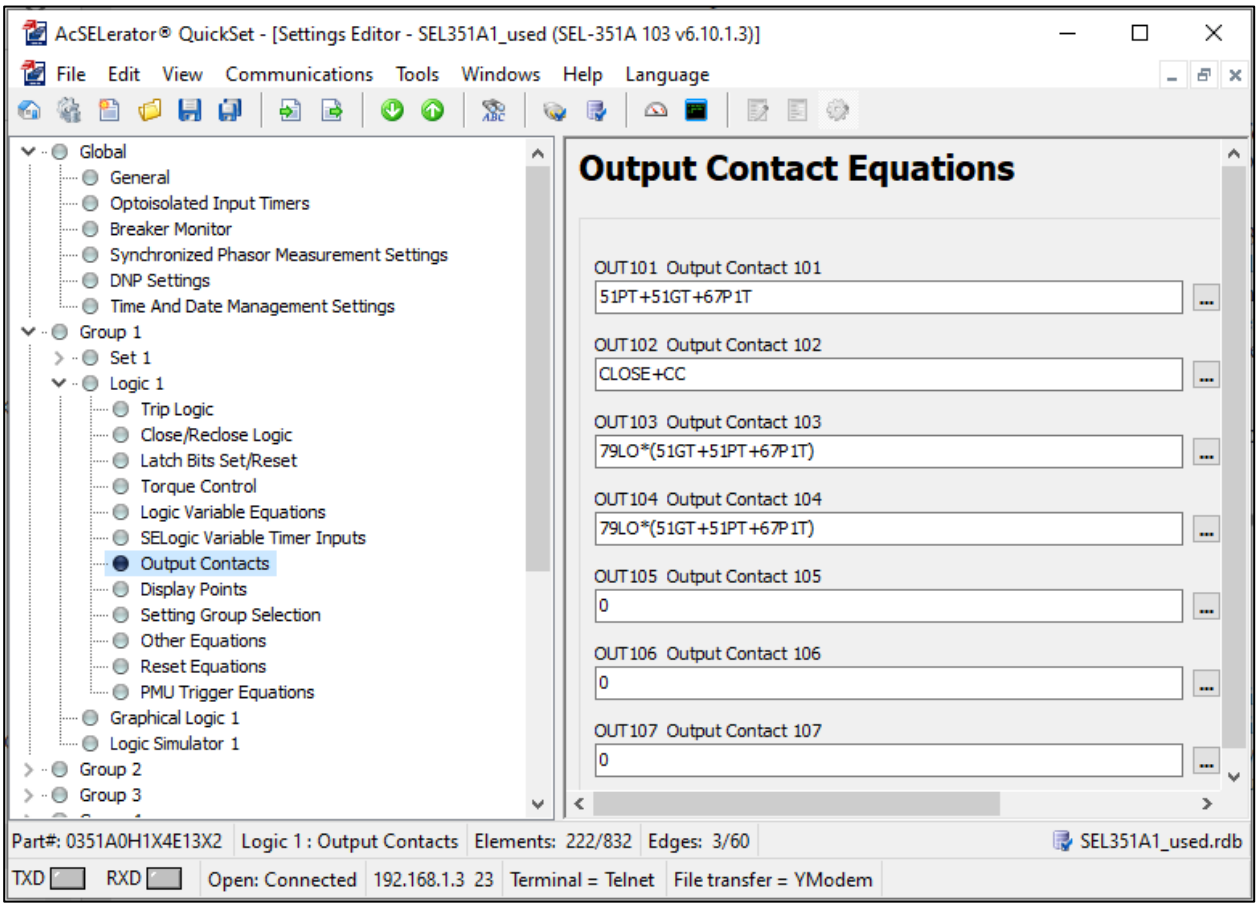

Figure 5.24: SEL-351A (R1) relay output port configuration settings

5.2.3 Configuration of the engineering settings for the relay SEL-351A (R2)

Figure 5.25 depicts the overall global configuration of the SEL-351A (R2) overcurrent reclosing relay. The system phase rotation is set to ABC, with a nominal frequency of 50Hz.

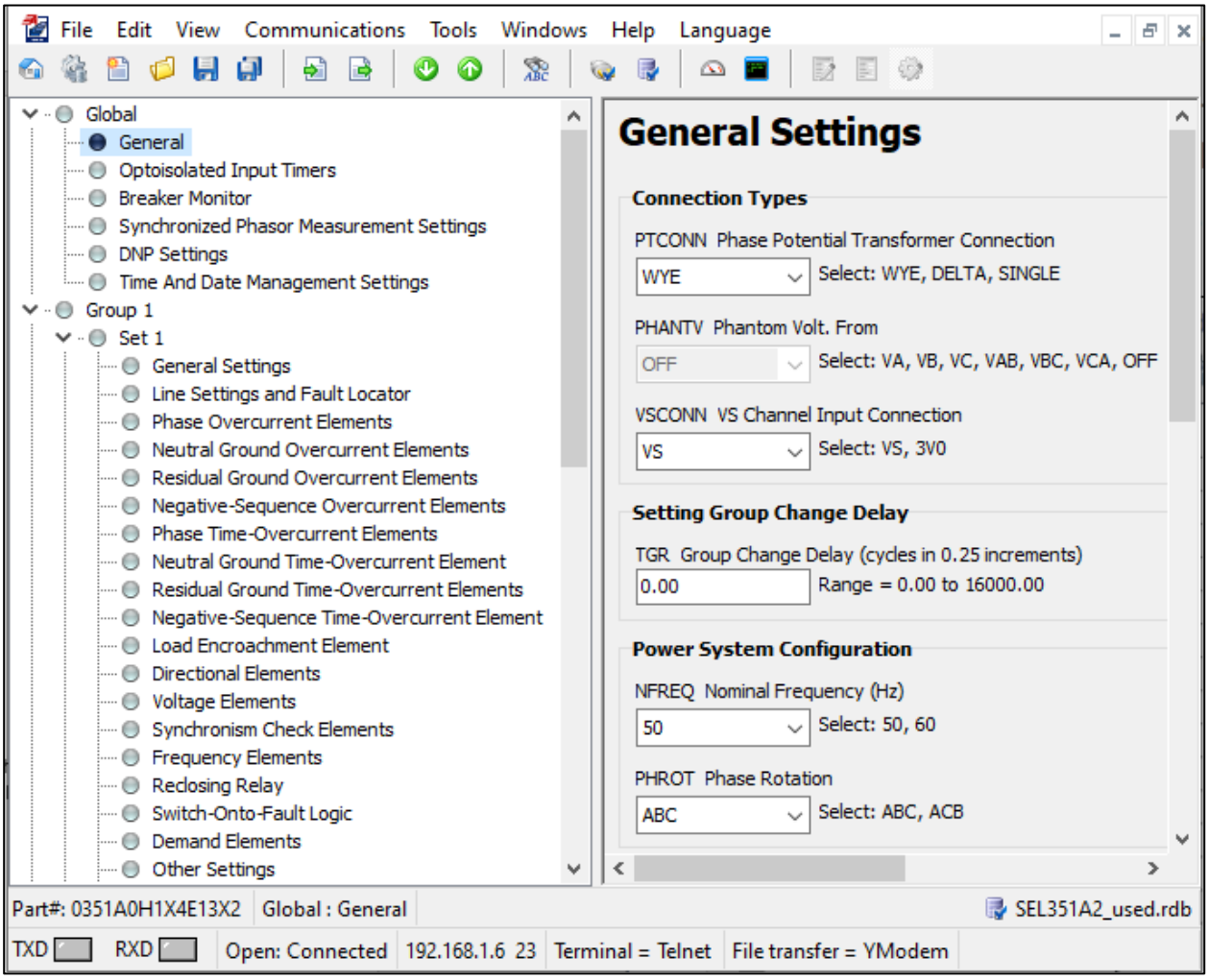

Figure 5.25: Global general settings of the SEL-351A (R2) relay

The CT ratios of SEL-351A (R2) are 300:1 for both phase and neutral elements, as illustrated in Figure 5.26. The CT ratio selection procedure is described in Chapter 4, section 4.4.5.

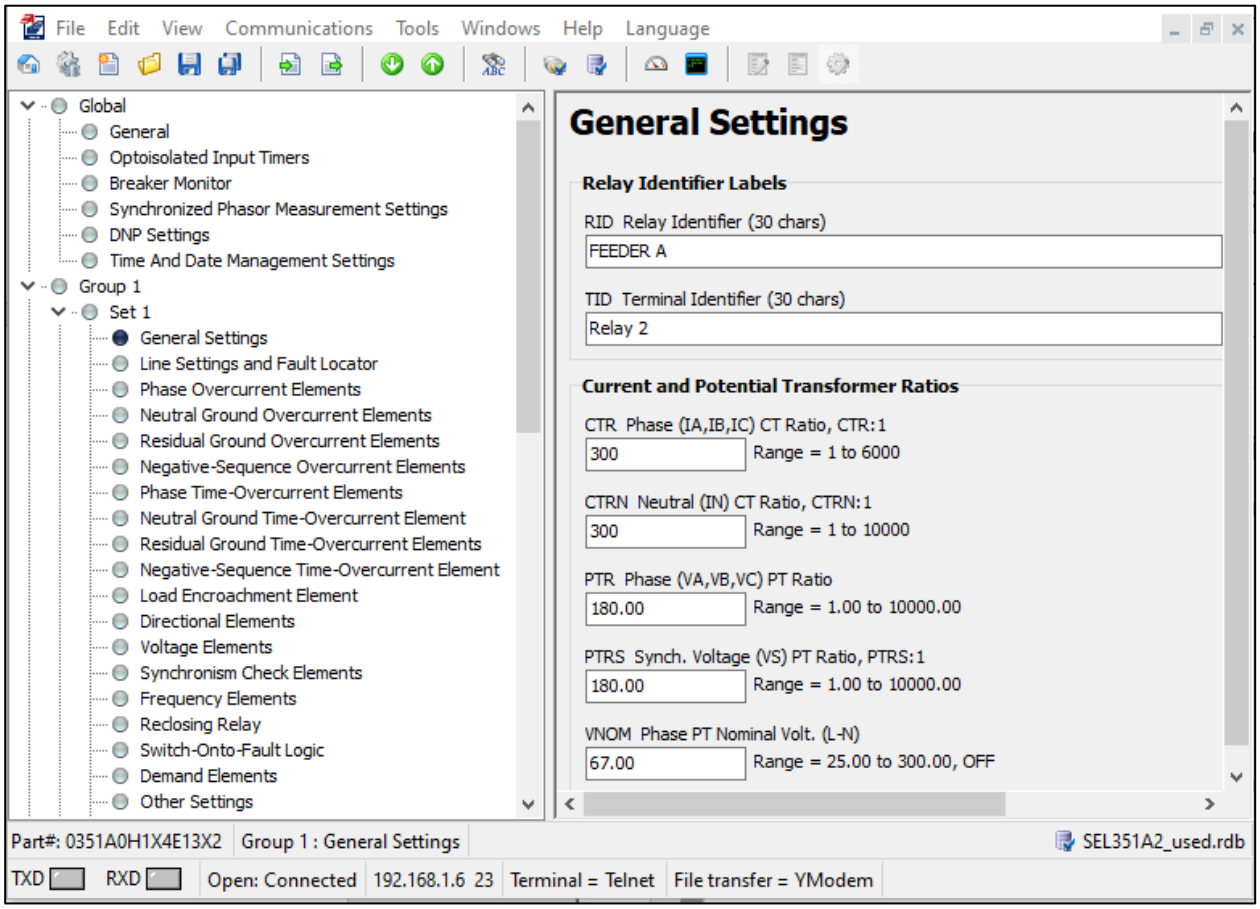

Figure 5.26: The SEL-351A (R2) relay's current transformer settings

The settings in Table 5.6 are used to configure the phase time-overcurrent element "51PP" pickup, time overcurrent curve selection "51PC", time dial "51PTD", electromechanical reset delay "51PRS", and torque control "51PRS".

Table 5.6: SEL-351A (R2) relay maximum phase time-overcurrent configuration settings

Relay word bits	Definition	Threshold value
51PP	Pickup	0.68A
51PC	Type of curve	C1
51PTD	Time dial	0.05 seconds
51PRS	Electromacanical reset timing	N
51PTC	SELOGIC for torque control setting	1

Figure 5.27 depicts the maximum phase time overcurrent setting of the SEL-351A (R2) on AcSELerator Quickset.

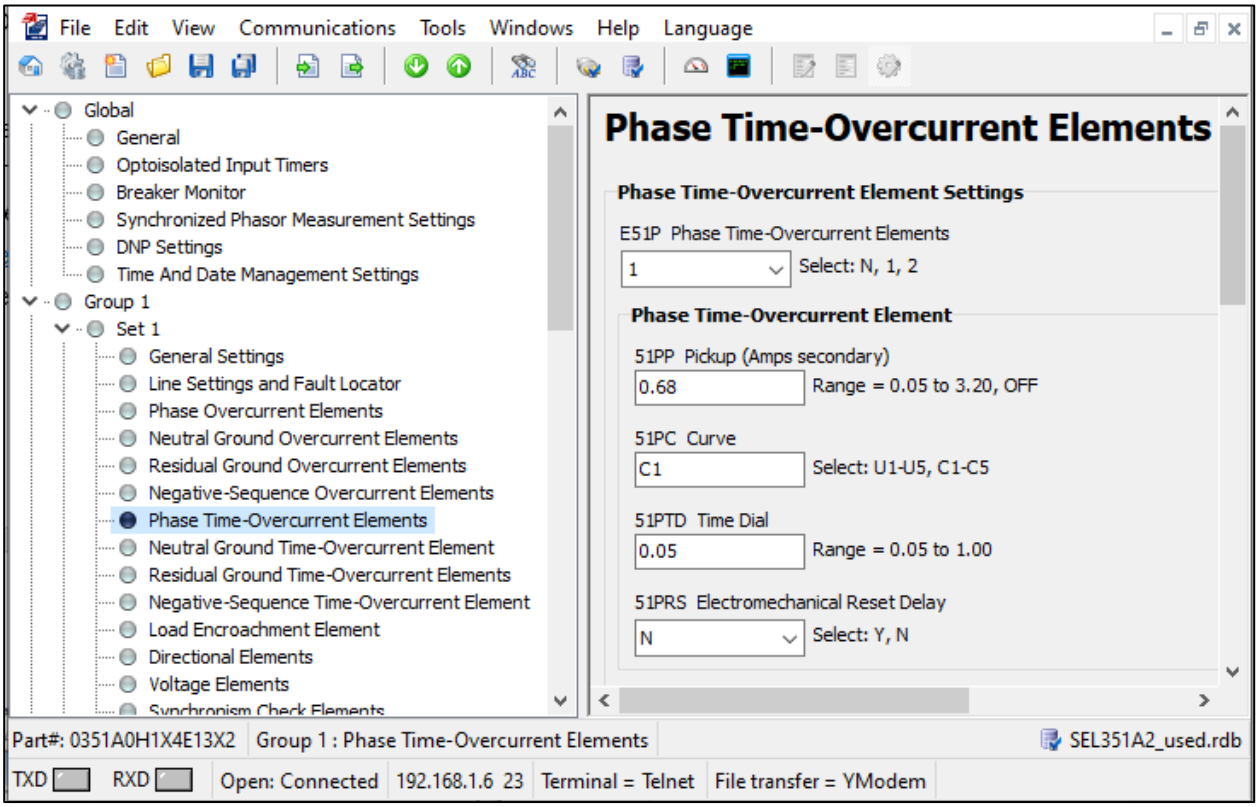

Figure 5.27: SEL-351A (R2) relay maximum phase time overcurrent configuration

The settings in Table 5.7 are used to define the residual ground time-overcurrent element "51GP," time overcurrent curve selection "51GC," time dial "51GTD," electromechanical reset delay "51GRS," and torque control "51GRS."

Table 5.7: SEL-351A (R2) relay residual ground time-overcurrent configuration settings

Relay word bits	Definition	Threshold value
51GP	Pickup	0.68A
51GC	Type of curve	C1
51GTD	Time dial	0.05 seconds
51PRS	Electromacanical reset timing	N
51PTC	SELOGIC for torque control setting	1

The SEL-351A (R2) residual ground time overcurrent configuration on AcSELerator Quickset is shown in Figure 5.28 below.

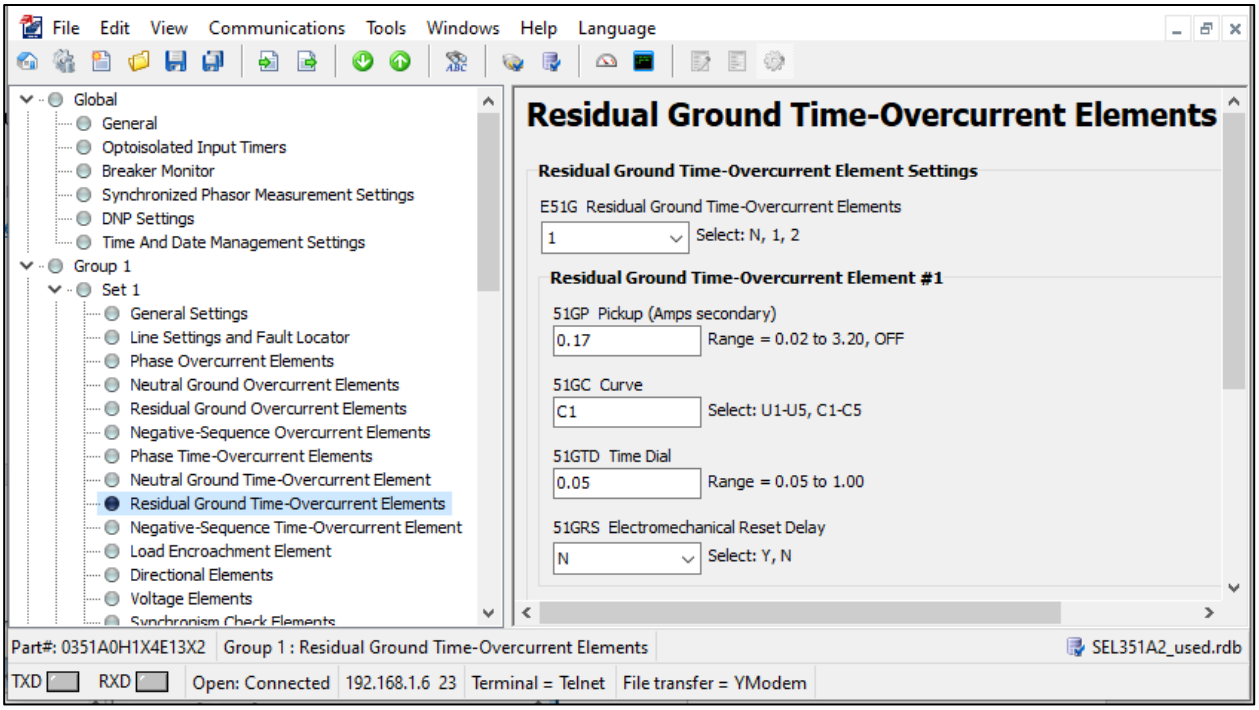

Figure 5.28: SEL-351A (R2) relay residual ground time-overcurrent configuration

The SEL-351A (R2) reclosing relay configuration and function are identical to those of the SEL-351A (R1) as shown in Figure 5.22. The SEL-351A (R2) reclosing relay settings are not shown in this section to avoid repetition.

The trip logic configuration of the SEL-351A (R2) is shown in Figure 5.29 below. The phase and residual ground time time-overcurrent trip elements are included in the logic. These settings correspond to the elements of phase and residual ground overcurrent protection functions. The trip signal sent by SEL-351A (R1) is mapped to output port OUT103. The remaining parameters in this section are all set to default.

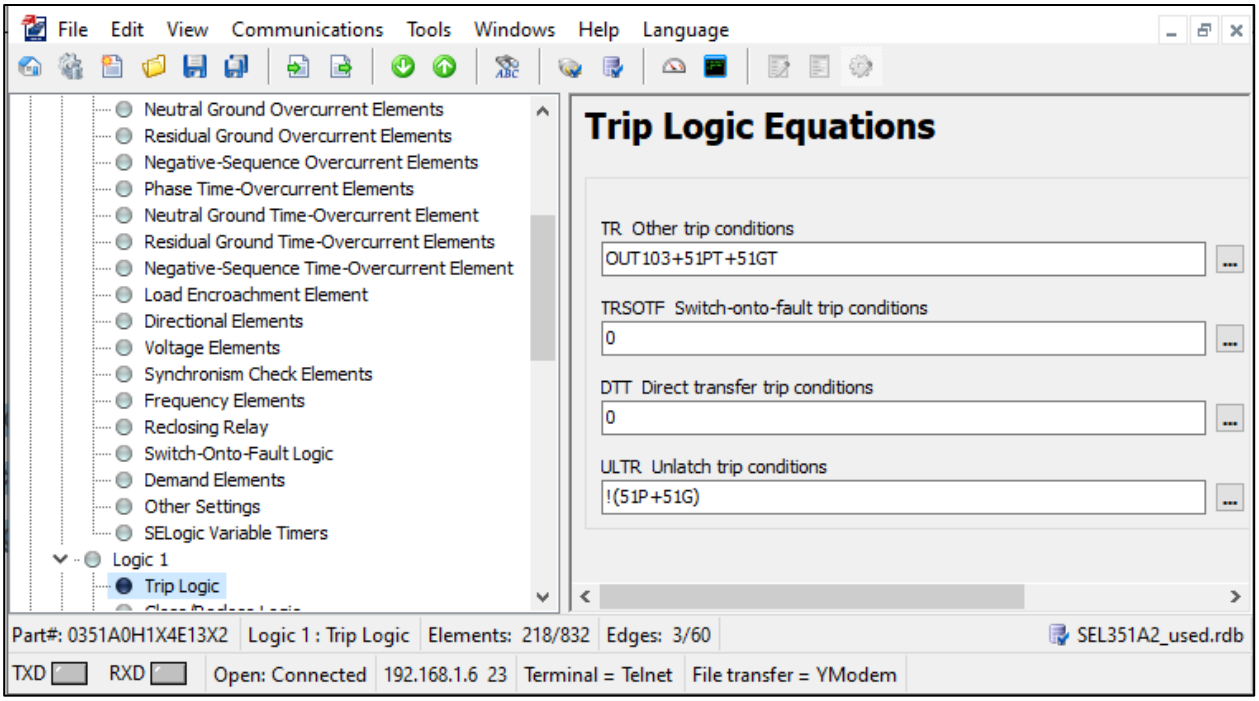

Figure 5.29: SEL-351A (R2) relay trip logic

The configuration and functioning of SEL-351A (R2) Close logic is the same as that of SEL-351A (R1) as shown in Figure 5.22. The SEL-351A (R2) reclosing settings are not shown in this section to avoid repetition.

Figure 5.30 depicts the relay SEL-351A (R2) output port contacts setup. The elements OUT103, maximum phase, and residual ground time-overcurrent trip are assigned to relay output contact port OUT101. The CLOSE option is assigned to output port OUT102. The close logic signal sent to SEL-351 (NOP) confirms that SEL-351A (R2) has tripped and locked out due to 51PT or 51GT being triggered. Figure 5.31 depicts the graphical logic of the SEL-351A (R2) relay output port OUT103. The remainder of the options are set to default.

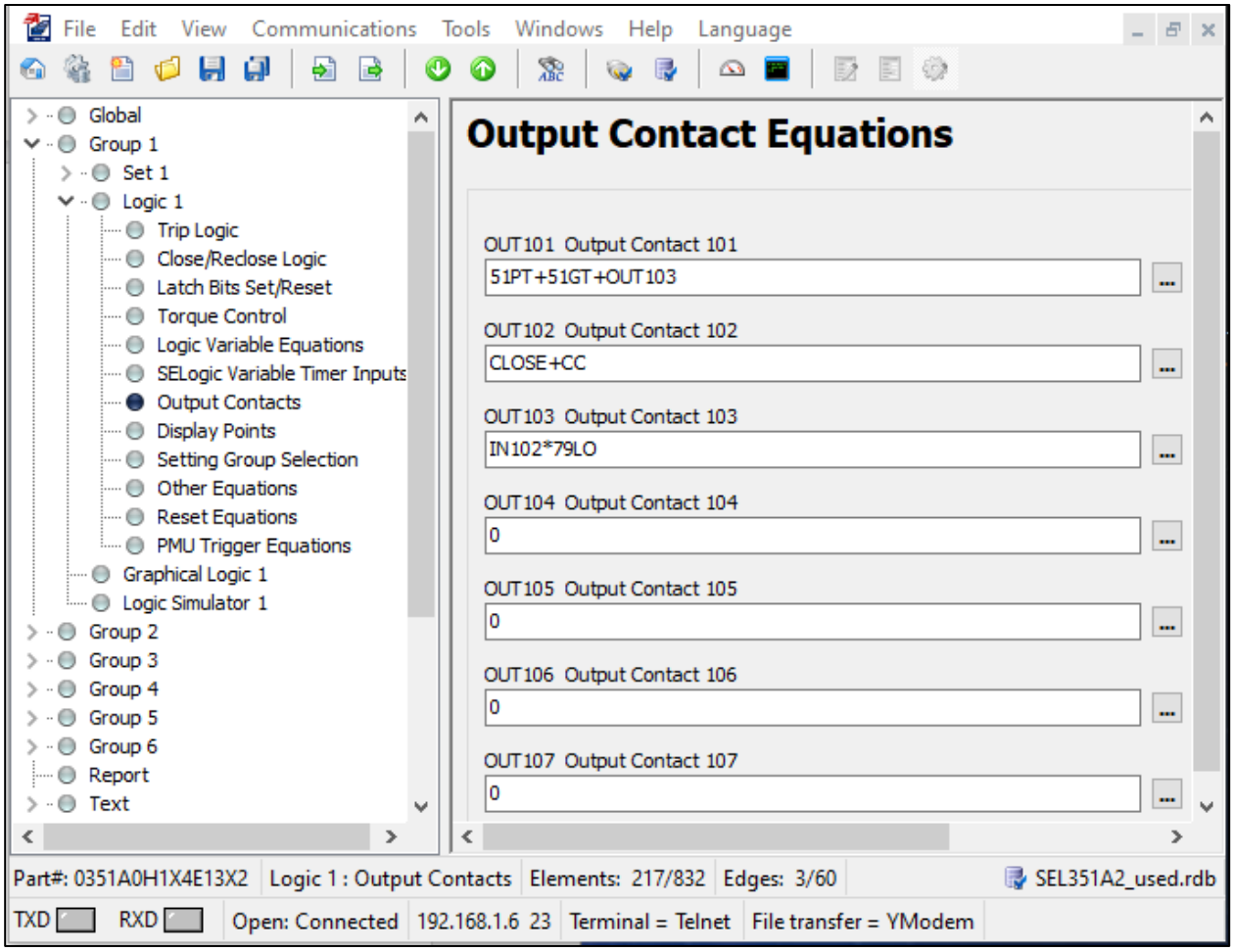

Figure 5.30: SEL-351A (R2) relay output ports configuration

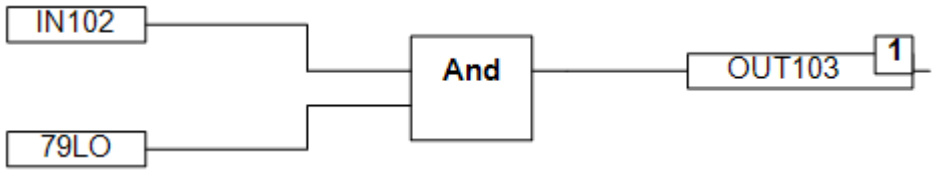

Figure 5.31: SEL-351A (R2) relay output port (OUT103) graphical logic configuration

5.2.4 Configuration of the engineering settings for the relay SEL-351A (NOP)

On the SEL-351 (NOP) relay, there are only three configurations. The configurations are performed on trip/communication assisted trip logic, close/reclose logic, and output logic under logic 1. The trip/communication assisted trip logic for the SEL-351 (NOP) relay is shown in Figure 5.32 below. The logic states that the NOP relay should not be opened

if the two inputs from SEL-351A (R1) and SEL-351A (R2) are both low (logical 0) and is represented ! (IN102 * IN103).

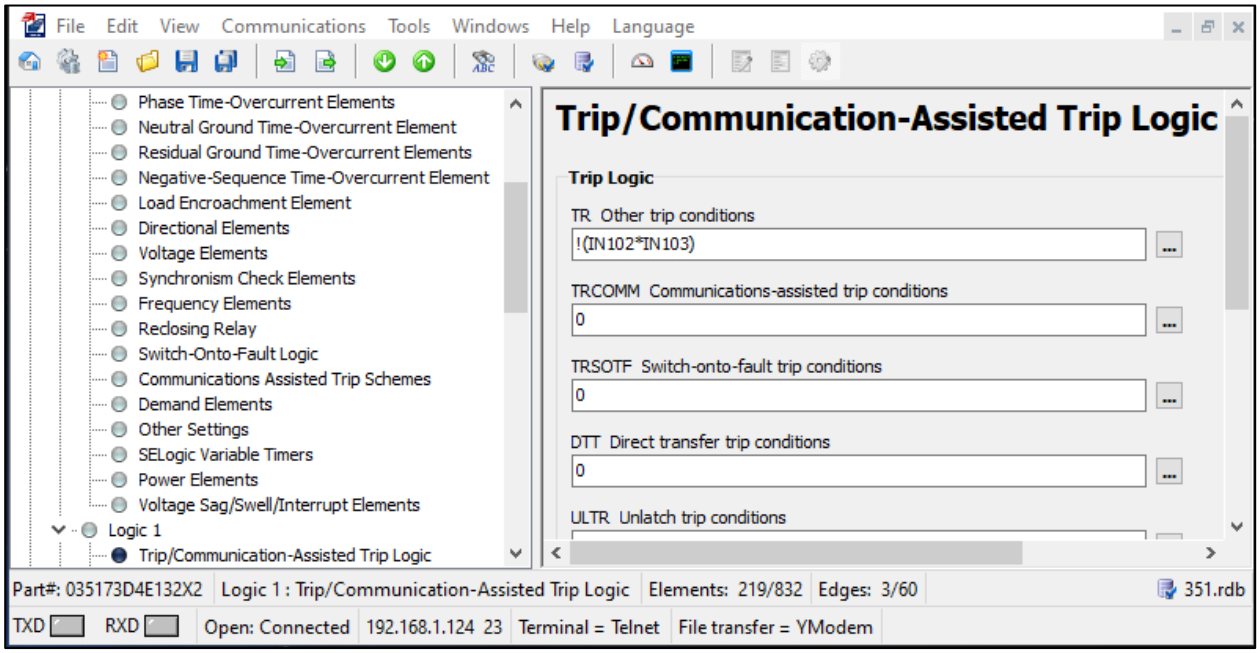

Figure 5.32: SEL-351 (NOP) relay trip/communication assisted logic

Figures 5.33 and 5.34 demonstrate the SEL-351 (NOP) relay's close command graphical logic and close command settings. When the two SEL-351A (R1) and SEL-351A (R2) inputs are both high (logical 1), the NOP relay should close. When both inputs are logical 1, the output port OUT102 is high, and close conditions other than automatic reclose (CL) are high (logical 1).

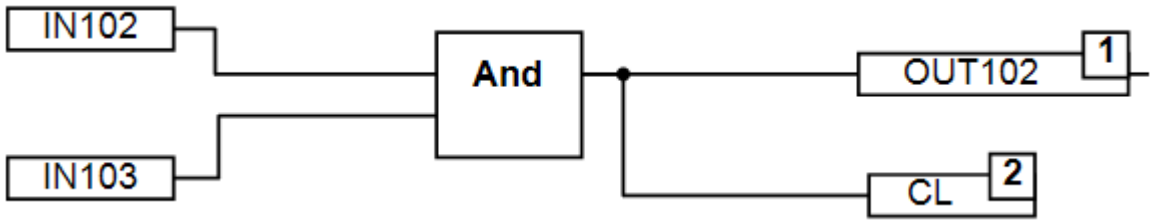

Figure 5.33: SEL-351 (NOP) relay Close command graphical logic

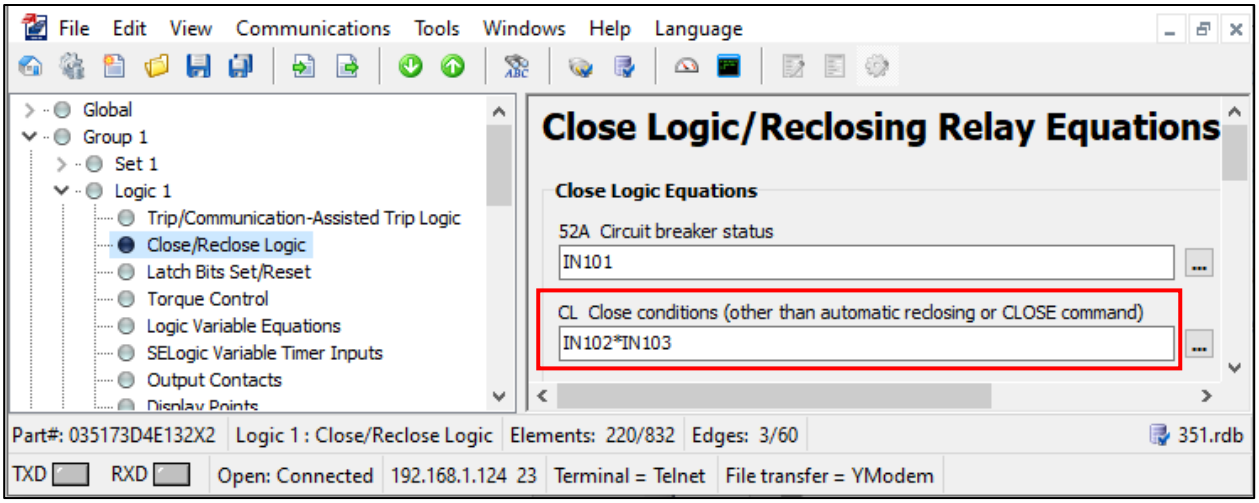

Figure 5.34: SEL-351 NOP relay close logic

The resulting output contact logic is depicted in Figure 5.35.

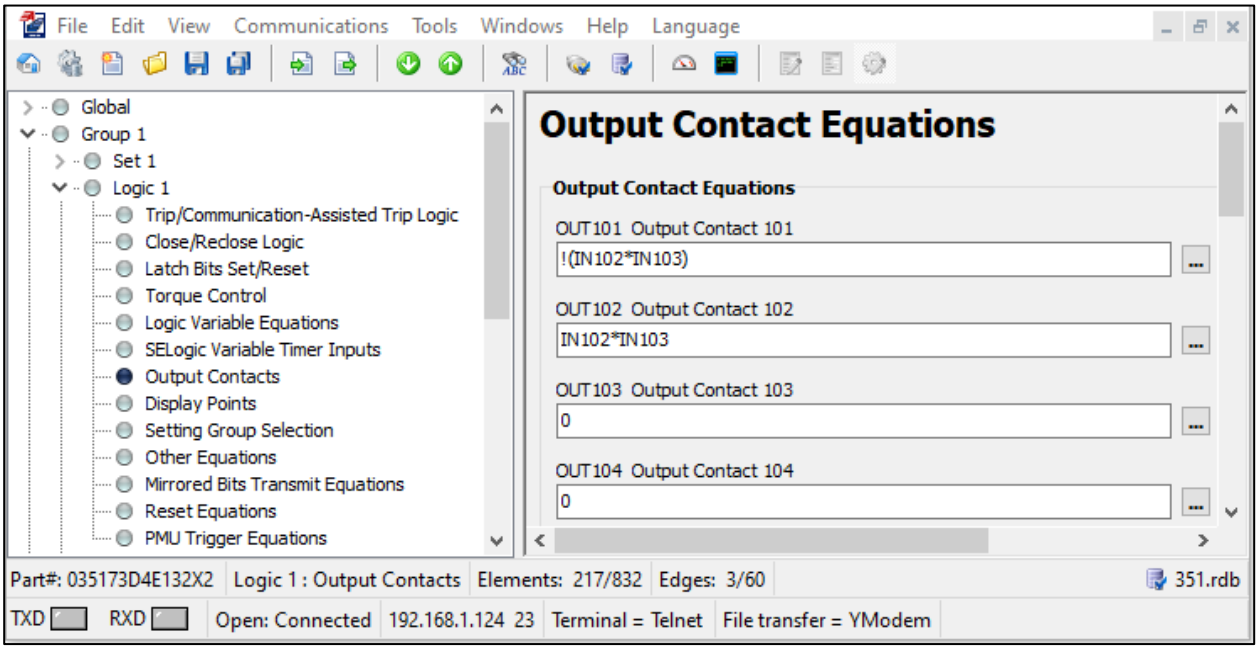

Figure 5.35: SEL-351 NOP relay output logic

5.3 The auto-reclose protection scheme's Omicron test universe configuration setting

The injection device Omicron CMC 356 is used to mimic and inject current and voltage signals to the SEL-351A (R1) and SEL-351A (R2) relays. It should be noted that this paper only shows the test set configuration for the SEL-351A (R1) relay utilizing the omicron test universe. The engineering configuration of the Omicron test-set device is

performed using test universe software. Omicron test universe software includes a number of functional-oriented modules for testing protection features, commissioning, and factory acceptance testing. Figure 5.36 depicts the omicron test universe software home screen. The first step in setting the omicron test universe is to associate the omicron CMC 356 device by clicking "Test set association," as shown in Figure 5.36 in red.

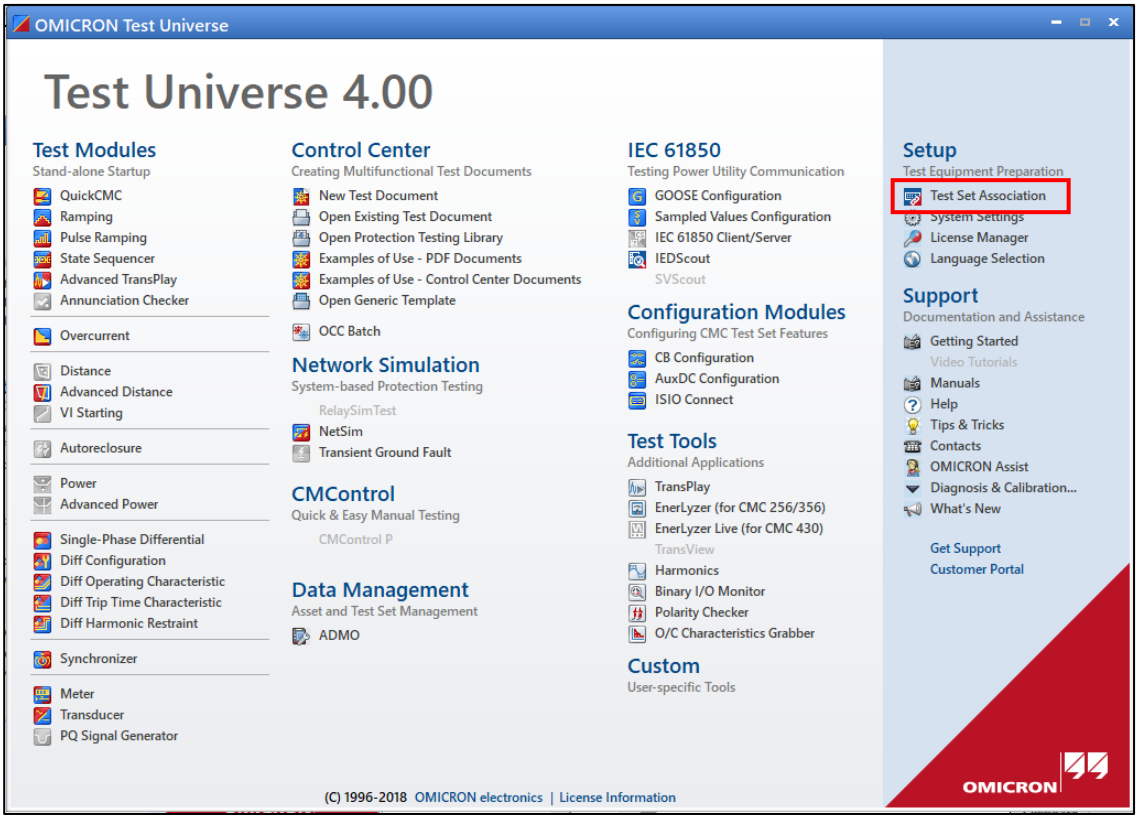

Figure 5.36: Window pane of the Omicron test universe program

After selecting Test Set Association in Figure 5.36, the first omicron device link screen encircled 1 in Figure 5.37 appeared. As of now, the computer is not affiliated with the omicron CMC 356, as shown by the description on the omicron device link screen, "Not associated with this computer (ETH1)." The taskbar on the red square is selected to display the circled 2 omicron device link screen. To attach the computer with the omicron CMC 356, the associated device option in the omicron device link section 2 is selected. The Omicron device link screen circled 3 appeared, and the test associate button on the rear of the Omicron CMC 356 was pressed. The following screen circled 4 showed, indicating that the omicron CMC 356 is ready, indicating that both the PC and the omicron CMC 356 are connected.

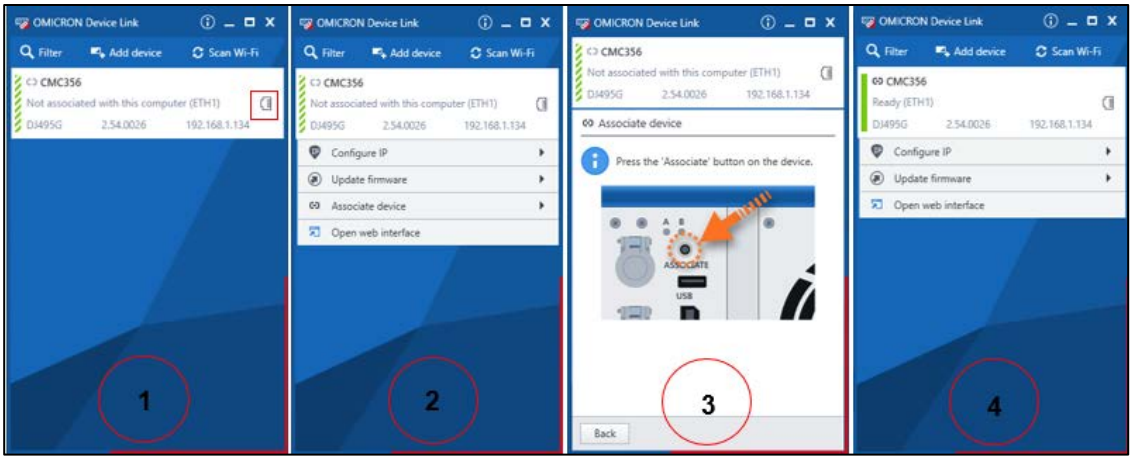

Figure 5.37: Omicron device link screen

The next step is to open the Omicron test universe software window in Figure 5.36 and create a "new test document." Four test modules are built on the new test document, as shown in Figure 5.38 below. The state sequencer module, overcurrent module, GOOSE configuration module, and Aux DC configuration module are among the test modules. Each module is explained in detail in its own section. The following steps are taken to complete the omicron test universe configuration: configure object parameters, hardware, overcurrent test module, state sequencer module, and finally Aux DC configuration.

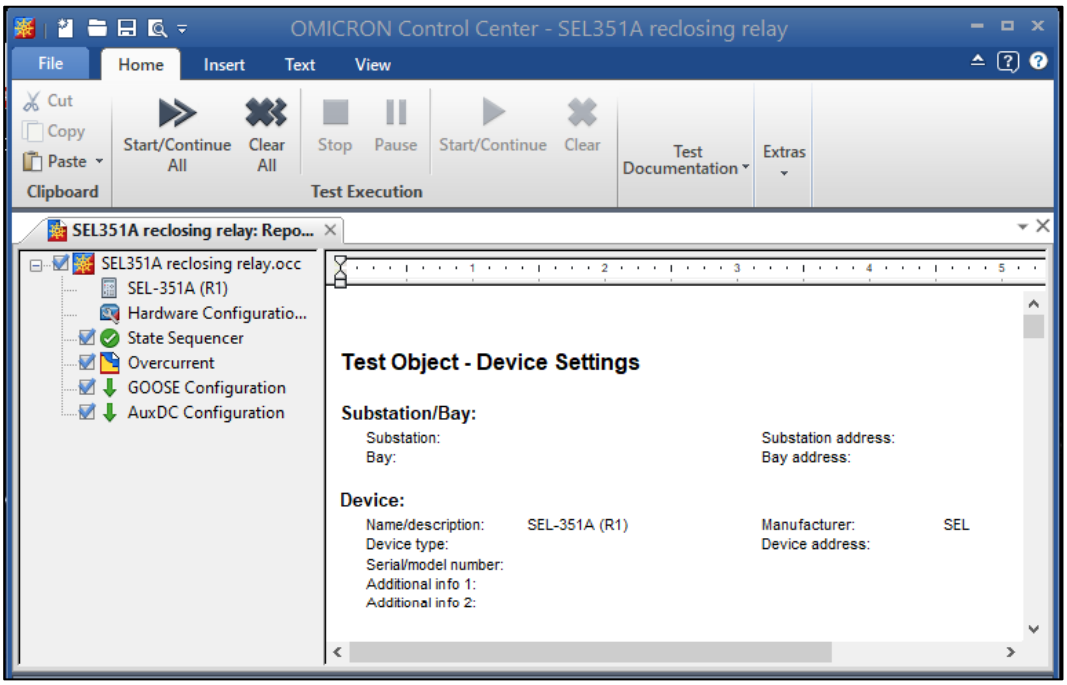

Figure 5.38: Omicron test universe project setup

5.3.1 Configuration of SEL-351A (R1) test object parameters using omicron test universe software

"SEL-351A (R1)" in Figure 5.38, which depicts the test object setup parameters. When the test object is opened, As illustrated in Figure 5.39, the test item has a Relay Interface by Omicron (RIO) function, which contains four functions: device, distance, overcurrent, and CB settings. Only the device and overcurrent functions are configured for this project.

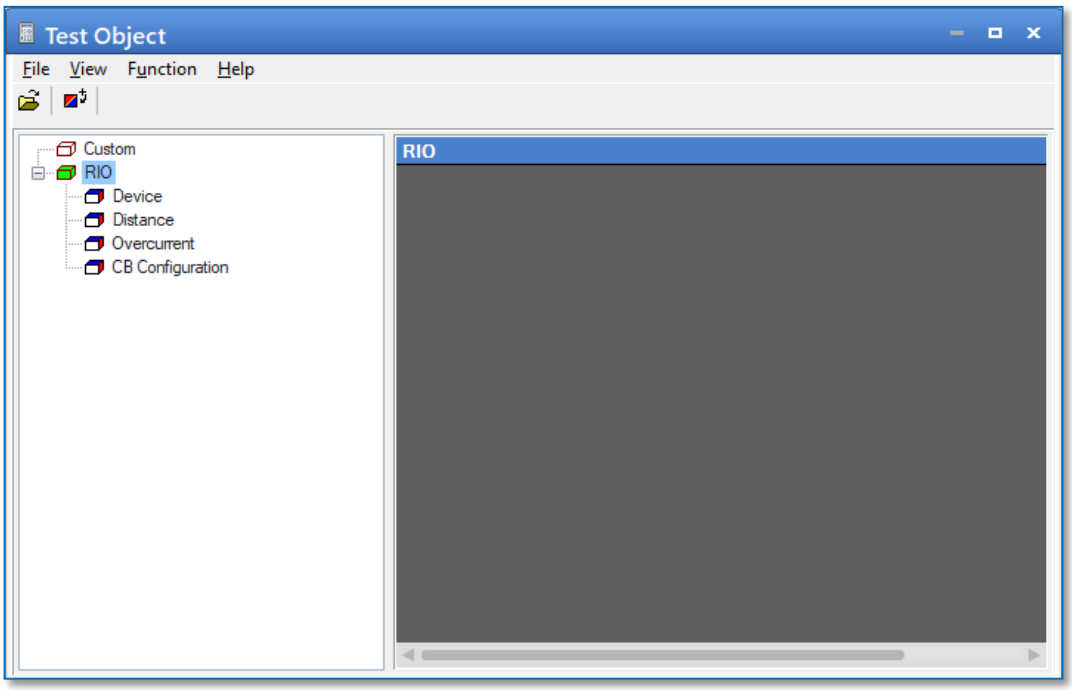

Figure 5.39: Test object configuration

The following step is to launch the device function and configure the device settings, as shown in Figure 5.40 below. The priority settings for this project are to ensure that the number of phases selected is 3, the nominal frequency is 50Hz, and the CT ratio is 300:1A. The rest of the options are kept at their defaults. It should be noted that the device parameters in Figure 5.31 that are configured in this section are the same settings that are configured in AcSELerator Quickset software for SEL-351A (R1) relay as shown in Figures 5.7 and 5.9 for the system frequency and CT ratio settings respectively.

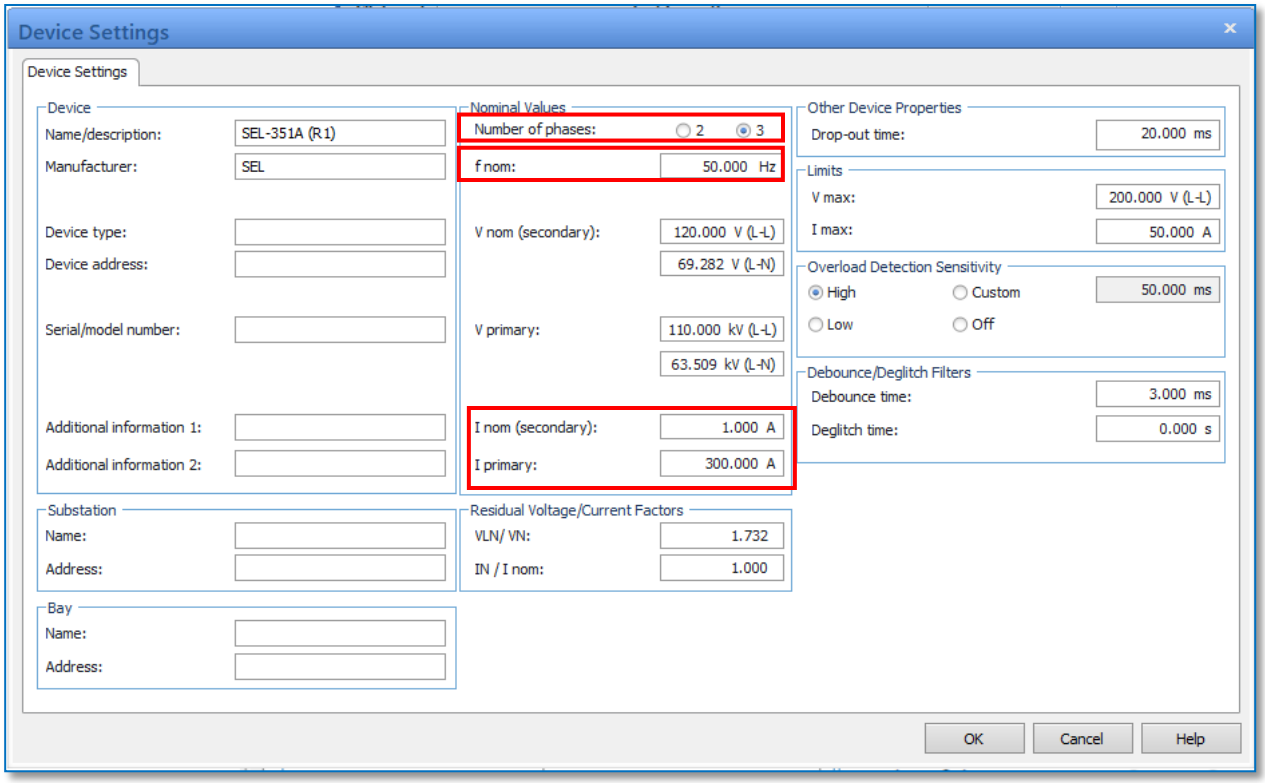

Figure 5.40: Device configuration settings

Figure 5.41 shows the relay parameters tab, which contains the definitions for non-directional and directional behaviors, as well as relay tolerances. The non-directional overcurrent is tested in this project, hence it is turned on. Tolerances are set to default.

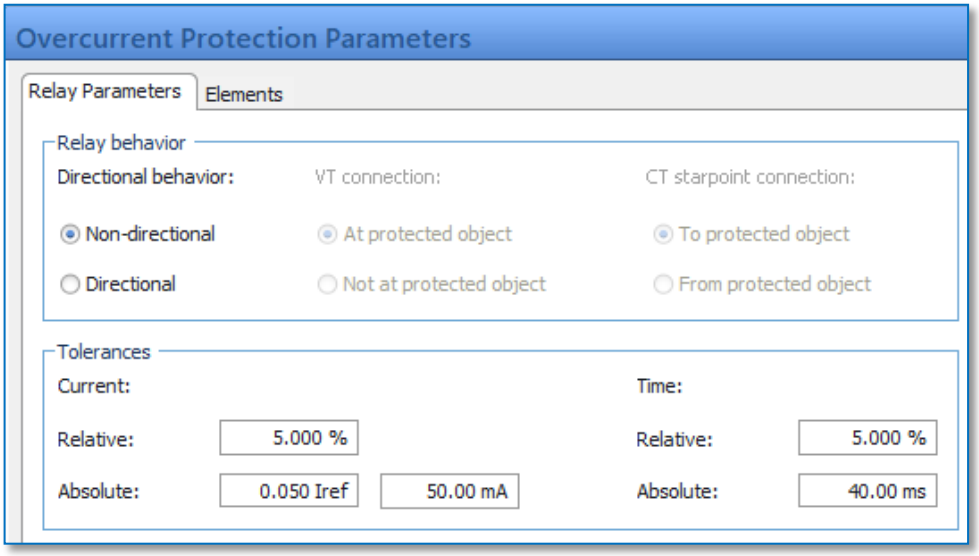

Figure 5.41: Overcurrent relay directional behaviour and tolerances settings

The overcurrent protection elements must then be configured. The elements tab has two windows for configuring the overcurrent element's characteristics and viewing the resulting TOC characteristic curve. The define element tab is chosen in Figure 5.42. The circle number 1 is used to configure either phase or residual elements. In Figure 5.42, the circle number 2 indicates the technical configuration of the overcurrent protection devices. These OC configuration options are identical to those utilized in the AcSELerator Quickset program. Circle 3 is chosen to determine the type of curve to use: IEC normal inverse or IEC definite time characteristic curve. It should be noted that Figure 5.42 simply depicts the configuration of phase elements. Figure 5.43 depicts the configuration of residual overcurrent elements.

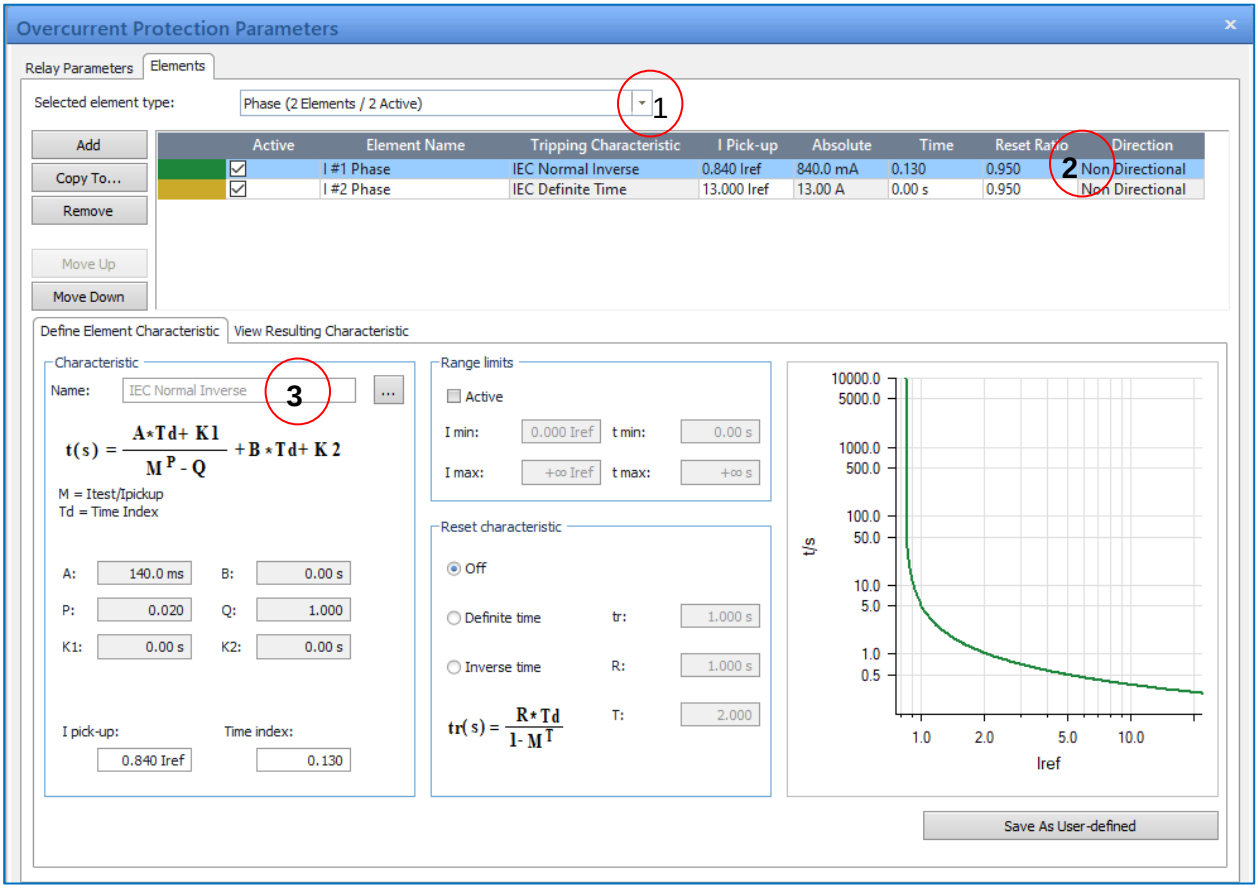

Figure 5.42: Configuration of phase overcurrent elements

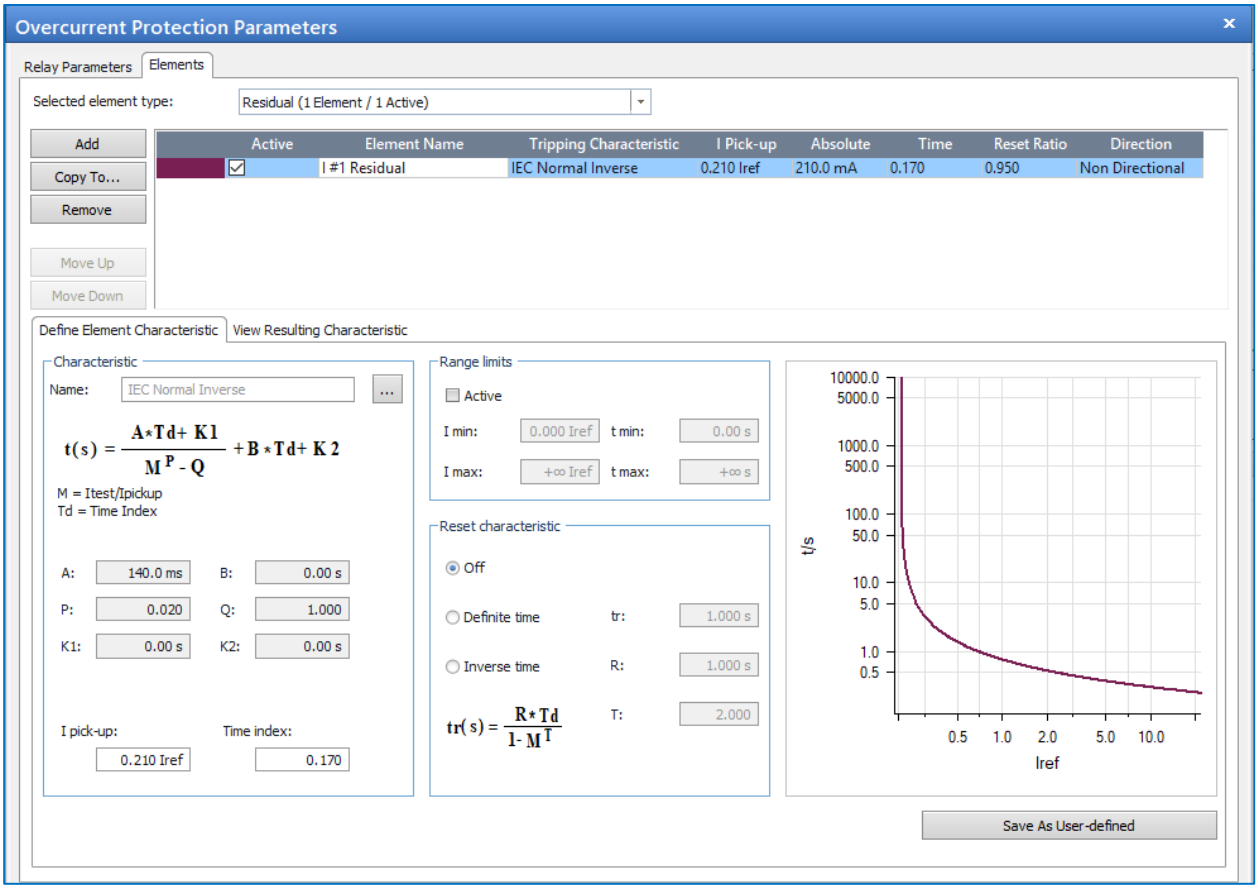

Figure 5.43: Configuration of residual overcurrent elements

Table 5.8 shows the configuration settings for the IEC normal inverse and definite time overcurrent of phase and residual elements utilized in the test case scenario used in this project.

Table 5.8: SEL-351A (R1) relay Phase and residual overcurrent elements parameters in test universe

Active	Name	Tripping characteristic	I Pick-up	Time dial	Reset ratio	Direction
Yes	I #1 Phase	IEC Normal Inverse	0.84 Iref	0.13	0.95	Non-Directional
Yes	I #2 Phase	IEC Definite Time	13 Iref	0	0.95	Non-Directional
Yes	I #1 Residual	IEC Definite Time	0.21 Iref	0.17	0.95	Non-Directional

The phase and residual overcurrent characteristic curves in the omicron test universe are depicted in Figure 5.44 below. The phase time-overcurrent curve element is set to 0.84 Iref with a time delay of 0.13s for the phase IDMT overcurrent element, and the definite time OC is set to 13 Iref with a time dial of 0s. 0.21 Iref is assigned to the residual definite time OC element.

(a) Phase OC element characteristic curve **(b) Residual OC element characteristic curve**

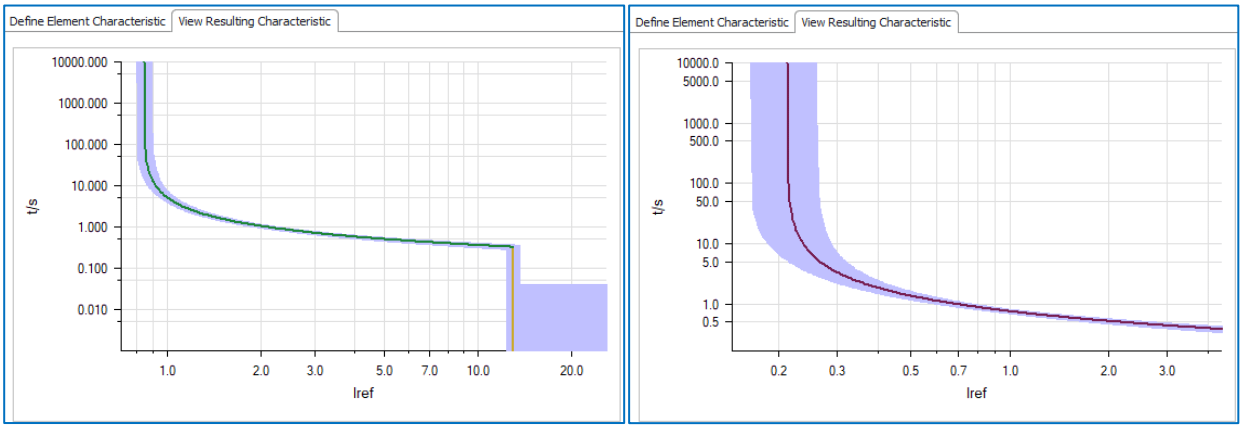

Figure 5.44: SEL-351A (R1) relay Phase and Residual OC elements characteristic curves

IEC 60255 and IEEE C37.112 describe the operation time of TOC characteristic curves. The equation for calculating the operational time of an overcurrent relay, as defined by by the above mentioned standard is given in Equation 5.1 as follows:

$$\mathrm{t(s)} = \frac{A \times Td + K1}{M^{P} - Q} + B \times Td = K2 \qquad (5.1)$$

Where:

t is the operating time of the relay in seconds

Td is the time dial or time multiplier M is the ratio of the fault current over pickup current setting

A is a slope constant

B is a slope constant

P is a slope constant

The constant values of the inverse time overcurrent curves established by the IEC 60255 standard are shown in Table 5.9. These are the constants A, B, P, Q, K1, and K2.

Table 5.9: Inverse time-overcurrent relay constants defined by IEC 60255 standard

Characteristic curve	A	B	P	Q	K1	K2
IEC Normal Inverse	0.14	0.0	0.02	1.0	0.0	0.0
IEC Very Inverse	13.5	0.0	1.0	1.0	0.0	0.0
IEC Extremely Inverse	80.0	0.0	2.0	1.0	0.0	0.0

Note: Very inverse and extremely inverse curves are employed in certain applications, the two case studies provided in this chapter only used IEC normal inverse curves.

5.3.2 Configuration of the SEL-351A (R1) relay hardware in the test universe

The Omicron CMC 356 device's general input/output configuration is specified in hardware configuration settings. These inputs/outputs are defined in SEL-351A (R1) connection diagram in Figure 5.10. The hardware configuration setup is depicted in Figure 5.45 below.

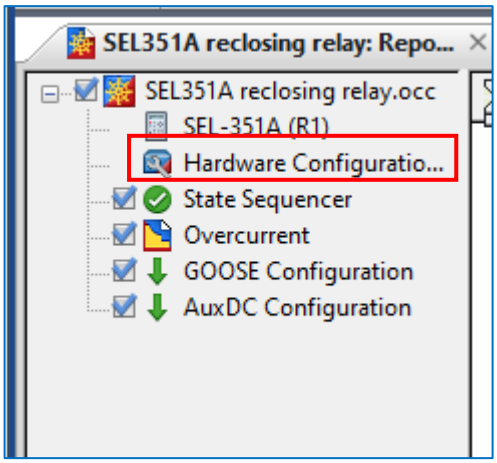

Figure 5.45: Setting the hardware configuration of the auto-reclose relay SEL 351(R1)

Figure 5.46 shows the global hardware configuration window pane, after double-clicking the hardware configuration tab in Figure 5.45.

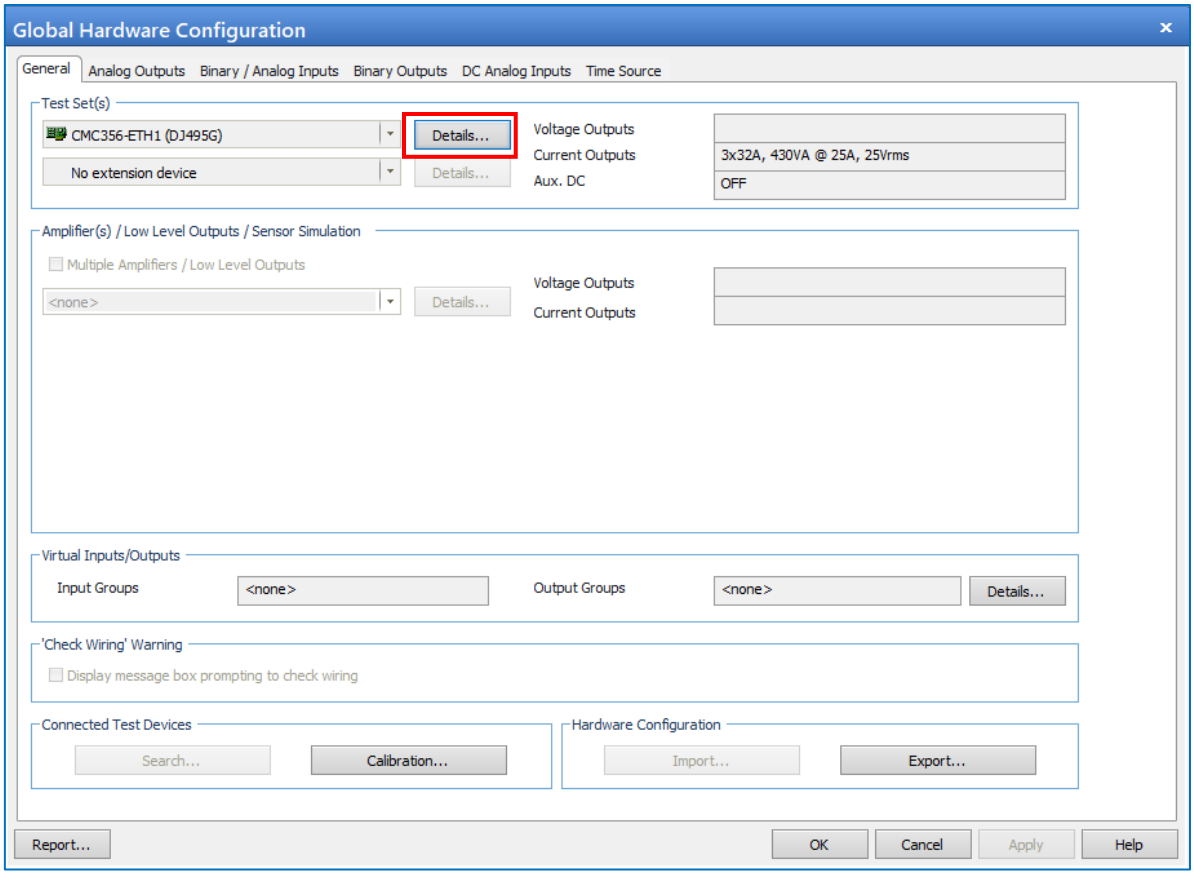

Figure 5.46: Global hardware configuration

When configuring general settings, double-click the configuration details tab in Figure 5.46 to configure current output connections, as illustrated in Figure 5.47. It should be noted that this project does not use voltage output because only the OC recloser protection function is tested.

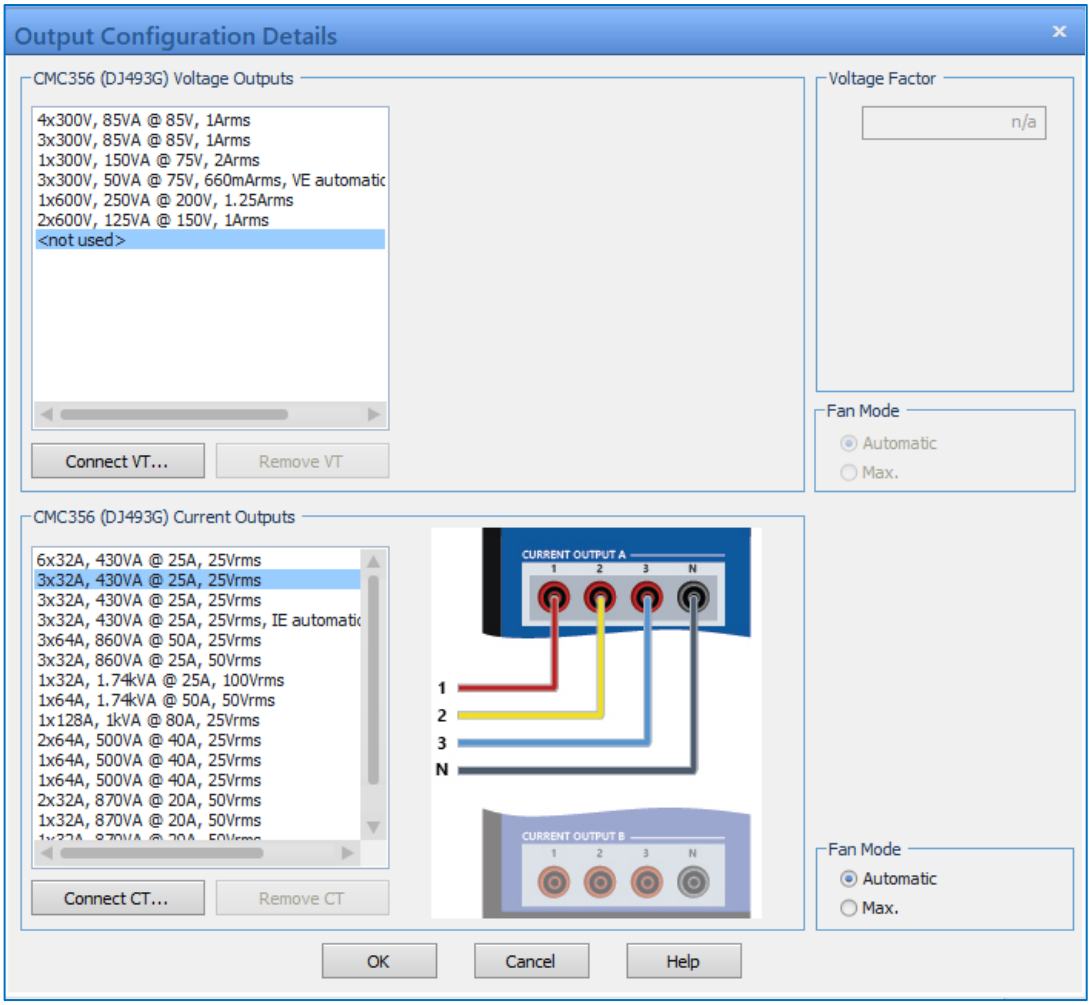

Figure 5.47: CMC356 device channel A connection for current outputs

The analog outputs are set up as illustrated in Figure 5.48 below.

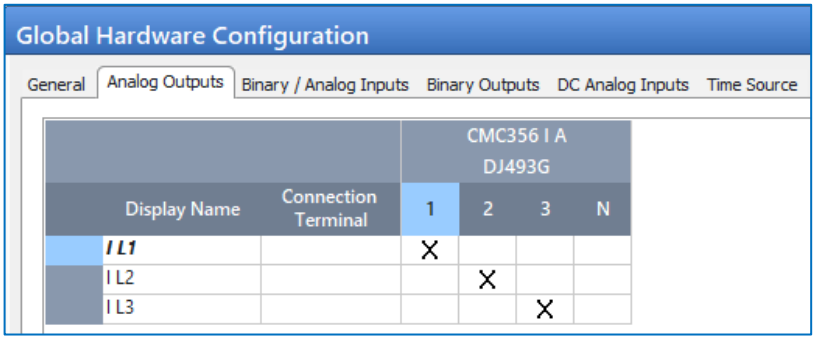

Figure 5.48: CMC356 device analog current channel connected to SEL351A(R1) relay current coils.

As illustrated in Figure 5.49, the trip and close command binary signals from CMC356 device are connected to SEL351(R1) relay output ports 1 and 2 respectively.

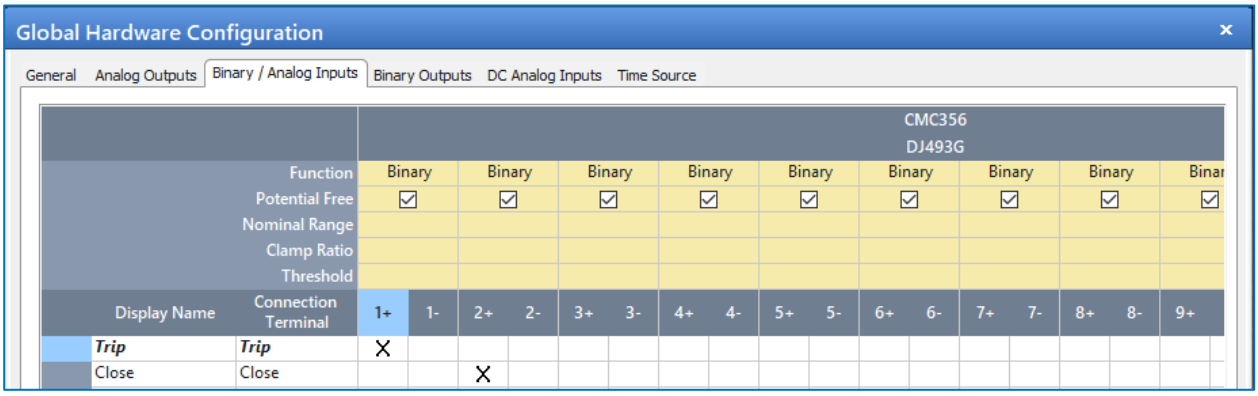

Figure 5.49: Trip and close binary input singals configuration

The binary output arrangement is shown in Figure 5.50 below. The status of the circuit breaker is assigned to binary output 1, and the remaining binary outputs are not used in this project.

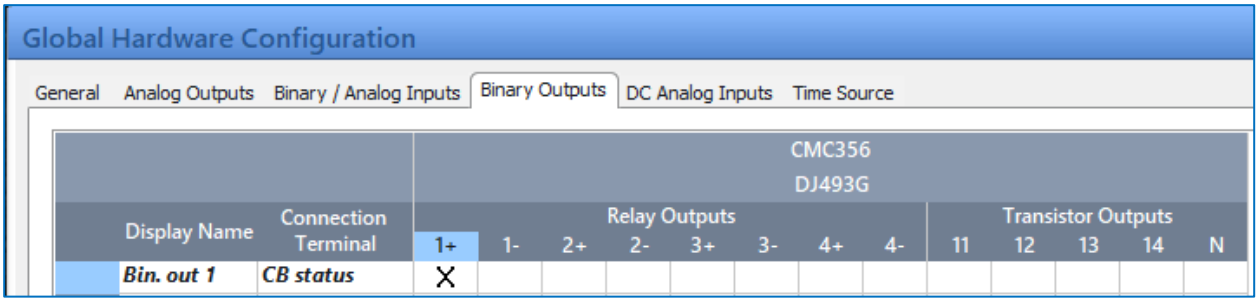

Figure 5.50: Binary output configuration to simulate the CB status

5.3.3 State Sequence configuration of the SEL-351A (R1) relay in the test universe

To test the auto-reclose protection function, the state sequencer module is included. The state sequencer module is intended to provide a versatile automated testing tool for the auto-reclose scheme. On the state sequencer module, a complete sequence of states is defined, and measurements are automatically assessed. Figure 5.45 shows how to add the state sequencer module by clicking on the Insert tab. The test module configuration includes a number of test modules, one of which is the state sequencer module.

The created state sequencer module is depicted in Figure 5.51 below. The table view labeled 1 contains a summary of all defined states. The state tab is where you can navigate and add new states. The various states are set up in the detail view window numbered 2. The currents are defined on the analog output tab, the binary position (opened/closed) for each state is specified on the Binary output tab, and the trigger tab is used to define the trigger that ends each state on the detail view window. The graphic overview for the auto-reclose sequence, record trip, and close signals is shown by the time signal view window labeled 3. The time measurement criteria and open interval periods are defined and evaluated using the test assessment window labeled 4.

The workflow of the eight states specified in Figure 5.51 is depicted in Figure 5.52. The analog output current is set to 560mA in the first state, defined as the normal state, the binary output is closed, and the trigger/state termination is set to (17s). 560mA is the normal secondary load current with a CT ratio of 300:1 at outgoing feeder A, as observed from DIgSILENT simulation findings in section 4.4.5 of chapter 4. 17s is the time required for the relay to reset in 850 cycles (850 X 0.02=17s).

State 2, described as Fault 1, has an analog output secondary current of 8.456A, the binary output is closed, the trigger/state termination initiates a trip signal with logic high (logical 1), and the state time out is set to 0. (5s). The fault current seen by relay 1 from the DIgSILENT simulation results shown in Table 4.25 in section 4.6.1 is 8.456A. (5s) is the time allotted to allow the SEL-351A's open interval of 3 seconds/150 cycles (R1). State 3 is specified as auto-reclose 1 (ARC1), with the analog output current set to 0A, the binary output open, and the trigger/state termination defined as a close signal with a logic high (logical 1). Because there is no current flow during the open interval period, 0A current is measured.

State 4 is classified as fault 2, and its configuration is identical to fault 1. State 5 is specified as auto-reclose 2 (ARC3); the configuration of this state is identical to that of ARC1, with the exception that ARC3 time outs at 12s. (12s) is the time allowed for the SEL-351A's (R1) relay open interval (10 seconds/500 cycles). Fault 3 with the same setup as faults 1 and 2 is characterized as state 6. ARC3 with the same settings as ARC2 is classified as state 7. Fault 4 is defined by State 8 as a fault state that is simulated to ensure that the circuit breaker trips and locks out. For this condition, the analog output secondary current is set to 8.456A, the binary output is closed, and the trigger/state termination is ignored.

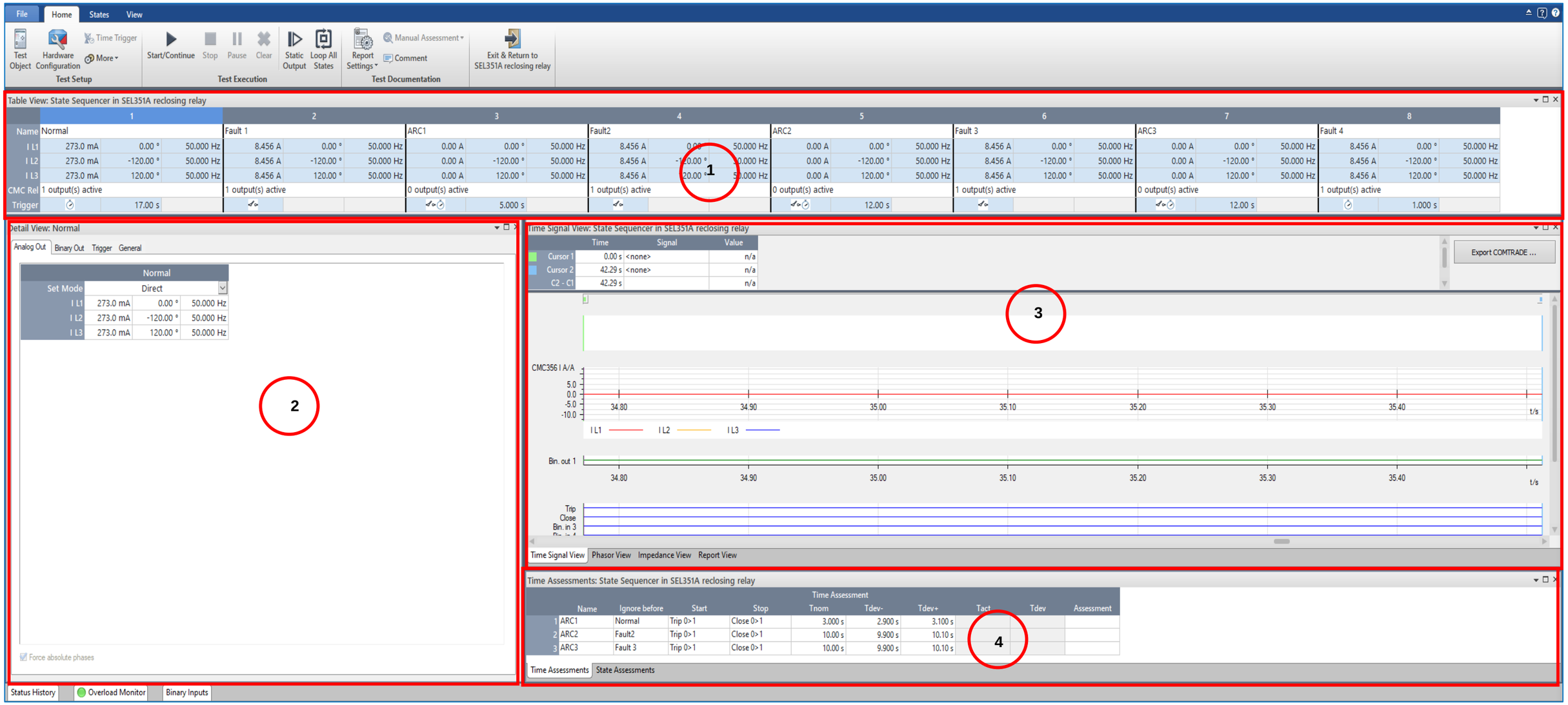

Figure 5.51: Configuration of the state sequencer test module

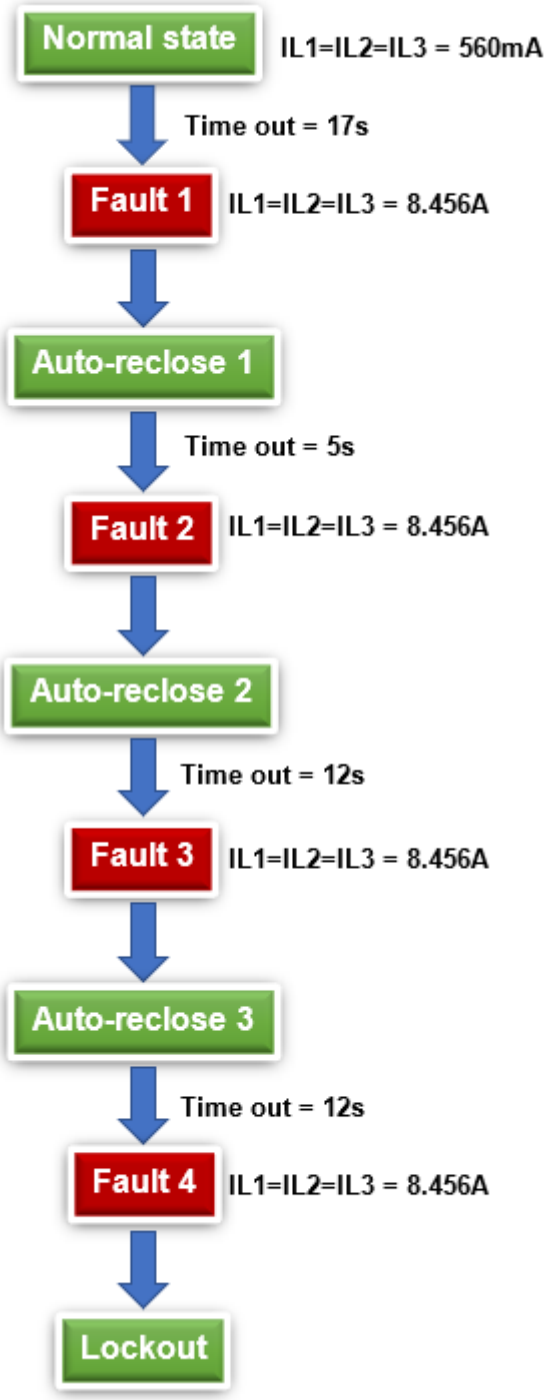

Figure 5.52: State sequencer Workflow to mimic the auto-reclose protection system

5.3.4 Auxiliary DC configuration of the omicron test universe software

An auxiliary DC supply is utilized to give auxiliary voltage to the SEL-351A (R1) and SEL-351A (R2) modules. In Figure 5.45, add the AuxDC test module by clicking on the insert tab, then the test module. The AuxDC test module is chosen from the list of available test modules. As seen in Figure 5.53, the DC voltage is set to 110V. The

DC voltage in this project is used to power the input port IN101 of the SEL-351A (R1) and SEL-351A (R2) relays. When the circuit breaker is closed, input port 101 is energized; when the circuit breaker is open, it is de-energized. Furthermore, when input port 101 is energized, the circuit breaker state changes to logical 1, and when it is de-energized, the status changes to logical 0.

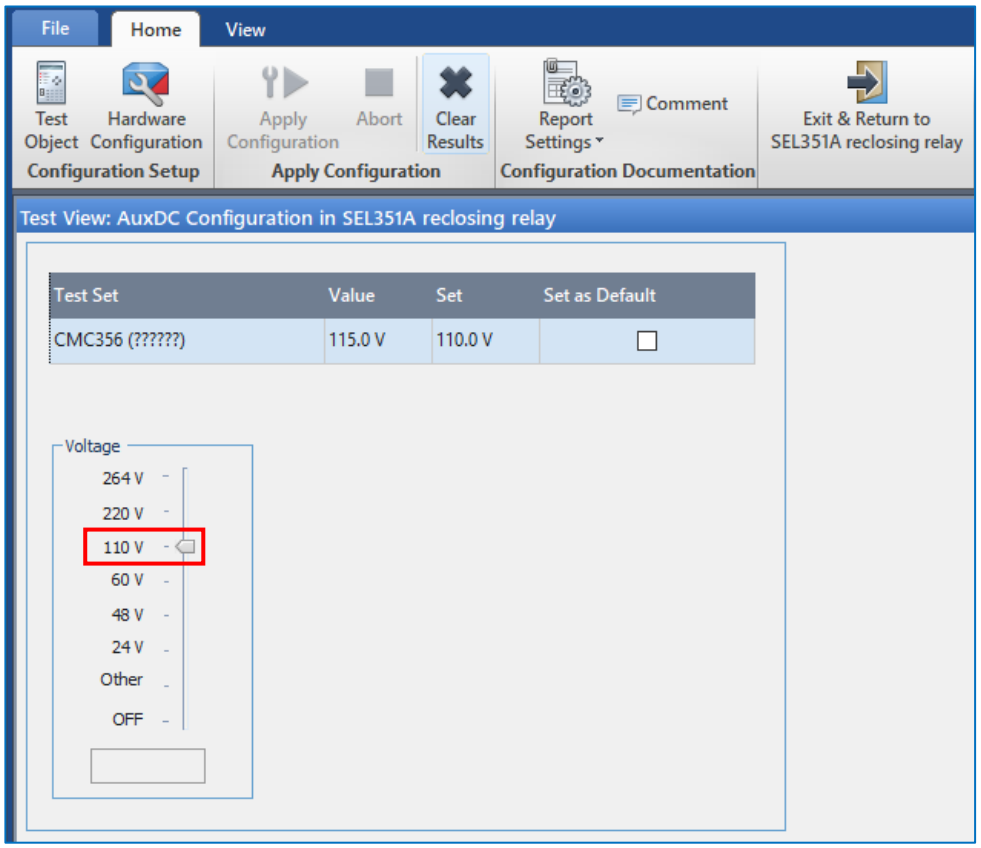

Figure 5.53: Configuration of the AuxDC test module

5.4 The auto-reclose scheme's lab-scale testing and simulation findings

This section presents the results of the lab-scale testing of the recloser protection functions and their simulation work for the investigated distribution system. The protective functional testing performance of each relay is studied in two case studies utilizing the following scenarios in accordance with Figure 5.1.

1. Case one: Three-phase fault and a single-phase to ground fault on the SEL-351A (R1) reclosing relay
2. Case two: Three-phase fault and a single-phase to ground fault on the SEL-351 (R2) reclosing relay

The outcomes of the two case studies are compared to the DIgSILENT simulation findings reported in section 4.6 of Chapter 4.

Table 5.10 shows the fault current magnitudes simulated to the two relays SEL-351A (R1) and SEL-351A (R2). These fault current estimates were obtained using DIgSILENT simulations in section 4.6 of Chapter 4.

Table 5.10: Simulated fault currents

Relay	**Three-phase fault currents**		**Single-phase to ground fault currents**	
	Primary current	Secondary current	Primary current	Secondary current
SEL-351A (R1)	2536.76A	8.456A	1727.1A	5.757A
SEL-351A (R2)	1456.65A	4.856A	843.12A	2.81A

5.4.1 Case one: Three-phase fault and a single-phase to ground fault on the SEL-351A reclosing relay (R1)

5.4.1.1 Three-phase fault on the SEL-351A reclosing relay (R1)

This case study is carried out using the hardwired recloser control system lab-scale test bench depicted in Figure 5.2. DIgSILENT three-phase fault current simulation produced a primary fault current of 2536.76A and a secondary current of 8.456A with a CT ratio of 300:1 in chapter 4 section 4.6. The 300:1 CT ratio is chosen in section 4.4.5 of Chapter 4 based on the entire load current in Feeder A. As a result, a secondary current of 8.456A is injected into the SEL-351A relay (R1) via the state sequencer module depicted in Figure 5.51. When the fault is simulated, the digital and analog events are depicted in Figure 5.54. Bin out 1 refers to the binary output 1 of the CMC 356 device, which is assigned to circuit breaker 1 (BRK 1). The hardwired signals "Close" and "Trip" are supplied to the circuit breaker (BRK 1) to imitate the close and trip operations.

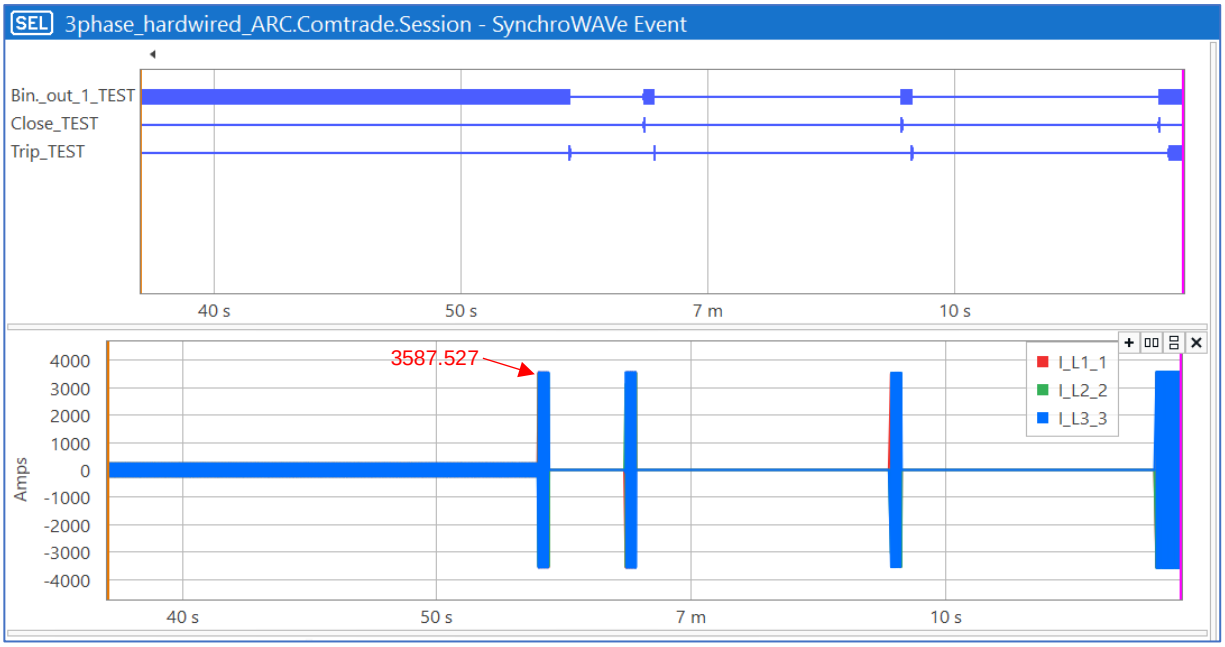

Figure 5.54: Results of auto-recloser lab scale simulation

The labels listed below are used to describe the lab-scale simulation results provided in this chapter:

- Bin_out_1_TEST is abbreviated as BRK 1
- Close_TEST is abbreviated as CLOSE
- Trip_TEST is abbreviated as TRIP

Binary output 1 (BRK 1) is closed for 15 seconds (from 38 to 53s), as seen in the digital chart at the top of Figure 5.54, to allow SEL-351A (R1) to reset. A normal load current of 560mA secondary and 168A primary is injected while BRK 1 is closed, as indicated in the analog chart at the bottom. The DIgSILENT simulation shows that the secondary current flowing at the outgoing of feeder A is 560mA. This current is also depicted in Figure 5.51 on the state sequencer module. After 15 seconds, a fault current of 8.456A secondary and 3587.57 primary current (8.456 X 300 X $\sqrt{2}$ = 3587.57 A) is automatically simulated, and the SEL-351A (R1) relay detects the fault current and sends a signal signal to the open CB contacts of BRK 1.

The SEL-351A (R1) relay is now reset and ready to go through a cycle state (CY). When the BRK 1 receives the trip signal, it opens the CB contacts and the SEL-351A relay has a 3-second open interval. After 3 seconds, the SEL-351A (R1) relay transmits a close signal to the circuit breaker contacts. When the BRK 1 switch is closed and a fault current of 8.456A is simulated, the SEL-351A (R1) relay detects

the fault and sends a trip signal to open the circuit breaker contacts. The circuit breaker was tripped, and the SEL-351A (R1) relay had a 10-second open interval.

When the open interval of 10 seconds completed, the SEL-351A relay (R1) transmitted a close signal to the circuit breaker. The circuit breaker was closed, and an 8.456A fault current was simulated; the SEL-351A (R1) relay identified the fault and delivered a trip signal to open the CB contact (BRK 1). The circuit breaker was tripped, and the SEL-351A (R1) relay went through another 10-second open interval. When the open interval of 10 seconds expired, the SEL-351A (R1) relay issued a close signal to the circuit breaker. The circuit breaker was closed, and an 8.456A fault current was simulated. The SEL-351A (R1) relay recognized the fault current and transmitted a trip to open the contacts, and a lockout signal was delivered to BRK 1. At this time, the relay transitions from the cycle state (CY) to the lockout state (LO).

The SEL-351A (R1) relay event files when the four auto-reclose shots happened during the auto-reclose process are shown in Figures 5.55 to 5.58 depict the fault current waveforms, operating time, and triggered elements for each fault.

When the first shooting took place, the SEL-351A (R1) relay operated after 385 milliseconds, as illustrated in Figure 5.55. The peak current value is 2A, which is derived using Equation 5.2 below. Figures 5.55 to 5.58 depict the protection elements that are triggered along with its ANSI codes as a result of the fault conditions. When the fault current is simulated, the pick-up "51P" is asserted, and the trip element 51PT is asserted to clear the fault. When the circuit breaker is closed for a qualifying reset time, 79RS is asserted and de-asserted; 79CY is asserted and de-asserted when the circuit breaker open and reclose initiation is successful, 79LO is not triggered because there is no lockout condition; and 52A is asserted when the circuit breaker is closed and de-asserted when the circuit breaker sends the trip signals and opens the contacts.

$$Ip = \sqrt{2} \times Irms \quad (5.2)$$

Where:

Ip is the pick current value

Irms is the RMS current

$$Ip = \sqrt{2} \times 2536.76$$

$$= 3587.57A$$

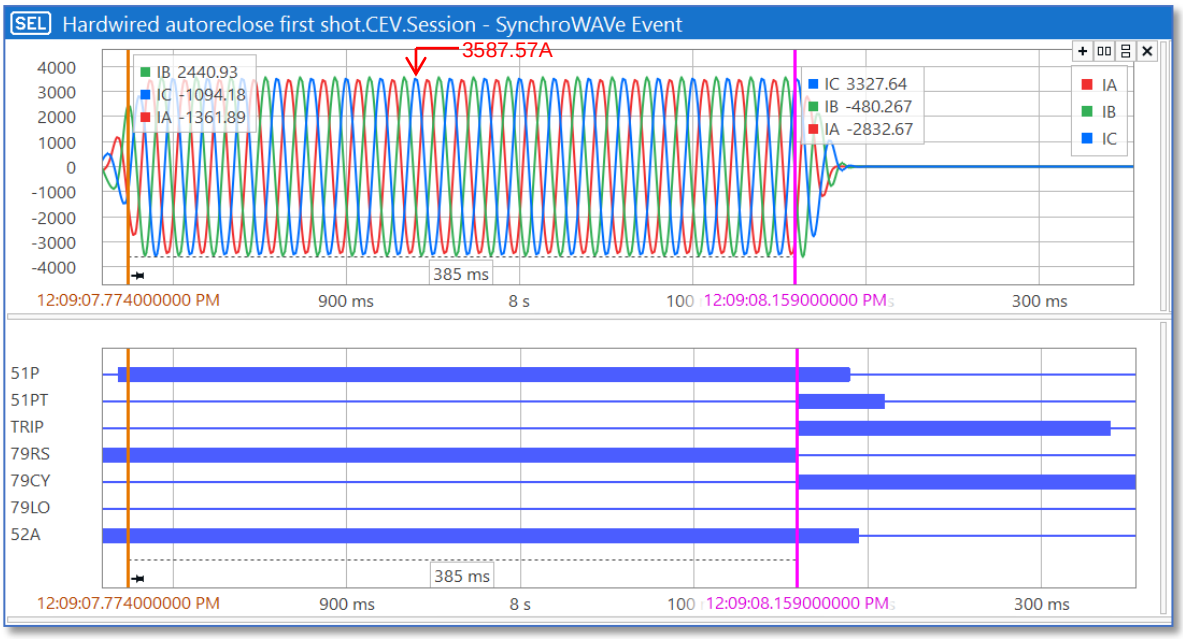

Figure 5.55: Results of the first shot's auto-reclose SEL351A (R1) relay simulation

The SEL-351A (R1) relay simulation results for the second shot event are shown in Figure 5.56 below. When the circuit breaker is reclosed, the SEL-351A (R1) operates after 385 ms. 51P is asserted to the fault, 51PT is asserted to clear the fault, 79RS is de-asserted because the SEL-351A (R1) is in the cycle state, 79CY is asserted because the SEL-351A (R1) is in a reclose cycle, 79LO is de-asserted because there is no lockout condition yet, and 52A is asserted when the circuit breaker is closed and de-asserted when the circuit is opened.

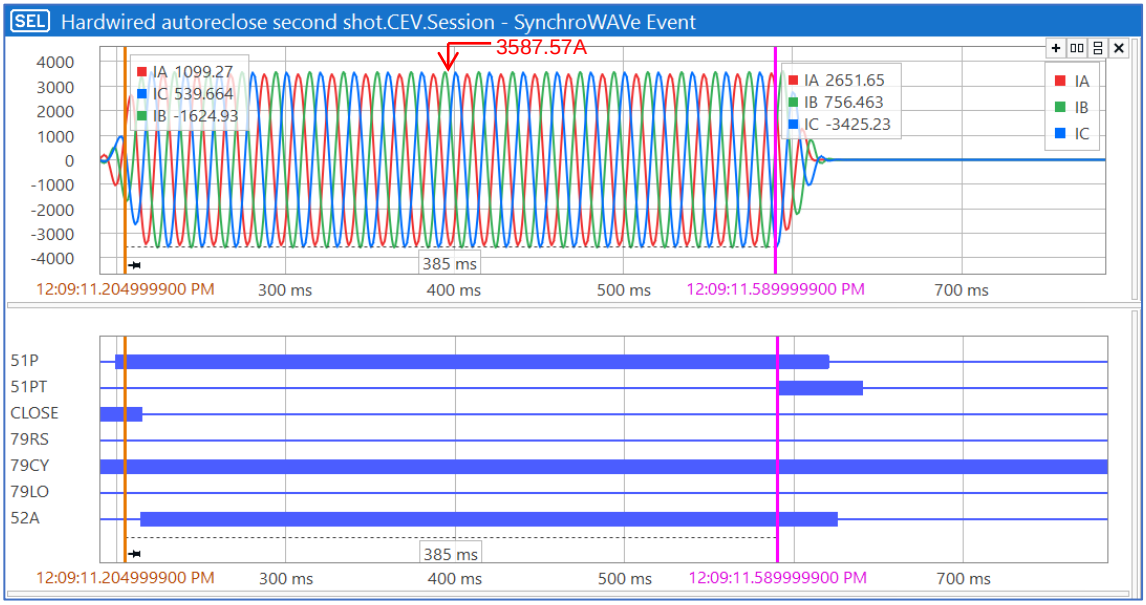

Figure 5.56: Results of the second shot's auto-reclose SEL351A (R1) relay simulation

The SEL-351A (R1) results of the third shot event are shown in Figure 5.57 below. The second shot event operates in the same manner as the third shot event.

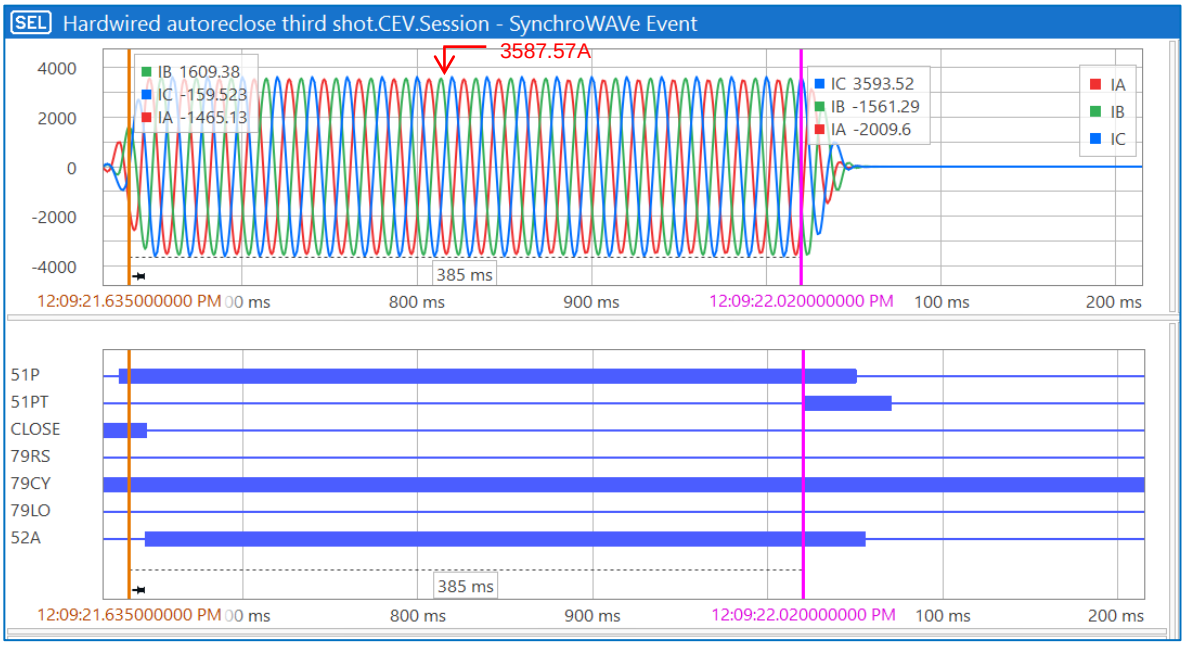

Figure 5.57: Results of the third shot's auto-reclose SEL351A (R1) relay simulation

The fourth shot's SEL-351A (R1) results are shown in Figure 5.58 below. When the SEL-351A (R1) is reclosed, 51P is asserted due to the fault, 51PT is asserted after 385 ms to clear the fault, 79CY is asserted for the entire reclosing cycle and de-asserted, when 51PT is asserted, 79LO is asserted to lockout the circuit since it is the last shot, OUT103 and OUT104 are asserted to send a trip signal to SEL-351A (R2) and a close signal to SEL 351A (NOP), since SEL351A relay trip and lock out.

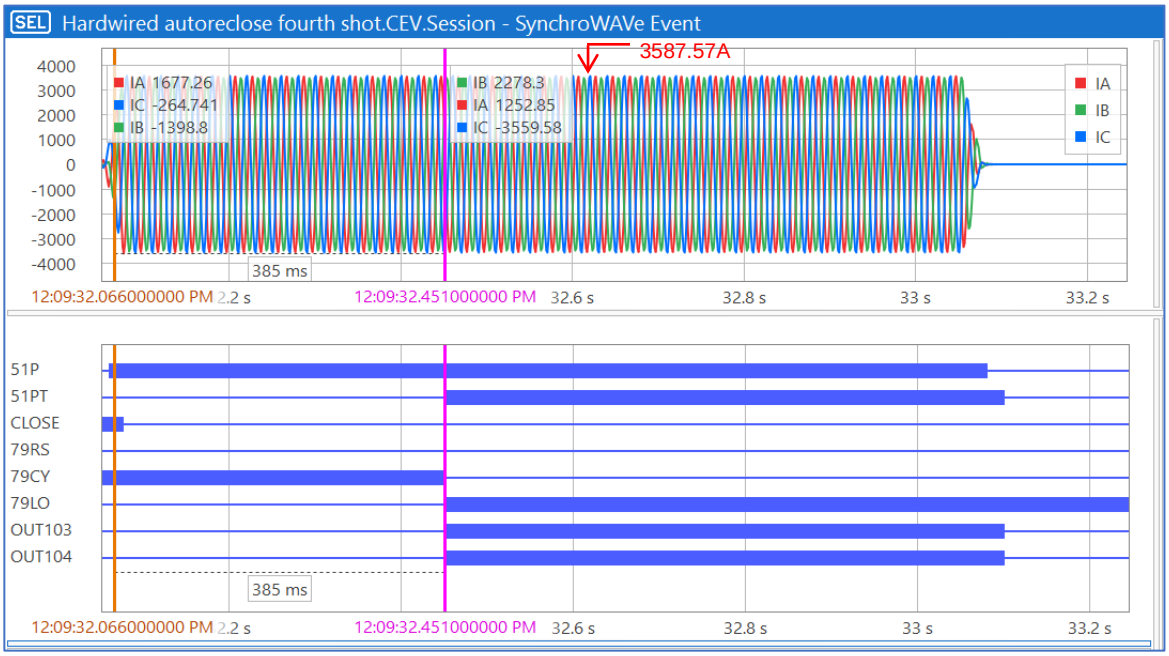

Figure 5.58: Results of the fourth shot's auto-reclose SEL351A (R1) relay simulation

The response of the SEL-351A (R2) relay to the trip signal sent by the SEL-351A (R1) relay through OUT103 is shown in Figure 5.59 below. Because there is no current injection on SEL-351A (R2), lockout element 79LO is asserted. The trip signal sent by SEL-351A (R1) through OUT103 is delivered to SEL-351A's (R2) input port IN102. When powered with 110V DC, IN102 is asserted to receive the trip signal given by SEL-351A. (R1). When 79LO and IN102 are both asserted, SEL-351A (R2) trips to isolate the part of the line between SEL-351A (R1) and SEL-351A (R2), as illustrated in Figure 5.59. OUT101 is asserted because the trip elements are mapped to SEL-351A (R1) output 101. When OUT103 is asserted, a close signal is sent to the SEL-351 relay (NOP). The SEL-351 relay trip signal and lockout state is used to close the NOP.

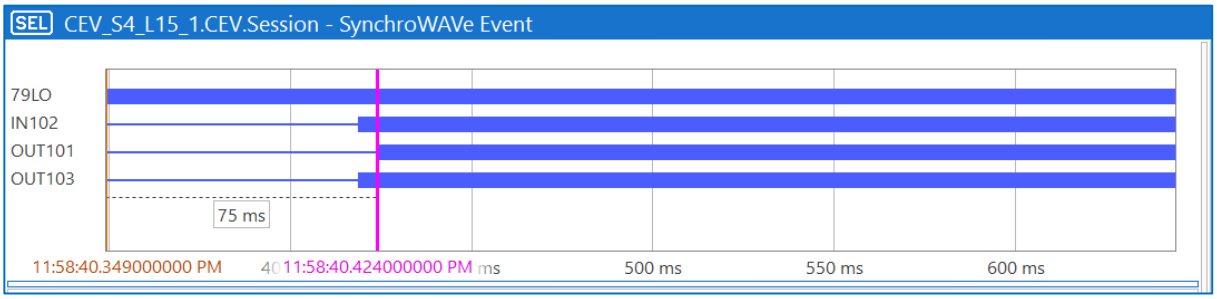

Figure 5.59: Trip signal response of the SEL-351A (R2) relay

SEL-351A relay (R1) output port OUT104 and SEL-351A relay (R2) output port OUT103 are mapped to SEL-351 relay (NOP) input ports IN102 and IN103, respectively. IN101 and IN102 in Figure 5.60 are asserted and confirm receipt of the two close input signals transmitted by SEL-351A relays (R1) and (R2). OUT102 is assigned to the close signal. When both IN102 and IN103 are asserted, the NOP is closed by asserting OUT102. When the NOP is closed, the line segment between SEL-351A (R2) and the NOP in Figure 5.1 is back-fed by Feeder B to avoid consumers in that section of the line from losing supply.

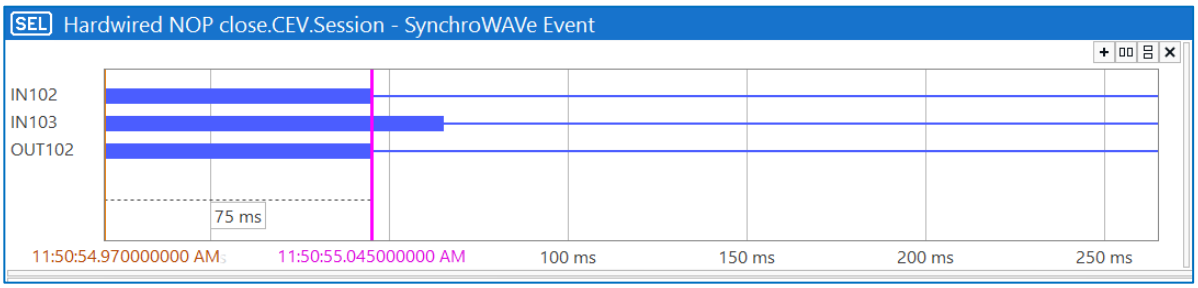

Figure 5.60: SEL-351 relay (NOP) close command

5.4.1.2 Single-phase to ground fault on the SEL-351A reclosing relay (R1)

Based on a CT ratio of 300:1, a single-phase to ground fault current simulation using DIgSILENT in chapter 4, section 4.6 produced a primary fault current of 1727.1A and a secondary current of 5.757A. An omicron overcurrent test module is used to simulate a secondary current of 5.757A to the SEL-351A (R1) relay. The maximum current is 2442.49A (1727.1A × $\sqrt{2}$ = 2442.49A). The fault current is generated by simulating the connection between the red phase and ground. Figure 5.61 shows how the SEL-351A (R1) relay cleared the fault in 345 milliseconds.

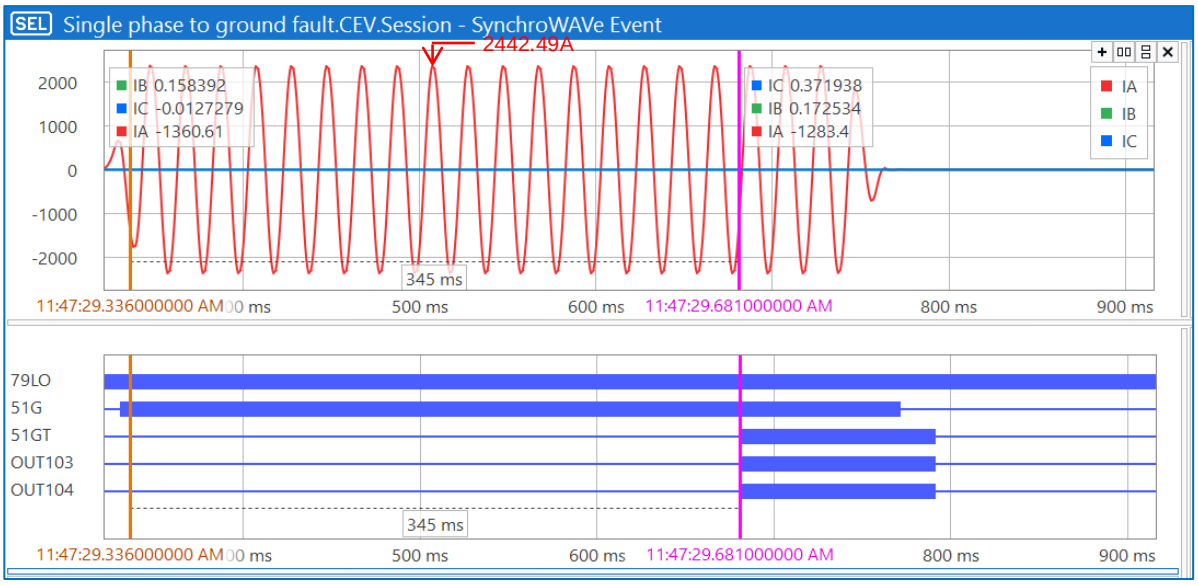

Figure 5.61: Single phase to ground fault on the SEL-351A reclosing relay (R1)

Because there is no injection to SEL-351A relay (R1), 79LO element is already asserted, 51G asserted to pick up the 5.757A secondary fault current is injected, 51GT asserted to clear the fault and operated at 345 ms. Output ports OUT103 and OUT104 are asserted, and trip signals are sent to open the contacts of the SEL-351A relay (R2) and the SEL-351 relay (R1) (NOP).

Figure 5.62 depicts the SEL-351A (R2) response to a trip signal sent by the SEL-351A relay (R1).

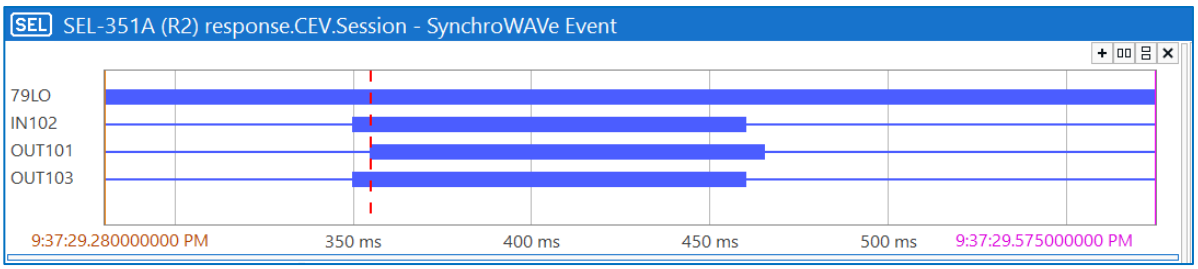

Figure 5.62: Response of the SEL-351A relay (R2) to the trip signal sent by the SEL-351A (R1)

Because there is no injection to the SEL-351A (R2) device, the 79LO element is already asserted; the input port IN102 is asserted when receiving a trip signal sent by the SEL-351A relay (R1); the output port OUT101 is asserted because the SEL-351A relay (R1)trip signal is mapped to OUT101; and the output port OUT103 is asserted when sending a trip to open a trip signal to the SEL (NOP).

Figure 5.63 depicts the response of the SEL-351 relay (NOP) to trip signals sent by the SEL-351A (R1) and SEL-351A (R2) relays.

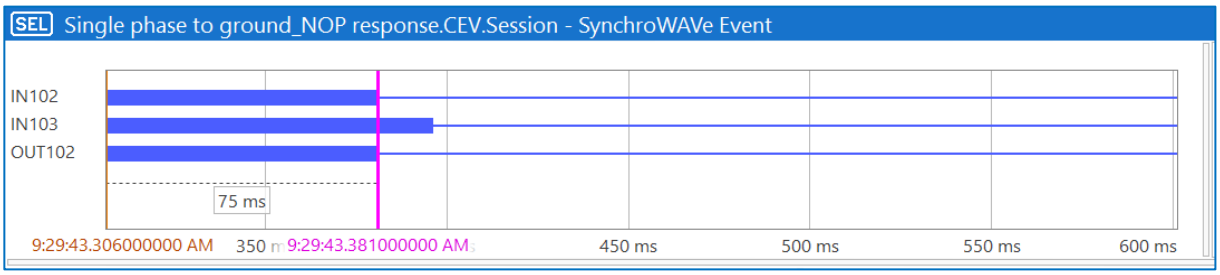

Figure 5.63: The SEL-351 relay (NOP) responds by sending the trip signal to the SEL-351A relay (R1) and the SEL-351A relay (R2)

SEL-351 relay (NOP) input ports IN102 and IN103 asserted in response to the close signal sent by SEL-351A relay (R1) and SEL-351A relay (R2), respectively. Because the close signal is assigned to output port OUT102, it is asserted. When SEL-351 relay (NOP) IN102 and IN103 are asserted, it signifies that both SEL-351A relay (R1) and SEL-351A relay (R2) tripped to open and SEL-351 relay (NOP) can safely close NOP to back feed line section between NOP and SEL-351 relay (R2) in Figure 5.1.

5.4.2 Case two: Three-phase fault and a single-phase to ground fault on the SEL-351A reclosing relay (R2)

5.4.2.1 Three-phase fault on the SEL-351A reclosing relay(R2)

This case study is carried out on the recloser control scheme lab scale test bench shown in Figure 5.3. Based on the CT ratio of 300:1, a three-phase fault current simulation in DIgSILENT in chapter 4 section 4.6 produced a fault current of 1456.65A primary and 4.856A secondary current. A peak value of 2060.01A shown in Figure 5.64 by multiplying the rms value by square root two (1456.65A × $\sqrt{2}$ = 2060.01A). The 300:1 CT ratio is chosen in chapter 4 section 4.4.5. Using the omicron state sequencer module, 4.856A of current is injected into the SEL-351A relay (R1). When the problem is simulated, the digital and analog chart events are

depicted in Figure 5.64. Bin out 1 is the binary output 1 of the CMC 356 device, which is mapped to circuit breaker 2 (BRK 2). The words "Close" and "Trip" are hardwired cable signals that are sent to the circuit breaker to close and trip it. The auto-reclose simulation results retrieved in test universe software are shown in Appendix E. These simulation results are the same as the results simulated for relay 1 in Figure 5.54 and for relay 2 in Figure 5.64.

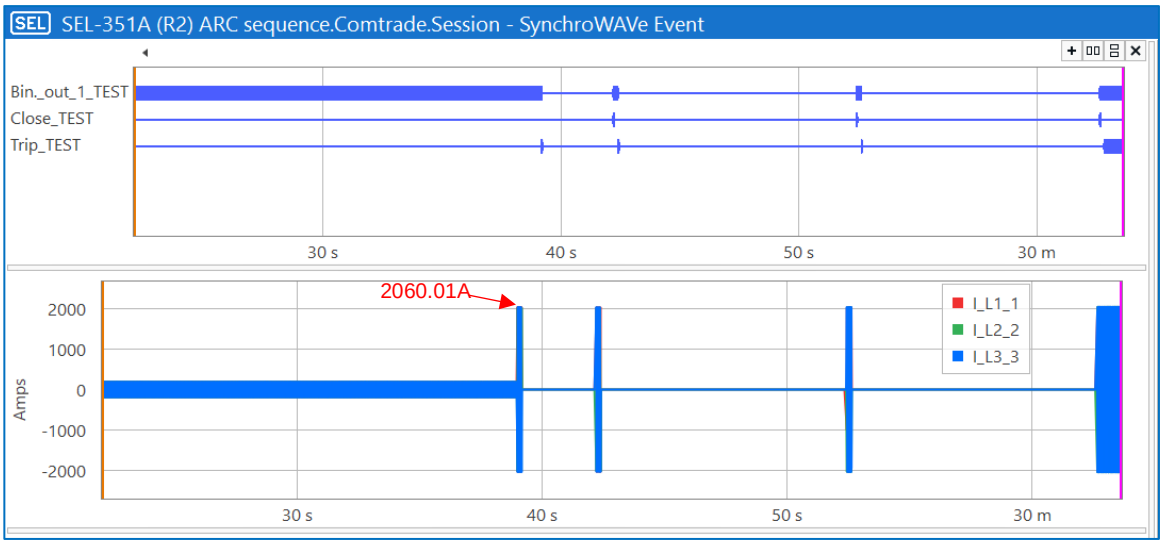

Figure 5.64: Results of the auto-reclose SEL351A (R2) relay simulation

The labels listed below are used to describe the lab-scale simulation results provided in this chapter:

- Bin_out_1_TEST is abbreviated as BRK 1
- Close_TEST is abbreviated as CLOSE
- Trip_TEST is abbreviated as TRIP

The SEL-351A relay (R2) is subjected to the identical auto-reclose cycle described in case study one, in which a three-phase permanent fault is simulated for the SEL-351A relay (R1). Figures 5.65 to 5.68 depict the SEL-351A relay (R2) events during the four auto-reclose shots. Each event displays fault current waveforms, relay (R2) operation time, and ANSI code of the triggered elements. The peak current value obtained is 2060.01A.

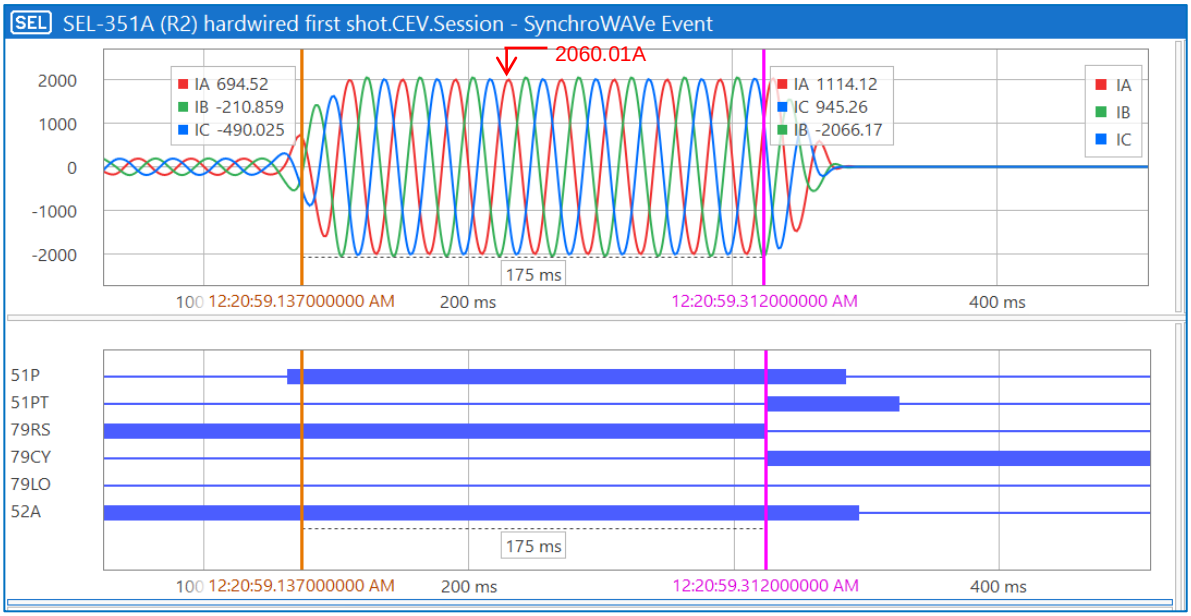

Figure 5.65: Results of the first shot's auto-reclose SEL351A (R2) relay simulation

The SEL-351A (R2) operated the fault in 175 ms for the first short, as illustrated in Figure 5.65. 51P is asserted when the fault current is detected, 51PT is asserted to clear the fault, 79RS is asserted when the circuit breaker is closed for a qualifying reset time and de-asserted when the circuit breaker tripped to open and reclose initiation is successful, 79CY is asserted when reclose initiation is successful, 79LO is not asserted because there is no lockout condition, 52A is asserted when the circuit breaker is open.

The auto-reclose results for the second shot are shown in Figure 5.66 below. As indicated in Figure 5.66, it took 175 milliseconds for the SEL-351A relay (R2) to operate and clear the fault. 51P is asserted to pick up the fault, 51PT is asserted to clear the fault, CLOSE is asserted to automatically reclose the circuit breaker, 79RS is de-asserted because the SEL-351A (R2) is in a cycle state, 79CY is asserted because the SEL-351A (R2) is undergoing auto-reclose cycle, 79LO is de-asserted because there is no lockout condition yet, When the circuit breaker is open, 52A is de-asserted, and when it is closed, 52A is asserted.

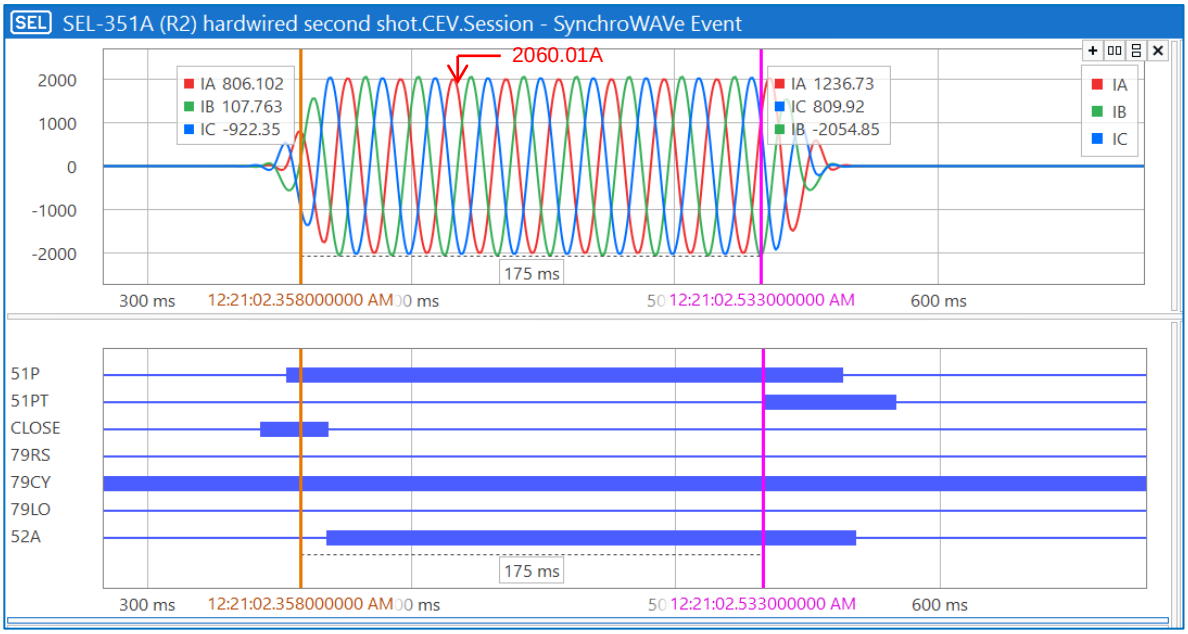

Figure 5.66: Results of the second shot's auto-reclose SEL351A (R2) relay simulation

The auto-reclose results for the third shot are shown in Figure 5.67 below. The third shot yields the same outcomes as the second shot.

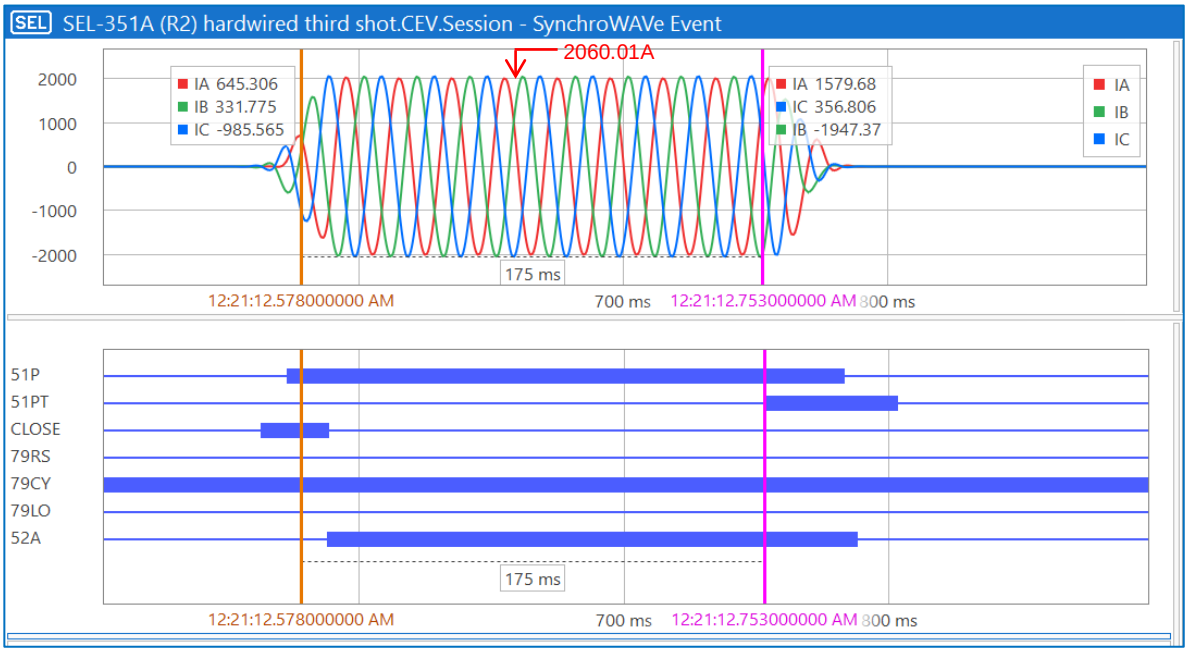

Figure 5.67: Results of the third shot's auto-reclose SEL351A (R2) relay simulation

Figure 5.68 depicts the auto-reclose results of the SEL-351A relay (R2) for the fourth short. CLOSE asserted to automatically reclose the circuit breaker when the last shot occurred, 51P picked up the fault and asserted, 51PT asserted to clear the fault, 79CY is asserted when the SEL-351A is in the recycle state and de-asserted when 51PT tripped to lockout, and 79LO asserted to prevent the circuit breaker from

closing. When the circuit breaker is closed, 52A is asserted; when the circuit breaker is open, 52A is de-asserted.

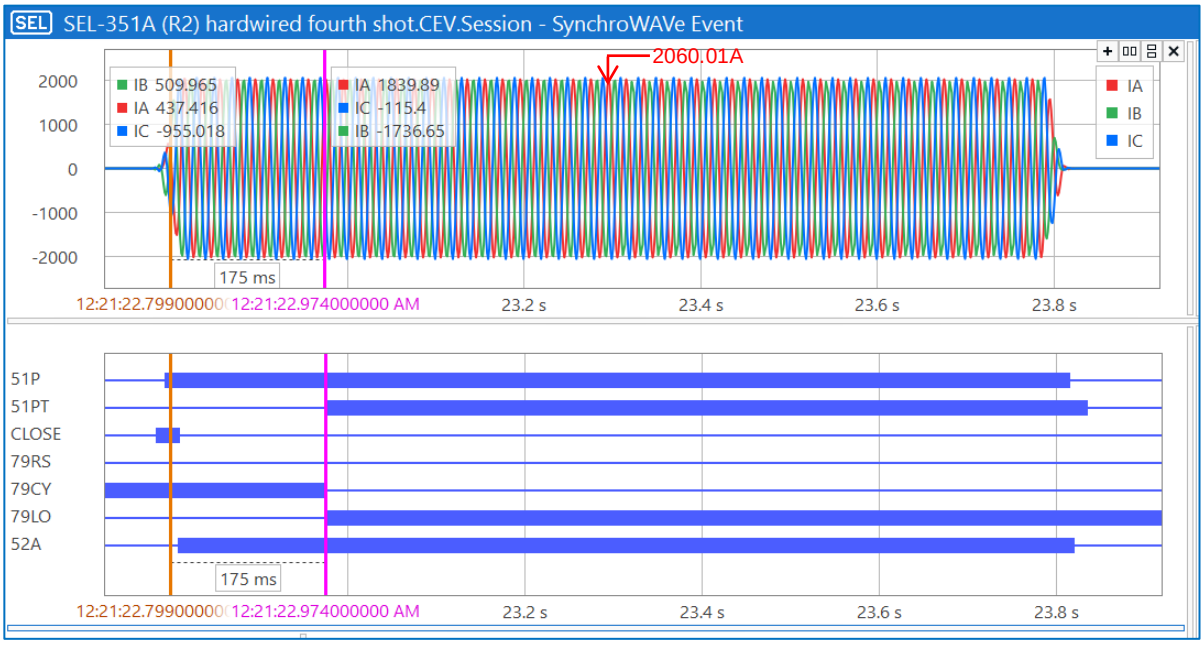

Figure 5.68: Results of the fourth shot's auto-reclose SEL351A (R2) relay simulation

Figure 5.69 depicts three-phase fault outcomes for the SEL-351A relay (R1) in the event that the SEL-351A relay (R2) fails to trip. After providing SEL-351A (R2) time to remove the fault, SEL-351A relay (R1) would operate 505 ms later. The SEL-351A (R1) 51P is also picked up in the Figure 5.69 as a result of the 4.856A secondary fault current injected. 51PT asserted that the fault had been cleared.

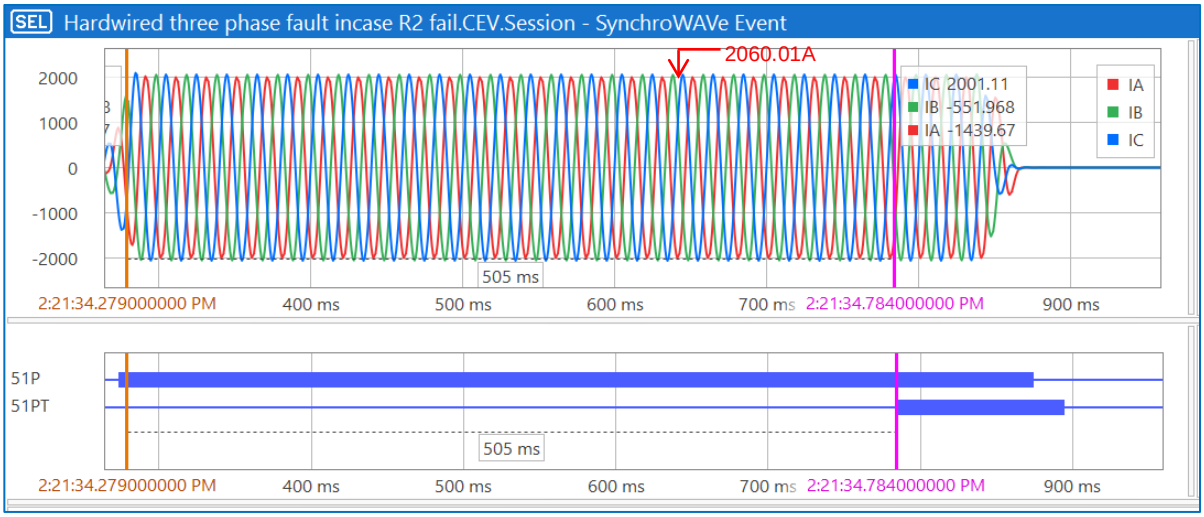

Figure 5.69: In the event that the SEL-351A relay (R2) fails to operate, the SEL-351A relay (R1) operate

The obtained grading margin between relay R2 and R1 is (505 ms – 175 ms =0.33s)

5.4.2.2 Single-phase to ground fault on the SEL-351A reclosing relay(R2)

The hardwired recloser control scheme lab-scale test bench shown in Figure 5.3 is used for this study scenario. Based on the CT ratio of 300:1, a single-phase to ground fault current simulation in DIgSILENT produced a fault current of 842.88A primary and a secondary current of 2.81A. The 300:1 ratio A secondary fault current of 2.81A is injected between the red phase and ground to the SEL-351A (R2) relay. Figure 5.70 depict a peak value of (842.88A × $\sqrt{2}$ = 1192.01A). This is done to ensure that the SEL-351A (R2) relay is tested for faults between the SEL-351A (R2) relay and the NOP. Figure 5.70 depicts the fault current waveform, relay (R2) operation time, and ground elements triggered. As illustrated in Figure 5.70, the 51G element detected the 2.81A fault current and the 51GT element asserted to clear the fault in 115 ms.

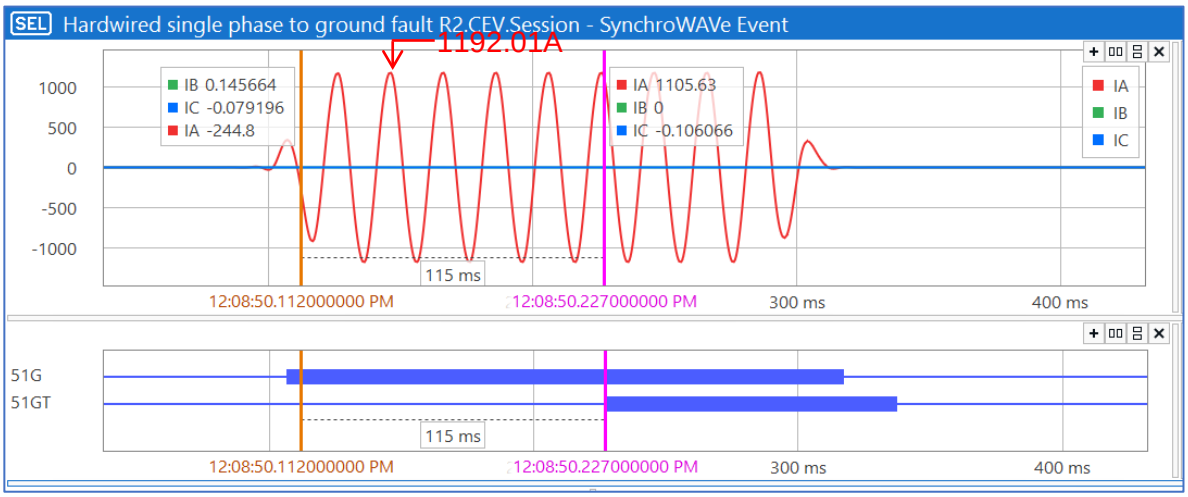

Figure 5.70: For a *fault condition* between SEL-351A (R2) and NOP, SEL-351A relay (R2) is operated for a single phase to ground.

In the event that the SEL-351A (R2) relay fails to operate, Figure 5.71 displays the single-phase to ground fault results for the SEL-351A (R1) relay. The SEL-351A (R1) relay operates in 445 milliseconds. Figure 5.71 also shows SEL-351A (R1) relay 51G picking up as a result of the simulated 2.81A secondary fault current and 51GT asserted to clear the fault.

The difference in operation timings between the two reclosing relays SEL-351A (R2) and SEL-351A (R1) will be graded as 445ms -115ms = 0.33 seconds.

.

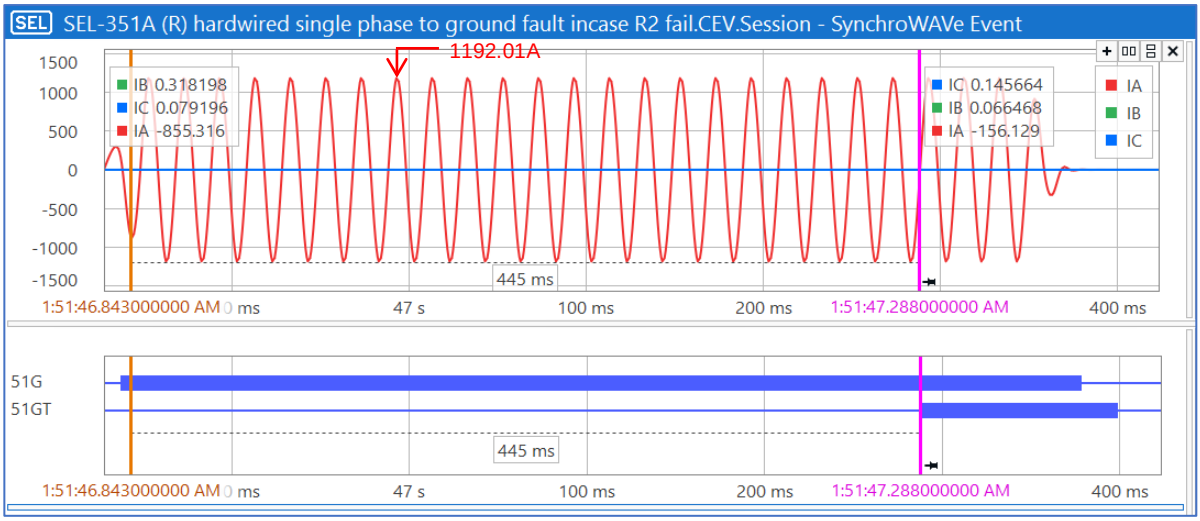

Figure 5.71: SEL-351A relay (R1) operation for a single phase to ground for a fault between SEL-351A (R2) and NOP

5.4.3 DIgSILENT simulation versus hardwired lab-scale testing results

Table 5.11 compares DIgSILENT recloser control protection functions to lab-scale protection testing simulation findings utilizing the SEL-351A relay and Omicron Test injection device due to a failure simulated at Feeder A. The comparison is based on the identical simulated fault current magnitudes and tripping timings. The fault currents value are taken from section 4.6 of chapter 4.

Table 5.11: DIgSILENT auto-recloser simulation results versus lab-scale testing using the SEL-351A relay are compared

Relay (R1/R2)	Type of fault	Fault current magnitude in amperes (A)	Tripping times in seconds	
			DIgSILENT simulation results	SEL-351A lab-scale test bench results
R1	Three-phase fault	8.456	0.385	0.385
R1	Single-phase to ground	5.757	0.348	0.345
R2	Three-phase fault	4.856	0.175	0.175
R2	Single-phase to ground	2.81	0.121	0.115
R1(back-up when R2 fail)	Three-phase fault	4.856	0.510	0.505
R1(back-up when R2 fail)	Single-phase to ground	2.81	0.447	0.445

The simulation results of DIgSILENT and lab-scale testing of the recloser control protection functions are benchmarked according to the recloser operation time as specified in IEEE Std C37.104-2012. Table 5.11 compares the protection speed tolerance of DIgSILENT to lab-scale simulation results. Tripping time tolerances compasrion are less than 5%, ensuring the recloser protection operational speed is within the specified limit.

5.5 Conclusion

This chapter reveals a hardwired lab-scale implementation of a distribution system auto-reclose scheme. This chapter covered the engineering setups of the auto recloser scheme in both the AcSELerator quickset and the Test Universe software environments.

This chapter investigates two case studies. Case study one looked at a three-phase fault and a single-phase to ground fault on a SEL-351A (R1) reclosing relay, while case study two looked at a three-phase fault and a single-phase to ground fault on a SEL-351 (R2) reclosing relay. The findings of the two case studies are presented and evaluated in depth.

The following chapter implements the IEC 61850 GOOSE message application for the recloser control system.

CHAPTER SIX

LAB-SCALE IMPLEMENTATION OF THE IEC 61850 STANDARD-BASED GOOSE MESSAGE APPLICATION FOR THE RECLOSER CONTROL SCHEME

6.1 Introduction

Traditionally, hardwire was utilized as a means to transfer signals between protection and monitoring devices while monitoring and controlling substation equipment. As a result of this strategy, there are a lot of wires connecting the substation equipment. When signals are conveyed from a sending device to a receiving device, this mode of communication causes temporal delays.

This chapter describes the IEC 61850 GOOSE message-based lab-scale implementation of the distribution system's auto-reclose scheme. Using IEC 61850 GOOSE signals between the devices, the proposed recloser control approach simulates automatic reconfiguration of the distribution system under fault conditions. To set up the recloser control scheme, the lab-scale implementation incorporates SEL-351A (R1), SEL-351A (R2), and SEL-351 (NOP) IEDs. This chapter describes the engineering configuration and testing of the simulation of the IEC 61850 standard-based GOOSE messaging application for the auto-reclose scheme.

The following is a list of the chapter's contents: Section 6.2 explains the implementation of the auto-reclose method utilizing the IEC 61850 standard. Section 6.3 describes the established auto-reclose logic system. Section 6.4 details the IEC 61850 GOOSE message engineering configuration for the auto-reclose method. Section 6.5 contains case studies and simulation results. Conclusion of Section 6.6

6.2 Implementation of the recloser control scheme using the GOOSE message based on the IEC 61850 standard

This section provides an IEC61850 standard-based lab-scale implementation GOOSE message communication configuration between two SEL-351A devices, SEL-351 and omicron CMC 356. To exchange digital signals, these devices use the IEC 61850 standard GOOSE messages. Data is sent between these recloser controllers in an event-based method. The mechanism of the publisher/subscriber

system is used for data exchange. The IEC 61850 GOOSE message implementation of a recloser control scheme for the 22kV distribution network is shown in Figure 6.1 below.

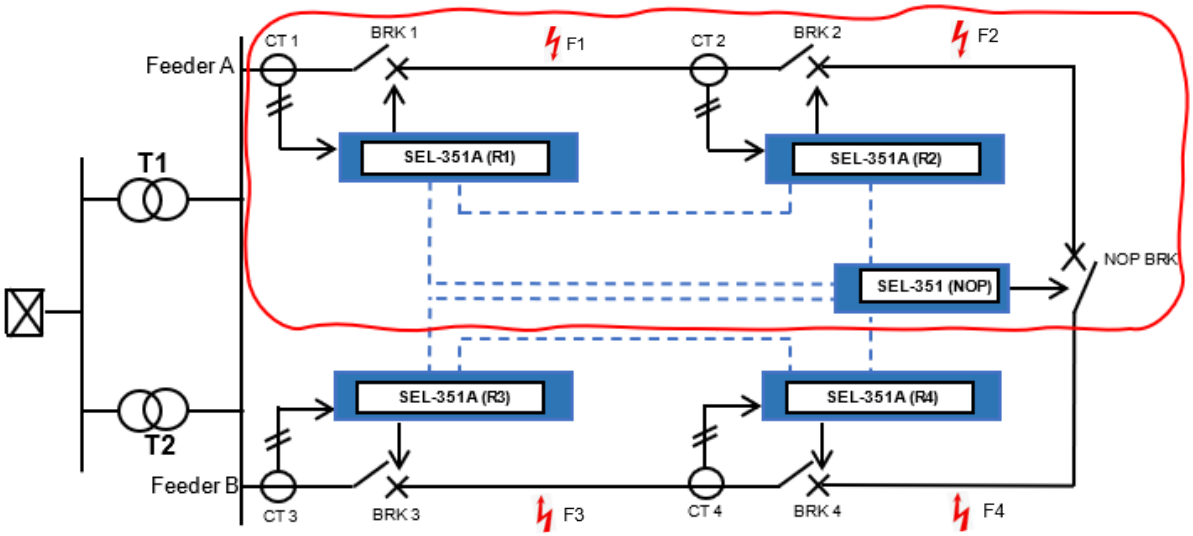

Figure 6.1: Recloser control scheme based on the IEC 61850 GOOSE messaging application

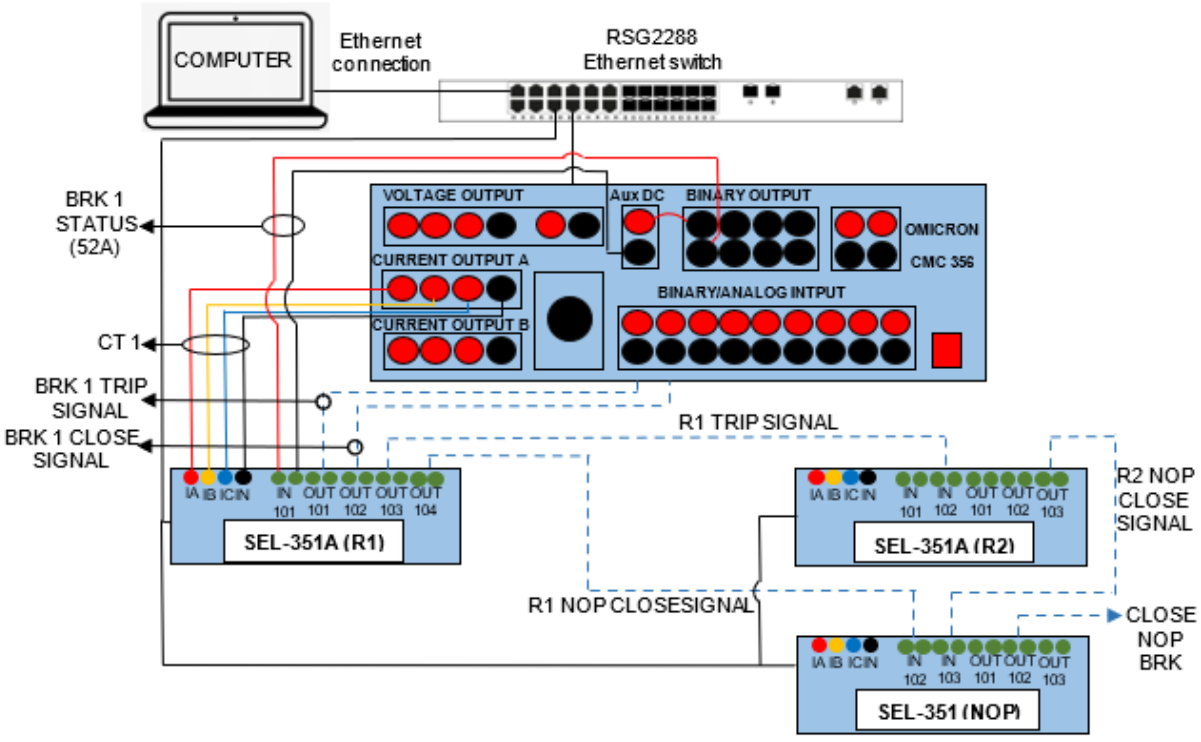

Figure 6.2: IEC 61850 GOOSE message-based lab-scale setup of a recloser control scheme to test the fault conditions between SEL-351 (R1) and SEL-351A (R2)

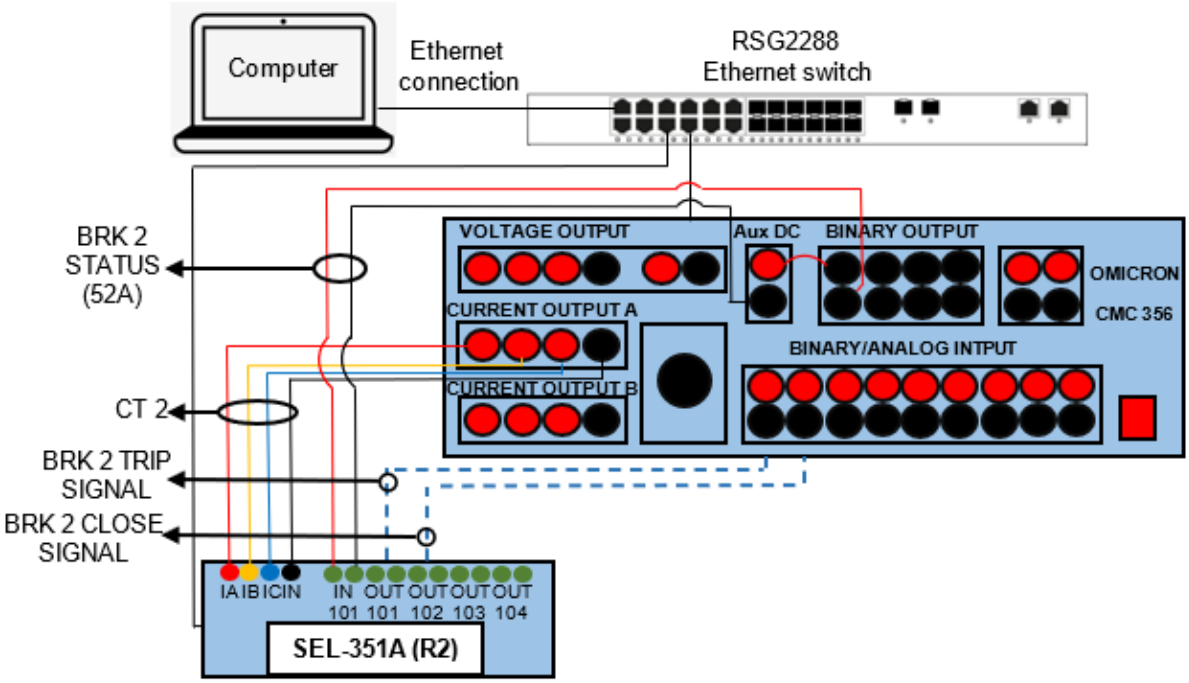

Figure 6.3: IEC 61850 GOOSE message-based lab-scale setup of a recloser control scheme to test the fault conditions between SEL-351 (R2) and SEL-351A (NOP)

Figure 6.1 depicts the whole recloser control scheme in a distribution system network, with the area encircled in red representing the developed IEC 61850 GOOSE-based recloser control scheme. Figure 6.2 below shows a lab-scale setup of the IEC 61850 GOOSE-based auto-reclose scheme to test the fault conditions between SEL-351 (R1) and SEL-351A (R2), while Figure 6.3 shows a lab-scale setup to test the fault conditions between SEL-351 (R2) and SEL-351 (NOP).

Figure 6.4 depicts the installed recloser control scheme at CPUT, DEECE, CSAEMS lab for the distribution system, which automatically reconfigures the network in the event of a fault.

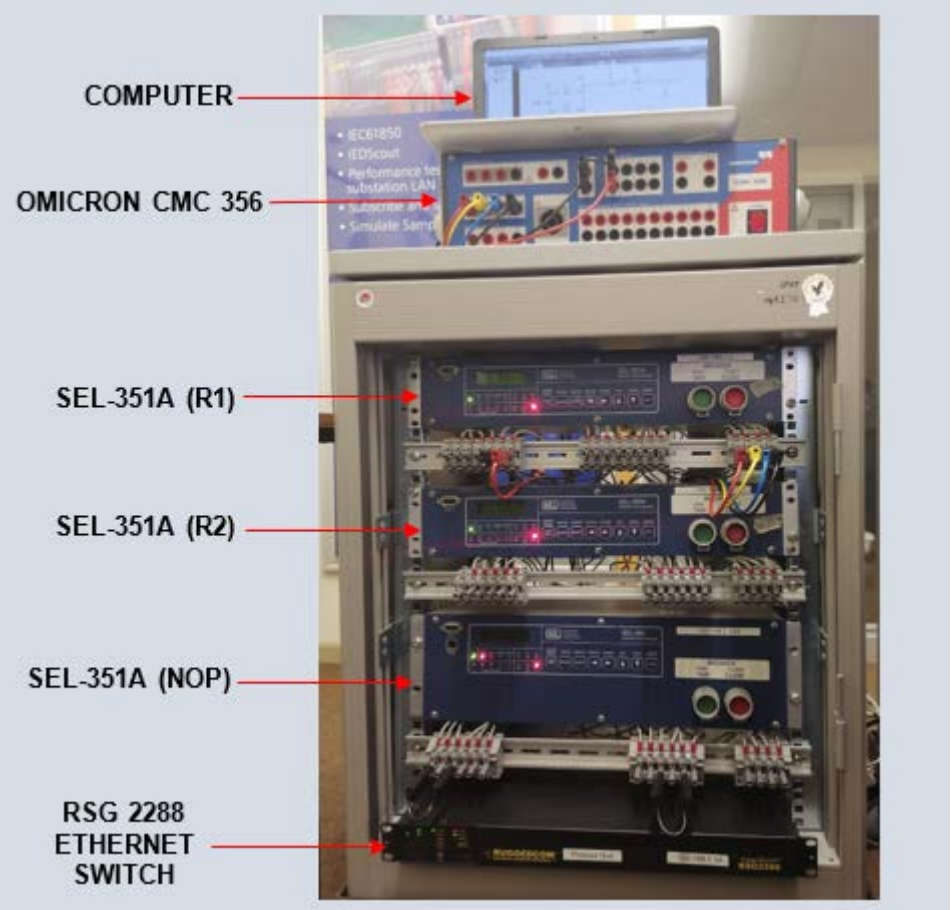

Figure 6.4: CPUT CSAEMS lab has built up a test bench for the distribution system auto-reclose scheme.

The computer is utilized to do relay engineering configuration using the AcSELerator Quickset and AcSELerator Architect software, as well as Omicron CMC 356 test injection device configuration using the test universe program. The CMC 356 device is used to mimic fault currents on the SEL-351A IEDs (R1 and R2). The RUGGEDCOM Ethernet switch was utilized to connect the three IEDs (R1, R2, and NOP) to the computer and the CMC 356 device.

According to section 4.5 of Chapter 4, R1 is set with three overcurrent elements: phase time overcurrent (51PP), instantaneous overcurrent element (50P1P), and residual overcurrent element (51G1P). These three elements are configured with their respective trip elements 51PT, 67P1T, and 51GT. For safety concerns, 67P1T and 51GT are not configured to initiate auto-reclose; only 51PT is configured to do so. Only 51PP and 50P1P, along with their associated trip elements 51PT and 51GPT, are configured for Relay 2. The auto-reclose system is triggered for Relay 2 via the 51PT element.

According to Figure 6.1, there are two fault locations on each side of the NOP, namely between SEL-351A (R1) and SEL-351 (R2), SEL-351A (R2) and SEL-351 (NOP),

SEL-351A (R3) and SEL-351A (R4), and SEL-351A (R4) and SEL-351 (NOP). The power restoration process can be detailed for a permanent fault that occurs between SEL-351A (R1) and SEL-351A (R2) or between SEL-351 (R3) and SEL-351 (R4). This section mainly concentrates on fault conditions on one side of the feeder (Feeder A), in order to minimize duplicating effort, as the same approach would be followed for faults happening in feeder B.

6.3 Developed auto-reclose logic

In Figure 6.1, if a permanent fault condition involving 51PT occurs between R1 and R2, R1 will detect the fault and attempt three auto-reclosing attempts. During R1 tripping and closure, multicast GOOSE signals are delivered to trip and close binary inputs on the omicron 356 device, thereby opening and closing the virtual circuit breaker mapped at the binary output. Figure 6.2 is used to accomplish this. R1 will lockout if it is unable to reclose due to a permanent fault. Figure 6.5 depicts the reasoning that is followed after R1 locks out.

Table 6.1 presents the protective function ANSI codes and their related logical nodes as stated in the IEC61850-7-4 part of the standard; this table is used to comprehend the description of the protective functions and the developed recloser logics represented in Figures 6.5 to 6.7.

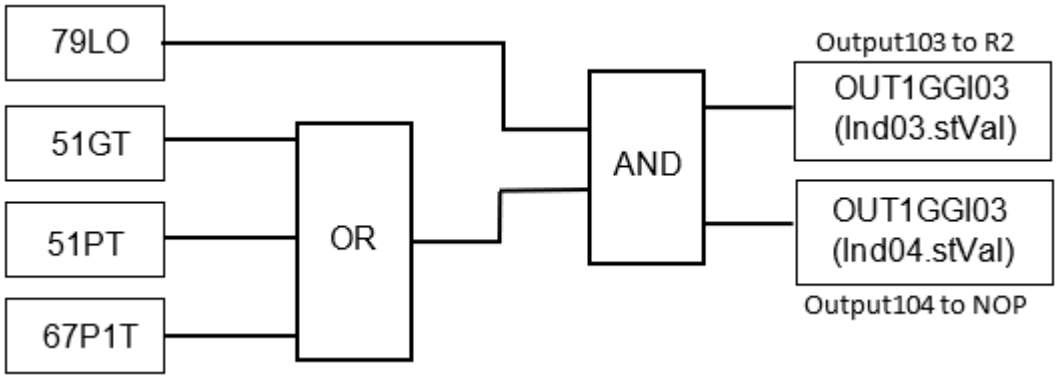

Figure 6.5: Developed auto-reclose logic for SEL-351A (R1)

Both the high status (logical 1) from the 79LO and 51PT trip element input signals to the AND gate, as well as the AND gate's high output, are delivered to R2 and NOP via outputs 103 and 104 via the GOOSE signal, as shown in Figure 6.5. The identical operation occurs with no auto-reclose operation for a permanent fault involving 51GT and 67PT. Power is restored after a reclosure when a temporal fault involving 51PT occurs.

Relay R1's lockout and trip GOOSE message serves as an input to R2. When R2 trips and locks out as a result of R1 input, a close GOOSE message is sent to the NOP through output 103. Figure 6.3 is used to accomplish this. The relay R2 logic is depicted in Figure 6.6 below.

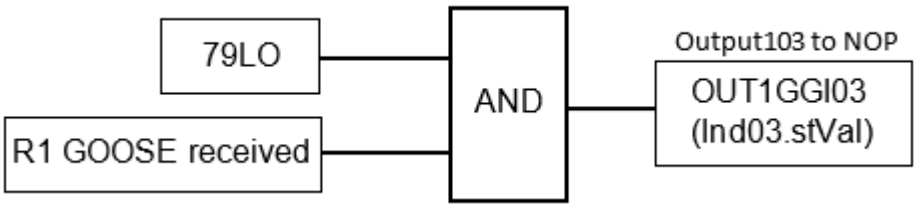

Figure 6.6: Developed auto-reclose logic for SEL-351A (R2)

As shown in Figure 6.7, the trip and lockout GOOSE messages from R1 and R2 are used as inputs for the SEL-351 (NOP). These two GOOSE input signals instruct the SEL-351 (NOP) to close its circuit breaker and feed feeder B to the line section between the NOP and the SEL-351 (R2). Figure 6.1 depicts the back-fed line segment.

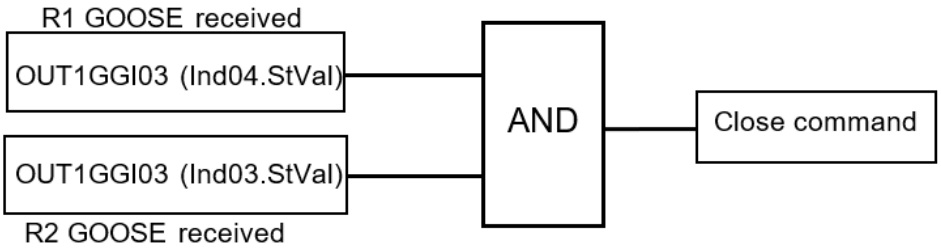

Figure 6.7: Developed auto-reclose logic for SEL-351 (NOP)

In Figure 6.1, when a permanent fault involving 51PT occurs between R2 and NOP, R2 auto-recloses and locks out. During the tripping and closing of R1, multicast GOOSE messages are sent to the omicron 356 device's trip and close binary inputs to open and close the virtual circuit breaker mapped at binary output 2. When a 51GT fault occurs, no auto-reclose is initiated, and R2 trips and locks out.

6.4 IEC 61850 GOOSE message engineering configuration for the auto-reclose scheme

This section aims to configure SEL-351A (R1) to send GOOSE messages when the 51PT, 67P1T, and 50GT are triggered. Configure SEL-351A (R2) to subscribe to a trip GOOSE message broadcast by R1 and to publish a close GOOSE message subscribed to by SEL-351A. (NOP). Finally, NOP IED should be configured to subscribe to a close GOOSE message published by R1 and R2.

Figure 6.8 shows the flow chart used to configure auto-reclose scheme GOOSE messages on AcSELerator Architect.

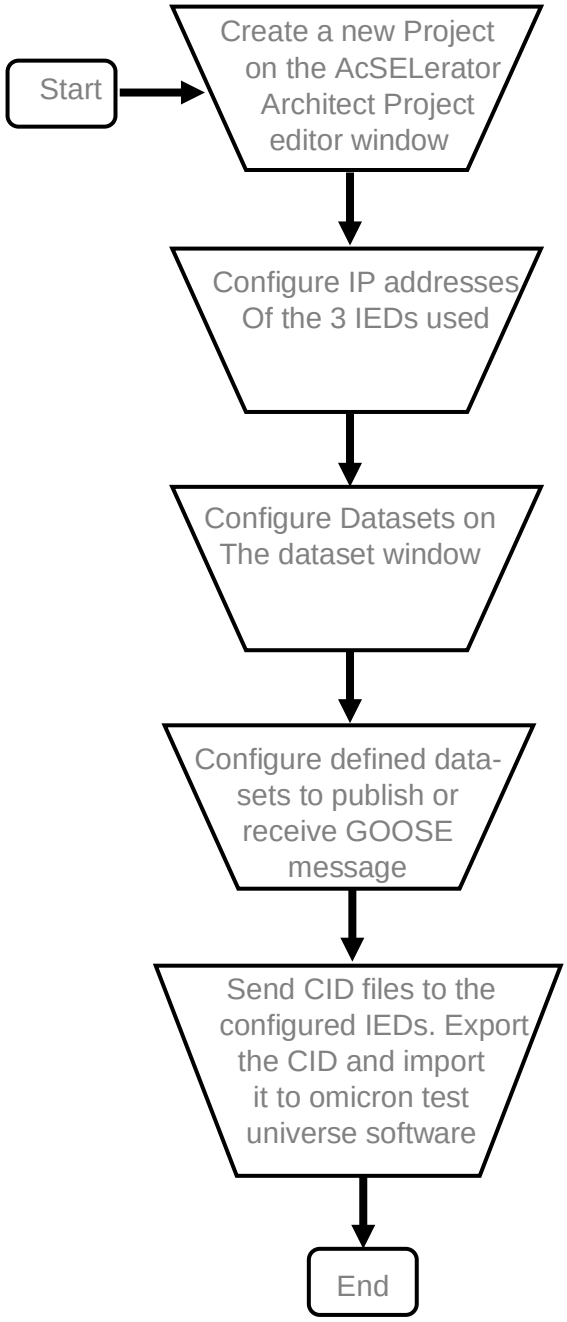

Figure 6.8: Flow chart for configuring IEC61850 datasets for the auto-reclose scheme

The AcSELerator Architect software home page is comprised of four panes, as shown in Figure 6.9.

- The project editor window is used to create a new project.
- The IED properties window is used to complete the IP address parameters of the IEDs used in the project editor window.

- IED palette window for selecting IEDs SEL-351.
- The output pane displays information about the configured IEC61850 project.

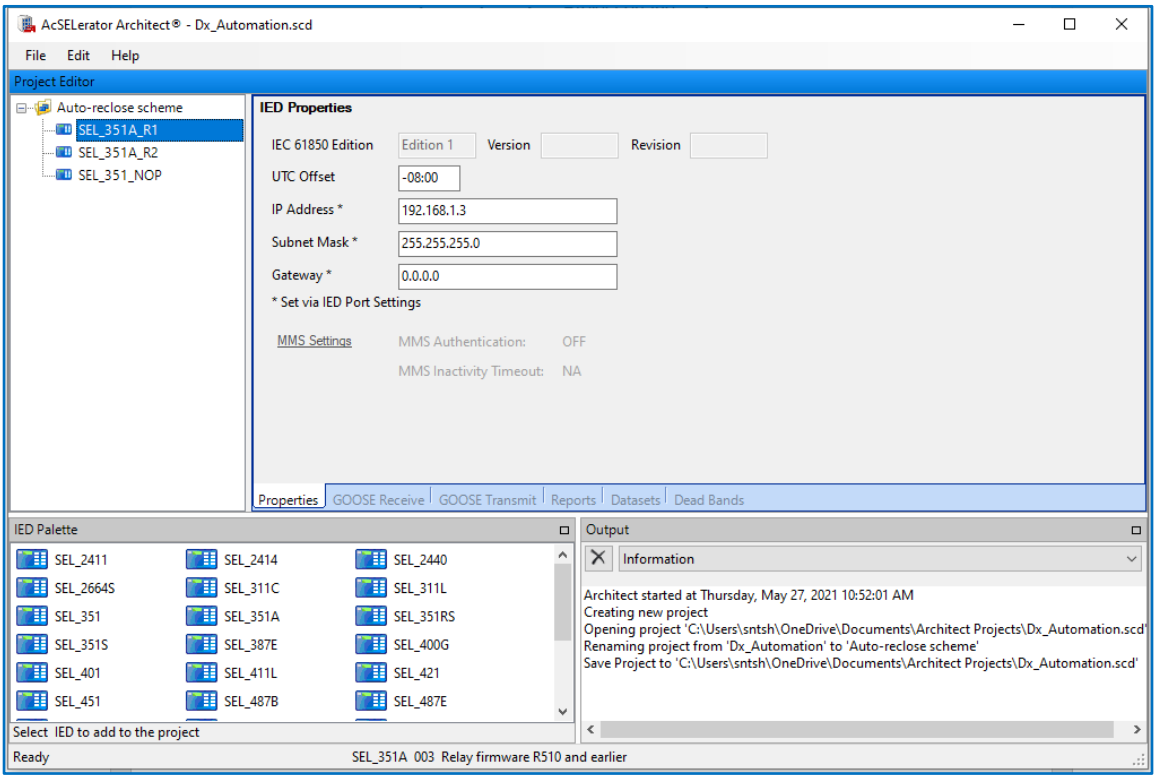

Figure 6.9: AcSELerator Architect GOOSE message configuration tool

To implement the auto-reclose system based on IEC61850 GOOSE signals, the following steps are taken:

Step 1: In the project editor window, a new project named "Auto-reclose scheme" was created. As shown in Figure 6.9, three IEDs (SEL-351A (R1), SEL-351A (R2), and SEL-351 (NOP) are selected from the IED palette and added to the project editor window. Each of the IED properties is defined under IED properties. IP address, Subnet Mask, and Gateway are among the IED attributes.

Step 2: The datasets required for the auto-reclose technique are defined in this step. New datasets are established for each IED under the Dataset tab. seven datasets are developed for R1 as shown in Figure 6.10a, five datasets are developed for R2 as shown in Figure 6.10b, and no datasets are created for NOP. NOP only receives R1 and R2's trip and locked out signals. Following the creation of the datasets, the necessary logical nodes and data attributes are assigned. The logical nodes, data attributes, and the overcurrent element that triggers attributes of the configured logical nodes in each IED are listed in Table 6.1 below.

Table 6.1: Configured datasets for the auto-reclose scheme

		SEL-351A_R1		SEL-351A_R2		SEL-351_NOP
Description	**Trigger**	**Logical node**	**Data attribute**	**Logical node**	**Data attribute**	**Logical node**
Phase time-overcurrent operate	51PT	P51PTOC1	Op.general	P51PTOC1	Op.general	-
Residual time-overcurrent operate	51GT	G51PTCO1	Op.general	G51PTCO1	Op.general	-
Definite time, torque-controlled 50P1	67P1T	P67PTCOC1	Op.general	-	-	-
Digital ouput 2	OUTPUT102 (Close)	OUT1GGIO3	Ind002	OUT1GGIO3	Ind002	-
Digital output 3	OUTPUT103 (79LO+TRIP)	OUT1GGIO3	Ind003	OUTPUT103	Ind003	OUT1GGIO3
Digital output 4	OUTPUT104 (79LO+TRIP)	OUT1GGIO3	Ind004	-	-	OUT1GGIO3
Trip indication	TRIP	TRIPPTRC1	Tr.general	TRIPPTRC1	Tr.general	-

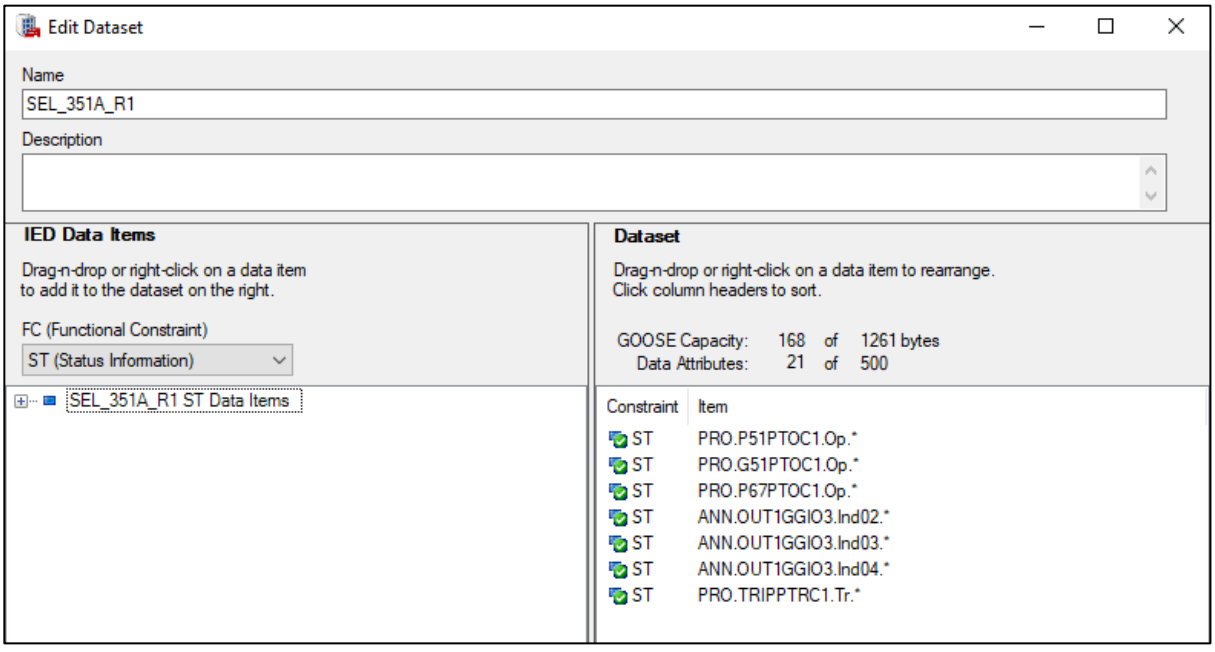

Figure 6.10: Dataset configuration for SEL-351A (R1)

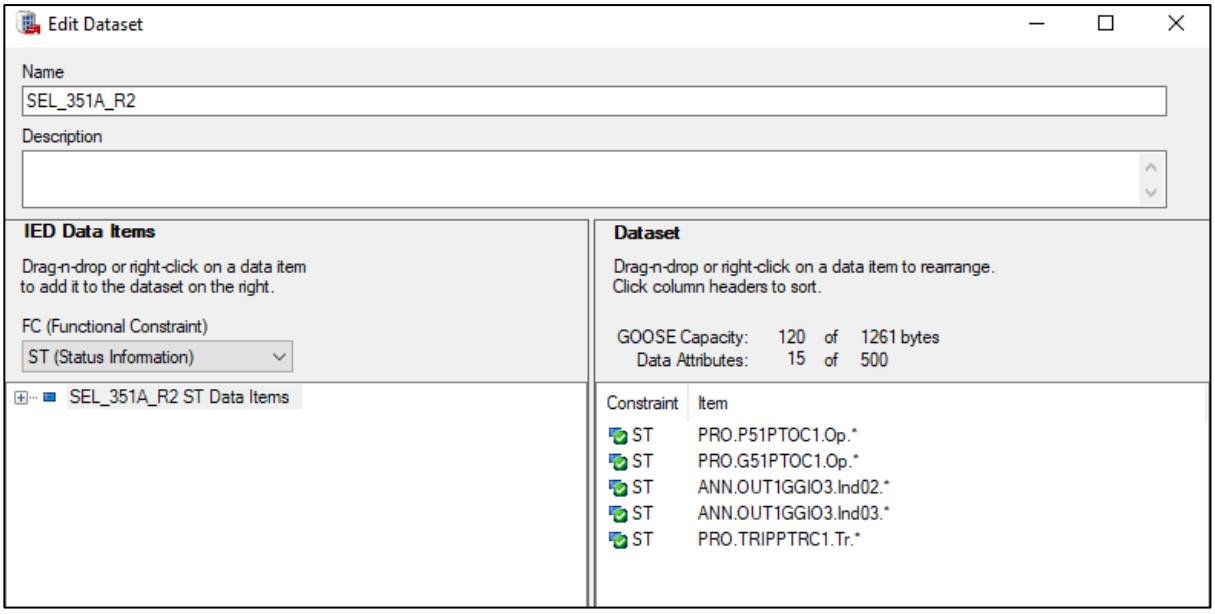

Figure 6.11: Dataset configuration for SEL-351A (R2)

Step 3: The NOP's SEL-351 is set up to receive GOOSE messages broadcast by relays R1 and R2. When both R1 and R2 are open due to a fault, this step is used to achieve the CLOSE command on the NOP. This setting is done on the GOOSE receive tab by mapping R1 output 104 to SEL-351 virtual bit 1 (VB001) and R2 output 103 to SEL-351 virtual bit 2 (VB002). Figure 6.12 depicts the GOOSE message mapping of the two IEDs (R1 and R2) to SEL-351 virtual bits.

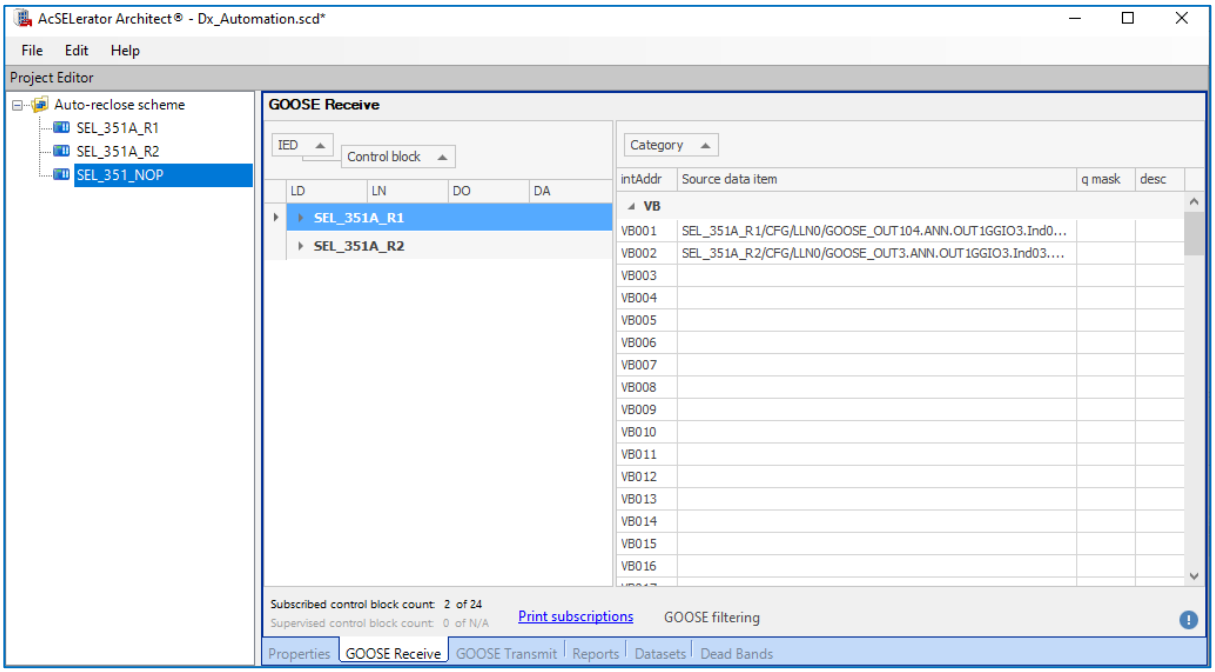

Figure 6.12: GOOSE message mapping to SEL-351 (NOP) for a CLOSE command

Step 4: The Configured IED description files (CID) that are transmitted to their corresponding IEDs SEL-351A (R1), SEL-351A (R2), and SEL-351A (R3) (NOP). On omicron test universe software, the configured CID files for R1 and R2 IEC61850 datasets are exported, stored, and imported as Substation Configuration Files (SCL). The imported SCL file on the test universe software is shown in Figure 6.13 below. As illustrated in Figure 6.13's input tab, the operation logical node P51PTOC1 was mapped to binary input input 1 and the "CLOSE" signal to binary input 2. All R1 datasets configured on AcSELerator Architect are listed under GOOSEs. All remaining logical nodes are mapped similarly.

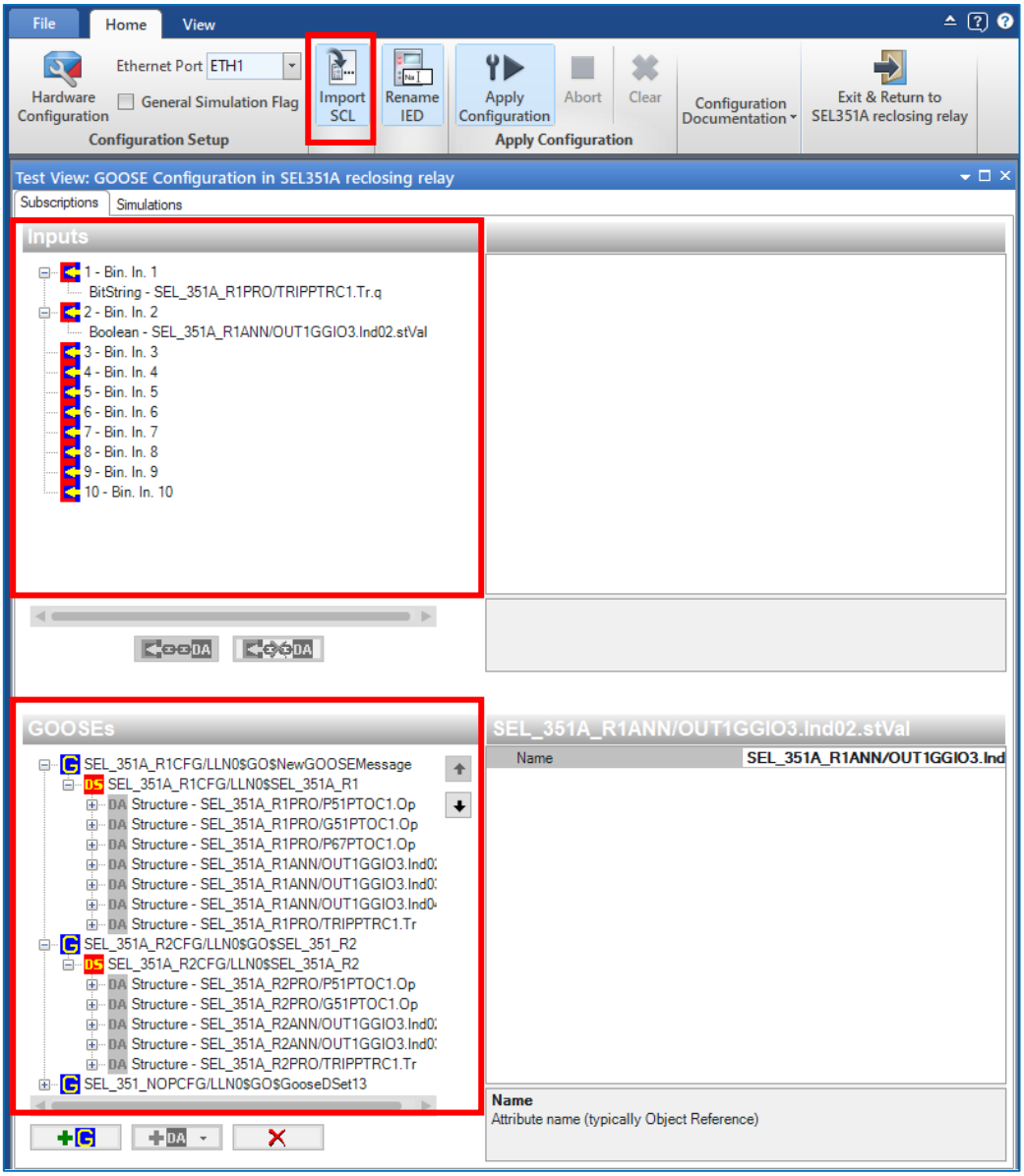

Figure 6.13: GOOSE dataset mapping in the omicron test universe

6.5 Case studies

Two case studies were conducted utilizing the IEC 61850 standard-based GOOSE auto-reclose scheme to investigate the performance of the overcurrent recloser control scheme for the distribution system. The following scenarios were simulated, and the performance of each IED was analyzed.

1. Case one: Three-phase fault and single-phase to ground fault on a SEL-351A (R1)
2. Case two: Three-phase fault and single-phase to ground fault on a SEL-351A (R2)

Table 6.2 shows the fault current magnitudes simulated to the two relays SEL-351A (R1) and SEL-351A (R2). It should be noted that the fault current estimates in this section are obtained from DIgSILENT simulations in section 4.6 of Chapter 4 and Table 5.10 in section 5.4 of chapter 5.

Table 6.2: Simulated fault currents to relays R1 and R2

	Three-phase fault currents		**Single-phase to ground fault currents**	
Relay	Primary current	Secondary current	Primary current	Secondary current
SEL-351A (R1)	2536.76A	8.456A	1727.1A	5.757A
SEL-351A (R2)	1456.65A	4.856A	843.12A	2.81A

6.5.1 Case one: Three-phase fault and single-phase to ground fault on a SEL-351A (R1)

6.5.1.1 Three-phase fault on a SEL-351A (R1)

The omicron test universe state sequencer module is used to mimic a three-phase permanent fault scenario by injecting 8.456A secondary current on R1. When the fault is simulated, the digital and analog chart sequence of events is depicted in Figure 6.14. Bin out 1 is the CMC 356 device's binary output 1 where the circuit breaker for the SEL-351A (R1) IED is mapped. "Close" and "Trip" are GOOSE signals that are sent to the circuit breaker to trigger it to close and trip. Calculations to obtain 3587.52A are discussed in section 5.4.1.1 of chapter 5.

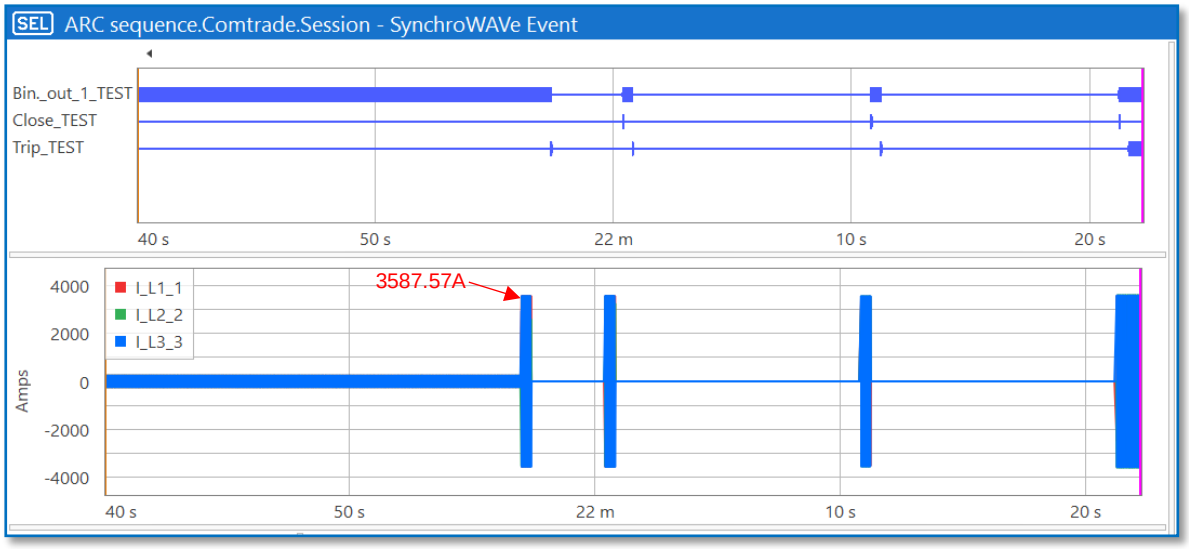

Figure 6.14: Sequence of Auto-reclosure

The circuit breaker is closed during the first 15 seconds of the simulation, as shown on the digital chart at the top of Figure 6.14. A usual load current of 0.56A secondary was simulated while the circuit breaker was closed, as indicated in the analog chart at the bottom. After 15 seconds, a secondary fault current of 8.456A (8.456 secondary current X CT ratio (300) = 2536.8 RMS current in primary, then 2536.8 X √2 = 3587.57 peak current in primary amps as depicted in Figure 6.14 above) was simulated, and the SEL-351A (R1) detected it by sending a GOOSE signal to open the circuit breaker. In the auto-reclose cycle, the SEL-351A (R1) resets and is ready for the automatic reclosing sequence (CY). When the trip signal is received, the circuit breaker opens, and the SEL-351A (R1) opens the contacts for 3 seconds. After 3 seconds, the SEL-351A (R1) transmits a GOOSE signal to close the circuit breaker. After closing the circuit breaker and simulating a fault current of 8.456A, the SEL-351A (R1) detected the fault and transmitted a GOOSE signal to open the circuit breaker. The circuit breaker tripped, and the SEL-351A (R1) opened the connections for 10 seconds.

When the time delay of 10 seconds had elapsed, the SEL-351A (R1) transmitted a GOOSE signal to close the circuit breaker. The circuit breaker was closed, and an 8.456A fault current was simulated; the SEL-351A (R1) detected the fault and transmitted a GOOSE signal to open the circuit breaker. The circuit breaker was tripped, and the SEL-351A (R1) went through another open interval of 10 seconds. When the time delay of 10 seconds had lapsed, the SEL-351A (R1) transmitted a GOOSE signal to close the circuit breaker. The circuit breaker was closed, and an 8.456A fault current was simulated; the SEL-351A (R1) detected the fault current and

sent a GOOSE signal trip to open and lockout the circuit breaker. At this time, the relay transitions from the Cycle State (CY) to the Lockout State (LO).

Figures 6.15–6.18 illustrate the event files for the four shots that happened during the auto-reclose sequence. In each event, those Figures show the fault current waveforms, operational time, and triggered overcurrent elements.

When the first shot was occurred, the SEL-351A (R1) operated after 385 milliseconds, as illustrated in Figure 6.15. The elements that are triggered by the fault condition are also depicted in Figure 6.15. When the fault current is simulated, the pick-up "51P" asserts, and the trip element 51PT asserts to clear the fault, 79RS asserts when the circuit breaker closes for a defined reset time and de-asserted when the circuit breaker tripped open and reclose initiation is successful, 79CY asserts when reclose initiation is successful, Because there is no lockout condition, 79LO is not triggered, and 52A is asserted when the circuit breaker is closed and de-asserted when the circuit breaker is tripped and opened.

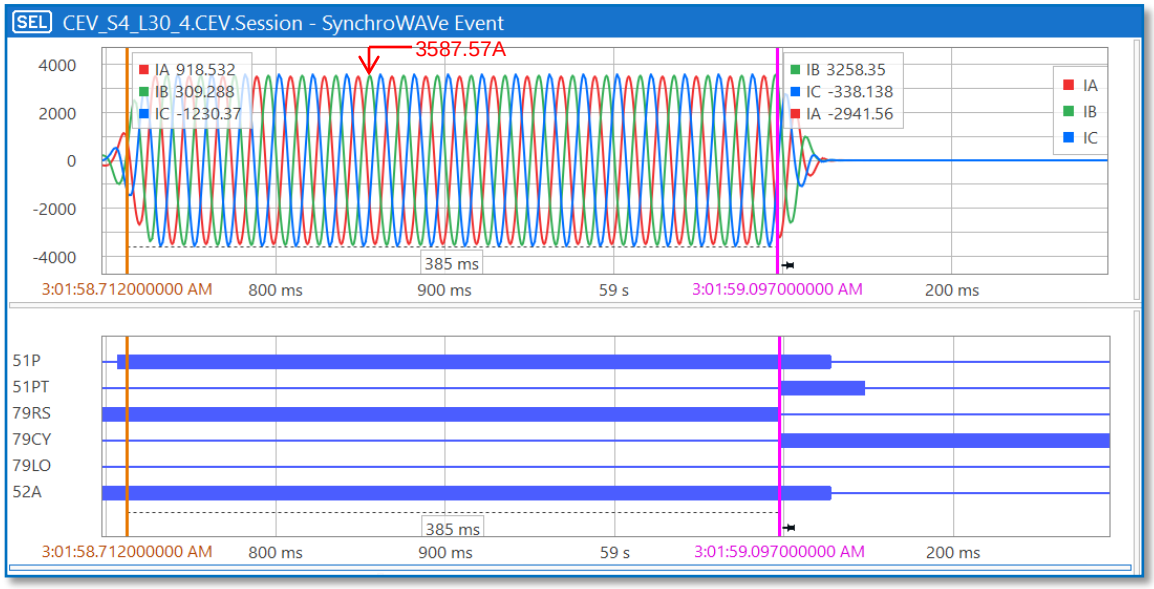

Figure 6.15: SEL-351A (R1) event report for the first shot

The SEL-351A (R1) results for the second shot event are shown in Figure 6.16 below. When the circuit breaker was reclosed, the SEL-351A (R1) started to operate after 385 ms. 51P asserted after closing to the fault, 51PT asserted to clear the fault, 79RS de-asserted because the SEL-351A (R1) is in Cycle State, 79CY asserted, 79LO de-asserted because the lockout condition has not yet been reached, and 52A asserted when the circuit breaker closed and de-asserted when the circuit breaker tripped and opened.

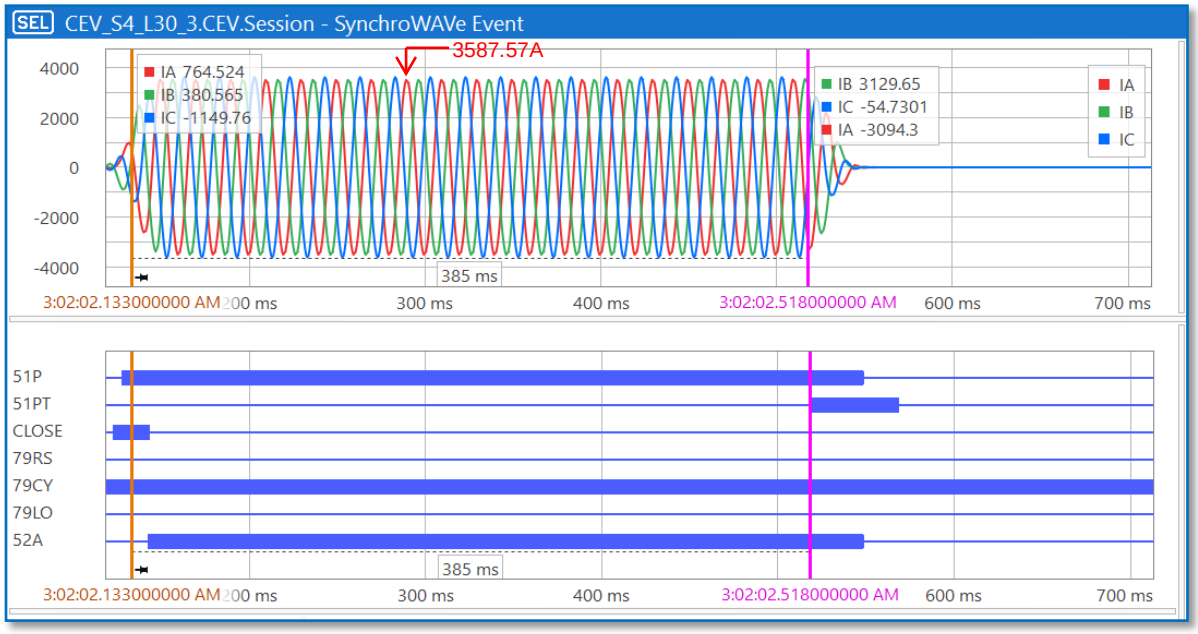

Figure 6.16: SEL-351A (R1) event report for the second shot

The SEL-351A (R1) results for the third shot event are shown in Figure 6.17 below. The operation for the second shot event is the same as for the third shot event.

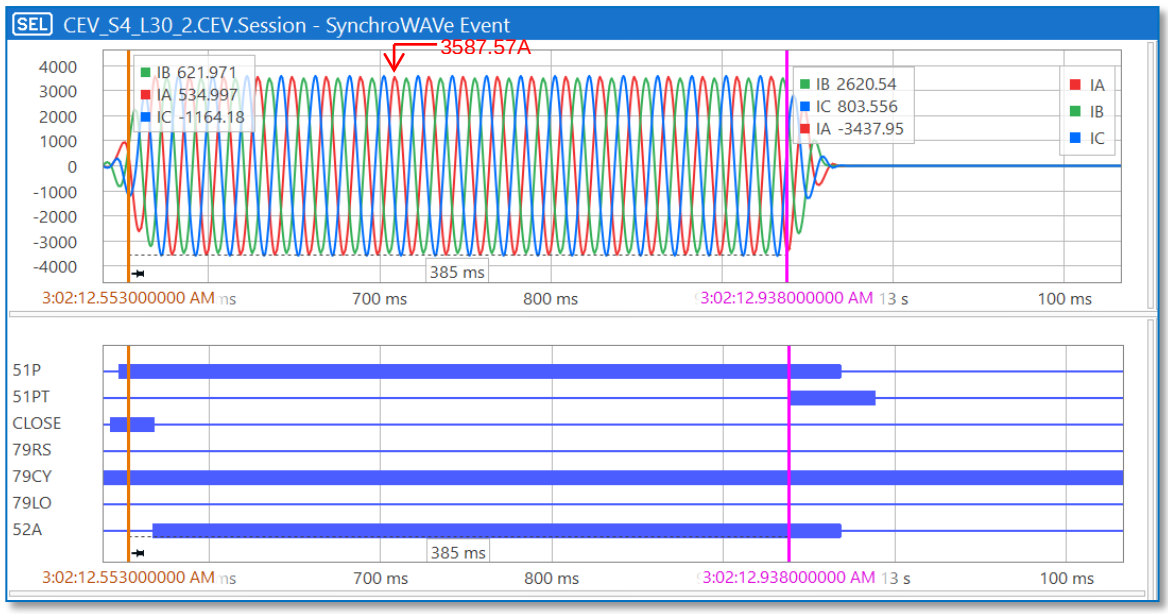

Figure 6.17: SEL-351A (R1) event report for the third shot

The SEL-351A (R1) event results for the fourth shot are shown in Figure 6.18 below. When the SEL-351A (R1) reclosed, 51P asserted due to the fault, 51PT asserted to clear the fault, 79CY asserted for the entire reclosing cycle and de-asserted when 51PT asserted, 79LO asserted to lockout the circuit because it is the last shot, Since

SEL-351A (R1) tripped and locked out, OUT103 and OUT104 asserted to deliver GOOSE message-based trip signals to SEL-351A (R2) and SEL-351A (NOP), respectively.

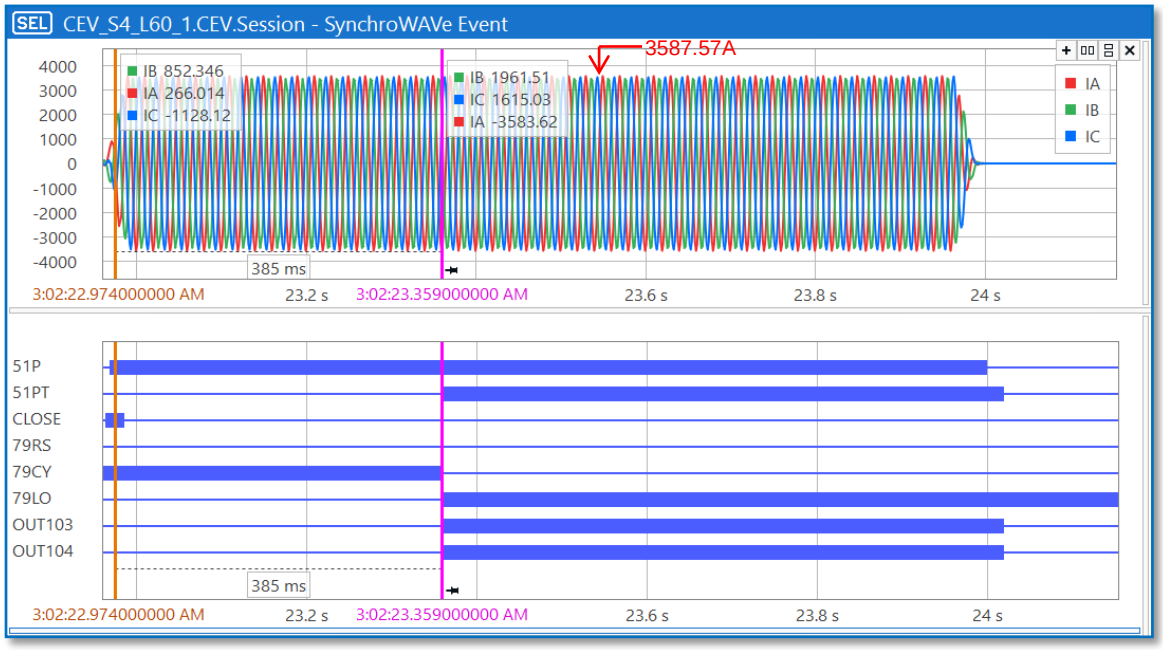

Figure 6.18: SEL-351A (R1) event report for the fourth shot

Figure 6.19 depicts SEL-351A (R2 response) to the trip GOOSE message sent by SEL-351A (R1) through OUT103. Because there is no current injection on SEL-351A, lockout element 79LO is asserted (R2). The GOOSE message sent by SEL-351A (R1) through OUT103 is mapped to SEL-351A's virtual bit "VB001" (R2). Based on the GOOSE message published by SEL-351A, VB001 declared that it will subscribe to the trip signal (R1). When 79LO and VB001 are both asserted, SEL-351A (R2) trips to isolate the part of the line between SEL-351A (R1) and SEL-351A (R2) (R2). OUT101 is asserted, and its trip elements are mapped to SEL-351A output 101. (R2). OUT103 was activated in order to transmit a GOOSE message to SEL-351 (NOP). The purpose of this GOOSE message is to close SEL-351 (NOP).

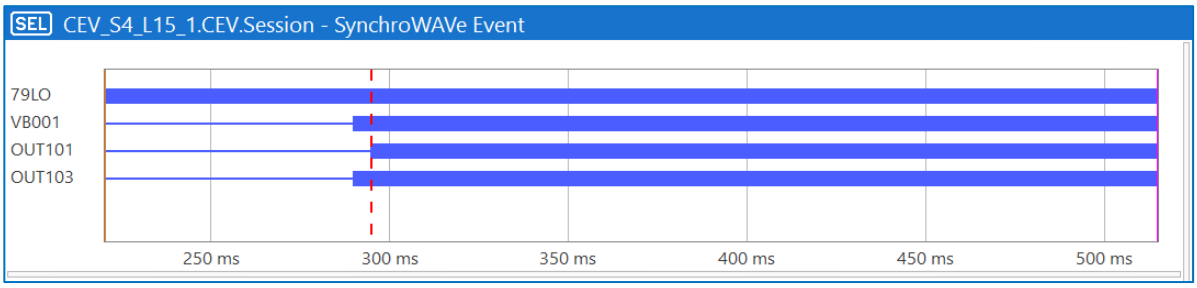

Figure 6.19: SEL-351A (R2) trip response

OUT104 (R1) and OUT103 (R2) of SEL-351A (R2) are mapped to VB001 and VB002 of SEL-351 (NOP), respectively. Figure 6.20 shows VB001 and VB002 as confirmations of receipt of the two GOOSE signals sent by SEL-351A (R1) and SEL-351A (R2) (R2). OUT102 is assigned to a close signal. When both VB001 and VB002 are asserted, the NOP is closed by asserting OUT102. When the NOP is closed, the line segment on Figure 6.1 between SEL-351A (R2) and the NOP is back-fed by feeder B. This prevents the supply on this line section from being cut off due to an upstream fault.

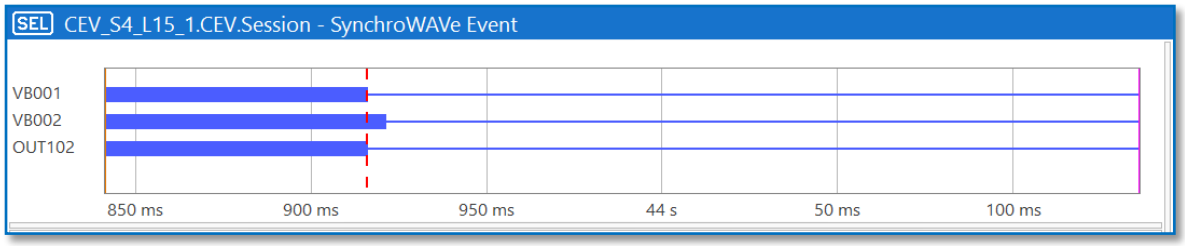

Figure 6.20: SEL-351 (NOP) relay close operational

6.5.1.2 Single-phase to ground fault on the relay SEL-351A (R1)

The omicron test universe overcurrent module was used to mimic a single-phase to ground fault condition by injecting 5.757A secondary current into SEL-351A (R1). The maximum current is 2442.49A (1727.1A × $\sqrt{2}$ = 2442.49A). The fault is simulated between the red phase and the ground. Figure 6.21 depicts the fault current waveform as well as the items that were triggered when the fault occurred. Due to this fault, the operational time of SEL-351A (R1) is 345ms.

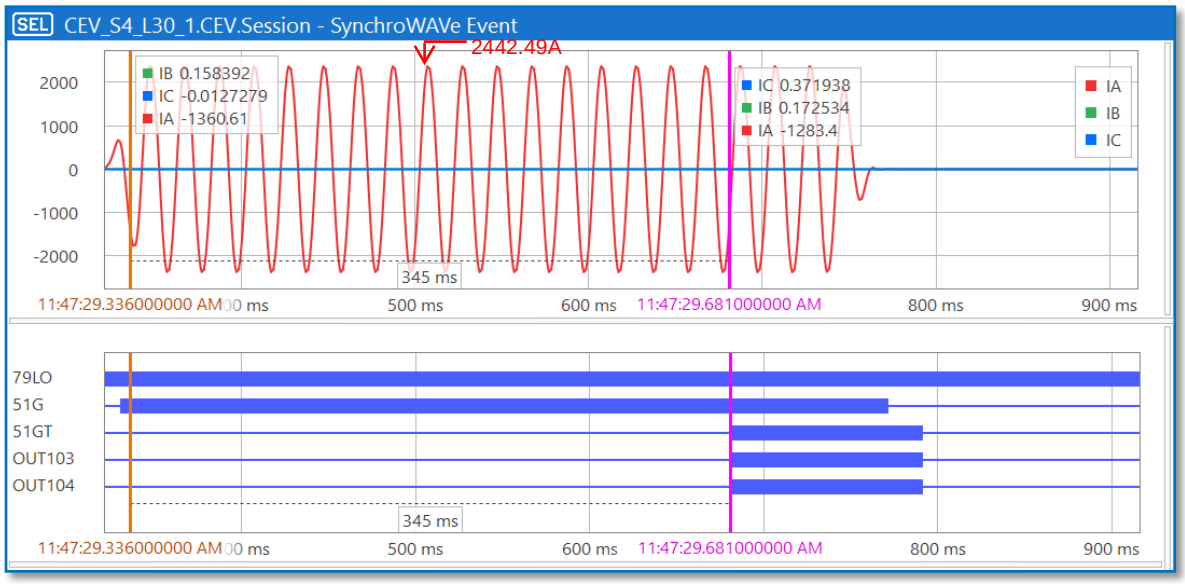

Figure 6.21: SEL-351A (R1) event report for single phase to ground fault

Since there was no injection to the SEL-351A (R1) device, the 79LO element was already asserted, 51G asserted to pick up the 5.757A fault current injected, 51GT asserted to clear the fault, and both OUT103 and OUT104 asserted to send the trip to open GOOSE signal to the SEL-351A (R2) and a close signal to SEL-351 (NOP) devices (NOP).

Figure 6.22 below shows the SEL-351A (R2) relay operational to the trip GOOSE signal published by the relay SEL-351A (R1).

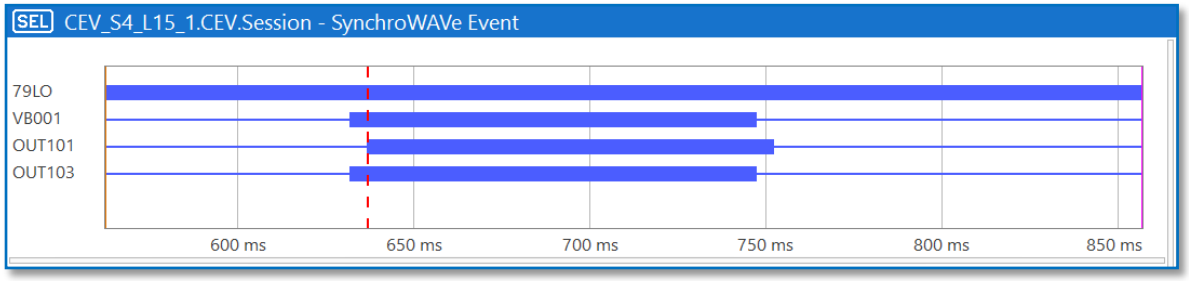

Figure 6.22: SEL-351A (R2) trip event report published by the relay SEL-351A (R1)

Because there was no injection to SEL-351A (R2) device, the 79LO element was already asserted, VB001 asserted to subscribe to the trip GOOSE message published by SEL-351A (R1), OUT101 asserted since the trip is mapped to OUT101, and OUT103 asserted to send a closeGOOSE signal to SEL-351 (NOP).

Figure 6.23 below show the SEL-351 (NOP) relay response to the trip GOOSE message published by SEL-351A (R1) and SEL-351A (R2)

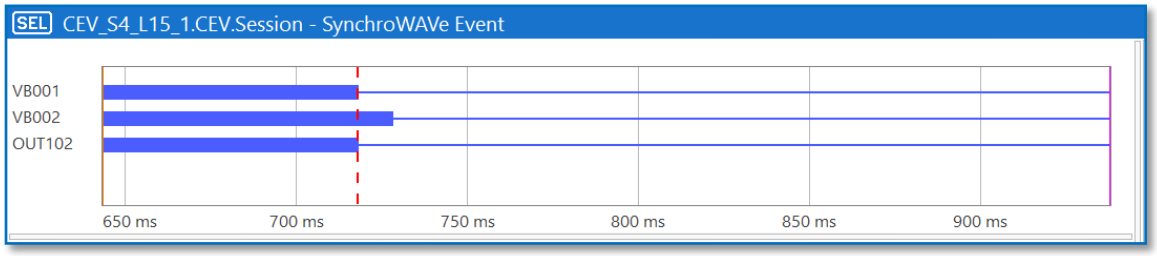

Figure 6.23: SEL-351 (NOP) relay close operational

VB001 and VB002 of SEL-351 (NOP) asserted to subscribe to the GOOSE message broadcast by SEL-351A (R1) and SEL-351 (R2). Because the close signal is mapped to output 102, OUT102 is asserted. When both VB001 and VB002 of SEL-351 (NOP) are asserted, it signifies that both SEL-351A (R1) and SEL-351 (R2) tripped to open and SEL-351 (NOP) can securely close NOP to the back-feed line section between the NOP and SEL-351A (R2) illustrated in Figure 6.1.

6.5.2 Case two: Three-phase fault and single-phase to ground fault on a SEL-351 (R2)

6.5.2.1 Three-phase fault on a SEL-351A (R2)

The omicron test universe state sequencer module is used to mimic a three-phase permanent fault condition by injecting 4.856A secondary current into SEL-351A (R2). A peak value of 2060.01A shown in Figure 5.64 by multiplying the rms value by square root two (1456.65A × $\sqrt{2}$ = 2060.01A). When the fault is simulated, the digital and analog chart sequence of events is shown in Figure 6.24. The circuit breaker for the SEL-351A (R2) is mapped to the CMC 356 device at binary output 1, which is designated as "Bin out 1." The GOOSE messages "Close" and "Trip" instruct the circuit breaker to close or trip.

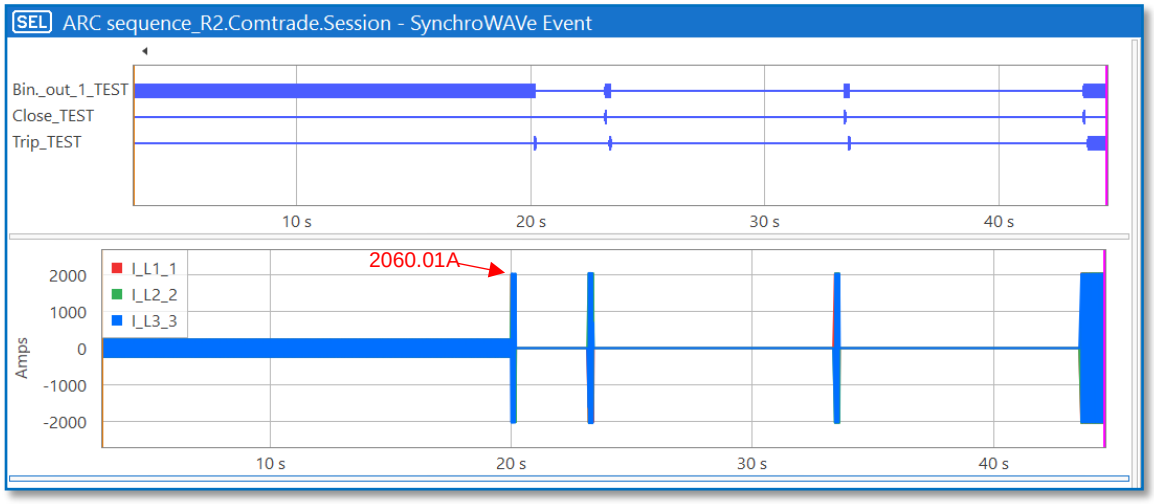

Figure 6.24: Auto-reclose cycle for the SEL-351A (R2) relay

The identical auto-reclose cycle as in Case Study 1 is simulated on SEL-351A (R2), where a three-phase permanent fault is simulated for SEL-351A. (R1). Figures 6.25 to 6.28 show the SEL-351A (R2) events during the four auto-reclose shots. The event display fault current waveforms, the operation time of the SEL-351A (R2), and the items that are triggered in each event.

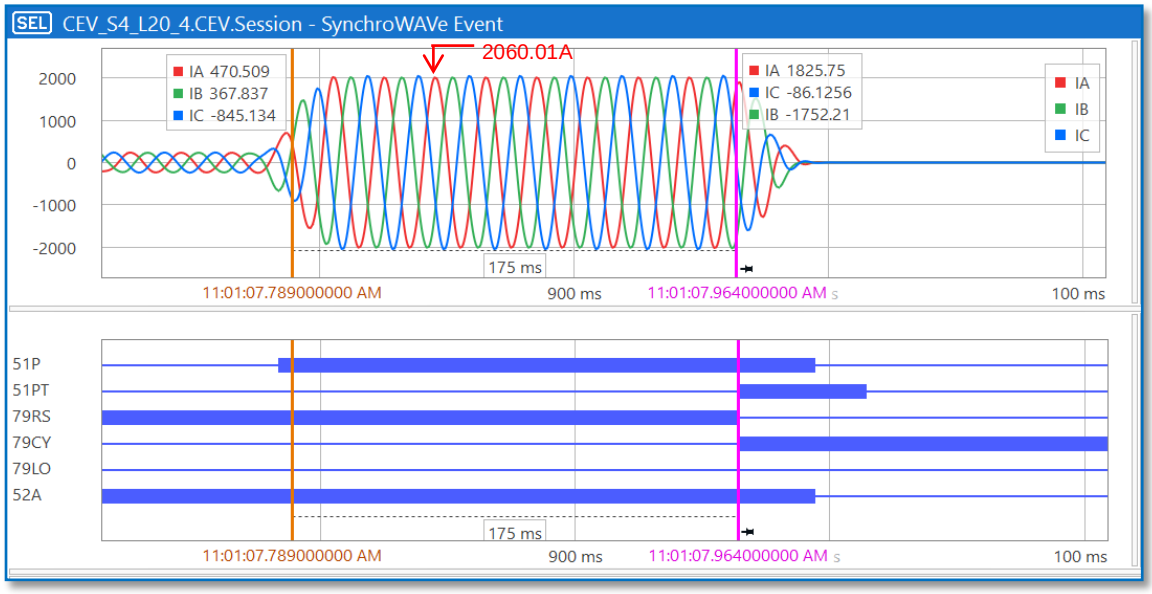

Figure 6.25: SEL-351A (R2) auto-reclose results for the first shot

Figure 6.25 shows how the first short SEL-351A (R2) operated in 175ms to clear the fault. 51P was asserted when the fault current was detected, 51PT was asserted to clear the fault, 79RS was asserted when the circuit breaker was closed for a qualifying reset time and de-asserted when the circuit breaker tripped to open and reclose initiation was successful, 79CY was asserted when reclose initiation was successful, 79LO was not asserted because there is no lockout condition, 52A is asserted when the circuit breaker.

The auto-reclose results for the second shot are shown in Figure 6.26 below. The SEL-351A (R2) took 175 ms to function, as seen in the Figure 6.25s. 51P was asserted to pick up the fault, 51PT was asserted to clear the fault, CLOSE was asserted to automatically reclose the circuit breaker, 79RS was de-asserted because the SEL-351A relay (R2) was in a cycle state, 79CY was asserted because the SEL-351A (R2) was undergoing auto-reclose cycle, 79LO is de-asserted because there is no lockout condition yet.

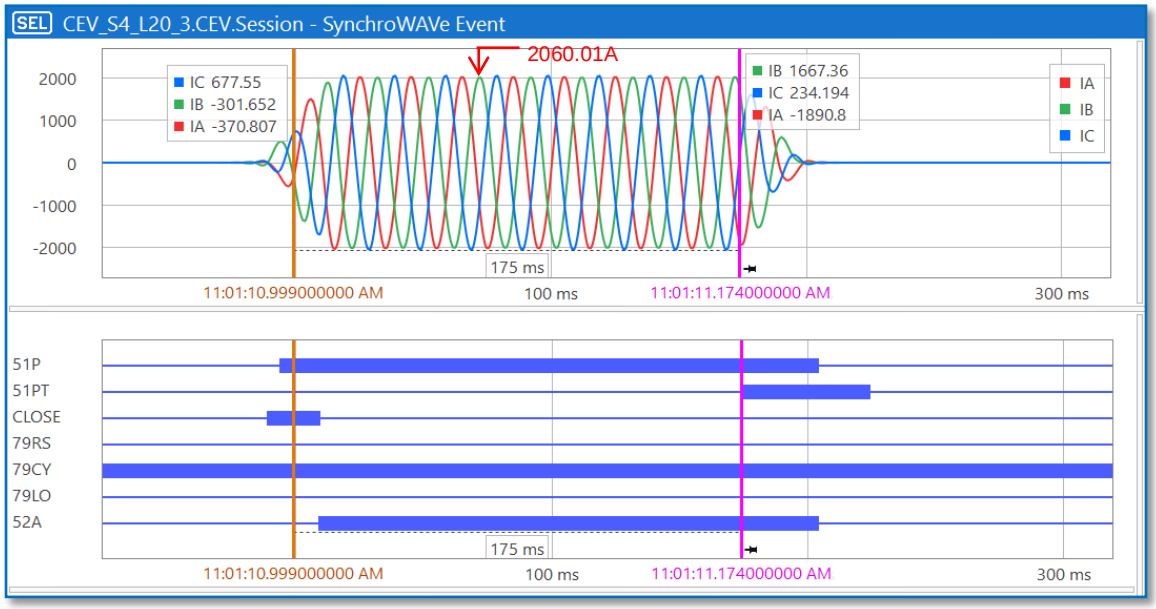

Figure 6.26: SEL-351A (R2) auto-reclose results for the second shot

The auto-reclose results for the third shot are shown in Figure 6.27 below. The third shot yields the same outcomes as the second shot.

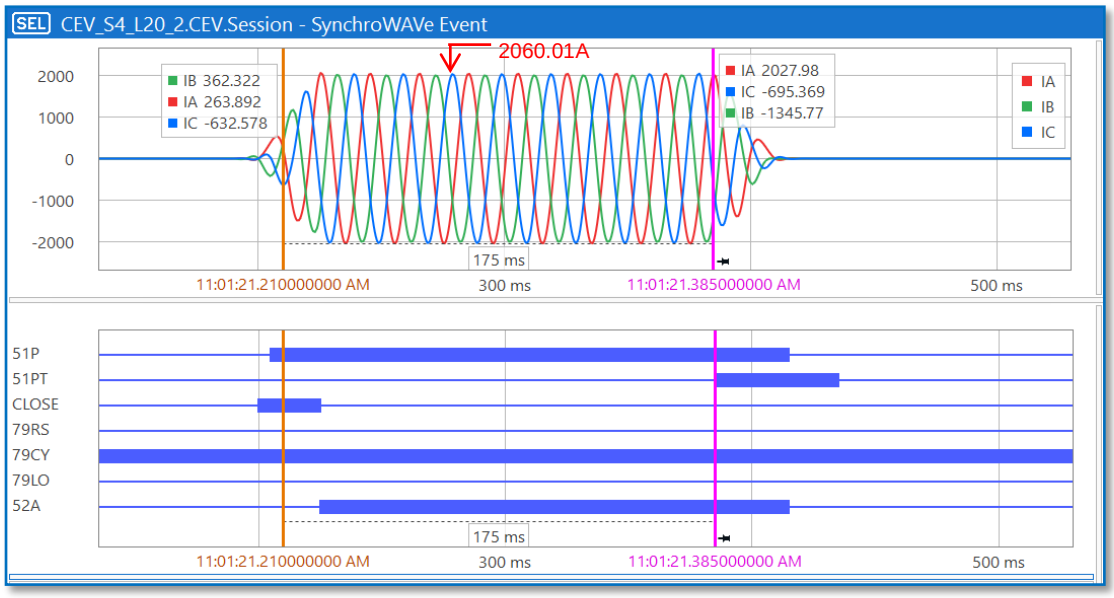

Figure 6.27: SEL-351A (R2) auto-reclose results for the third shot

The SEL-351A (R2) auto-reclose results for the fourth short are shown in Figure 6.28 below. CLOSE asserted to automatically reclose the circuit breaker when the last shot occurred, 51P picked up the fault and asserted, 51PT asserted to clear the fault, 79CY was asserted when the SEL-351A was in recycle state and de-asserted when 51PT tripped to lockout, and 79LO asserted to prevent the circuit breaker from

closing. When the circuit breaker is closed, 52A is asserted; when the circuit breaker is open, 52A is de-asserted.

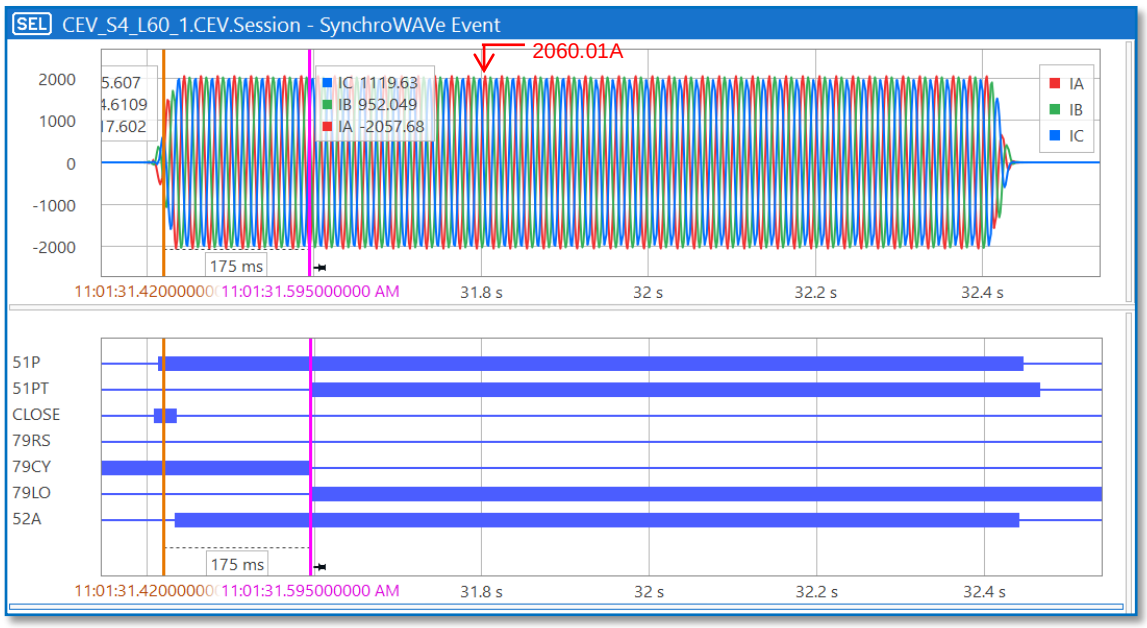

Figure 6.28: SEL-351A (R2) auto-reclose results for a fourth shot

Figure 6.29 depicts three-phase fault results for SEL-351A (R1) in the event that SEL-351A (R2) fails to trip. After allowing SEL-351A (R2) time to clear the fault, SEL-351A (R1) would operate 505 ms later. The SEL-351A (R1) 51P is also picked up in the figure as a result of the 4.856A secondary fault current injected. 51PT asserted that the fault had been cleared.

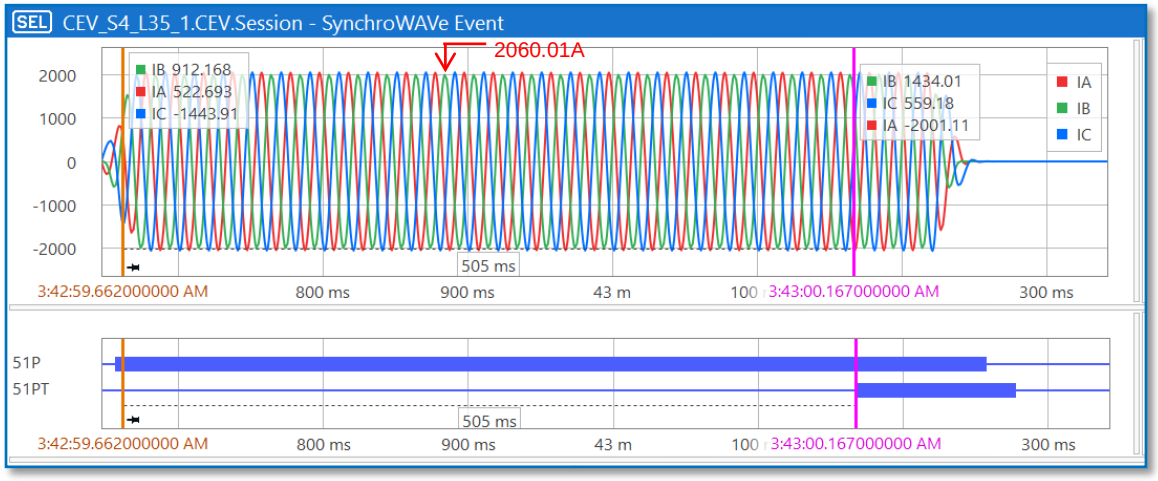

Figure 6.29: SEL-351A (R1) simulation results for three-phase fault between the SEL-351A (R2) and NOP devices.

The obtained grading margin will be the difference in the operating times due to the three-phase fault. The grading margin in this situation is 505 ms – 175 ms = 0.33 seconds.

6.5.2.2 Single-phase to ground fault on relay SEL-351A (R2)

A secondary fault current of 2.81A is simulated between the red phase and ground on SEL-351A (R2). Figure 6.30 depict a peak value of (842.88A × $\sqrt{2}$ = 1192.01A). In Figure 6.1, the simulation is conducted to identify the SEL-351A (R2) response for single-phase to ground faults that occur between SEL-351A (2) and NOP. Figure 6.30 depicts the fault current waveform, SEL-351A (R2) operational time, and triggered ground elements. The SEL-351A (R2) has an operating time of 115ms. The 2.81A fault current was detected by 51G, and 51GT asserted to clear the fault.

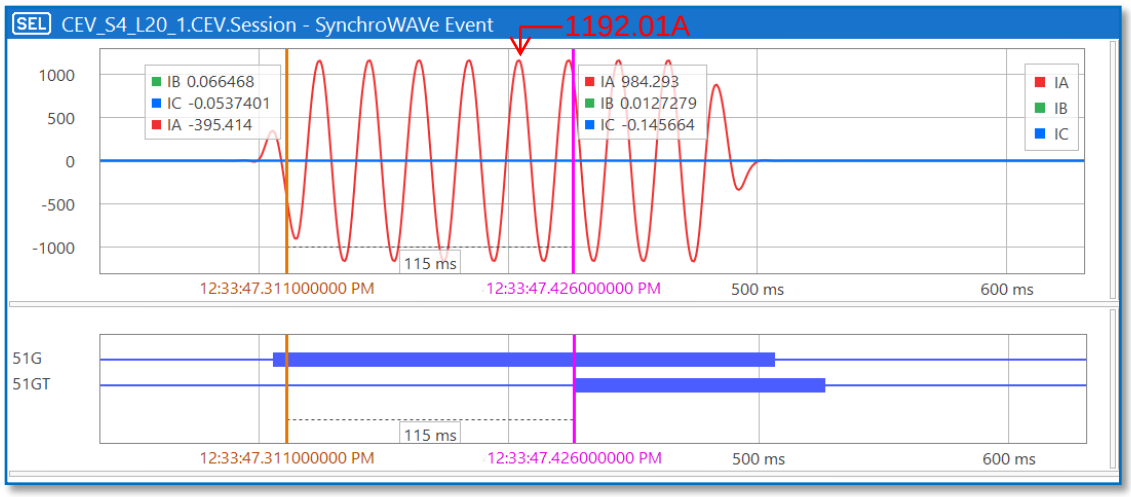

Figure 6.30: SEL-351A (R2) simulation results for a single-phase to ground fault between SEL-351A (R2) and NOP

In the event that SEL-351A (R2) fails to operate, Figure 6.31 depicts the single-phase to ground fault consequences for SEL-351A (R1). The SEL-351A (R1) would operate in 445 ms. The image also shows the SEL-351A (R1) 51G picking up due to the injected 2.81A secondary fault current. 51GT asserted that the fault had been cleared.

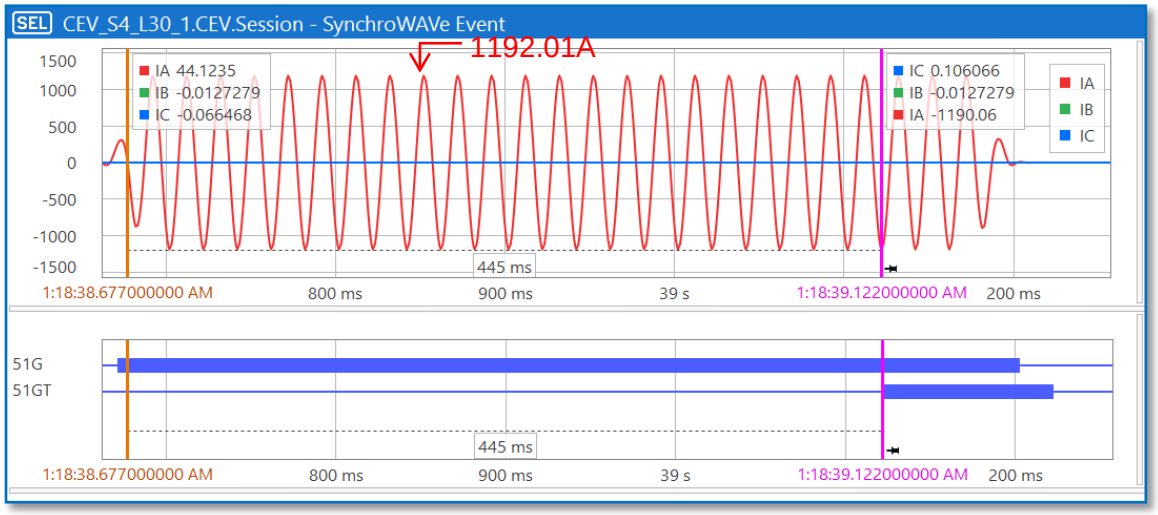

Figure 6.31: SEL-351A (R1) results for single-phase to ground fault between SEL-351A (R2) and NOP

The difference in operation times between the two IEDs SEL-351A (R2) and SEL-351A (R1) will be graded as 445ms -115ms = 0.33 seconds.

6.6 Conclusion

The IEC 61850 GOOSE-based auto-reclose scheme simulation test was carried out at DEECE CPUT's CSAEMS lab. Using the omicron test injection device CMC 356, different fault circumstances for different fault locations are simulated, and relay operating parameters are monitored. The simulation results are analyzed using the two case studies under consideration.

The practical implementation of the IEC 61850 GOOSE-based auto-reclose scheme was shown in this chapter. Simulations on case studies demonstrated that the designed IEC 61850 auto-reclose technique may reconfigure the distribution system in the event of a fault. This technique enhances the distribution system's reliability. The practical information gained in this chapter will instruct protection engineers on how to configure and deploy the recloser control scheme for any industrial distribution network in order to increase network protection performance through automatic reconfiguration under fault conditions.

The next chapter discusses the thesis deliverables, the complete scope of the developed method, future work, and publications related to this Thesis.

CHAPTER SEVEN

CONCLUSION

7.1 Introduction

This research work aimed to develop and implement a feasible and reliable IEC 61850 standard-based recloser control scheme for automatic reconfiguration of the distribution system. A 22kV distribution network is used to investigate the overcurrent, automatic reclosing, and automatic reconfiguration schemes. The test results are studied and analyzed.

Simulations of fault current conditions were conducted at different sections (upstream and downstream) of the distribution network using a DIgSILENT environment. DIgSILENT simulation results were used to determine to pick up settings of the relays, and the settings were used for both DIgSILENT software relays and lab-scale recloser control scheme relays.

The implementation and testing of the lab-scale recloser control scheme were performed. The development and implementation of the reliable recloser control scheme based on IEC 61850 standard GOOSE messages for automatic reclosing and network reconfiguration under fault conditions were done. The recloser control scheme was achieved using three relays (SEL-351A (R1), SEL-351A (R2), and SEL-351 (NOP)). The auto-reclose and overcurrent configuration settings of the relays are configured using AcSELerator Quickset software. The Omicron CMC 356 injection device is used to inject currents and voltages to test the auto-reclose and overcurrent protection functions. The omicron CMC 356 configuration settings are configured using omicron test universe software. The engineering configuration of both AcSELerator Quickset and test universe software are performed using a personal computer. The configuration of the IEC 61850 GOOSE communication between relays was achieved using AcSELerator Architect software tool.

7.2 Deliverables

When a permanent fault condition occurs at the outgoing of a radial distribution feeder, the relay recloses three times and lockout. The whole feeder will be out of supply up until the field engineers are dispatched to the site to open the downstream recloser and close the normally open point (NOP) (manually reconfigure the distribution network) to supply customers beyond a faulted section with an alternative

healthy feeder. After the upstream recloser has been locked out due to a permanent fault, this research work sends IEC 61850 GOOSE signal to the downstream recloser to open and the NOP to close, after the downstream recloser has opened, it also sends a close signal to the NOP. When the NOP receive both close signals from both upstream and downstream relays, it closes to supply customer between downstream and relay and NOP.

7.2.1 Literature review

The literature study offered in Chapter 2 outlined various methods for feeder automation in distribution networks. A survey of several types of distribution networks was conducted (radial, ring, and mesh). The literature review examined the coordination of the recloser with other protective devices, a review of relevant studies on reliability indices, and a comparison of different methods used on feeder automation, including techniques with and without the IEC 61850 standard.

7.2.2 Theory on overcurrent and recloser protection

This research work provided a theory on distribution system faults. It discussed different types of faults and how they are calculated. The application of reclosers in a distribution system, recloser grading and coordination, distribution reliability measures, and distribution automation were covered.

7.2.3 DIgSILENT implementation of overcurrent and recloser protection scheme

A 22kV distribution network was considered as a case study. This distribution network was modeled and simulated on the DIgSILENT software tool. The DIgSILENT simulations were focused on studying the performance of the overcurrent relaying system through the simulation of fault conditions in different sections of the distribution network. The auto-reclose function is studied and analyzed. The load flow and fault studies were used to determine the relay settings. The simulation results presented a need for auto reclosers to restore power downstream of the distribution lines due to faults upstream of the network.

7.2.4 Implementation of the recloser control scheme using feeder protection using numerical relays

The lab-scale recloser control scheme test bench setup was implemented and tested at the CSAEMS lab at CPUT. The recloser control scheme used (SEL-351A (R1),

SEL-351A (R2), and SEL-351 (NOP), These relays are positioned at the outgoing feeder, downstream and at the NOP respectively. Two sets of tests were studied and analyzed. The first set was tested using hardwired communication, the second set used GOOSE signal communication and both results were compared. To inject fault currents for upstream and downstream relays, an Omicron CMC 356 device was used. The overcurrent and reclosing engineering configuration of the relays was done using both AcSELerator Quickset and test universe software. GOOSE configuration was done using the AcSELerator Architect software tool.

7.3 Project application in academia, research and industry

The developed DIgSILENT simulation model results for the distribution system can equally benefit undergraduate and post-graduate students to understand the behavior of a distribution system feeder operation, under normal and fault conditions.

This research work offers a standard benchmark for academic and industrial applications through the implementation of the distribution system recloser control scheme. Implementation of a lab-scale test bench setup for overcurrent protection, automatic reclosing and network reconfiguration using numerical relays is provided and test results are studied and analyzed.

The practical knowledge studied in this research will guide the protection engineers on how to configure and apply the recloser control scheme for any industrial distribution network to improve the network protection performance through automatic reconfiguration under fault conditions.

7.4 Future work

The overcurrent, automatic reclosing and network reconfiguration was tested in a lab-scale environment. For future research, it will be interesting to see these functions tested in a real-time system. This would demonstrate that when a normal open closes during network reconfiguration, customers on the interrupted feeder would be reconnected by the alternative healthy feeder. This thesis used only SEL relays. It will be interesting to see the network reconfiguration using different vendors. This would benefit researchers and protection engineers to demonstrate interoperability. The research work was only focused at automatic reclosing at distribution system level, and it would be interesting to apply the auto-reclose function at transmission system level. In this research work there are no distributed generators, it will be

interesting to study the performance of the network with multiple sources of supply, as this will have an influence on protection and monitoring functions.

The future work also proposes to investigate distributed load modeling and reliability indices study.

7.5 Publications and project demostration

1. S.Ntshiba and S. Krishnamurthy. April 2021. A distribution system's auto-recloser control method. The idea was showcased during the research festival at Cape Peninsula University of Technology (CPUT).
2. S.Ntshiba and S. Krishnamurthy. October 2021. Control strategy for automatic reclosers in a distribution system. This paper was presented at the CPUT Centre for Postgraduate Studies (CPGS) conference.
3. S.Ntshiba and S. Krishnamurthy, 2021. Digital implementation of an auto-reclose protection scheme for a distribution system. Submitted to Southern Africa University Power Engineering Conference (SAUPEC), 1-8.
4. S.Ntshiba and S. Krishnamurthy, “Implementation, simulation, and validation of the IEC61850 GOOSE recloser control scheme application on a 22kV distribution system” submitted to International Journal of Electrical Power & Energy Systems, Science Direct , Elsevier, ISSN 0142-0615.

BIBLIOGRAPHY

ABB (2011) *Distribution Automation Handbook*. Finland.

Abidi, S. and Yokoyama, A. (2005) 'An Appropriate Distributed Generation Sizing Considering Recloser-Fuse Coordination', *IEEE/PES Transmission and Distribution Conference & Exhibition*, pp. 1–6.

Adamiak, M., Baigent, D. and Mackiewicz, R. (2009) 'IEC 61850 Communication Networks and Systems In Substations: An Overview for Users', *Protection & Control Journal*, pp. 61–68. doi: 10.1.1.698.1497.

Aguero, J. R. (2012) 'Applying self-healing schemes to modern power distribution systems', *IEEE Power and Energy Society General Meeting*, pp. 1–4.

Allan, R. R. and Silva, M. G. (1995) 'EVALUATION OF RELIABILITY INDICES AND OUTAGE COSTS IN DISTRIBUTION SYSTEMS', 10(1), pp. 413–419.

Alstom Grid (2011) *Network protection and automation guide*. Third edit. Stafford: GEC Measurements.

Altuve, H. J., Zimmerman, K. and Tziouvaras, D. (2015) 'Maximizing Line Protection Reliability, Speed, and Security', *42nd Annual Western Protective Relay Conference*.

Arthi, S. R. V. and Vittal, K. P. (2013) 'Modeling of recloser and sectionalizer and their coordination using PSCAD', *Proceedings of IEEE International Conference on Circuit, Power and Computing Technologies (ICCPCT)*, pp. 679–684.

Bakhtiari, N. S. and Frarahani, N. K. (2012) 'Improvement of distribution automation by implementing MasterRTU', *IEEE Conference on Industrial Electronics and Applications (ICIEA)*, pp. 834–837.

Baningobera, B. E. (2018) 'the Iec61850 Standard-Based Protection Scheme for Power Transformers', (November).

Bentarzi, H., Chafai, M., *et al.* (2012) 'A new computer based auto-recloser framework', *24th Proceedings of the International Conference on Microelectronics (ICM)*.

Bentarzi, H., Chafi, M., *et al.* (2012) 'A new computer based auto-recloser framework', *Proceedings of the International Conference on Microelectronics, ICM*, (Icm), pp. 3–6.

Billinton, R. and Wang, P. (1999) 'Teaching distribution system reliability evaluation using Monte Carlo simulation', *IEEE Transactions on Power Systems*, 14(2), pp. 397–403.

Bosisio, A. *et al.* (2019) 'IEC 61850-based smart automation system logic to improve reliability indices in distribution networks', *APAP 8th IEEE International Conference on Advanced Power System Automation and Protection*, pp. 1–5.

Brahma, S. M. and Girgis, A. A. (2002) 'Microprocessor-based reclosing to coordinate fuse and recloser in a system with high penetration of distributed generation', *Proceedings of the IEEE Power Engineering Society Transmission and Distribution Conference*, pp. 453–458.

Chaitusaney, S. and Yokoyama, A. (2008) 'Prevention of Reliability Degradation from', *IEEE TRANSACTIONS ON POWER DELIVERY*, 23(4), pp. 2545–2554.

Chan, F. C. (2009) 'Electric Power Distribution Systems', *Encyclopedia of Life*

Support (EOLSS), 3(1).

Chen, C. R., Lee, C. H. and Chang, C. J. (2012) 'Optimal overcurrent relay coordination in power distribution system using a new approach', *International Journal of Electrical Power and Energy Systems*, 45(1), pp. 217–222.

Chow, M., Taylor, L. S. and Chow, M.-S. (1996) 'Time of Outage Restoration Analysis in Distribution Systems', 11(3), pp. 1652–1658.

Cutler-Hammer (1999) *Fundamentals of Electrical Distribution*, *101 Basics Series*. Milwaukee: Cutler-Hammer and Eaton Corp.

DIgSILENT (2020) 'PowerFactory 2020'. Germany.

Fahmi, D. et al. (2014) 'Evaluation of distribution network reliability index using Loop Restoration Scheme', 1st International Conference on Information Technology, Computer, and Electrical Engineering: Green Technology and Its Applications for a Better Future, ICITACEE - Proceedings, pp. 239–244.

Fardo, S. W. (2009) *Electrical power systems technology*. 3rd ed. Edited by D. R. Patrick. Lilburn, Georgia: Fairmont Press.

Fazanehrafat, A. *et al.* (2008) 'Maintaining the recloser-fuse coordination in distribution systems in presence of DG by determining DG's size'.

Gers, J. M. (2004) *Protection of electricity distribution networks*. 2nd. ed. Edited by E. J. Holmes. London: Institution of Electrical Engineers (IEE power and energy series ; 47).

Gilligan, S. R. (1992) 'A METHOD FOR ESTIMATING THE RELIABILITY OF DISTRIBUTION CIRCUITS', *IEEE Transactions on Power Delivery*, 7(2), pp. 694–698.

Glover, J. D., Sarma, M. S. and Overbye, T. (2012) *Power system analysis & design, SI version*. Cengage Learning.

Goodin, R. E., Fahey, T. S. and Hanson, A. (1999) 'Distribution reliability using reclosers and sectionalisers', (13).

Goryunov, V. N., Osipov, D. S. and Dolgikh, N. N. (2016) 'The application of wavelet transform for identification of single phase to earth fault in power system', *2nd International Conference on Industrial Engineering, Applications and Manufacturing (ICIEAM)*, pp. 1–6.

Gruenemeyer, D. (1991) 'Distribution automation: How should it be evaaluated?', pp. 1–10.

Guner, S. and Ozdemir, A. (2020) 'Reliability improvement of distribution system considering EV parking lots', *Electric Power Systems Research*, 185, pp. 1–8.

Habib, H., Fawzy, N. and Brahma, S. (2020) 'Hardware in the Loop Testing of a Protection Scheme for Microgrid using RTDS with IEC 61850 Protocol', *IEEE Industry Applications Society Annual Meeting*, 2020, pp. 1–8.

Hao, K. and Keckalo, D. (2021) 'Adaptive Coordination Schemes to Reduce Fault Energy in Distribution Feeders Using Wireless Protection Sensors Adaptive Coordination Schemes to Reduce Fault Energy in Distribution Feeders Using Wireless Protection Sensors', *74th Annual Conference for Protective Relay Engineers*.

Heidari, S., Fotuhi-firuzabad, M. and Kazemi, S. (2015) 'Power Distribution Network

Expansion Planning Considering Distribution Automation', 30(3), pp. 1261–1269.

Hoang, T. T., Tuan, T. Q. and Besanger, Y. (2019) 'A Multiagent and IEC 61850-Based Fault Location and Isolation System for Distribution Network with High PV Integration - A CHIL Implementation', *IEEE International Conference on Environment and Electrical Engineering and IEEE Industrial and Commercial Power Systems Europe, (EEEIC/I&CPSEurope)*, pp. 1–6.

Hong, J., Ishchenko, D. and Kondabathini, A. (2021) 'Implementation of resilient self-healing microgrids with iec 61850-based communications', *Energies*, 14(3).

Hosseinzadeh, H. (2008) 'Distribution System Protection', pp. 2–16.

Hou, D. and Dolezilek, D. (2010) 'IEC 61850 – What It Can and Cannot Offer to Traditional Protection Schemes', *SEL Journal of Reliable Power*, 1(2), pp. 1–12.

Huda, A. S. . and Rastko, Z. (2016) 'Distribution System Reliability Assessment Using Sequential Monte Carlo Method', *IEEE Innovative Smart Grid Technologies (ISGT)*, pp. 867–872.

Hussain, A., Choi, M. S. and Lee, S. J. (2014) 'A novel algorithm for reducing restoration time in smart distribution systems utilizing reclosing dead time', *Journal of Electrical Engineering and Technology*, 9(6), pp. 1805–1811.

Hussain, M. H., Rahim, S. R. A. and Musirin, I. (2013) 'Optimal overcurrent relay coordination: A review', *Procedia Engineering*, 53, pp. 332–336.

IEC 60255 (2009) 'International Standard'.

IEC 62271-111 (2012) 'High-voltage switchgear and controlgear – Part 111: Automatic circuit reclosers and fault interrupters for alternating current systems up to 38 kV'.

IEC standard 60909 (2001) 'International Standard Short-circuit currents in three-phase a.c. systems'.

IEEE C37.112 (2018) 'IEEE Std C37.112. Standard for Inverse- Time Characteristics Equations for Overcurrent Relays'.

IEEE Std 1366 (2012) 'IEEE Guide for Electric Power Distribution Reliability Indices'.

IEEE Std 141 (1993) 'IEEE Recommended Practice for Electric Power Distribution for Industrial Plants'.

IEEE Std C37.104-2012 (2012) 'IEEE Guide for Automatic Reclosing of Circuit Breakers for AC Distribution and Transmission Lines'.

IEEE Std C37.110 (1996) 'IEEE Guide for application of current transformers used for protection relaying purposes'.

IEEE Std C37.230 (2007) 'IEEE Guide for Protective Relay Applications to Distribution Lines'.

Islam, F. R. *et al.* (2017) 'Aromatic network: A novel structure for power distribution system', *IEEE Access*, 5, pp. 25236–25257.

Jamborsalamati, P. *et al.* (2015) 'Implementation of an agent based distributed FLISR algorithm using IEC 61850 in active distribution grids', *4th International Conference on Renewable Energy Research and Applications (ICRERA)*, pp. 606–611.

Janaka, E. *et al.* (2012) *Smart Grid:Technology and applications*. Chichester: John Wisley and tdson L. Available at: http://www.renewables-made-in-germany.com.

Konarski, M. and Wegierek, P. (2018) ‘The use of power restoration systems for automation of medium voltage distribution grid’, *Przeglad Elektrotechniczny*, 94(7), pp. 167–172.

Koozehkanani, S., Salemi, S. and Sadr, S. (2015) ‘Optimal implementation of feeder automation in medium voltage distribution networks’, *20th Electrical Power Distribution Conference, EPDC 2015*, (April), pp. 16–21.

Kumar, T. B., Sekhar, O. C. and Ramamoorty, M. (2017) ‘Composite power system reliability evaluation using modified minimal cut set approach’, *Alexandria Engineering Journal*, pp. 4–11.

Le, D. P. *et al.* (2018) ‘FLISR approach for smart distribution networks using e-terra software—a case study’, *Energies*, 11(12), pp. 1–33.

Lei, H., Singh, C. and Sprintson, A. (2014) ‘Reliability modeling and analysis of IEC 61850 based substation protection systems’, *IEEE Transactions on Smart Grid*, 5(5), pp. 2194–2202.

Li, W. (2014) Risk assessment of power systems: models, methods, and applications. John Wiley & Sons.

Lin, C. H. *et al.* (2009) ‘Fault detection, isolation and restoration using a multiagent-based distribution automation system’, *4th IEEE Conference on Industrial Electronics and Applications, ICIEA*, pp. 2528–2533.

Mackiewicz, R. (2006) ‘Technical Overview and Benefits of the IEC 61850 Standard for Substation Automation’, pp. 1–8.

Makarov, Y. V. and Moharari, N. S. (1999) ‘A generalized power system reliability and security index’, *International Conference on Electric Power Engineering, PowerTech Budapest*, pp. 1–6.

Markushevich, N. S., Herejk, I. C. and Nielsen, R. E. (1994) ‘Functional requirements and cost-benefit study for distribution automation at B.C.hydro’, *IEEE Transactions on Power Systems*, 9(2), pp. 772–781.

Mo-yuen, C., Taylor, L. S. and Mo-Suk, C. (1996) ‘Time of Outage Restoration Analysis in Distribution Systems’, 11(3), pp. 1652–1658.

Mohagheghi, S. (2010) ‘A fuzzy cognitive map for data integrity assessment in a IEC 61850 based substation’, *IEEE PES General Meeting, PES 2010*, pp. 1–7. doi: 10.1109/PES.2010.5588058.

Mohagheghi, S., Stoupis, J. and Wang, Z. (2009) ‘Communication protocols and networks for power systems - Current status and future trends’, *2009 IEEE/PES Power Systems Conference and Exposition, PSCE 2009*, pp. 1–9.

Momoh, J. A., Dias, L. G. and Laird, D. N. (1997) ‘An implementation of a hybrid intelligent tool for distribution system fault diagnosis’, *IEEE transactions on power delivery*, 12(2), pp. 1035–1040.

Mostafa, M., Elshahed, M. and Elsobki, M. S. (2018) ‘The impact of distributed energy resources on the reliability of smart distribution system’, *Majlesi Journal of Electrical Engineering*, 12(4), pp. 1–4.

Motoki, É. M. *et al.* (2015) ‘Use of computational system for analysis of power quality in smart grid’, *IEEE PES Innovative Smart Grid Technologies Latin America, ISGT LATAM*, pp. 423–428.

Nagaraj, B., Subramanyam, S. V. and Richard, D. C. (2014) ‘Modeling and Analysis

of Distribution Reliability Indices Nagaraj', *IEEE TRANSACTIONS ON POWER DELIVERY*, 19(4), pp. 1950–1955.

Nagata, T. *et al.* (2005) 'A multiagent approach to distribution system restoration', *4th IEEE International Midwest Symposium on circuits and Systems*, 152(3), pp. 333–336.

Paci, A., Bualoti, R. and Celo, M. (2021) 'Evaluation of Distribution System Reliability Indices Using Fuzzy Reasoning Approach', *European Journal of Electrical Engineering and Computer Science (EJECE)*, 5(3), pp. 1–8.

Paci, A., Celo, M. and Bualoti, R. (2018) 'Distribution System Reliability Indices. Case Study Albanian Distribution System', *Journal of Multidisciplinary Engineering Science and Technology (JMEST) ISSN*, 5(12), pp. 9137–9143.

Pahwa, A. (2005) 'Planning and analysis tools to evaluate distribution automation implementation and benefits', *IEEE Power Engineering Society General Meeting*, pp. 1–2.

Parikh, P., Voloh, I. and Mahony, M. (2013) 'Distributed fault detection, isolation, and restoration (FDIR) technique for smart distribution system', *66th Annual Conference for Protective Relay Engineers, CPRE*, pp. 172–176.

Prakash, K. et al. (2016) 'Review of Power System Distribution Network Architecture', Proceedings - Asia-Pacific World Congress on Computer Science and Engineering and Asia-Pacific World Congress on Engineering , APWC on CSE/APWCE, pp. 124–130.

Qin, Q. and Wu, N. E. (2014) 'Recloser and sectionalizer placement for reliability improvement using discrete event simulation', *IEEE Power and Energy Society General Meeting*, pp. 1–5.

Razavi, F. *et al.* (2008) 'A new comprehensive genetic algorithm method for optimal overcurrent relays coordination', *Electric Power Systems Research*, 78, pp. 713–720.

Rones, V. A. . and Vittal, K. P. (2013) 'Modeling of recloser and sectionalizer and their coordination using PSCAD', *Proceedings of IEEE International Conference on Circuit, Power and Computing Technologies, ICCPCT*, pp. 679–684.

Roos, F. (2005) Electricity Supply Reliability: Evaluation of Improvement Solutions for Existing Electricity Networks.

Ruihua, R. *et al.* (2008) 'The realization of the feeder automation function in distribution automation systems', *China International Conference on Electricity Distribution, CICED*, pp. 1–4.

Ruschel, W. J. and Ashley, W. A. (1989) 'Coordination of Relays, Reclosers, and Sectionalizing Fuses for Overhead Lines in the Oil Patch', *IEEE Transactions on Industry Applications*, 25(6), pp. 1041–1048.

Saadat, H. (1999) *Power system analysis*. McGraw-hill.

Sadhu, P. K. and Das, S. (2016) *Elements of Power Systems*. Boca Raton: Taylor & Francis Group.

Safari, M., Haghifam, M. R. and Zangiabadi, M. (2021) 'A hybrid method for recloser and sectionalizer placement in distribution networks considering protection coordination, fault type and equipment malfunction', *IET Generation, Transmission and Distribution*, 15(19), pp. 2176–2190.

Salim, R. H. *et al.* (2009) 'Extended fault-location formulation for power distribution

systems', *IEEE Transactions on Power Delivery*, 24(2), pp. 508–516.

Saran, A. and Fu, Y. (2015) 'Comparison of FDIR technique between passive and active distribution systems', *North American Power Symposium (NAPS)*, pp. 1–6.

Sardina, D. V. (2015) FAULT LOCATION , ISOLATION AND NETWORK RESTORATION AS A SELF-HEALING FUNCTION.

Schwarz, K. (2020) 'The Standard Message Specification for Industrial Automation Systems ISO 9506 (MMS)', *Industrial Communication Technology Handbook*.

SEL-351A Instruction manual (2020) 'SEL-351A, -1 Protection system Instruction Manual'.

Shahin, M. . (2013) 'Smart Grid Self-healing Implementation for Underground Distribution Networks', *In IEEE Innovative Smart Grid Technologies-Asia (ISGT Asia)*, pp. 1–5.

Silos, S. A., Villafafila, R. R. and Lloret, G. P. (2020) 'Novel fault location algorithm for meshed distribution networks with DERs', *Electric Power Systems Research*.

Skoonpong, A. and Sirisumrannukul, S. (2008) 'Network reconfiguration for reliability worth enhancement in distribution systems by simulated annealing', *5th International Conference on Electrical Engineering/Electronics, Computer, Telecommunications and Information Technology, ECTI-CON*, pp. 937–940.

So, C. W. and Li, K. K. (2002) 'Protection relay coordination on ring-fed distribution network with distributed generations', *Proceedings of IEEE TENCON'02*, 3, pp. 1885–1888.

Solanki, J. M., Sarika, K. and Schulz, N. N. (2007) 'A Multi-Agent Solution to', *IEEE Transactions on Power Systems*, 22(3), pp. 1026–1034.

Souza, J. C. S. de *et al.* (2001) 'Fault location in electrical power systems using intelligent systems techniques', *IEEE Transactions on power delivery*, 16(1), pp. 59–67.

Su, C. L. and Teng, J. H. (2006) 'Economic evaluation of a distribution automation project', *IEEE Industry Applications Conference*, 3, pp. 1402–1409.

Teo, C. Y. and Gooi, H. B. (1998) 'Artificial intelligence in diagnosis and supply restoration for a distribution network', *IEE Proceedings-Generation, Transmission and Distribution*, 145, pp. 444–450.

Valtari, J. and Verho, P. (2011) 'Efficient Secondary System Configuration Process Utilizing Centralized Substation Functions', *InPACW Protection, Automation & Control World Conference*, pp. 1–8.

Vasant, P. (2011) Innovation in power, control, and optimization: Emerging energy technologies: Emerging energy technologies. Hershey PA: IGI Global.

Wang, B. *et al.* (2018) 'New reward and penalty scheme for electric distribution utilities employing load-based reliability indices', *IET Generation, Transmission and Distribution*, 12(15), pp. 3647–3654.

Weedy, B. M. (2012) *Electric power systems, fifth edition*. 5th ed. Chichester, West Sussex, U.K: John Wiley & Sons Ltd.

Willis, H. L. (2004) *Power distribution planning reference book*. 1st edn. Boca Raton: Tylor & Francis Group.

Wright, A. and Christopoulos, C. (1999) *Electrical power system protection*. Nottingham: Springer Science & Business Media.

Zeinalzadeh, A., Estebsari, A. and Bahmanyar, A. (2019) 'Multi-Objective Optimal Placement of Recloser and Sectionalizer in Electricity Distribution Feeders', *IEEE International Conference on Environment and Electrical Engineering EEIC(E/I) and IEEE Industrial and Commercial Power Systems (CPS)*, pp. 1–4.

Zhou, X. *et al.* (2016) 'An overview on distribution automation system', *Proceedings of the 28th Chinese Control and Decision Conference, CCDC*, pp. 3667–3671.

Zidan, A. *et al.* (2017) 'Fault Detection, Isolation, and Service Restoration in Distribution Systems: State-of-the-Art and Future Trends', *IEEE Transactions on Smart Grid*, 8(5), pp. 2170–2185.

Zidan, A. and El-Saadany, E. F. (2012) 'A cooperative multiagent framework for self-healing mechanisms in distribution systems', *IEEE Transactions on Smart Grid*, 3(3), pp. 1525–1539.

Zidan, A. and El-Saadany, E. F. (2013) 'Incorporating load variation and variable wind generation in service restoration plans for distribution systems', *Energy*, 57, pp. 682–691.

APPENDICES

Appendix A: Distribution network modeling

A.1.1: External grid modelling

DIgSILENT software is used to model the distribution network under consideration. The external grid data are shown in Table A.1 below, and Figure A.1 depicts an illustrative modeling of the external grid data in DIgSILENT. The grid data comprises the type of bus, voltage, and short circuit current, which is the maximum current supplied by the grid to the network in the event of a three-phase fault in the network. At the start of the load flow, the Slack Bus Real and reactive power are assumed zero. Following the load flow, DIgSILENT compute the actual real and reactive network requirements based on the network's loading condition using the Newton Raphson load flow algorithm.

Table A.1: External Grid data

Description	Rated Voltage in kV	Bus type	Angle in degree	Voltage setpoint in p.u	Short circuit current (I_k'' max) in kA
External Grid	66kV	Slack	0	1.0	6.81

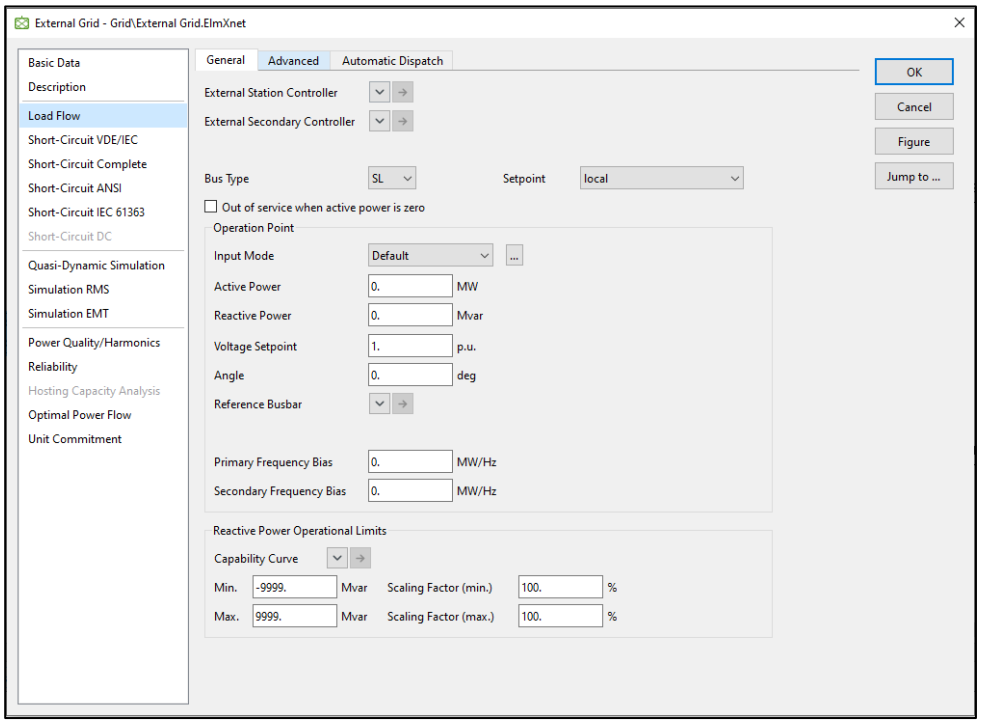

Figure A.1: Modelling of External grid parameters

A.1.2: Busbar modelling

Busbar data includes rated voltage, system type, and phase technology. Table A.2 and Figure A.2 show busbar data and busbar modeling, respectively. All other busbars are modelled in the same way, using the rated voltages shown in Table A.2. The ABC phase technique refers to a 120 phase shift between phases.

Table A.2: Busbar data

Description	Rated Voltage in kV	System type	Phase technology
Busbar 1	66	AC	ABC
Busbar 2	22	AC	ABC
Busbar 3	22	AC	ABC
Busbar 4	22	AC	ABC

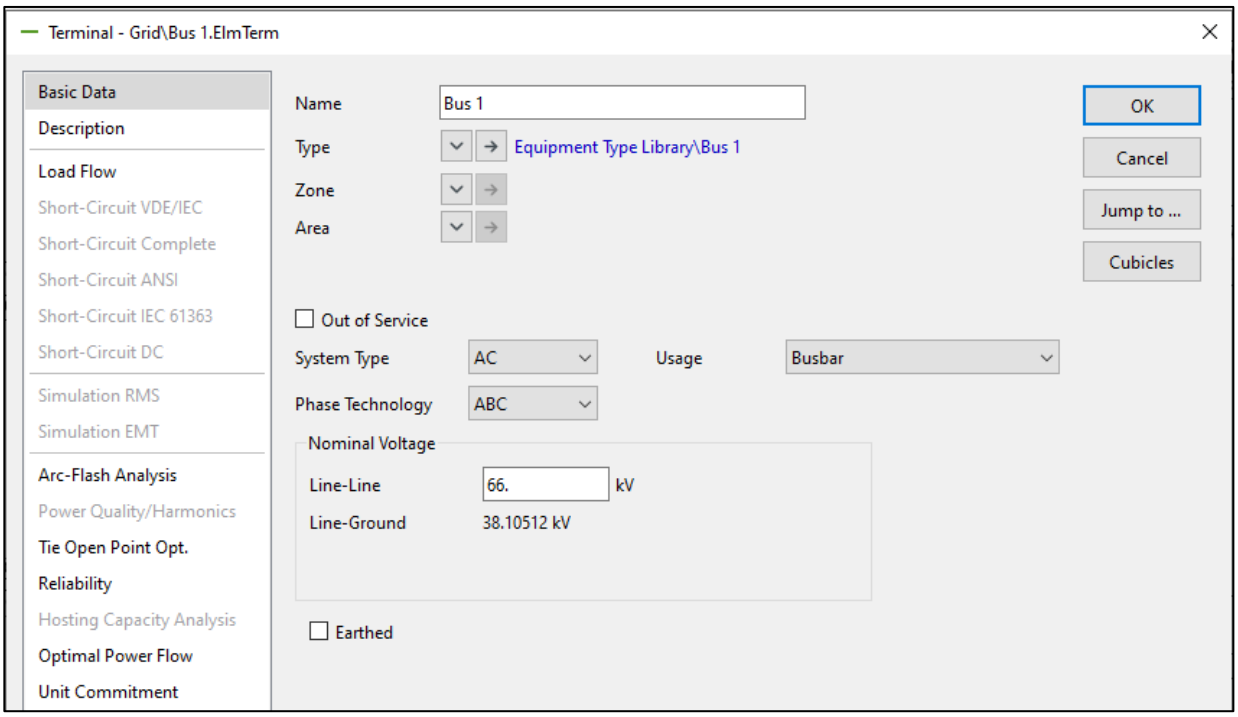

Figure A.2: Busbar modelling

A.1.3: Transformer modelling

Table 4.2 contains the data used to model both transformer 1 and transformer 2. Both of these transformers are connected in parallel and have the same characteristics. Figure A.3 depicts the modeling of transformer 1 in DIgSILENT software; transformer 2 is modelled in the same approach as transformer 1. Rated voltage, vector group, short circuit voltage, copper losses, rated power, and tap changer settings are among some of the transformer parameters given in Table A.3.

Table A.3: Transformer data

Description	Rated Voltage in kV	Vector group	Short circuit voltage uk	Copper losses in kW	Rated power in MVA
Transformer 1	HV 66kV LV 22kV	YNY11	8.97%	89.7	10
Transformer 2	HV 66kV LV 22kV	YNY11	8.97%	89.7	10

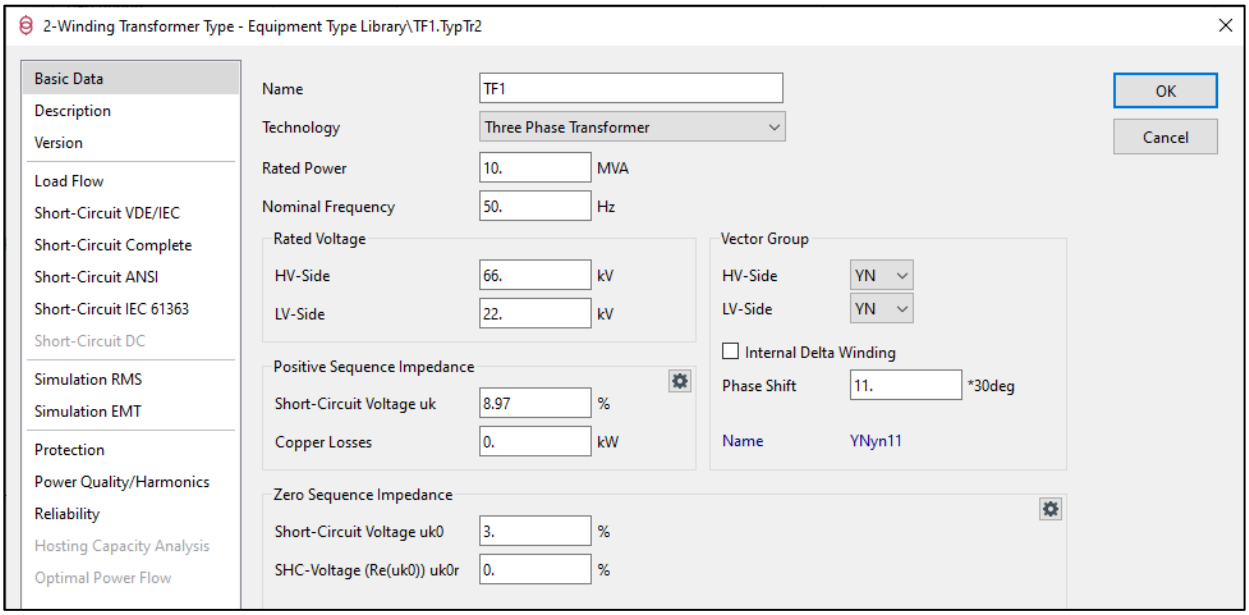

Figure A.3: Modelling of transformer parameters on DIgSILENT software

Tap changers are located on the primary side of each of the two transformers. The tap changers are used to regulate the transformer's output voltage by changing the number of turns on the transformer winding, which changes the transformer's turns ratio. Regulating the transformer's output voltage helps in maintaining the distribution system voltage within the limitations stated in the IEEE 141-1993 standard. The tap changer data is shown in Table A.4 and Figure A.4 below provides the transformer tap-changer parameter configuration in DIgSILENT software.

Table A.4: Tap changer data

Tap changer position	Additional voltage per tap	Phase of du	Neutral position	Minimum position	Maximum position
HV side	1.25%	0 degree	5	1	17

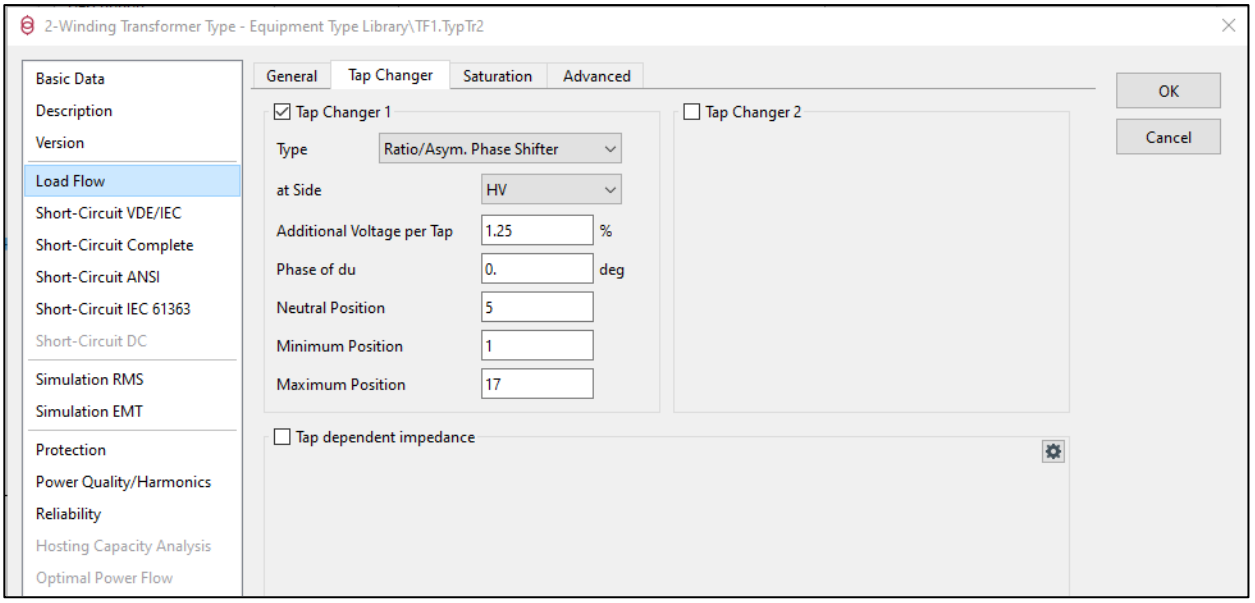

Figure A.4: Modelling of tap changer configuration parameters in DigSILENT simulation software

A.1.4: Overhead line modelling

Table A.5 shows the overhead line parameters. Figures A.5 and A.6 depict the overhead line modeling in DIgSILENT software. The rated voltage, rated current, and impedance values of the overhead lines are the same, but their lengths varied, as indicated in Table A.5.

Table A.5: Overhead line data of the Distribution system

Description	Conductor material	Rated Voltage in kV	Rated current in kA	Line length in km	AC - Resistance R^{l} in Ω/km	Reactance X^{l} in Ω/km	AC - Resistance $R0^{l}$ in Ω/km	Reactance $X0^{l}$ in Ω/km	Susceptance B^{l} in uS/km	Susceptance $B0^{l}$ in uS/km
Line 1	Aluminium	22	0.25	7	0.195	0.355	0.342	1.667	3.24	1.54
Line 2			0.25	7						
Line 3			0.25	6.5						
Line 4			0.25	6						
Line 5			0.25	6						
Line 6			0.25	5						

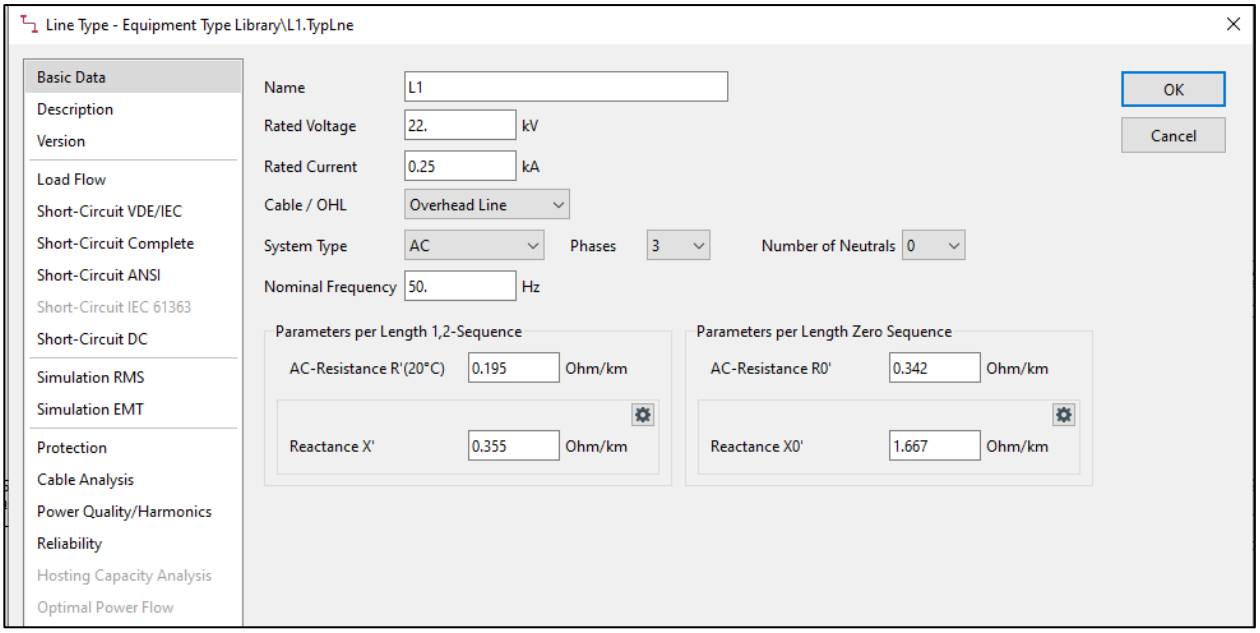

Figure A.5: Overhead line ratings and sequence Impedances

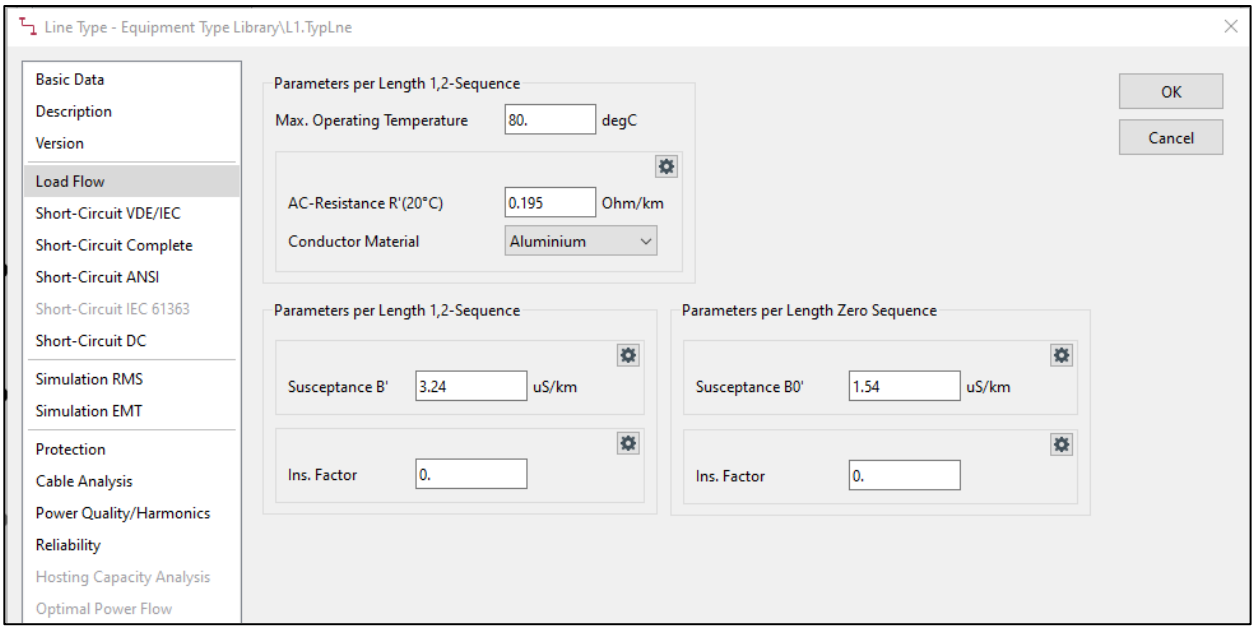

Figure A.6: Overhead line conductor material and susceptance data

A.1.4: Load modelling

The type of loads determines the load parameters. Load types include single-phase, two-phase, three-phase with and without earth, and neutral. Load data and its modeling in DIgSILENT can be seen in Table A.6 and Figure A.7, respectively. Active power, power factor, and P.U. voltage are all part of the load data.

Table A.6: Load data

Description	Active power in MW	Power factor	Voltage in p.u
Load 1	1.2	0.95	1.0
Load 2	0.9	0.95	1.0
Load 3	0.9	0.95	1.0
Load 4	1.4	0.95	1.0
Load 5	0.75	0.95	1.0
Load 6	0.75	0.95	1.0

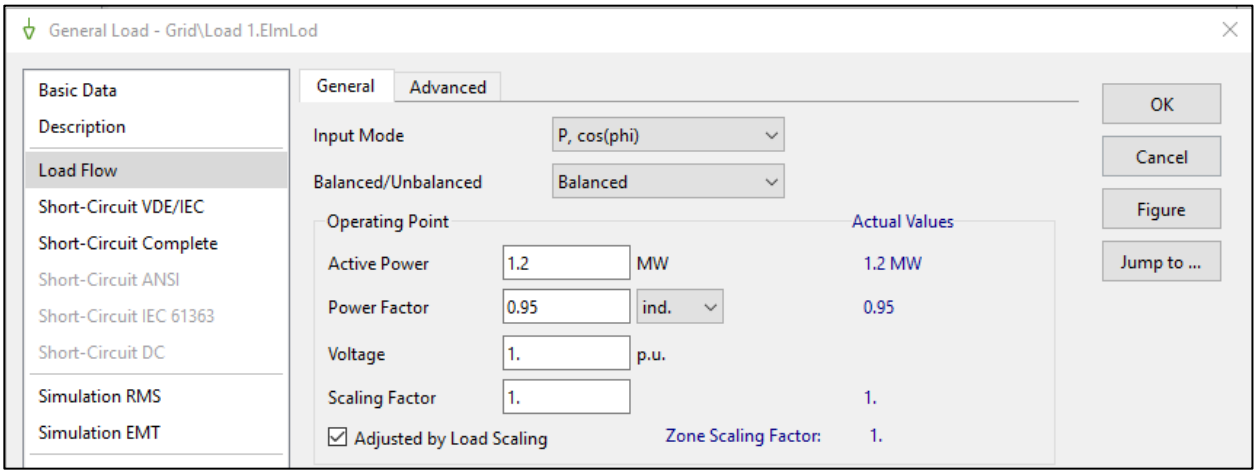

Figure A.7: Load data modelling

Appendix B: SEL-351A wiring diagram

This appendix provides the wiring diagram for configuring the overcurrent and auto-reclose schemes. Figure B.1 depicts the wiring diagram.

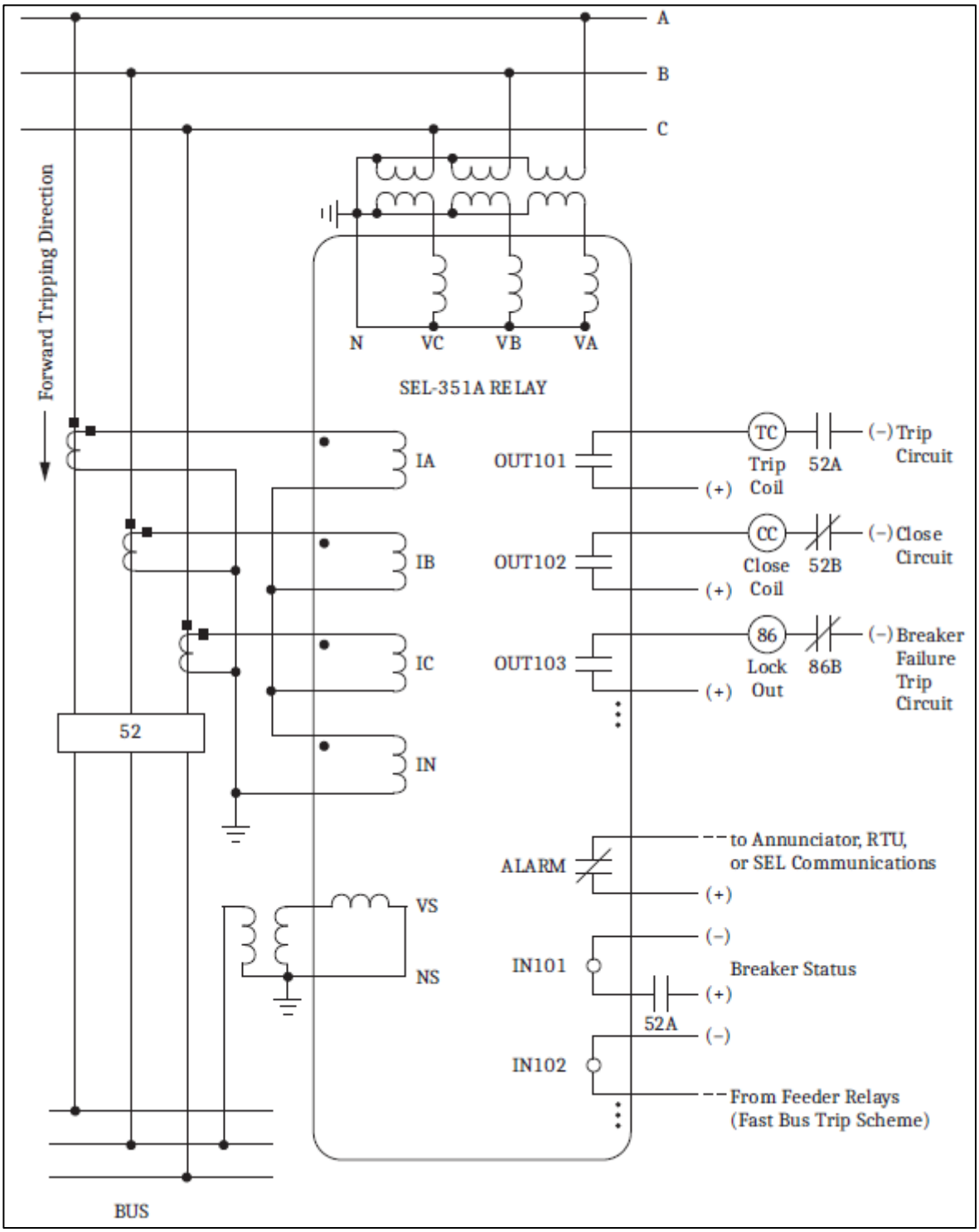

Figure B.1: SEL-351A wiring diagram

Appendix C: SEL-351A Recloser protection configuration settings

This appendix section provides the overcurrent protection settings for Relays 1 and 2 received from the SEL-351A AcSELerator Quickset terminal window. The resultant settings are depicted in Figures C.1 and C.2.

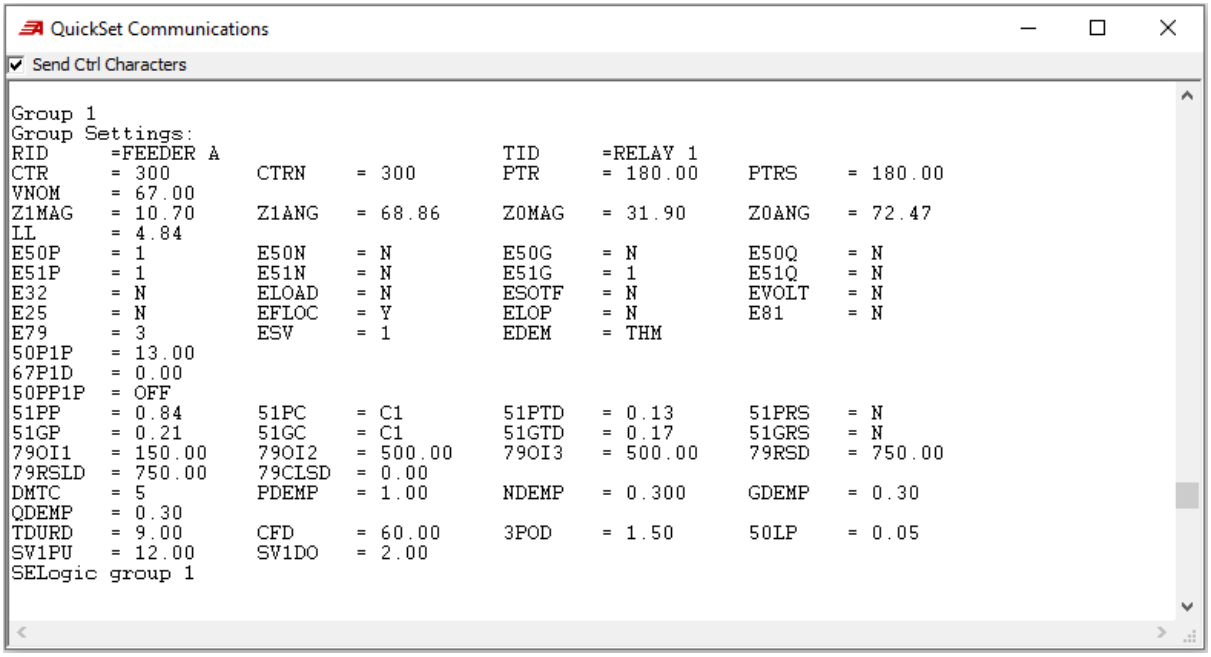

Figure C.1: SEL-351A (R1) overcurrent and auto-reclose settings

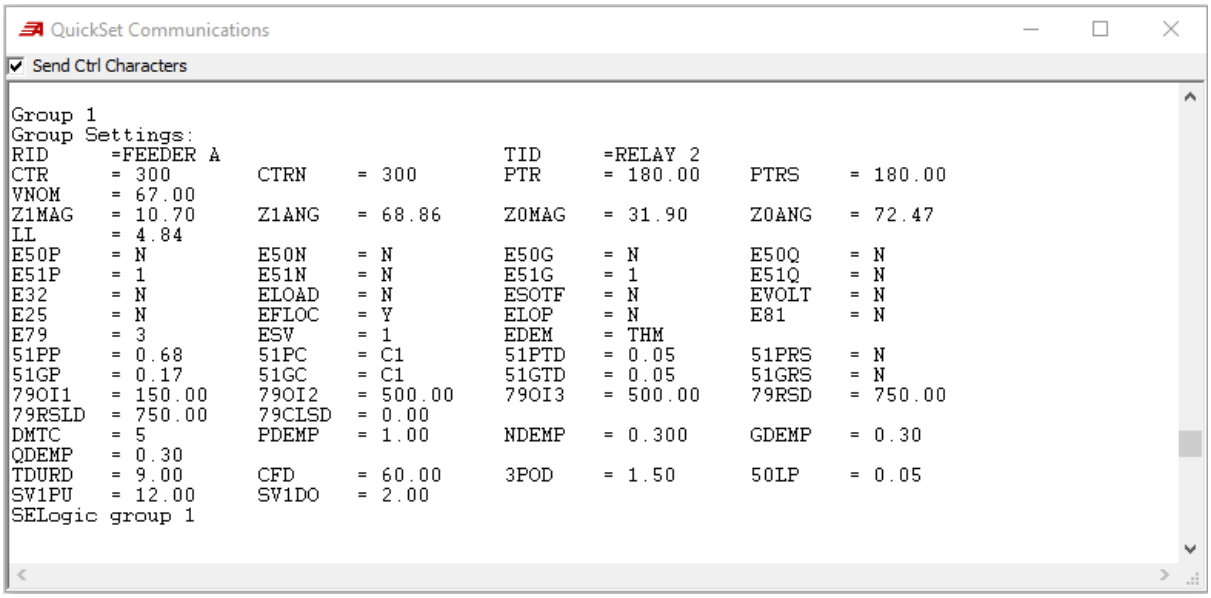

Figure C.2: SEL-351A (R2) overcurrent and auto-reclose settings

Appendix D: Sequential Events Recorder (SER) Report

This section provides sequence of events when the overcurrent and auto-reclose functions were tested. Tables D.1 and D.2 provides the sequence of reports retrieved from SEL-351A (R1) and SEL-351A (R2) respectively.

Table D.1: SER retrieved from SEL-351A (R1) relay

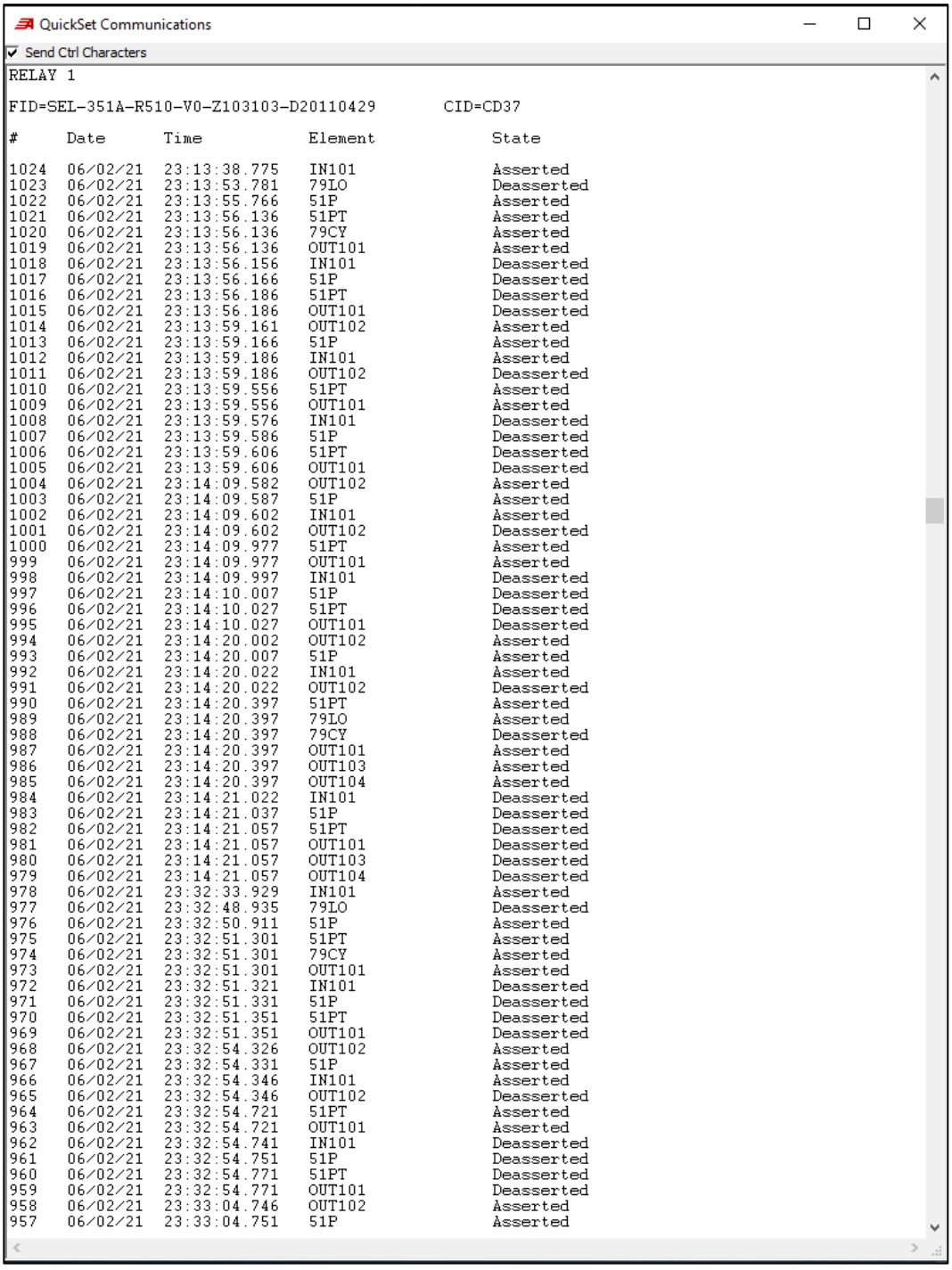

QuickSet Communications

Send Ctrl Characters

RELAY 1

FID=SEL-351A-R510-V0-Z103103-D20110429 CID=CD37

#	Date	Time	Element	State
1024	06/02/21	23:13:38.775	IN101	Asserted
1023	06/02/21	23:13:53.781	79LO	Deasserted
1022	06/02/21	23:13:55.766	51P	Asserted
1021	06/02/21	23:13:56.136	51PT	Asserted
1020	06/02/21	23:13:56.136	79CY	Asserted
1019	06/02/21	23:13:56.136	OUT101	Asserted
1018	06/02/21	23:13:56.156	IN101	Deasserted
1017	06/02/21	23:13:56.166	51P	Deasserted
1016	06/02/21	23:13:56.186	51PT	Deasserted
1015	06/02/21	23:13:56.186	OUT101	Deasserted
1014	06/02/21	23:13:59.161	OUT102	Asserted
1013	06/02/21	23:13:59.166	51P	Asserted
1012	06/02/21	23:13:59.186	IN101	Asserted
1011	06/02/21	23:13:59.186	OUT102	Deasserted
1010	06/02/21	23:13:59.556	51PT	Asserted
1009	06/02/21	23:13:59.556	OUT101	Asserted
1008	06/02/21	23:13:59.576	IN101	Deasserted
1007	06/02/21	23:13:59.586	51P	Deasserted
1006	06/02/21	23:13:59.606	51PT	Deasserted
1005	06/02/21	23:13:59.606	OUT101	Deasserted
1004	06/02/21	23:14:09.582	OUT102	Asserted
1003	06/02/21	23:14:09.587	51P	Asserted
1002	06/02/21	23:14:09.602	IN101	Asserted
1001	06/02/21	23:14:09.602	OUT102	Deasserted
1000	06/02/21	23:14:09.977	51PT	Asserted
999	06/02/21	23:14:09.977	OUT101	Asserted
998	06/02/21	23:14:09.997	IN101	Deasserted
997	06/02/21	23:14:10.007	51P	Deasserted
996	06/02/21	23:14:10.027	51PT	Deasserted
995	06/02/21	23:14:10.027	OUT101	Deasserted
994	06/02/21	23:14:20.002	OUT102	Asserted
993	06/02/21	23:14:20.007	51P	Asserted
992	06/02/21	23:14:20.022	IN101	Asserted
991	06/02/21	23:14:20.022	OUT102	Deasserted
990	06/02/21	23:14:20.397	51PT	Asserted
989	06/02/21	23:14:20.397	79LO	Asserted
988	06/02/21	23:14:20.397	79CY	Deasserted
987	06/02/21	23:14:20.397	OUT101	Asserted
986	06/02/21	23:14:20.397	OUT103	Asserted
985	06/02/21	23:14:20.397	OUT104	Asserted
984	06/02/21	23:14:21.022	IN101	Deasserted
983	06/02/21	23:14:21.037	51P	Deasserted
982	06/02/21	23:14:21.057	51PT	Deasserted
981	06/02/21	23:14:21.057	OUT101	Deasserted
980	06/02/21	23:14:21.057	OUT103	Deasserted
979	06/02/21	23:14:21.057	OUT104	Deasserted
978	06/02/21	23:32:33.929	IN101	Asserted
977	06/02/21	23:32:48.935	79LO	Deasserted
976	06/02/21	23:32:50.911	51P	Asserted
975	06/02/21	23:32:51.301	51PT	Asserted
974	06/02/21	23:32:51.301	79CY	Asserted
973	06/02/21	23:32:51.301	OUT101	Asserted
972	06/02/21	23:32:51.321	IN101	Deasserted
971	06/02/21	23:32:51.331	51P	Deasserted
970	06/02/21	23:32:51.351	51PT	Deasserted
969	06/02/21	23:32:51.351	OUT101	Deasserted
968	06/02/21	23:32:54.326	OUT102	Asserted
967	06/02/21	23:32:54.331	51P	Asserted
966	06/02/21	23:32:54.346	IN101	Asserted
965	06/02/21	23:32:54.346	OUT102	Deasserted
964	06/02/21	23:32:54.721	51PT	Asserted
963	06/02/21	23:32:54.721	OUT101	Asserted
962	06/02/21	23:32:54.741	IN101	Deasserted
961	06/02/21	23:32:54.751	51P	Deasserted
960	06/02/21	23:32:54.771	51PT	Deasserted
959	06/02/21	23:32:54.771	OUT101	Deasserted
958	06/02/21	23:33:04.746	OUT102	Asserted
957	06/02/21	23:33:04.751	51P	Asserted

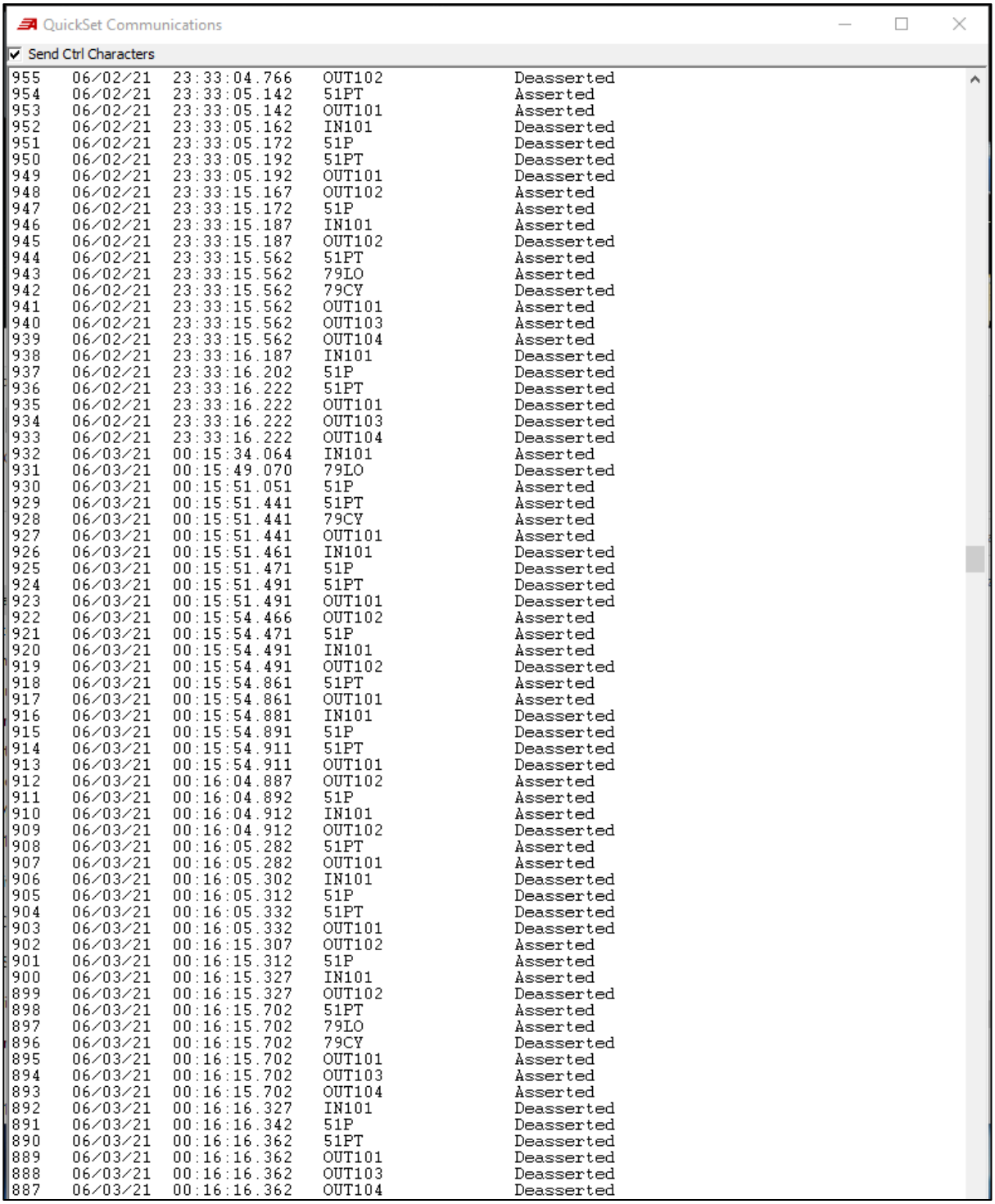

955	06/02/21	23:33:04.766	OUT102	Deasserted
954	06/02/21	23:33:05.142	51PT	Asserted
953	06/02/21	23:33:05.142	OUT101	Asserted
952	06/02/21	23:33:05.162	IN101	Deasserted
951	06/02/21	23:33:05.172	51P	Deasserted
950	06/02/21	23:33:05.192	51PT	Deasserted
949	06/02/21	23:33:05.192	OUT101	Deasserted
948	06/02/21	23:33:15.167	OUT102	Asserted
947	06/02/21	23:33:15.172	51P	Asserted
946	06/02/21	23:33:15.187	IN101	Asserted
945	06/02/21	23:33:15.187	OUT102	Deasserted
944	06/02/21	23:33:15.562	51PT	Asserted
943	06/02/21	23:33:15.562	79LO	Asserted
942	06/02/21	23:33:15.562	79CY	Deasserted
941	06/02/21	23:33:15.562	OUT101	Asserted
940	06/02/21	23:33:15.562	OUT103	Asserted
939	06/02/21	23:33:15.562	OUT104	Asserted
938	06/02/21	23:33:16.187	IN101	Deasserted
937	06/02/21	23:33:16.202	51P	Deasserted
936	06/02/21	23:33:16.222	51PT	Deasserted
935	06/02/21	23:33:16.222	OUT101	Deasserted
934	06/02/21	23:33:16.222	OUT103	Deasserted
933	06/02/21	23:33:16.222	OUT104	Deasserted
932	06/03/21	00:15:34.064	IN101	Asserted
931	06/03/21	00:15:49.070	79LO	Deasserted
930	06/03/21	00:15:51.051	51P	Asserted
929	06/03/21	00:15:51.441	51PT	Asserted
928	06/03/21	00:15:51.441	79CY	Asserted
927	06/03/21	00:15:51.441	OUT101	Asserted
926	06/03/21	00:15:51.461	IN101	Deasserted
925	06/03/21	00:15:51.471	51P	Deasserted
924	06/03/21	00:15:51.491	51PT	Deasserted
923	06/03/21	00:15:51.491	OUT101	Deasserted
922	06/03/21	00:15:54.466	OUT102	Asserted
921	06/03/21	00:15:54.471	51P	Asserted
920	06/03/21	00:15:54.491	IN101	Asserted
919	06/03/21	00:15:54.491	OUT102	Deasserted
918	06/03/21	00:15:54.861	51PT	Asserted
917	06/03/21	00:15:54.861	OUT101	Asserted
916	06/03/21	00:15:54.881	IN101	Deasserted
915	06/03/21	00:15:54.891	51P	Deasserted
914	06/03/21	00:15:54.911	51PT	Deasserted
913	06/03/21	00:15:54.911	OUT101	Deasserted
912	06/03/21	00:16:04.887	OUT102	Asserted
911	06/03/21	00:16:04.892	51P	Asserted
910	06/03/21	00:16:04.912	IN101	Asserted
909	06/03/21	00:16:04.912	OUT102	Deasserted
908	06/03/21	00:16:05.282	51PT	Asserted
907	06/03/21	00:16:05.282	OUT101	Asserted
906	06/03/21	00:16:05.302	IN101	Deasserted
905	06/03/21	00:16:05.312	51P	Deasserted
904	06/03/21	00:16:05.332	51PT	Deasserted
903	06/03/21	00:16:05.332	OUT101	Deasserted
902	06/03/21	00:16:15.307	OUT102	Asserted
901	06/03/21	00:16:15.312	51P	Asserted
900	06/03/21	00:16:15.327	IN101	Asserted
899	06/03/21	00:16:15.327	OUT102	Deasserted
898	06/03/21	00:16:15.702	51PT	Asserted
897	06/03/21	00:16:15.702	79LO	Asserted
896	06/03/21	00:16:15.702	79CY	Deasserted
895	06/03/21	00:16:15.702	OUT101	Asserted
894	06/03/21	00:16:15.702	OUT103	Asserted
893	06/03/21	00:16:15.702	OUT104	Asserted
892	06/03/21	00:16:16.327	IN101	Deasserted
891	06/03/21	00:16:16.342	51P	Deasserted
890	06/03/21	00:16:16.362	51PT	Deasserted
889	06/03/21	00:16:16.362	OUT101	Deasserted
888	06/03/21	00:16:16.362	OUT103	Deasserted
887	06/03/21	00:16:16.362	OUT104	Deasserted

Table D.2: SER retrieved from SEL-351A (R2) relay

QuickSet Communications

Send Ctrl Characters

```
RELAY 2

FID=SEL-351A-R510-V0-Z103103-D20110429       CID=CD37

#      Date       Time            Element             State

1024   05/31/21   22:23:35.936    TRIP                Deasserted
1023   05/31/21   22:23:39.121    TRGTR               Asserted
1022   05/31/21   22:23:39.126    TRGTR               Deasserted
1021   05/31/21   22:37:28.193    OUT103              Asserted
1020   05/31/21   22:37:28.193    VB001               Asserted
1019   05/31/21   22:37:28.198    OUT101              Asserted
1018   05/31/21   22:37:28.198    TRIP                Asserted
1017   05/31/21   22:37:28.283    OUT103              Deasserted
1016   05/31/21   22:37:28.283    VB001               Deasserted
1015   05/31/21   22:37:28.288    OUT101              Deasserted
1014   05/31/21   22:37:28.378    TRIP                Deasserted
1013   05/31/21   23:03:05.924    OUT103              Asserted
1012   05/31/21   23:03:05.924    VB001               Asserted
1011   05/31/21   23:03:05.929    OUT101              Asserted
1010   05/31/21   23:03:05.929    TRIP                Asserted
1009   05/31/21   23:03:06.014    OUT103              Deasserted
1008   05/31/21   23:03:06.014    VB001               Deasserted
1007   05/31/21   23:03:06.019    OUT101              Deasserted
1006   05/31/21   23:03:06.109    TRIP                Deasserted
1005   05/31/21   23:14:59.868    TRGTR               Asserted
1004   05/31/21   23:14:59.873    TRGTR               Deasserted
1003   06/01/21   09:15:20.267     Relay newly powered up
1002   06/01/21   09:15:52.198    TRGTR               Asserted
1001   06/01/21   09:15:52.203    TRGTR               Deasserted
1000   06/01/21   10:59:29.186    OUT103              Asserted
999    06/01/21   10:59:29.186    VB001               Asserted
998    06/01/21   10:59:29.191    OUT101              Asserted
997    06/01/21   10:59:29.191    TRIP                Asserted
996    06/01/21   10:59:29.286    OUT103              Deasserted
995    06/01/21   10:59:29.286    VB001               Deasserted
994    06/01/21   10:59:29.291    OUT101              Deasserted
993    06/01/21   10:59:29.371    TRIP                Deasserted
992    06/01/21   10:59:44.267    OUT103              Asserted
991    06/01/21   10:59:44.267    VB001               Asserted
990    06/01/21   10:59:44.272    OUT101              Asserted
989    06/01/21   10:59:44.272    TRIP                Asserted
988    06/01/21   10:59:44.357    OUT103              Deasserted
987    06/01/21   10:59:44.357    VB001               Deasserted
986    06/01/21   10:59:44.362    OUT101              Deasserted
985    06/01/21   10:59:44.452    TRIP                Deasserted
984    06/01/21   10:59:47.132    TRGTR               Asserted
983    06/01/21   10:59:47.137    TRGTR               Deasserted
982    06/01/21   10:59:57.578    OUT103              Asserted
981    06/01/21   10:59:57.578    VB001               Asserted
980    06/01/21   10:59:57.583    OUT101              Asserted
979    06/01/21   10:59:57.583    TRIP                Asserted
978    06/01/21   10:59:57.678    OUT103              Deasserted
977    06/01/21   10:59:57.678    VB001               Deasserted
976    06/01/21   10:59:57.683    OUT101              Deasserted
975    06/01/21   10:59:57.763    TRIP                Deasserted
974    06/01/21   11:00:00.438    TRGTR               Asserted
973    06/01/21   11:00:00.443    TRGTR               Deasserted
972    06/01/21   11:01:11.108    OUT103              Asserted
971    06/01/21   11:01:11.108    VB001               Asserted
970    06/01/21   11:01:11.113    OUT101              Asserted
969    06/01/21   11:01:11.113    TRIP                Asserted
968    06/01/21   11:01:11.603    OUT103              Deasserted
967    06/01/21   11:01:11.603    VB001               Deasserted
966    06/01/21   11:01:11.608    OUT101              Deasserted
965    06/01/21   11:01:11.608    TRIP                Deasserted
964    06/01/21   11:11:04.535    TRGTR               Asserted
963    06/01/21   11:11:04.540    TRGTR               Deasserted
962    06/01/21   11:11:20.911    OUT103              Asserted
961    06/01/21   11:11:20.911    VB001               Asserted
960    06/01/21   11:11:20.916    OUT101              Asserted
```

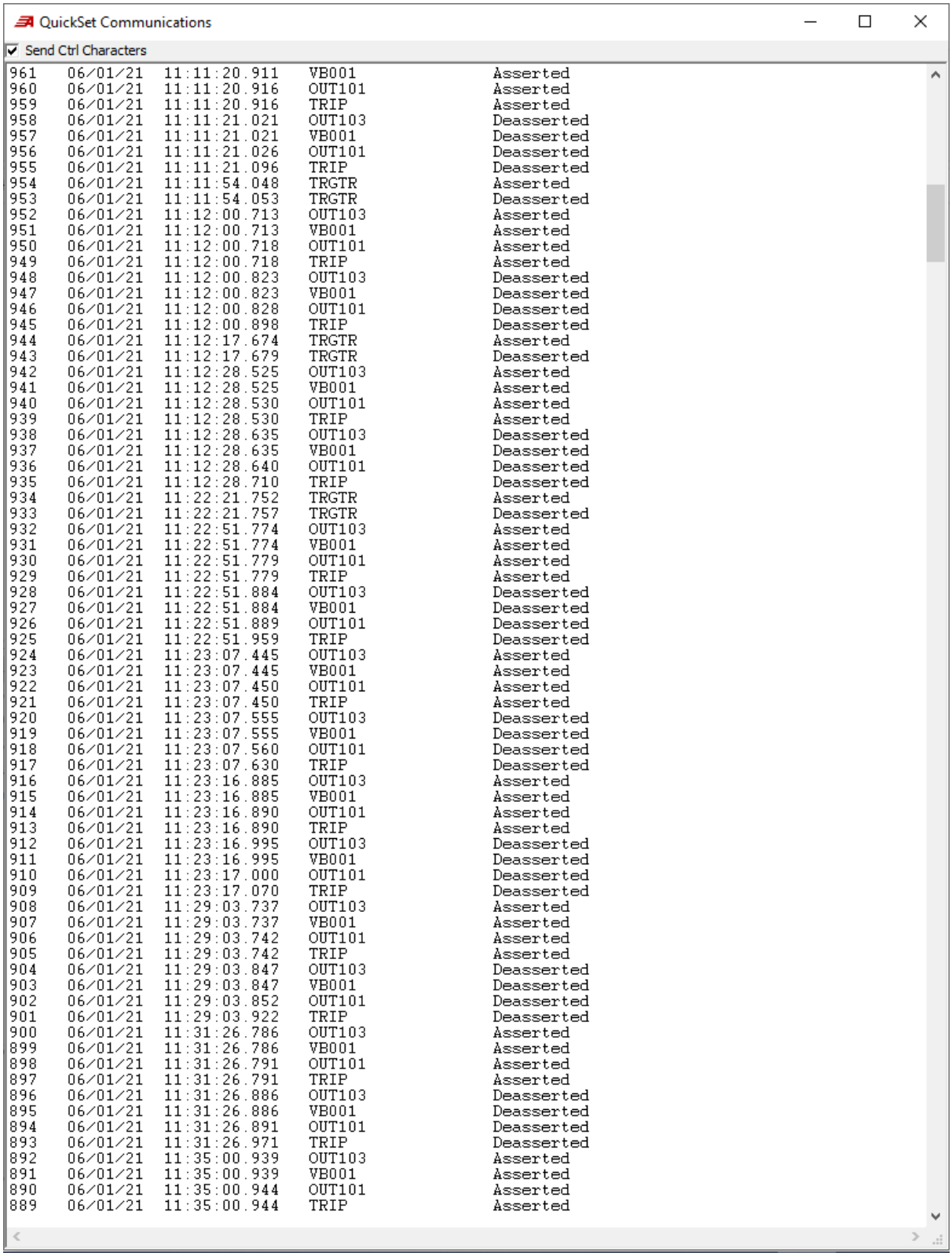
QuickSet Communications
Send Ctrl Characters
961 06/01/21 11:11:20.911 VB001 Asserted
960 06/01/21 11:11:20.916 OUT101 Asserted
959 06/01/21 11:11:20.916 TRIP Asserted
958 06/01/21 11:11:21.021 OUT103 Deasserted
957 06/01/21 11:11:21.021 VB001 Deasserted
956 06/01/21 11:11:21.026 OUT101 Deasserted
955 06/01/21 11:11:21.096 TRIP Deasserted
954 06/01/21 11:11:54.048 TRGTR Asserted
953 06/01/21 11:11:54.053 TRGTR Deasserted
952 06/01/21 11:12:00.713 OUT103 Asserted
951 06/01/21 11:12:00.713 VB001 Asserted
950 06/01/21 11:12:00.718 OUT101 Asserted
949 06/01/21 11:12:00.718 TRIP Asserted
948 06/01/21 11:12:00.823 OUT103 Deasserted
947 06/01/21 11:12:00.823 VB001 Deasserted
946 06/01/21 11:12:00.828 OUT101 Deasserted
945 06/01/21 11:12:00.898 TRIP Deasserted
944 06/01/21 11:12:17.674 TRGTR Asserted
943 06/01/21 11:12:17.679 TRGTR Deasserted
942 06/01/21 11:12:28.525 OUT103 Asserted
941 06/01/21 11:12:28.525 VB001 Asserted
940 06/01/21 11:12:28.530 OUT101 Asserted
939 06/01/21 11:12:28.530 TRIP Asserted
938 06/01/21 11:12:28.635 OUT103 Deasserted
937 06/01/21 11:12:28.635 VB001 Deasserted
936 06/01/21 11:12:28.640 OUT101 Deasserted
935 06/01/21 11:12:28.710 TRIP Deasserted
934 06/01/21 11:22:21.752 TRGTR Asserted
933 06/01/21 11:22:21.757 TRGTR Deasserted
932 06/01/21 11:22:51.774 OUT103 Asserted
931 06/01/21 11:22:51.774 VB001 Asserted
930 06/01/21 11:22:51.779 OUT101 Asserted
929 06/01/21 11:22:51.779 TRIP Asserted
928 06/01/21 11:22:51.884 OUT103 Deasserted
927 06/01/21 11:22:51.884 VB001 Deasserted
926 06/01/21 11:22:51.889 OUT101 Deasserted
925 06/01/21 11:22:51.959 TRIP Deasserted
924 06/01/21 11:23:07.445 OUT103 Asserted
923 06/01/21 11:23:07.445 VB001 Asserted
922 06/01/21 11:23:07.450 OUT101 Asserted
921 06/01/21 11:23:07.450 TRIP Asserted
920 06/01/21 11:23:07.555 OUT103 Deasserted
919 06/01/21 11:23:07.555 VB001 Deasserted
918 06/01/21 11:23:07.560 OUT101 Deasserted
917 06/01/21 11:23:07.630 TRIP Deasserted
916 06/01/21 11:23:16.885 OUT103 Asserted
915 06/01/21 11:23:16.885 VB001 Asserted
914 06/01/21 11:23:16.890 OUT101 Asserted
913 06/01/21 11:23:16.890 TRIP Asserted
912 06/01/21 11:23:16.995 OUT103 Deasserted
911 06/01/21 11:23:16.995 VB001 Deasserted
910 06/01/21 11:23:17.000 OUT101 Deasserted
909 06/01/21 11:23:17.070 TRIP Deasserted
908 06/01/21 11:29:03.737 OUT103 Asserted
907 06/01/21 11:29:03.737 VB001 Asserted
906 06/01/21 11:29:03.742 OUT101 Asserted
905 06/01/21 11:29:03.742 TRIP Asserted
904 06/01/21 11:29:03.847 OUT103 Deasserted
903 06/01/21 11:29:03.847 VB001 Deasserted
902 06/01/21 11:29:03.852 OUT101 Deasserted
901 06/01/21 11:29:03.922 TRIP Deasserted
900 06/01/21 11:31:26.786 OUT103 Asserted
899 06/01/21 11:31:26.786 VB001 Asserted
898 06/01/21 11:31:26.791 OUT101 Asserted
897 06/01/21 11:31:26.791 TRIP Asserted
896 06/01/21 11:31:26.886 OUT103 Deasserted
895 06/01/21 11:31:26.886 VB001 Deasserted
894 06/01/21 11:31:26.891 OUT101 Deasserted
893 06/01/21 11:31:26.971 TRIP Deasserted
892 06/01/21 11:35:00.939 OUT103 Asserted
891 06/01/21 11:35:00.939 VB001 Asserted
890 06/01/21 11:35:00.944 OUT101 Asserted
889 06/01/21 11:35:00.944 TRIP Asserted

Appendix E: Test universe auto-reclose reports

This appendix section describes the test universe software's auto-reclose sequence for relays 1 and 2. Figures E1 and E2 show the results of the auto-reclose simulation. Both figures depict the auto-reclose sequence and show that the testing were successful.

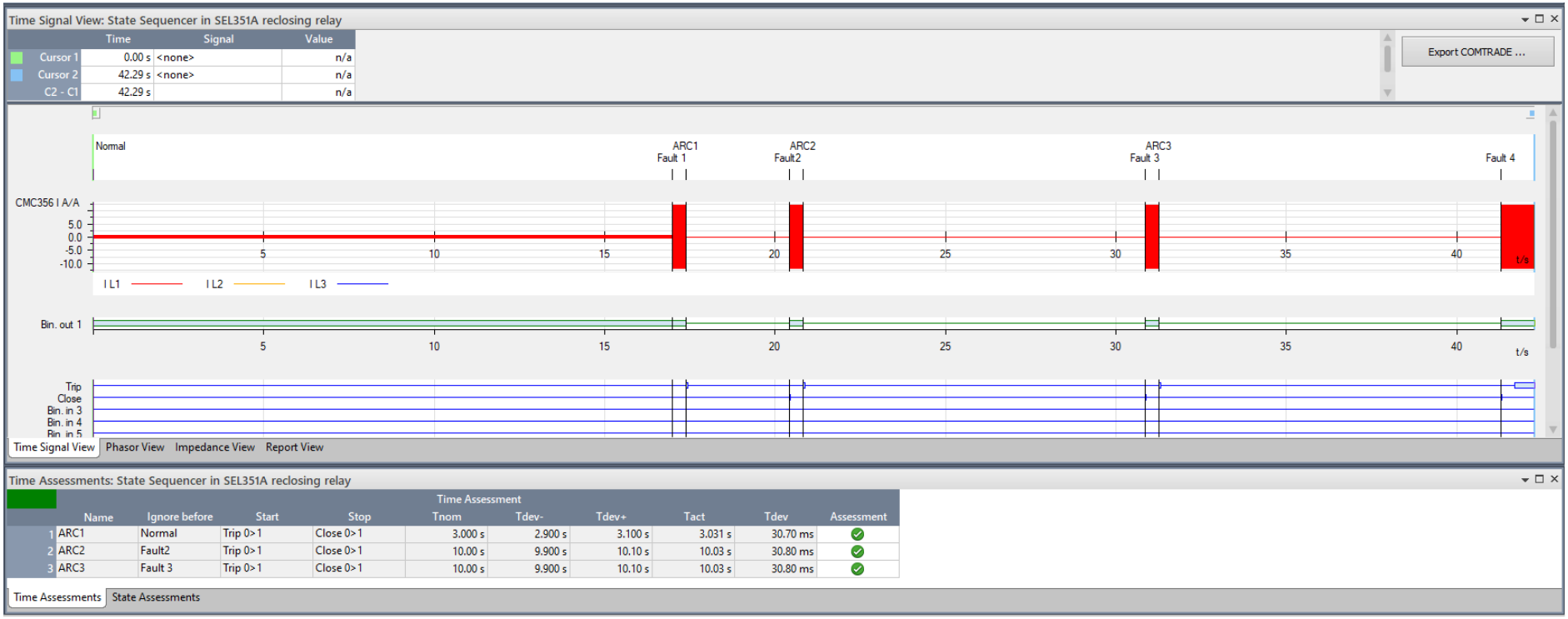

Figure E.1: Auto-reclose simulation results for SEL-351A (R1) obtained from test universe

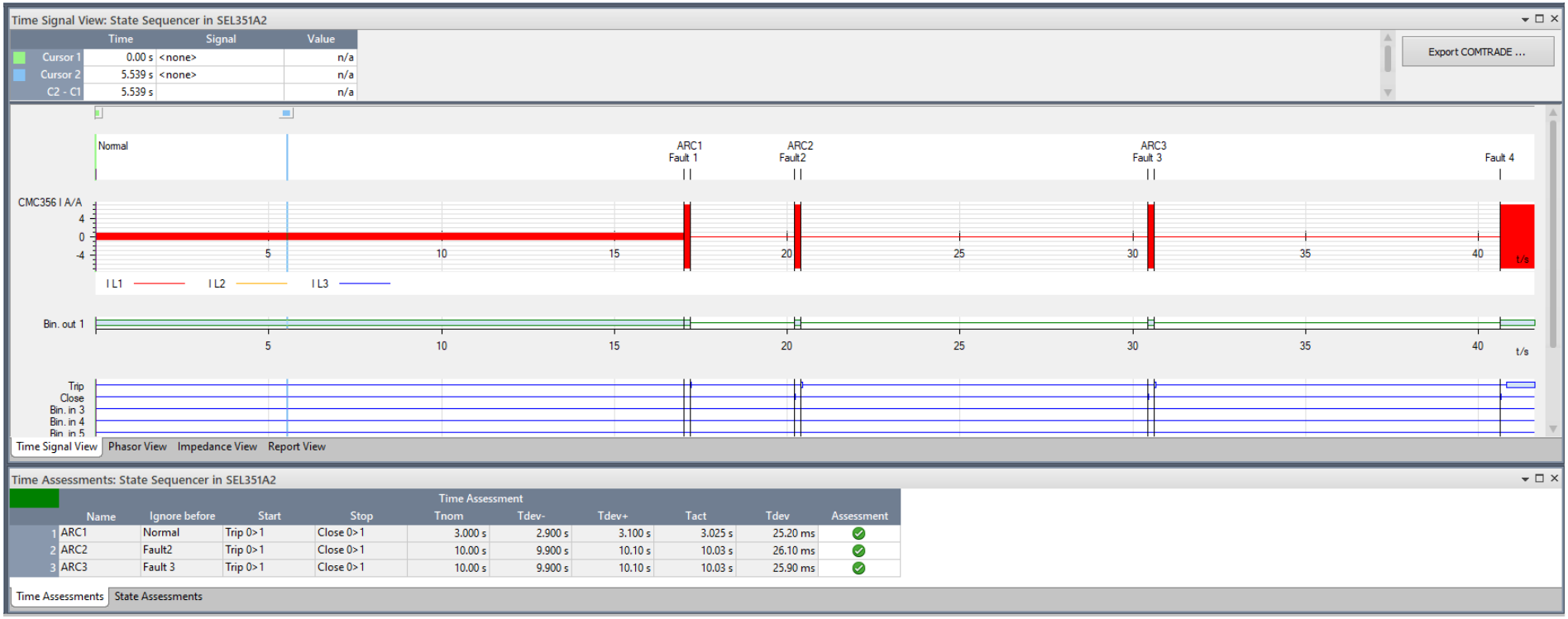

Figure E.2: Auto-reclose simulation results for SEL-351A (R2) obtained from test universe